THE CELL MODEL AND GAS SOLUBILITY THEORY

A thesis submitted for the degree of Doctor of Philosophy of The University of London.

by

William Ieuan Jenkins.

Department of Chemistry
Imperial College of Science and Technology.
London S.W.7. July 1966.

ABSTRACT

The development of the cell model of Lennard-Jones and Devonshire is discussed and the reasons for its failures noted.

Various mathematical forms of the intermolecular potential are examined together with some current ideas on the strict pair additivity of the intermolecular potential.

The thermodynamic properties of solid argon and neon have been predicted using a quantum version of the Lennard-Jones cell model, which utilizes the W.K.B. approximation to solve the Schroedinger equation. Excellent agreement between theoretical and experimental properties is observed and the critical dependence of the predicted data on the source of the parameters for the intermolecular potential clearly shown.

The above examination has been extended for various forms of the bi-reciprocal (m:n) potential. For predictions of the high density state of the inert gases the 12:6 potential is markedly superior to any alternative form.

A Corresponding States approach has been used to study the high density state of quantum molecules. The equation of state is regarded as the sum of a classical term and a quantum correction term. Theoretical isotherms were unsuccessfully predicted using an L.J. 12:6 model. However, better agreement was obtained using a uniform potential approximation to this theory.

An experimental determination of partial molar volumes at 25°C. was made for twenty four systems of non-polar gases in organic solvents. In all cases a dilatometric technique was used.

The experimental results were found to be in excellent agreement with those predicted through a simple hard sphere theory. A quantal version of this theory also successfully explained the solution behaviour of hydrogen and deuterium at room temperature.

The application of a more rigorous but correspondingly more complex "free volume" theory to solubility phenomena has also been examined but found unsatisfactory.

Dedication

To my father.

Acknowledgements

The work presented in this thesis owes much to the inspiration and guidence of John Walkley Ph.D., who first as tutor and then as supervisor has influenced the author throughout his college career. For his radical ideas, many of which appear here, his interest and most of all his constant approachability go the authors sincere thanks.

Thanks are also due to Ian Hillier who produced the prototypes of the majority of computer programs extensively used in these investigations.

These programs were taken over and developed by Barry Utting who for two years has had the fortune (or misfortune) to be the authors research collegue. This period has been marked by discussions, arguements and debates which have sometimes touched on scientific topics-but more importantly by a true and lasting friendship.

In fact the last six years at Imperial College have produced a multitude of persons and personalities who academically and socially have done much to make the author's somewhat chequered career a happy one. Too numerous to list here they are perhaps typified in two sets of initials - D.J.H. and J.C.T.. To these and to the above thanks alone might be inadequate but, in the present context, must suffice.

CONTENTS

CONTENTS (cont.)

Introduction

"And like a man to double business bound
I stand in pause when shall I first begin."

Hamlet III, 2, 40.

The ultimate quest of the scientific researcher is a complete understanding of the basic properties of matter. This optimistic and indeed far distant objective is, of necessity, attacked on two fronts; by experiments which are planned observations of physical phenomena, and by theories which seek to correlate observables by ideas.

At the present time the scientific picture on all levels is in a constant state of flux and upheaval, but although theories rapidly appear, are extended or are superceded, one paramount fact remains. This is that any theory concerning the properties of matter must have as its objectives a satisfactory description of structure on the molecular level and a quantitative correlation between macroscopic or experimental observations and the properties of individual molecules or atoms.

The problem of molecular structure is therefore one of the most challenging and intriguing in physical chemistry. It is, however, also one of the most complex, and in an attempt to arrive at situations that may be conceivably studied theoretically we are forced to adopt methods that make wide use of simplifying assumptions. Through these assumptions mathematical theories can be applied to natural

phenomena, and we are immediately involved with the discipline of statistical mechanics.

Statistical mechanics was described by Henry Eyring as, "Simply a game, a mathematical game with the rules made up as we go along" (1). This observation may well be true but it does not detract from the utility of a method which enables us, by averaging over systems of molecules, to predict macroscopic properties that compare favourably to the corresponding physical measurements.

Thus by astute use of the appropriate mathematical techniques we may compound theories to explain experimental phenomena. However, the picture given above is not quite as simple or as justifiable as has been stated. The reason for this is that in order to satisfactorily perform our averaging techniques i.e. to produce the tractable from the intractable, we are forced to impose conditions which have no physical reality. These conditions, often in the form of artificial boundaries or arbitrary assumptions as to molecular positions, can sometimes be justified by experimental observations, but almost as often their chief reason for existence is simply that of mathematical expediency.

These sets of artificially imposed conditions constitute a model on the molecular level. The following chapters are devoted to theories and experiments linked with one such model, the cell model, and especially in the form proposed some thirty years ago by Lennard-Jones and Devonshire (2-5).

The cell theory of Lennard-Jones and Devonshire (henceforth called L.J.&D.) was first developed to facilitate theoretical calculations on liquids and dense gases. It is one of the simplest models propounded for this phase of matter and over the last few decades has been the basis of many discussions and suggested improvements in the theories of liquids and solutions. Unfortunately this model does not give a good description of the fluid state and due to the assumptions on which it is formulated describes (as will be shown later) solids rather better than it describes fluids.

The most attractive media for any theoretical study are the crystals of the inert gases. These molecules are spherical units with closed electron shells, bound by central molecular forces which are to a first approximation additive i.e. the total potential energy of an inert gas crystal can be thought of as the sum of the two body interactions of all constituent atoms. This assumption of pair additivity is one of the basic concepts of the Lennard-Jones (henceforth L.J.) theory which considers intermolecular forces in terms of a bi-reciprocal potential. It is also a concept that perhaps suffers from being too elementary and during the last few years the subjects of pair additivity and the form of the intermolecular potential have stimulated much discussion and theory.

In this thesis it is proposed to study in some detail the limitations and successes of the cell model, in particular the

model of L.J.&D., which utilises the bi-reciprocal potential. We will first trace the development of the model as a description of the fluid state, study the assumptions on which it is based and consider the inherent limitations they impose. The form and nature of the potential will be examined in the light of contemporary ideas and in particular whether these sophisticated and often complex postulates lend themselves as simply, productively and successfully as those used in the L.J.&D. theory.

A detailed account of a theoretical investigation into the inert gas solids will then be presented, an investigation which,as will be shown, leads to extensive and accurate predictions of the temperature dependent properties of argon (6) and neon (7) at high densities. In all cases an L.J.&D. cell theory is employed assuming both pair additivity and a bi-reciprocal potential. Further studies on the second virial coefficients of these substances have been made, and the results of a rigorous generalised approach to the potential it its bi-reciprocal form are also given (8).

Following the success of the above model under strongly favourable conditions we have imposed a strain on the model by using it in a "Corresponding States" approach to study the compressibility of hydrogen and deuterium at fluid densities (9). These studies harshly expose the limitations of the potential, limitations moreover that are emphasised by comparison of the results with those from similar studies using an empirical potential.

The above investigations were in the greater part made on systems at low temperature and high densities. However, there exist in the range of normal temperatures and pressures (298°K., 1 atmos.) several physical situations that invite the application of the cell model. Chief amongst these is gas solubility theory and it is to this topic that the second part of this thesis is devoted.

The solubility of non-polar gases in non-polar solvents has been studied by Hildebrand and co-workers (10-16), resulting in an extensive array of data for a wide range of two component systems. The majority of measurements have been of the solubilities and entropies of solution. Together with these there exists another experimental property, the partial molar volume (expressed as V_2 cc/mole) which represents the expansion of the solution due to the dissolution of the solute. This is essentially a property of the solution as a whole but since these measurements can, to a good approximation, be considered on the basis of infinitely dilute solutions a cell theory which pictures the gas molecule as creating a spherical cavity the size of which is dependent on the partial molar volume is quite defensible.

Available experimental data for partial molar volumes were found to be both limited and incomplete. In order to extend these results, as well as to confirm or disprove several observations made by previous workers we have carried out an experimental determination of the partial molar volumes for twenty four gas-liquid systems. The results

of this project and their interpretation when compared with the data already available is comprehensively presented in the text.

The results of our experiments together with those from other sources are initially investigated by a hard sphere theory first proposed by Smith and Walkley (17) and later refined by Hillier and Walkley to allow for quantum effects (18). Further calculations were then made using the more complete cell theory of Kobatake and Alder (19), which should enable estimates as to the effect of distant neighbours and to the degree of order remaining in the liquid to be made. However, the complications arising in this treatment were substantial and it is doubtful whether the final results can be taken as a satisfactory picture of gas solubility phenomena.

We therefore present this work as a comprehensive investigation of the predicative value of the cell model under varying physical conditions. It should perhaps be stressed that at no time do we forward the model as an absolute theory of the fluid state, but we do claim that it may act as a simple and versatile framework in situations where it has often been rejected or ignored. The authenticity or otherwise of this statement will be ably demonstrated in subsequent chapters.

CHAPTER 1.

The Evolution of the Cell Model

"All the inventions that the world contains
Were not by reason first found out, nor brains
But pass for theirs who had the luck to light
Upon them by mistake or oversight"

Samuel Butler (1612-1680)

1.1 The Liquid State

The obstacles that stand between us and a clearer understanding of the liquid state may be better understood by a consideration of the three discreet phases of matter. To the one side lies the solid state characterised by cohesion, rigidity and regular crystalline structure, to the other the gaseous state, a state of complete molecular disorder. Liquids, however, represent a peculiar compromise between these two extremes, exhibiting forces strong enough to lead to a condensed state but not strong enough to prevent considerable translational energy between the individual molecules.

There seems to be little doubt from experimental evidence that a certain degree of order exists in the liquid. How permanent or substantial this may be is difficult to say. However, it is on the strength of this order that a collection of theories known as lattice theories have been developed.

These lattice theories immediately introduce the model of a distorted crystal in which long range order has been lost. It is well to consider here the basic differences between solids and liquids. The solid consists of molecules without internal degrees of freedom executing small vibrations about their equilibrium positions - "a static structure only slightly blurred by thermal motions..." (20). In the liquid there are

no lattice sites and the instantaneous picture is continually changing. How then can an assumption of order be justified? To answer this we examine the experimental evidence. The most important direct results arise from neutron diffraction or X ray studies. The latter, performed by Eisenstein and Gingrich (21) indicated that a liquid, though lacking the long range order found in the crystal structure, had considerable short range order and possessed intermolecular distances similar to those observed in solids. The experiments of Henshaw (22), in which he studied the scattering of slow neutrons by liquids, confirmed Eisenstein's observations and also indicated that molecular motions in a liquid can approximately be described as vibrations interrupted by occasional jumps. These findings give considerable weight to the picture of Alder and Wainwright (23) who used the methods of molecular dynamics to make extensive calculations of molecular trajectories.

If we accept this picture of a liquid when forming a theoretical model we are forced to ignore occasional jumps from one molecular position to another. Lattice theories essentially do this and, therefore, find their greatest usage in predicting equilibrium rather than transport properties, in which these disregarded jumps are all important.

The calculation and comparison of theoretical equilibrium properties with experimentally measured values is a critical test of liquid state theories that employ the methods of

equilibrium statisitical mechanics. As mentioned previously (see introduction), the use of statistical mechanics of necessity introduces the idea of a model or ideal structure. Starting from this model it should be possible to derive the correct results for the equilibrium properties through a series of direct approximations. This, though theoretically feasible, is almost practically impossible and imposes the condition that any model or ideal structure chosen should be as close as possible to the true liquid structure.

From the strictly statistical viewpoint the two most satisfactory methods used in the problems of liquid theory are those of Monte Carlo and molecular dynamics. They both depend on averaging procedure and follow the trajectories of many molecules moving in large cells. They differ only in their methods of averaging, obtain results by direct numerical techniques and should by all theoretical reasoning yield complete and accurate solutions. They are, however, hamstrung by mathematical complexity, in the frightening number of calculations they involve, and in general their progress is parallel to the increase in power of numerical techniques and the capacity of modern electronic computers.

This leaves us with theories based on a regular lattice structure, the earliest of which was developed between 1936-41 by Eyring and co-workers (24-26). They introduced the "hole theory", which correlates liquid properties through a model of a lattice structure with some sites vacant. Soon after this, Lennard-Jones and Devonshire placed the theory

on a more quantitative basis by introducing assumptions regarding the geometry of distibution of the lattice sites and the size of cell surrounding each site, to which they assumed the molecule confined. This theory is the best known example of a cell model - a theory based on a lattice with all sites occupied.

In the past few years other theories of the liquid state have been forwarded - the tunnel model of Barker (20), amended hole theories (27), worm models (28) and significant structure theories (1). However, we will not dwell on these here but move on to a discussion of intermolecular forces and a more detailed examination of the cell model.

1.2 Intermolecular Forces and the Bi-reciprocal Potential

The successful prediction of any experimental property from a theoretical model depends to a large extent on a clear knowledge of intermolecular forces, irrespective of phase or conditions. In all cases that we investigate the molecules are assumed to be non-polar, chemically saturated and neutral. The forces between these molecules are electrostatic in origin and are ultimately based on Coulomb's law of attraction and repulsion between like and unlike charges. Thus, the force of interaction (F) between two non polar molecules is taken as a function of the separation between the centres. In most instances it is better to investigate the potential energy of interaction, $W(r)$,

rather than the force of interaction, F(r). These two quantities are related, the force being the gradient of the potential function. Hence:-

$$F(r) = -\partial\omega(r)/\partial r \qquad (1.2.1)$$

$$\omega(r) = \int_r^\infty F(r)\,dr \qquad (1.2.2)$$

We may now investigate how this potential energy between molecules varies with the distance between their centres. On close approach their electron clouds overlap and they repel each other strongly. This short range repulsion varies exponentially with the separation but its true form is more complex. At larger intermolecular distances a force of attraction appears to exist. This observation at once poses two problems, i.e. what is the nature of the attractive force and how can the total potential be expressed as a function of the distance between the molecular centres?

As early as 1903 Mie (29) proposed that the interaction energy between two atoms could be expressed in the form of a bi-reciprocal potential, which involved a negative term proportional to the power $-\underline{n}$ of the distance $\underline{r}$ and a positive term proportional ot the power $-\underline{m}$ of $\underline{r}$, $(m>n>0)$. This was termed the "m:n" potential and was written as:-

$$\omega(r) = \lambda_m/r^m - \lambda_n/r^n \qquad (1.2.3)$$

where λ_m, λ_n are constants.

The origin of the repulsive term has been given above, its form in (1.2.3) being justifiable only on the grounds of mathematical convenience. The explanation of the more important attractive term posed more difficult problems.

That it was due to Van der Waals or "dispersion forces" was unquestionable but attaching a theoretical explanation to this proved somewhat complex. Keesom (30) and later Debye (31) theorised that the attraction was due to permanent dipoles, postulating an attractive index of six. These theories, however, failed to explain the case of the inert gas molecules which exhibited considerable attractive forces while possessing no trace of permanent dipoles. Then in 1930 London (32) solved the problem by the application of quantum mechanics. London pictured a neutral molecule as a positive nucleus surrounded by a cloud of negative charge. Although the time average of this charge distribution was spherically symmetrical, at any specific instant it was also somewhat distorted. Thus, an instantaneous picture would reveal an orientated dipole. The time average of these dipoles would be zero but the instantaneous dipole on one molecule would polarise a second molecule, attract the resultant reduced dipole and produce an average attractive force.

This dispersion interaction generally known as dipole-dipole led to the attractive force W_a, being given as:-

$$\omega_a = -\frac{3}{4} h \nu_0 \alpha^2 / r^6 \qquad (1.2.4)$$

where h=Planck's constant, α=polarisability, ν_0=characteristic frequency of oscillation of charge distribution. (For derivation of the above see Ref. 33.)

London also showed that there were further terms in the interaction energy arising from contributions from the

dipole-quadrupole (varying as r^{-8}) and from quadrupole-quadrupole(varying as r^{-10}). These are usually ignored in the simple potential, an omission that may possibly not be fully justified.

On the basis of London's work Lennard-Jones (34) re-adjusted the "m:n" potential that he had used for the argon interaction (38) and produced the potential in the form:-

$$\omega(r) = \lambda_m/r^{12} - \lambda_n/r^6 \qquad (1.2.5)$$

This is the form used extensively in the cell theory. It is, as are most formulae describing the intermolecular potential, essentially empirical, depending on constants that are obtained from the properties of the substance being studied. The graphical form of the "L-J." potential is shown in Fig. 1 and equation (1.2.5) may be written:-

$$\omega(r) = 4\epsilon\left[\left(\sigma/r\right)^{12} - \left(\sigma/r\right)^{6}\right] \qquad (1.2.6)$$

Here σ and ϵ are constants having dimensions of length and energy respectively. We now consider the origin of these constants. On consultation of Fig. 1 we see that they indicate unique values of the potential.

Thus $r=\sigma$ when $W(r)=0$ (1.2.7)

and $W(r)=-\epsilon$ when $dW(r)/dr=0$ (1.2.8)

The values of these parameters or scale factors are determined from the properties of the gas or solid. The second virial coefficient, B(T), or transport properties are the best known sources and tabulated values of σ and ϵ for a variety of molecules have been given (35). Knowledge of the parameters also leads to a law of corresponding states.

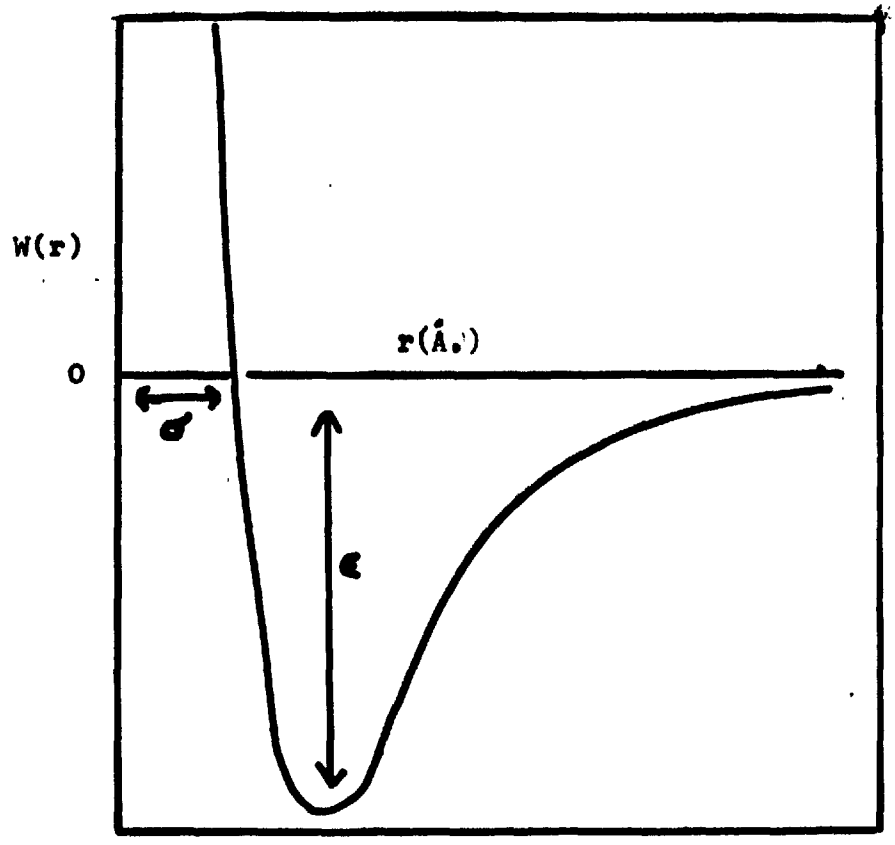

Fig 1.1 Lennard-Jones bi-reciprocal potential.

Potential energy W(r), expressed as a function of the distance r(Å), between the centres of two molecules.

However, a discussion of this and the sensitivity of the parameters to the nature of the potential will be given later. At present it suffices to note that (1.2.6) is the most commonly used form of the bi-reciprocal potential and is generally know as the "Lennard-Jones 12:6".

Having traced the development of the bi-reciprocal potential, we must now consider another basic assumption made in calculations involving intermolecular forces, namely that of pair additivity. This postulates that for an N body system the potential is given by N/2x the pair interaction, summed over all pairs of molecules, viz.

$$W = \frac{1}{2} \sum_{i,j \; i \neq j}^{N} \phi(r_{ij}) \qquad (1.2.9)$$

where W=total potential energy of the system and $\phi(r_{ij})$=potential energy between molecules $\underline{i}$ and $\underline{j}$. The very mode by which London forces are derived indicates that the concept of pair additivity cannot be completely true. Thus, the problem of non-additivity corrections arises and has been of considerable interest since the early calculations on three body forces by Axilrod and Teller (36). There has recently been renewed discussion on the effect of non-additivity on the form of the intermolecular potential (37), and it appears that a satisfactory explanation of certain experimental phenomena demand a consideration of the three body effect. (For further discussion see 3.3).

1.3 The Cell Theory of Lennard-Jones and Devonshire.

In the introduction to their original paper Lennard-Jones and Devonshire stated that their object was "...to find an equation of state and other properties at high concentrations in terms of interatomic forces of a general type...."(2).

In order to develop this equation of state they proceeded to make several basic assumptions, which although mostly intuitive have, from the time they were suggested, only undergone minor improvements(39-42).

These assumptions are:-

(i) The available volume is divided into cells and each molecule is confined to it's cell by nearest neighbours.

(ii) The cells are chosen so that their centres occupy sites on a regular lattice.

(iii) The molecules are regarded as moving independently in their cells

The second assumption is required to relate the distance between cell centres to the density. It is in fact made because no satisfactory alternative is known and immediately imposes the concept of long range order, so typical of the solid and so unwanted in any fluid theory.

We now digress for a moment into statistical mechanics and consider a system of N molecules, of mass m, occupying a volume V. The partition function for this system may be

written as -

$$Z = \lambda^{-3N} Q \qquad (1.3.1)$$

where $\lambda = (2\pi mkT/h^2)^{-\frac{1}{2}}$

and Q, the configurational integral is given by -

$$Q(N,V,T) = \frac{1}{N!} \int \cdots \int \exp\left(\frac{-w}{kT}\right) dx_1 \cdots dz_n \qquad (1.3.2)$$

The third assumption in the L.J. theory is needed to make the evaluation of the integral(1.3.2) practicable. It does this by approximating the potential energy(W) of the system as the sum of terms each depending on the position of one molecule.This assumption which is essentially that made in the Einstein model of a solid enables us to write

$$w = w(0) + \sum_i [\varphi(r_i) - \varphi(0)] \qquad (1.3.3)$$

where W(0) is the energy when all molecules are at the centres of their cells and $\varphi(r_i) - \varphi(0)$ is the change in potential energy when a molecule i is displaced from the cell centre by a vector r_i .

The configurational integral Q, may now be written as

$$Q(N,V,T) = 1/N! \sum' \exp\left[-w(0)/kT\right] v_f^N \qquad (1.3.4)$$

$$= \exp\left[-w(0)/kT\right] v_f^N \qquad (1.3.5)$$

where the summation is taken over all arrangements of molecules with one in each cell.

We introduce at this point the free volume term v_f, which is the volume available to the centre of a molecule in it's cage. It is defined as-

$$v_f = \int_{cell} \exp\left\{-\left[\varphi(r_i) - \varphi(0)\right]/kT\right\} dr_i \qquad (1.3.6)$$

The integration for (1.3.6) is taken throughout the interior of a cell who's volume is equal to the volume per molecule. The lattice of cell centres is chosen on energy considerations, the lattice with the most stable structure(i.e. the lowest free energy) being the one normally adopted

The partition function (1.3.1) may now be written as-

$$Z = \lambda^{-3N} v_f^N \exp[-\omega(0)/kT] \qquad (1.3.7)$$

At low densities this equation may be simplified and an inherent difficulty of the cell theory exposed. Hence within this low density limit

$$\varphi(r) \to 0, \quad v_f \to (V/N)$$

and
$$Z = \lambda^{-3N}(V/N)^N. \qquad (1.3.8)$$

which differs from the partition function for a perfect gas by a factor of e^N. This extra factor gives rise to an additional contribution Nk to the entropy and is known as the "communal entropy"(24-26), since it arises from sharing the volume. Erying and later Lennard-Jones and Devonshire suggested that this extra e^N should be included in the partition function, but recent work by Alder (43) indicates that it appears more gradually.

We may now consider each molecule in it's cell moving in a field defined by $[\varphi(r) - \varphi(0)]$. If the potential energy function W(r) for the interaction of pairs of molecules is known this cell field may be calculated. To simplify this calculation it is assumed that the number of nearest neighbours Z, are uniformly smeared over the face of a spherical surface, radius $\underline{a}$, (equal to the nearest neighbour

distance), further neighbours being smeared over concentric shells. Over this surface nearest neighbours take up all positions with equal probability and $\varphi(r)$, is the field of surrounding molecules averaged over all directions. In the next section this procedure is described explicitly.

1.4 The Calculation of the Cell Potential.

The calculation of the sphericalised field involves the cell geometry as shown in Fig 1.2. Initially we will consider only one shell of neighbours and hence -

$$\text{Area of annulus } A = 2\pi a^2 \operatorname{Sin}\theta \, d\theta \qquad (1.4.1)$$

It contains a fraction of smoothed neighbours N, where

$$N = Z/2 \operatorname{Sin}\theta \, d\theta. \qquad (1.4.2)$$

with Z = Number of neighbours in first shell.

Thus the potential at a distance $\underline{r}$ from cell centre is given by-

$$\varphi(r) = \int_0^{\pi} \omega(R) \frac{Z}{2} \operatorname{Sin}\theta \, d\theta \qquad (1.4.3)$$

W(R) being a potential of the m:n type

i.e. $$\omega(R) = K\epsilon \left\{ (\sigma/R)^m - (\sigma/R)^n \right\} \qquad (1.4.4)$$

where K is a constant depending on $\underline{m}$ and $\underline{n}$.

But from Fig (1.2)

$$R^2 = a^2 + r^2 - 2ar\operatorname{Cos}\theta.$$

and $2R.dR = 2ar\operatorname{Sin}\theta.d\theta$. From which (1.4.3) may be rewritten as

$$\varphi(r) = \int_{a-r}^{a+r} K\epsilon \left[(\sigma/R)^m - (\sigma/R)^n \right] \frac{Z}{2ar} . R \, dR. \qquad (1.4.5)$$

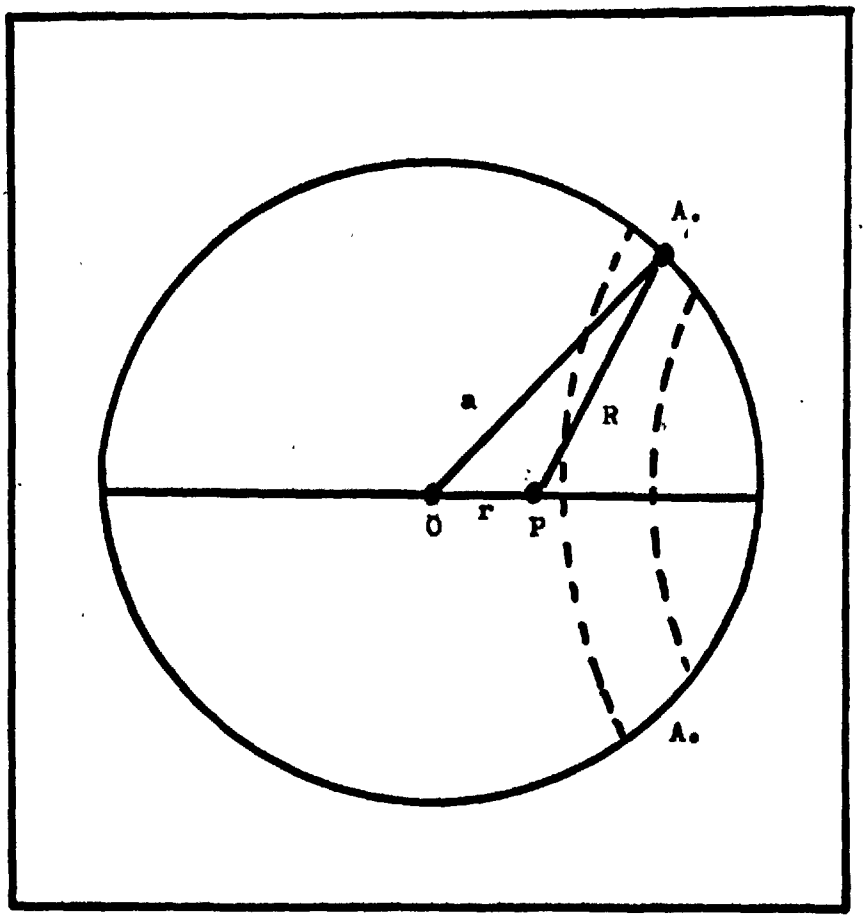

Fig 1.2 Cell geometry in the Lennard-Jones and Devonshire model.

now $$\int_{a-r}^{a+r} \omega(R)\, dR = -\int_{a+r}^{a-r} \omega(R)\, dR$$

$$= \left[\frac{\sigma^m}{m-2}\left\{\frac{1}{(a-r)^{m-2}} - \frac{1}{(a+r)^{m-2}}\right\} + \frac{\sigma^n}{n-2}\left\{\frac{1}{(a+r)^{n-2}} - \frac{1}{(a-r)^{n-2}}\right\}\right] \quad (1.4.6)$$

For a 12:6 potential m= 12, n= 6, K= 4, and $\varphi(r)$ becomes-

$$\varphi(r) = Z\epsilon\left[\frac{\sigma^{12}}{5ar}\left\{\frac{1}{(a-r)^{10}} - \frac{1}{(a+r)^{10}}\right\} + \frac{\sigma^6}{2ar}\left\{\frac{1}{(a+r)^4} - \frac{1}{(a-r)^4}\right\}\right] \quad (1.4.7)$$

Similarly the potential at the cell centre is given by

$$\varphi(o) = 4\epsilon\left[(\sigma/R)^{12} - (\sigma/R)^6\right] \quad (1.4.8)$$

and the total cell potential may be written as-

$$\varphi(r) - \varphi(o) = Z\epsilon\left[\left(\frac{\sigma^{12}}{5ar}\left\{\frac{1}{(a-r)^{10}} - \frac{1}{(a+r)^{10}}\right\} - \frac{4}{a^{12}}\right) + \left(\frac{\sigma^6}{2ar}\left\{\frac{1}{(a+r)^4} - \frac{1}{(a-r)^4}\right\} - \frac{4}{a^6}\right)\right] \quad (1.4.9)$$

This is the cell potential due to the first shell of neighbours at a distance $\underline{a}$. It may now be generalised for $\underline{j}$ shells, each containing Z_j molecules at a distance a_j i.e. $\varphi(r) - \varphi(o) =$

$$Z_j\epsilon\left[\left(\frac{\sigma^{12}}{5a_jr}\left\{\frac{1}{(a_j-r)^{10}} - \frac{1}{(a_j+r)^{10}}\right\} - \frac{4}{a_j^{12}}\right) + \left(\frac{\sigma^6}{2a_jr}\left\{\frac{1}{(a_j+r)^4} - \frac{1}{(a_j-r)^4}\right\} - \frac{4}{a_j^6}\right)\right] \quad (1.4.10)$$

The form of (1.4.10) may now be expanded and simplified as has been done by other workers(40).

Thus if we define $y = (r/a)^2$, assume from the lattice concept $a^3/2^{\frac{1}{2}} = V/N$ and introduce $V_o = N\sigma^3$ then (1.4.10) may be expanded to give-

$$\varphi(r) - \varphi(o) = Z_1\left[(V_o/V)^4 L(y) - 2(V_o/V)^2 M(y)\right] \quad (1.4.11)$$

where Z_1, is the number of neighbours in the first shell and from the assumption of a face centered cubic lattice $Z_1 = 12$. L(y) and M(y) are therefore written as-

$$L(y) = \sum_j Z_j/Z_1 (a_1/a_j)^{12}\, l(ya_1^2/a_j^2) \quad (1.4.12)$$

$$M(y) = \sum_j Z_j/Z_i (a_1/a_j)^6\, m(ya_1^2/a_j^2) \quad (1.4.13)$$

with $l(y) = \left(1 + 12y + 25.2y^2 + 12y^3 + y^4 \right)(1-y)^{-10} - 1$ (1.4.14)

$$m(y) = (1 + y)(1 - y)^{-4} - 1 \qquad (1.4.15)$$

Equations (1.4.12) and (1.4.13) may also be written as

$$L(y) = l(y) + \frac{1}{128} l(y/2) + \frac{2}{729} l(y/3) \ldots . \qquad (1.4.16)$$

$$M(y) = m(y) + \frac{1}{16} m(y/2) + \frac{2}{27} m(y/3) \ldots . \qquad (1.4.17)$$

In their original treatment Lennard-Jones and Devonshire considered only the first shell of neighbouring molecules and therefore neglected the second and third terms in (1.4.16) and (1.4.17) which result from taking the second and third shells containing 6 and 24 molecules, at a distance of $\underline{2^{\frac{1}{2}}a}$ and $\underline{3^{\frac{1}{2}}a}$ respectively, into consideration. This technique has been extensively employed by Wentorf et al(40).

The cell potential may be readily evaluated from the above equations. To calculate the partition function we must evaluate the free volume, which involves integration over the cell. Lennard-Jones and Devonshire arbitarily took this cell to be a sphere of radius $0.5a_1$. Wentorf et al(40) used a sphere of radius $0.55267\, a_1$, since the volume of this sphere is equal to the volume per molecule. Using this value the free volume is given as-

$$v_f = 2\pi a_1^3 G. \qquad (1.4.18)$$

$$= 2 \times 2^{\frac{1}{2}} \pi (V/N) G. \qquad (1.4.19)$$

where $$G = \int_0^{y_m} y^{\frac{1}{2}} \exp\left\{ -\left[\varphi(r) - \varphi(0)/kT \right] \right\} dy \qquad (1.4.20)$$

and $$y_m = \left(3/4\pi 2^{\frac{1}{2}} \right)^{\frac{2}{3}} = 0.30544.$$

The partition function-

$$Z = \lambda^{3N} . v_f^{\,N} . \exp(-NW(0)/kT) \qquad (1.4.21)$$

may now be developed to give the equation of state for the system.

$$\frac{PV}{NkT} = \left\{1 - \frac{12\epsilon}{kT}\left[2.4090\left(V_0/V\right)^2 - 2.0219\left(V_0/V\right)^4\right] - \frac{48\epsilon}{kT}\left[\left(\frac{V_0}{V}\right)^2 \frac{g_4}{G} - \left(\frac{V_0}{V}\right)^4 \frac{g_2}{G}\right]\right\} \quad (1.4.22)$$

where

$$g_n = \int_0^{0.30544} y^{1/2} L(y) \exp\left\{-\left[\varphi(r) - \varphi(0)/kT\right]\right\} dy \quad (1.4.23)$$

and

$$g_2 = \int_0^{0.30544} y^{1/2} M(y) \exp\left\{-\left[\varphi(r) - \varphi(0)/kT\right]\right\} dy \quad (1.4.24)$$

both integrals, as is G, are evaluated by numerical integration and have been tabulated by Wentorf et al(40) and by Fickett and Wood(44).

The equation of state (1.4.22) is for a L.J. & D. potential considering the first three shells of neighbours. It includes the static lattice term W(0), which is the potential energy when all molecules are at their lattice sites. This can be evaluated by a lattice summation. Hence-

$$W(0) = \frac{N}{2} \sum_{j=1}^{\infty} Z_j \, W(a_j) \quad (1.4.25)$$

which was given by Lennard-Jones and Ingram(207) as

$$W(0) = 6N\epsilon\left(1.0109\left(V_0/V\right)^4 - 2.4090\left(V_0/V\right)^2\right) \quad (1.4.26)$$

Having evaluated the mean potential in the cell by sphericalisation it is of interest to consider the nature of this field for cells of various sizes(i.e. differing values of V_0/V). This has been done by Hirschfelder, after the results of Lennard-Jones and Devonshire(35) and also by Prigogine(45).

In Fig (1.3a) the potential is uniform within the cell except for a region of low potential near the edge. The

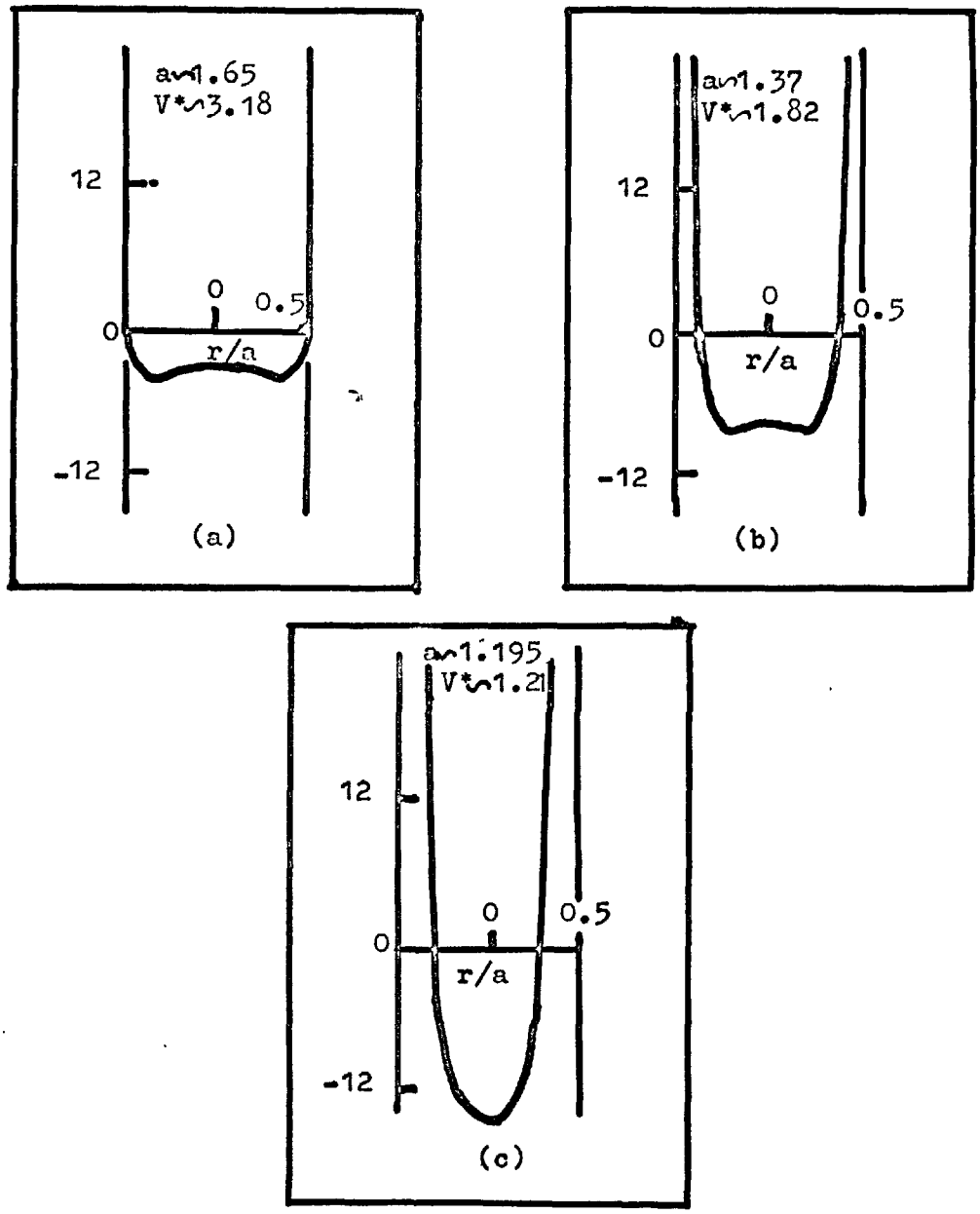

Fig. 1.3 Potential field within a cell for various cell sizes, after (2).

molecule is in fact "adsorbed" at the cell walls and the model becomes less justifiable since the ground state of the system no longer corresponds to a regular arrangement of the molecules. Fig (1.3b) represents the situation at liquid densities, the potential regions overlap and an energy barrier is formed between them. Finally in the region of normal crystal densities the energy barrier disappears and the potential assumes a parabolic shape as in Fig (1.3c). Further increase in density only serves to raise the minimum of this curve and it is in these situations that approximations based on a harmonic oscillator approach have their greatest appeal(45).

We have shown in (1.4.21) that once the potential is known the partition function may be evaluated and hence the thermodynamic properties of the system under study at once calculated. Most treatments of cell theory results employ reduced variables to express their equations of state, thermodynamic properties etc. and it would be as well to define these here. In the present treatment the reduction parameters are those of the L.J. cell theory i.e. ϵ and σ which are used to give -

$T^* = kT/\epsilon$, reduced temperature: $a^* = a/\sigma$, reduced neighbour dist.

$V^* = V/\sigma^3$ " volume : $r^* = r/\sigma$ " distance.

$v_f^* = v_f/\sigma$ " free volume: $p^* = p\sigma^3/\epsilon$ " pressure.

Using the above (1.4.22) may be written as-

$$\frac{PV}{NkT} = \left\{1 - \frac{12}{T^*}\left[\frac{2.4090}{V^{*2}} - \frac{2.0219}{V^{*4}}\right] - \frac{48}{T^*}\left[\frac{1}{V^{*2}G}g_m - \frac{1}{V^{*4}G}g_1\right]\right\} \qquad (1.4.27)$$

The expressions for the free energy etc. may be similarly formulated and hence with a knowledge of the appropriate integrals the thermodynamic properties evaluated over a range of V^* and T^*.

The results obtained, their correspondence to observed experimental data and suggested improvements to the theory will be discussed in the next chapter.

CHAPTER 2.

The failure of the Cell Theory at fluid densities.

"Seek simplicity and distrust it"

Alfred North Whitehead (1861-1946)

"And differing judgements serve but to declare
The truth lies somewhere- if we knew but where!"

William Cowper (1731-1800)

2.1 The Comparison of Experimental and Theoretical Results

The most extensive theoretical calculations on the Lennard-Jones theory are those in which Wentorf et al(40) considered the interaction of the wandering molecule with the first three shells of neighbours. In addition to the energy and entropy they presented both graphically and tabularly values of the reduced pressure over a wide range of reduced volumes for differing T*. The compressibility term, PV/NkT, was also given in a similar manner.

From these results it was possible to calculate a set of reduced critical constants, the critical point being defined as that where $(dP/dV)_T$ and $(d^2P/dV^2)_T$ vanish. These were found by the interpolation of tabular values and are presented in Table (2.1) together with the experimental values for argon reduced by the appropriate L.J. parameters.(Ref 35, Table 1A.)

Table 2.1 Reduced critical constants for argon(Theoretical and Experimental values.)

Source	T_c^*	V_c^*	P_c^*	P_cV_c/kT_c
L.J. &D.theory	1.30	1.77	0.434	0.591
Argon(expt.)	1.26	3.16	0.116	0.291

(Table from Ref 20, p61.)

From the above table it is immediately seen that although the calculated and experimental values of T_c^* are in good agreement the other quantities differ substantially. Prigogine and Garikian(41) showed that this agreement is relatively insensitive to the form of the potential. They

concluded that the model therefore needs considerable refinement in the critical region, where the density is too low to exclude all configurations besides those corresponding to one particle per cell.

A further comparison of theoretical and experimental data (20,45) for other substances underlines the fact that the theory is most satisfactory at low temperatures and high densities. Under such conditions the molecules are almost restricted to motions in their cells. At the other physical extreme i.e. at low densities and high temperatures, the substantially increased molecular motion makes the application of a cell theory less plausible.

This discrepancy between theoretical and experimental results at fluid densities led De Boer(46) to suggest an alteration in the number of nearest neighbours from 12 to 10. This idea is in some degree supported by experimental evidence(21) and employing a "hole" theory(24) can be easily incorporated into the calculations. On a strict lattice model however, no regular structures with Z_1 between 12 and 8 exist. De Boer avoided this difficulty by adjusting the values of his lattice parameter. The validity of such a step is highly dubious. Anomalies also exist regarding free energies and it is generally considered that the concept of decreasing the co-ordination number is not satisfactory.

A comprehensive comparison of the experimental properties of argon, against those calculated from the L.J. & D. theory has been given by Barker(20). In particular he

examined the properties of the theoretical condensed phase, comparing them with data from the solid and liquid state.

Table 2.2 Condensed phase compared with solid and liquid argon at the triple point($kT/\epsilon = 0.7$)

Source	V^*	E^{*a}	S^{*a}	C_v^{*a}
L.J.D. theory	1.037	-7.32	-5.51	1.11
Sld. argon[b]	1.035	-7.14	-5.33	1.41
Lqd. argon[b]	1.086	-5.96	-3.64	0.85

a. Properties expressed as excess quantities i.e. theoretical values in excess of an ideal gas.

b. Experimental properties

(Table from Ref 20,p57.)

The calculated values of the above properties are clearly closer to solid rather than liquid values and these observations are supported by a comparison of theory with Monte Carlo data(47). Pressures and energies from the L.J.D. model are in good agreement with Monte Carlo results on the solid side of the "freezing" transition but not on the compressed gas side. This comparison is thought to be particularly convincing, since Monte Carlo calculations employ the same concept of addivity as the L.J.D. model and it does not appear that any discrepancy may be attributed to this.

In the light of relations between experimental and predicted data, the high density results of the L.J.D. theory appear to describe the solid state. The low density situation must be regarded as a hypothetical ordered structure

which may be thought of as an "expanded solid" which is metastable with respect to a true gas, the latter having a lower free energy. The phase transition predicted by the theory is therefore neither a solid-gas nor a liquid-gas transition but rather a hypothetical transition from the condensed phase to the phase of the hypothetical expanded solid

The clear-cut failure of the cell theory to describe liquid phenomena may be traced to the assumptions from which it is developed. There have been several attempts to improve these, a comprehensive account of which is given elsewhere(20). We will briefly describe these attempts and comment on their relative success.

2.2 Improvements on the L.J. & D. Theory.

The major defects of the cell theoty lie in the smearing approximation which sphericalises the cell, in the incorrect calculation of the communal entropy- resulting from the postulate of one molecule per cell and the neglect of correlations between the molecules in their cells.

An early estimation as to the accuracy of the smearing approximation was carried out by Beuhler et al (48) for rigid spherical molecules on a face centered cubic lattice. The correction involves a straightfoward

numerical integration over the duodecahedral cell (the true cell that the molecule sits in formed by planes bisecting the distances from the neighbouring molecules to the origin). The correct free volumes were found to be 50% larger than the smeared free volumes. The cause of this difference is that the potential energy is averaged over the surface of a sphere and the term $\exp(-W_{av}/kT)$ formed whereas the correct procedure would be to average $\exp(-W/kT)$ itself.

The exact treatment for the 12:6 potential was given by Barker (50) who expanded the potential energy as a power series. At high densities and low temperatures the free volume is primarily determined from a harmonic oscillator model and as a result of lattice symmetry it can be shown that the change in the potential energy is proportional to r^2 (where $\underline{r}$ is the distance from the cell centre). The exact and smeared cell fields were found to be identical as far as the quadratic terms were concerned and thus the error due to smearing tends to zero with increasing density. At lower densities the ratio $v_f(\text{correct})/v_f(\text{smeared}) = 1.4$, but this may be easily corrected for.

The effect of correlated motions was studied, chiefly on account of computational difficulties, by an estimate of the effect of only binary correlations (50). However, it was found that an allowance for binary correlations corrects for the major part (75% - 85% for the harmonic force model), of the error due to independent motions - an

error that is itself rather small. Barker (20) performed these calculations by obtaining the correction Δ_{ij} which gives the difference between the **true** potential energy and the approximate potential energy for fixed neighbours. He expanded the expression

$$f_{ij} = \exp(-\Delta_{ij}/kT) - 1.$$

in a manner analogous to that used in imperfect gases (35) and found that at low temperatures the effect of these corrections appeared to improve the predictions of the cell model. At higher temperatures the agreement is not as good but the correction is considered adequate to account for correlations over the density range studied.

The last assumption, that of single occupency is more difficult to improve . Approximate corrections for the communal entropy were made by Pople (52) and by Jannsens and Prigogine (53) who estimated the possibilty of finding two molecules in a cell. The calculations were performed under the assumption that there was no correlation between the number of molecules in neighbouring cells. Although this is justified for a solid at high densities where there are few multiple occupied cells and for a gas at low densities where the cells are large and independent it's validity in the range of liquid densities is questionable.

The conclusion of these workers, that the effect of double occupation was negligable at densities as high as the liquid density at the triple point was not accepted. Calculations were made for a 12:6 fluid in the range of the critical density by Barker (49-51), who concluded that the

contribution of double occupency to the communal entropy was present even at liquid densities. His results also emphesised the difficulties of estimating the communal free energy at low densities and it was concluded that the approximations on which the work of Pople etc. were based would drastically underestimate the effect of multiple occupation in the fluid region.

From the above discussion it can be seen that while many of the fundimental faults of the cell model may be allowed for, the final product still does not yield a satisfactory description of the fluid state. Barker considers the main problem remaining to be that of evaluating the communal free energy, this would appear to necessitate calculations at liquid densities around the triple point, calculations that would involve the correlated motions of more than three molecules. However, any treatment of this type introduces severe mathematical problems that, within the framework of the present theory, are almost intractable.

If we acknowledge the failure of the detailed cell model, as given above, we are left with the conclusion that ideally the L.J. theory must describe a solid. At solid densities most of the corrections we have described have a low order of magnitude and considered from the viewpoint of mathematical expediency may, to a good approximation, be neglected.

The conclusion that the cell model is more valid in the solid state was in fact indicated by the later work of

Lennard-Jones and Devonshire (54-55) who introduced the order-disorder theory of melting in an effort to explain the difference between the solid and liquid phases.

In spite of it's limitations the cell theory should therefore give a reasonable description of the solid state especially of the simple inert gas solids. This of course assumes the validity of the basic concepts of the Lennard-Jones theory and in particular that of the bi-reciprocal potential normally employed. Doubts have been cast on the authenticity of this form, even with regard to the most elementary of systems and on this account we now propose to examine the form of the intermolecular potential in closer detail

CHAPTER 3.

The Intermolecular Potential.

"Matter exists only as attraction and repulsion
Attraction and repulsion are matter!"

Edgar Allan Poe (1809-1849)

3.1 Simple Potentials.

To date we have assumed the intermolecular interaction to be of the form shown in Fig (1.1) and to be mathematically described through the introduction of parameters of energy ϵ and distance $\underline{\sigma}$ so -

$$W(r) = \epsilon f(\sigma/r) \qquad (3.1.1)$$

where $\underline{f}$ is some universal function.

Furthermore it has been assumed that the function $\underline{f}$ is adequately described by the L.J. 12:6 potential, so that we are immediately able to introduce a law of corresponding states utilising the reduced variables given in (1.4).

Now while the general form of the potential is almost universally acknowledged, the mathematical representation of $\underline{f}$ in (3.1.1) is far from being completely and uniquely determined-even for the simplest of molecular systems, i.e. the solid phase of the inert gases. To test any theoretical potential it is essential to have a wide range of accurate experimental data to serve as a comparison with theoretical results. The inert gases, though a good theoretical medium , do not lend themselves easily to experimental measurements, most of which require extreme physical conditions. However over recent years many of these difficulties have been mastered and a wealth of experimental data, especially for argon, has been produced. These results have been admirably reviewed by Dobbs and Jones (56) for argon alone, and more recently by Pollack (58) and Boato (57)

for all inert gases except helium, while Hollis Hallet (59) has produced a comprehensive discussion and compilation of physical properties. Thus several hitherto unsolved problems may be considered in greater detail and especially whether even the simple Ar-Ar interaction can be adequately described by the L.J. potential.

The construction of almost any intermolecular potential involves a sample function containing several parameters which are fixed from the thermodynamic properties. Having set up the potential in this manner, it's ability to give a good description of the system under study is tested by using it to predict other experimentally known properties.

With regard to the inert gas solids, the properties generally used are the crystal lattice spacing (a_o) and the heat of sublimation (L_o) both at $0^oK.$, or gas phase properties,,such as second virial coefficients B(T) and transport data. If one is interested in the general description of the Ar-Ar interaction certain points immediately arise. The second virial coefficient, the first correction for non ideality in the gas phase, is essentially a two body property, being the result of two body interactions. The crystal properties at $0^oK.$ are by definition multi-particle properties. In view of this several workers have stated (60-63) that the pair potential parameters must be determined from properties dependent only on binary interactions and on these grounds, solid state data , reflecting the many body problem is unacceptable. The author, however shares

the view of Pollack (58) that parameters for solid state work should wherever possible be obtained from solid state data. The test of this surmise will come later in this text (4.4,4.6).

Returning to the determination of the potential parameters from second virial coefficients, it is as well to investigate the sensitivity of various parts of the potential curve. The limiting behaviour of B(T) at low temperatures in a classical system is determined by the shape and depth of W(r) near its minimum. This minimum occurs at a distance r_o, where for the L.J. 12:6, $r_o = 2^{1/6}\sigma$ (easily obtained from the first derivative of the potential). However, the low temperature limit is difficult to approach and its relation to the potential is complicated by quantum effects. The high temperature limit is determined by the details of molecular collisions which in turn shape the repulsive part of the potential.

Using accurate second virial data it is an easy matter to estimate $\underline{\epsilon}$ and $\underline{\sigma}$ (65). However, it has become abundently clear that not only is it often impossible to evaluate a unique set of $\underline{\epsilon}$ and $\underline{\sigma}$ to fit over the temperature range studied, but that parameters derived from one set of properties appear to predict other properties only fairly. The inability to find unique values for $\underline{\epsilon}$ and $\underline{\sigma}$ was ably demonstrated by the results of Halsey and Fender(64) and Stavely(66) and it has further been shown by Munn (62) that by considering wells of different shapes, a large number of potentials will fit second virial coefficient data.

With regard to other experimental properties which may be used for the determination of parameters it is noted that $\underline{a}_o$ is most sensitive to the form of the potential around the minimum, (the portion that controls lattice vibrations) while the sublimation energy (L_o) depends on the portion of the potential from the minimum out to large separations.

It therefore appears that the introduction of a two parameter law of interaction imposes an unnatural constraint on the potential. It has already been mentioned that the assumption of the repulsive term as $1/r^{12}$ was purely arbitrary (1.2) and that a more logical step would be to express this part of the potential in the form of an exponential. However, although earlier workers, including Corner (67) investigated potentials of this type, the most widely used form is that given by Kihara and Koba (68) and known as the "exp-6". This is written as-

$$W(r) = \frac{W_o}{\alpha - 6}\left(6\exp\alpha\left(1 - \frac{r}{r_o}\right) - \alpha(r_o/r)^6\right) \qquad (3.1.2)$$

where α = parameter controlling narrowness of bowl.

r_o = position of the minimum.

The above form, although quantum mechanically more reasonable than that of the L.J. at once introduces serious mathematical complexities. It has been investigated by Mason and Rice (69) who like Corner found their parameters by fitting crystal properties at 0^oK. However, their calculations of crystal data were only slightly better than those obtained by using a L.J. potential.

An extension of (3.1.2) was introduced in the four parameter Buckingham Corner exp-6 potential (70), which includes a correction in the attractive part of the potential. This correction is in the form of a dipole-quadrupole term (r^{-8}) which is added to the normal dipole-dipole(r^{-6}). It also introduces an extra parameter β which is the dimensionless ratio of the coefficients of the attractive terms and may be determined either from quantum mechanics or experiment.

Like those using (3.1.2), calculations involving the Buckingham-Corner potential have been made, but no significant improvement over the simpler potentials in fitting properties has been reported. Consequently there does not appear to be much gained by abandoning the bi-reciprocal potential in favour of either of the above. However, it should be stated that due to the complexities in the sphericalisation process etc., no reports have been given for a cell model employing an exponential repulsion. Such calculations are at present being performed in these laboratories and until their results are available it would be as well to reserve judgement.(71)

3.2 Multi-term Potentials.

In view of the apparent failure to produce a uniquely successful and moreover a general mathematical form for the potential, attempts were made by several authors to determine

the correct expression by utilisation of all available experimental data. The earliest work in this direction was by Rice (72-74) but he was hampered by a dearth of available experimental results. Further investigations of a similar nature were performed by Corner (67) using a L.J. n:n potential but it was not until Dobbs and Jones (56) published precise measurements for the density of solid argon that it was possible for any comprehensive treatment to be fowarded. These results were utilised by Guggenheim and McGlashan (75) who introduced a two piece intermolecular potential for the Ar-Ar interaction, a potential that involved six parameters. This potential has recently been extended by McGlashan (61) but in the present context it is perhaps better to concentrate on the origional equation that has provoked much comment and discussion.

The potential may be expressed (after Rice(72)) as

$$W(r) = -\epsilon + K\left(\frac{r-r_0}{r_0}\right)^2 - \alpha\left(\frac{r-r_0}{r_0}\right)^3 + \beta\left(\frac{r-r_0}{r_0}\right)^4 \qquad (3.2.1)$$

for $\underline{r}$ in the neighbourhood of r_o and

$$W(r) = -\lambda r_o^6/r^6 \qquad r \geqslant 1.40\ r_o \qquad (3.2.2)$$

The parameters in (3.2.1) and (3.2.2) are mostly determined from colid state data and are such that ϵ and r_o denote, as usual the energy and separation of the minimum. K describes the curvature of this minimum and α the rate of change of curvature there. The parameter β is related to the anharmonicity, a phenomenon present in argon even at lowest temperatures and having its origins in the non negligable zero point vibrations.

The factor λ which is found in the attractive part was determined a priori from the theory of dispersion forces, though it may also be obtained from experimental data. A unique determination of the parameters of this potential using only solid state equilibrium data was found to be impossible and this led to the introduction of a sixth parameter σ such that $W(r) = 0$, where $r = \sigma$. This distance, essentially a hard core repulsion, was estimated from the results of gas viscosity measurements.

Thus, having introduced their six parameters Guggenheim and McGlashan (henceforth G. and Mc.) then assumed $0 < \beta < \alpha$ which effectively ignored anharmonicity. The importance of anharmonicity for the potential was given by $\beta - \alpha$, and the assumption that this term was zero was equivalent to neglecting molecular correlations and implying only a single Einstein frequency. The justification for this step lay in the surmise that since the theoretical minimum of the potential was ill defined it would be satisfactory to assume a shape that made anharmonicity unimportant. It also ensured that the first order perturbation theory employed in the calculations was still permissible since large values of β would invalidate treatments involving this technique. McGlashan in his extension to the theory allowed for anharmonicity and found a best fit of experimental data with $\beta/\alpha = 1.25$. However, he states that the original assumption of $\beta/\alpha = 1.0$ did not appreciably effect the accuracy of the previous results.

To test their equation G. and Mc.,used it to make theoretical predictions of the temperature dependent properties of solid argon. These results were compared with those predicted using a 12:6 potential with or without anharmonicity corrections, from the lattice dynamical equations first proposed by Domb and Zucker (76)and later extended by Zucker (77). For second virials both potentials, as might be expected, give similar predictions but for the temperature dependence of entropy, energy and lattice constant the potential of G. and Mc. appeared to possess marked superiority.

Thus, on first impressions this potential is to a greater degree more successful than any of the simpler forms discussed previously. It would therefore be as well to make a careful examination of this potential and initially of its graphical shape as shown in Fig (3.1), where it is compared with the form of the L.J. 12:6. Several points are immediately noticable;the greater well depth and wider bowl for the G. and Mc. potential and also the complete absence of any repulsive (short range) section of the potential apart from the hard core $\underline{\sigma}$. This latter factor together with the other observed discontinuity are noticable failings. The lack of any continual representation of the repulsive term results in the failure to predict high temperature second virials (78) but while this cannot be treated as a serious fault the piecewise nature of the potential certainly is. Thus, certain sections of the curve must be constructed free hand (as above) or remain

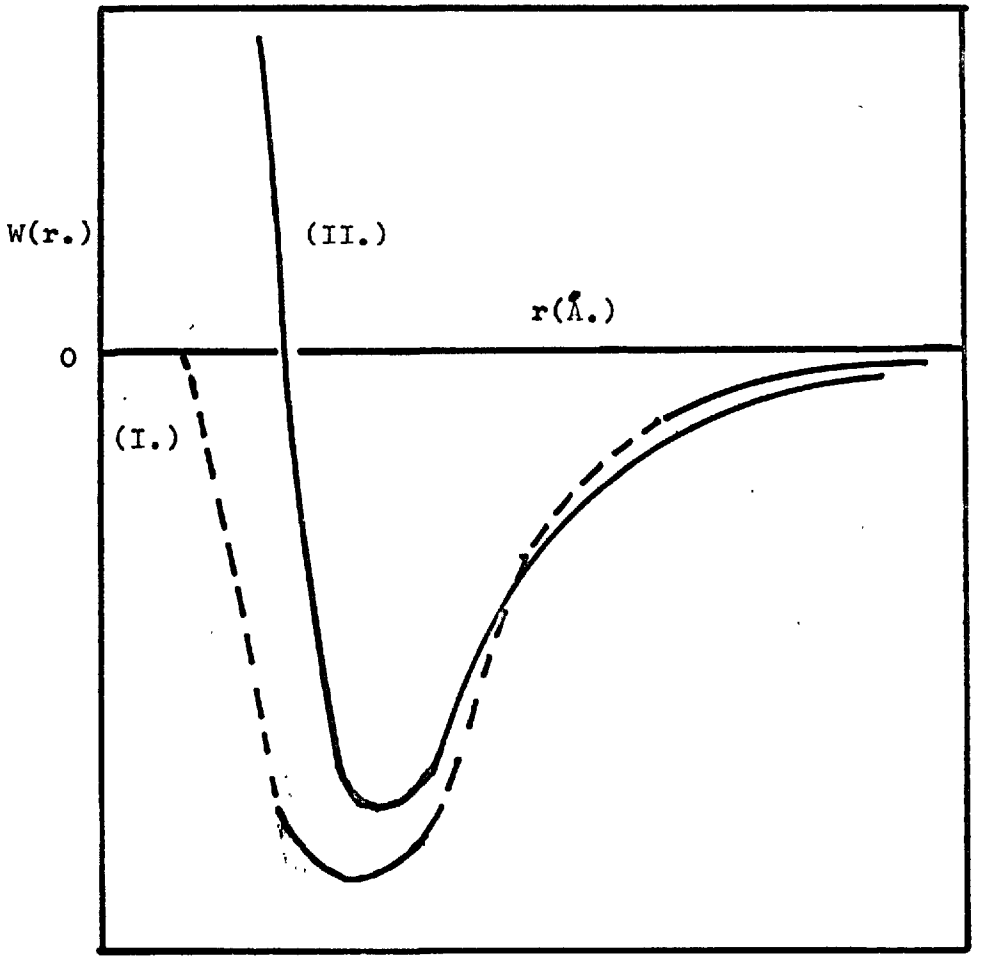

Fig 3.1 The potential of Guggenheim and McGlashan(I.) -(75.), for the Ar-Ar interaction compared with that of Lennard-Jones (II.)

hypothetical. It has been claimed that the attractive discontinuity is not critical. This conclusion, however, is open to discussion. The fact that the potential gives good agreement for many Ar-Ar temperature dependent properties is not too surprising, for by the use of so much experimental data to fit the parameters the curve itself is "tailored" to fit the model. Thus, Zucker (79) considers the above agreement to be expected and suggests that in the determination of potential functions from solid state data, volume dependent properties such as isotherms or bulk modulus should be used, these being insensitive to the model but sensitive to the potential.

Other criticisms have been leveled against this potential. Rowlinson finds that it does not give reasonable agreement with viscosity data (37), while both Rowlinson (37) and Munn (62) consider that the use of so many experimental properties involving multi-body interactions ensure that it cannot be the true pair potential, and hence yield little information regarding the importance of three body forces.

However the greatest criticism of the G. and Mc. potential must be its non-analytical nature. It also demands a detailed and exact knowledge of experimental data and in its final form can only be regarded as strictly valid for argon alone. There have been attempts to extend this approach to situations which lack the comprehensive data found for argon. Other inert gases were studied employing a corresponding states approach (80) and using

rather gross approximations. The results were claimed to be reasonable but serious discrepencies are observed especially in the predictions for the temperature dependence of the molar volume of xenon and krypton while in the case of neon the method fails completely.

The arguements against the G. and Mc. potential stressed above, i.e. discontinuity and multi-parameter nature are partially satisfied by the five term potential recently fowarded by Smith, Dymond and Rigby (60). This is expressed as-

$$W(r)=\epsilon(0.331(R_m/R)^{28}-1.7584(R_m/R)^{24}+2.07151(R_m/R)^{18} -1.74552(R_m/R)^{8}-0.39959(R_m/R)^{6}) \quad (3.2.3)$$

where R_m= the separation at the minimum.

The potential is continuous and involves two parameters only, these being derived from second virial data. It appears to interpret certain gas phase and solid state data to a high degree of accuracy and lends itself readily to calculations involving non-additivity (see 3.3). It is however substantially empirical. Its authors admit that the five coefficients of the powers of R, obtained from a machine fit, cannot be meaningful, while the attractive term in R^{-24} has no theoretical basis and is included for the sole reason of giving a broad bowl to the potential. However, it would not be justifiable for an account such as this, which defends the L.J. 12:6, to dismiss any potential function for its empirical basis alone. Within its objectivies of being an easily manipulated function with

substantial predicative value there can be little doubt of its general success or in its superiority over forms similar to that of G. and Mc. Its major disadvantage however, lies in its mathematical form which is considerably more difficult to handle than the simple L.J.

The above discussion has clearly emphasised the difficulties in obtaining a satisfactory form of the potential for even the simplest system. The next section discusses a further complication that may be present, the phenomon of three body interactions or non-additivity.

3.3 Non-additivity.

The strict additivity of intermolecular forces as required for the cell model has long been in doubt. If three body forces must be considered the question arises as to what properties are affected and the magnitude of any non-additive correction?

The relative stability of structure for inert gas crystals is a fundimental problem that has been linked with non-additivity. This problem arises since the molecules crystalise in the face centred cubic (f.c.c.) rather than in the hexagonal close packed(h.c.p.) structure which they should adopt from strict energy considerations, if the L.J. law was obeyed.

Barron and Domb (81) reviewed and recalculated the results of several previous workers on the static lattice energy and showed that the energy difference between the two

structures was dependent on the distribution of further neighbours. This energy difference was considered by Axilrod (82) who extended his work of almost ten years earlier (36). He computed the effect of the triple dipole over a large but finite cylindrical lattice. His calculations favoured the f.c.c. but not sufficiently to counteract the original lower value of the h.c.p.

Perturbation calculations by Jansen and co-workers (83-85) supported the views of Axilrod and others, that the stability of the f.c.c. structure in the rare gas solids could only be explained by the presence of many body forces. However Jansens estimation of the three body contribution (23% of the cohesive energy for solid argon) definitely appears to be too large.

Thus, although the presence of a non-pairwise additive term seems beyond dispute, the magnitude of the effect especially in the explanation of the above phenomena is still a matter of uncertainty. Another situation where ~~they~~ assume importance is in considerations of the third virial coefficients. Calculations by Kihara and others (86) indicate the contribution to be important in the cases of argon and krypton and this view was supported by the work of Sherwood and Prausnitz(87) who stated that non-additive forces made a significent contribution at low temperatures. Kihara estimated the leading term in Axilrod's dipole-dipole-dipole calculation (u_{123}) which is proportional to $(r_{12}r_{23}r_{31})^{-3}$ and which may be calculated from polarizability

measurements . Sherwood and Prausnitz used this term to indicate that the discrepency between the predictions of the two body potential and the observed virial coefficient could be assigned entirely to the leading term in u_{123}. This result has led Barker to conclude that the triple dipole interaction is the only important non-additive effect, this conclusion however awaits experimental confirmation.(208)

These observations stress the importance of obtaining an accurate estimation as to the magnitude of non-additivity. If the corrections are so small that they only account for the 0.01% difference in the relative lattice energies then the effect may generally be neglected, for this difference is less than the uncertainty in experimental properties. However, if the order of the effect is as high as predicted by Jansen the depth of the potential energy minimum would, of necessity, be substantially raised.

At the present time the position regarding non-additivity is far from clear and radically opposed opinions are rife. Thus Rowlinson and Stavely (88) have made low temperature measurements for Ar and Kr and fitting their results to a core potential of the type first proposed by Kihara (89) predict a value of $\epsilon/k=170^{\circ}K$.(approx.) for argon($\epsilon/k=120^{\circ}K$ from L.J.)

From the opposite viewpoint Batchelder et al (90) have recently published accurate measurements of the lattice constant for argon, and on comparing their results with theoretical predictions find "no experimental necessity

to invoke three body interactions".

In view of such conflicting statements, one must hesitate to draw any definite conclusions on non-additivity. However, the author feels that the effect is substantially less than that suggested by Rowlinson. In the subsequent theoretical studies of the inert gas solids no correction has been made for non-additivty. Its magnitude may possibly be reflected in the comparison of theoretical and experimental values.

3.4 Discussion.

The evidence presented earlier in this chapter indicated clearly the constraint imposed on the potential by a two parameter interaction law. However, potentials containing three or more parameters do not appear to justify their increased complexity by demonstrating a similar degree of improvement in their predicative value. The most successful multi-parameter potential, that of G. and Mc. must be considered as specific for a specific substance, demanding as it does a comprehensive knowledge of experinental data.

We therefore propose that a treatment of the solid state of the inert gases employing the cell model of Lennard-Jones and Devonshire is perfectly reasonable. The simple analytical form of the potential makes calculations relatively easy and enables the treatment to be generalised by a corresponding states approach- a treatment

that may be readily applied in situations where multi-parameter potentials appear to fail.

To date we have not mentioned quantum effects, which are markedly present in the low temperature states of the inert gases. These will be dealt with in the next chapter and we content ourselves here by stating that the simple analytical methods we employ are such that our treatment is readily and fully quantised.

The problem of the anharmonic vibrations of the crystal lattice at low temperatures has also been neglected. In lattice dynamical treatments these effects contribute measurably to the thermodynamic properties and must therefore be allowed for. To date most treatments that correct for anharmonicity have been long and detailed (76, 91-93). In cell methods however, these difficulties are not encountered and it is well known that the model of L.J. & D. deals exactly with anharmonicity (94).

Thus, neglecting three body forces and adopting a L.J. 12:6 interaction potential we will proceed to apply a quantised cell model to the solid state of the inert gases argon and neon.

CHAPTER 4.

A theoretical study of Argon and Neon at high densities.

"The essential fact is that all pictures which science now draws of nature and which alone seem capable of according with observational fact are mathematical pictures."

Sir James Jeans.

4.1 Quantum Effects.

Any attempt to investigate and interpret the properties of the inert gases, particularly at very low temperatures must account for the fact, that under these conditions the molecules behave quantum mechanically. This quantum behaviour can be conveniently described, as was pointed out by De Boer (95), by the introduction of a dimensionless quantum parameter Λ^* where

$$\Lambda^* = h/(m\epsilon)^{\frac{1}{2}}\sigma \qquad (4.1.1)$$

h = Planck's constant; m = mass of molecule

ϵ , σ are the potential constants.

Λ^* is the ratio of the De Broglie wavelength of the relative motion of the two molecules($\epsilon = mv^2/2$) to the molecular diameter σ. When $\Lambda^*$is of the order of unity for a particular element, large quantum effects are present at and below $\epsilon/k^{\circ}K$. However as the parameter becomes smaller the quantum effects noticably decrease in magnitude.

If we consider that the potential energy of a molecular system is expressed as the sum of pairwise interactions of the Lennard-Jones type, then the classical equation of state may be written (in reduced variables) as a universal function.

$$(p\sigma^3/\epsilon)_{classical} = f(V^*,T^*) \qquad (4.1.2)$$

which is the classical law of corresponding states. To extend this law into the region of quantum effects the Λ^* parameter must be introduced. As a result the

thermodynamic properties are no longer functions of the reduced variables alone, but unique functions of these variables and of Λ^* i.e. the thermodynamic properties become dependent on the mass of the molecule under consideration and -

$$(p\sigma^3/\epsilon)_{quantum} = f(V^*, T^*, \Lambda^*) \qquad (4.1.3)$$

We have already shown that the classical partition function for a system of molecules without internal degrees of freedom is-

$$Z_{cl} = \frac{1}{N!}\left(\frac{2\pi mkT}{h^2}\right)^{\frac{3N}{2}} \int \cdots \int \exp\left[-\omega(r)/kT\right] d\tau_1 \cdots d\tau_n \qquad (4.1.4)$$

In quantum mechanics the above equation must be replaced by the quantum or Slater sum, such that

$$Z_{qu} = \sum_n g_n \exp\left[-\lambda_n/kT\right] \qquad (4.1.5)$$

where g_n is the degeneracy and λ_n the eigen value of the n^{th} eigenstate satisfying the equation $H_n\psi_n = \lambda_n\psi_n$ and where the summation extends over all eigen values of which the system is capable.

Quantum effects are largest near $0^oK.$, where ordinary thermal effects are small. These have been widely investigated by examining the reduced static lattice energy U_o^* $(=U_o/N\epsilon)$ and the reduced molar volume $V_o^*(= V_o/N\sigma^3)$ for Xe, Kr, Ar and Ne at $0^oK.$, as functions of Λ^* (see 4.3). Quantum deviations are apparent for all rare gas solids and are most pronounced for neon (96). The deviations further increase as the molecular masses become smaller and any application of a statistical theory to investigate these regions must involve quantum corrections. The problem of introducing

such corrections into the cell model, although complex, has been solved and the solution is presented in the form of the quantum cell model.

4.2 The Quantum Cell Model.

The equation of state for a system obeying quantum statistical mechanics requires the solution of a Schroedinger wave equation, which describes the equilibrium configuration of a system of N particles. A straightfoward solution of this equation is virtually impossible and hence the introduction of a single particle theory such as the cell theory would simplify matters to a considerable extent.

The earliest attempts to introduce quantum corrections into the classical cell theory were by Lunbeck (97) who evaded a direct solution of the Schroedinger by expanding the Slater sum in powers of the quantum parameter. Another method initiated by Prigogine and Philpot (98), that of simplifying calculations by introducing an arbitary potential was extended by Henderson et al (99-100) and by Hamann and co-workers (101-103). The latter estimated the zero point energy in the cell by adopting a square well potential. This has appeal in limited circumstances (see 6.1), but in general these treatments are only approximate. The development of a fully quantised cell model for systems obeying a L.J. interaction is more rational and, as will be shown decidedly successful.

The first treatment of such a model was proposed by Levelt and Hurst (104) and later simplifed by Henderson and Reed (105). The approach we will describe here and which we have extensively employed in our calculations is that initially developed in these laborotories by Hillier and Walkley (106). It is more comprehensive than that of Henderson and Reed and less involved than the method used by Levelt and Hurst. It is also equally as rigerous, highly accurate and with regard to quantum systems, completely general in its application.

The assumptions of the cell theory have been described elsewhere (1.4) and, apart from a few relevant details will not be reiterated here.

The geometry of the cell is such that the cell centres lie on a hexagonal close packed lattice and

$$V/N = a^3/2^{\frac{1}{2}} \qquad (4.2.1)$$

The classical partition function (4.1.4) may be replaced by the product of one particle integrals.

$$Z_{class} = (1/N!)\left(\int_{cell} \exp -(W(r)-W(0)/kT)\, d\tau \right)^N \times \exp(-NW(0)/2kT) \qquad (4.2.2)$$

where $W(r) - W(0)$ is the potential experienced by the wandering molecule at a distance $\underline{r}$ from the cell centre.

The volume of the cell is taken as equal to the volume per particle and therefore the integral in the free volume term occuring in (4.2.2) is given by integrating over r_n where

$$4/3\pi r_n^3 = V/N \qquad (4.2.3)$$

The reduced cell volume $V^* = V/V_o$, is defined so that $V^* = a^3/2^{\frac{1}{2}}\sigma^3$ and the reduced cell radius $R_c = r_n/\sigma$ $= 0.55267\alpha$ (where $\alpha = a/\sigma$).

Assuming an L.J. potential we may rewrite the expression for the sphericalised potential, over k shells (1.4.10) as $W(r) - W(0) = \overline{W(r)}$

$$= \epsilon \sum_{i=1}^{k} \frac{Z_i}{\alpha_i R} \left\{ \frac{1}{2}\left[\frac{1}{(R+\alpha_i)^4} - \frac{1}{(R-\alpha_i)^4}\right] + \frac{1}{5}\left[\frac{1}{(R-\alpha_i)^{10}} - \frac{1}{(R+\alpha_i)^{10}}\right] \right\} + Z_i \epsilon \left[\frac{4}{\alpha_i^6} - \frac{4}{\alpha_i^{12}}\right] \quad (4.2.4)$$

where Z_i is the co-ordination number of the i^{th} shell at α_i and R is the reduced distance $R = r/\sigma$

We have already stated in (4.1) that for a system obeying quantum statistics the classical partition function must be replaced by the Slater sum (4.1.5) and adopting a one particle theory such as the cell theory this reduces to

$$Z_{qu} = \left(\sum_n g_n \exp(-\lambda_n/kT) \right)^N \times \exp(-NW(0)/2KT) \quad (4.2.5)$$

The energy levels λ_n of the particle in its cell are obtained by solving the Schroedinger equation

$$(-\hbar^2/2m)\nabla^2\psi + (\overline{W(r)} - \lambda_n)\psi = 0 \quad (4.2.6)$$

In the case of motion in a central field of force the generalised Hamiltonian allows a separation of variables (107). To determine the eigen values, only the radial component of this equation need be solved and denoting this by S(r) we may write the equation as--

$$S''(R) + (E_{l,n} - l(l+1)/R^2 - 8\pi^2/\Lambda^{*2}\overline{W(R)})S(R) = 0 \quad (4.2.7)$$

where $E_{l,n} = \frac{8\pi^2}{\Lambda^{*2}} \lambda^*_{l,n}$ and $\lambda^*_{l,n} = \lambda_{l,n}/\epsilon$

The boundary conditions for (4.2.7) are such that the wave function falls to zero at the cell boundary defined by r_n

$$\text{i.e. } \psi(0) = \psi(r_n) = 0 \qquad (4.2.8)$$

To obtain convergence of the partition function a large number of energy levels are required. An "exact" solution of the eigen value equation may be obtained either by a series expansion or through a finite difference method. The former approach was adopted by Levelt and Hurst who, using the fact that a Taylor expansion of $\overline{W(R)}$ contained only even powers of R, employed a Frobenius solution to solve the Schrodinger equation. For the light isotopes H_2 and D_2 which these workers investigated the method is capable of a limited degree of success. However, due to the complexities of the procedure no volume derivatives of the partition function (i.e. pressure) were obtainable and the mathematical evaluation of the eigen values was slow and involved. The other exact method, that of the finite difference is more versitile than a series expansion. It is however comprehensively described elsewhere (108) and since it is not employed in these calculations other than as a comparative medium we will not describe it in detail. Instead we have utilised an approximation, known as the Wentzel-Kramers -Brillouin (W.K.B.) approximation (109-110) that enables a large number of energy levels to be rapidly evaluated.

The W.K.B. method which is exact for a harmonic oscillator should be a good approximation for the sphericalised potential in the high density region, effectively

replacing the potential in the cell with a parabola split by a region of constant potential. It expands S(R) as a power series in R

$$S(R) = S_0(R) + \hbar_1 S(R) + \hbar^2/2\, S_2(R) + \ldots \qquad (4.2.9)$$

Neglecting terms above the second results in solutions that are singular at the classical turning points(111) i.e. those values of R for which the kinetic energy is zero. These solutions are linked by a relationship which is the determining equation for the eigen values:-

$$\int_a^b \left[E_{l,n} - \frac{l(l+1)}{R^2} - \frac{8\pi^2}{\Lambda^{*2}} \omega(R) \right]^{\frac{1}{2}} dR = \left(n+\tfrac{1}{2}\right)\pi \qquad (4.2.10)$$

where a and b are the classical turning points. However the formula (4.2.10) was found to give an incorrect solution unless l(l+1) was replaced by $(l+\frac{1}{2})^2$. This condition is requisite for the wave function to vanish at r=0 (i.e. that the boundary condition is satisfied). This modification is tantamount to raising the potential barrier, but is essential for a successful application of the approximation (112). Hence :-

$$\int_a^b \left[\frac{8\pi^2}{\Lambda^{*2}} \lambda^*_{l,n} - \frac{\left(l+\frac{1}{2}\right)^2}{R^2} - \frac{8\pi^2}{\Lambda^{*2}} \omega(R) \right]^{\frac{1}{2}} dR = \left(n+\tfrac{1}{2}\right)\pi \qquad (4.2.11)$$

for n = 0,1,2, ...

For each value of l, this equation computes an infinite number of eigen values corresponding to integral values of n.

An evaluation of the pressure for a quantum system requires the volume derivative of (4.2.5)

$$P = kT(d\ln Z_{qu}/dV)_T \qquad (4.2.12)$$

$$= \frac{\sum_n g_n(d\lambda_n/dV).\exp(-\lambda_n/kT)}{\sum_n g_n.\exp(-\lambda_n/kT)} - \frac{1}{2kT}\frac{d\overline{W(0)}}{dV} \qquad (4.2.13)$$

which in turn demands the evaluation of $d\lambda^*/dV^*$ where-

$$\frac{d\lambda^*_{l,n}}{dV^*} = \frac{2^{1/2}}{3\alpha^2}\frac{d\lambda^*_{l,n}}{d\alpha} \qquad (4.2.14)$$

This differential requires lengthy machine computation, but is readily obtainable from (4.2.11) by a solution of

$$\int_a^b \frac{1}{2}\left[\frac{8\pi^2}{\Lambda^{*2}}\frac{d\lambda^*_{l,n}}{d\alpha} - \frac{8\pi^2}{\Lambda^{*2}}\frac{dw(R)}{d\alpha}\right] x \left[\frac{8\pi^2}{\Lambda^{*2}}\lambda^*_{l,n} - \frac{(l+\frac{1}{2})^2}{R^2} - \frac{8\pi^2}{\Lambda^{*2}}w(R)\right]^{-\frac{1}{2}} dR \qquad (4.2.15)$$

We may directly proceed to evaluate the compressibility factor from (4.2.13) so-

$$\frac{\overline{PV}}{NkT} = \frac{(-V^*/T^*)\sum_{l=1}^{\infty}(2l+1)\left[\sum_{n=0}^{\infty}(d\lambda^*_{l,n}/dV^*)\exp(-\lambda^*_{l,n}/T^*)\right]}{\sum_{l=1}^{\infty}(2l+1)\sum_{\lambda=0}^{\infty}\exp(-\lambda^*_{l,n}/T^*)} - \frac{V^*}{2T^*}\frac{d\overline{W^*(0)}}{dV^*} \qquad (4.2.16)$$

where $W^*(0) = W(0)/\epsilon$

The corresponding classical expression is

$$\frac{\overline{PV}}{NkT} = \frac{((-V^*/T^*)\int_0^{R_c}(\overline{dW^*(R)/dV^*}).\exp(-\overline{W^*(R)}/T^*)\,4\pi R^2.dR}{\int_0^{R_c}\exp(-\overline{W^*(R)}/T^*)\,4\pi R^2.dR} - V^*/2T^*(dW^*(0)/dV^*) \qquad (4.2.17)$$

where $\overline{W^*(R)} = \overline{W(R)}/\epsilon$

It is clear that once the partition function (4.1.5) is evaluated the thermodynamic properties of the system can be immediately calculated. These are expressed as reduced internal properties (i.e. the value of the reduced property in excess of that of an ideal gas). The reduced internal energy (U_i^*), entropy (S_i^*) and specific heat (C^*_{vi}) are

given as -

$$U_i^* = U_i/N\epsilon = kT^2/\epsilon \ (d\ln Z_{qu}/dT) - 1.5T^* \qquad (4.2.18)$$

$$S_i^* = S_i/Nk = \frac{1}{N} \ln Z_{qu} + \frac{T}{N} \frac{d\ln Z_{qu}}{dT} - (\ln \frac{V}{N} + 2.5 + 1.5\ln(\frac{2\pi mkT}{h^2})) \qquad (4.2.19)$$

$$C_{vi}^* = C_{vi}/Nk = \frac{2T}{N} \frac{d\ln Z_{qu}}{dT} + \frac{T^2}{N} \cdot \frac{d^2 \ln Z_{qu}}{dT^2} - \frac{3}{2} \qquad (4.2.20)$$

In all calculations that follow we have performed our summations over the first three shells of neighbouring molecules. Hillier and Walkley (106) initially examined the effect of increasing from one to three the number of shells considered and observed a lowering of the energy levels of some 5% for the lowest levels, an effect that decreased with increasing n and l . The process of summing over more than three shells did not appreciably effect the values of the Slater sum and consequently exercised a negligable effect on the values of the thermodynamic properties. Calculations on H_2 and D_2 at $V^* = 5/3$ enabled the energy levels from the the approximate W.K.B. method to be compared with similar values from Henderson and Reed and with the exact solutions of Levelt and Hurst. A small inaccuracy for the W.K.B. values was observed but was insufficient to detract from the superiority of the approximation with regard to speed of computation. A more attractive alternative may well be a faster application of the finite difference method, this is under investigation (71) but to date comprehensive results are not available.

We finally refer to the reduced static lattice potential W*(0) occuring in (4.2.16) and (4.2.17). All compressibility terms involving the 12:6 potential were calculated using this in its asymptotic form.

$$W^*(0) = 12 \left\{ \frac{1.0110}{V^{*4}} - \frac{2.4091}{V^{*2}} \right\} \qquad (4.2.21)$$

which is developed from the expression for a cubic close packed structure

$$W(0) = 2N\epsilon \left(\frac{12.1318}{\alpha^{12}} - \frac{14.4539}{\alpha^{6}} \right) \qquad (4.2.22)$$

The co-ordination numbers were taken from the tables of Kihara and Koba (68) and the crystal lattice parameters used in (4.2.22) calculated by direct summation.(5.2)

The methods described in this section enable us to evaluate the compressibility and the thermodynamic properties for a quantum particle, experiencing a L.J. 12:6 potential over a wide range of temperatures and densities. Further the approach may be generalised for any bi-reciprocal potential of the Mie Lennard-Jones type (see Ch 5.). The mathematical techniques and the computational methods involved in this procedure are presented in Appendix 1, and for further details the reader is refered to this.

4.3 The Evaluation of the Potential Parameters.

The importance of determining a unique set of parameters for any system obeying a bi-reciprocal interaction law has already been stressed (3.1), as has the fact that second virial coefficient data noticably fails to meet this requirement. If we reject the latter as a suitable source of the parameters the only remaining thermodynamic state rigorous in its specification to determine ϵ and σ is the crystalline state at $0^{\circ}K.$, i.e. the values of the total lattice energy (U_o) and the molar volume (V_o) at this temperature. These quantities may be expressed in terms of the zero point energy (λ_o) and the static lattice potential ($W(0)$) as:-

$$U_o = N\lambda_o + NW(0)/2 \qquad (4.3.1)$$

$$-P_o = (dU_o/dV)_{T=0} = N(d\lambda_o/dV) + (N/2)(dW(0)/dV) \qquad (4.3.2)$$

The use of these properties to determine ϵ and σ essentially means that any thermodynamic data derived through them should reflect the multi-particle interaction and ipso facto should include any effects of non-additivity in the high density state. It is therefore of interest to compare parameters obtained from the zero point crystalline state with those found from second virial calculations and further to compare their relative merit in the prediction of other thermodynamic properties for the solid state.

Earlier workers who employed crystal data to characterise parameters include Corner (67) and Mason and Rice (69).

Corner used the lattice distance and the heat of sublimation (both at $0^{o}K$.). However, he was only able to uniquely determine his parameters by a combined consideration of virial (gas), zero point (solid) and Joule Thomson data. Mason and Rice performed similar work to Corner but on the exp-6 potential. They used the same experimental properties and in addition the viscosity coefficients only to reach similar conclusions.

The treatment used in this work was developed by Walkley and is completely different from any of the methods enumerated above. It makes extensive use of data available from the W.K.B. approximation, combined with an accurate knowledge of experimental properties.

The computed data allows λ_o^* and $d\lambda_o^*/dV$ to be determined for any range of reduced density over any given region of the Λ^* parameter. Equations (4.3.1) and (4.3.2) can be solved in their reduced form and hence considering the zero pressure ($P_o=0$) state these become:-

$$U_o^* = U_o/N\epsilon = \lambda_o^* + W^*(0)/2 \qquad (4.3.3)$$

$$d\lambda_o^*/dV^* + \tfrac{1}{2}dW^*(0)/dV^* = 0 \qquad (4.3.4)$$

The second term in (4.3.4) is independent of the Λ^* parameter, and therefore lends itself to a simple graphical method of solving these equations. For any given lattice (4.3.4) may be solved by a simultaneous plot of $d\lambda_o^*/dV^*$ and $\tfrac{1}{2}dW^*(0)/dV^*$ as functions of V^*. As will be seen from Fig (4.1) this results in a unique set of V^* at various Λ^* values. For any particle of known mass $\underline{m}$ it is then a

Volume derivatives of Zero point energy levels and of the Static lattice energy as functions of V*.

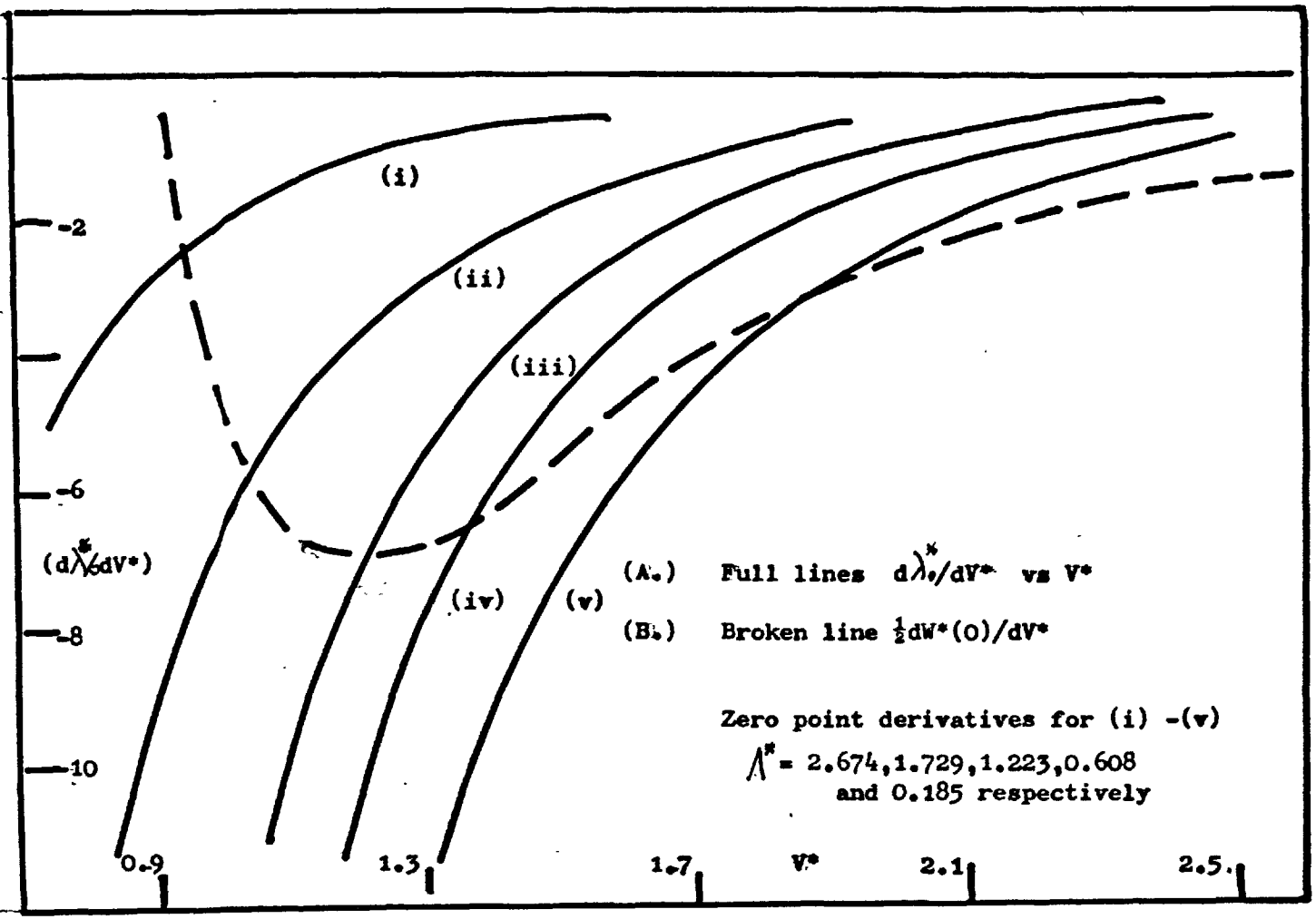

Fig 4.1

relatively simple matter to proceed graphically to a determination of ϵ and σ for the system. These calculations have been performed by the author for neon and by Islam (113) for argon and other inert gases. The detailed derivation of ϵ and σ for neon is given in Appendix 2. The results are presented in Table (4.1) together with values of ϵ/k and $N\sigma^3$ quoted from second virial data and the experimental data used in the calculations. Also included are values of the parameters obtained from a direct numerical solution of (4.3.3) and (4.3.4) using a method developed by Utting. This utilises the W.K.B. approximation and a Newton-Raphson technique in two variables. The equations may be satisfied to any predetermined degree of accuracy, and the procedure involves little computing time. A description of the method is also given in Appendix 2.

We now compare our zero point parameters with those obtained from second virial data. We first study the dependence of the reduced zero point volume $V_o^*(=V_o/N\sigma^3)$ and the crystal energy $U_o^*(=U_o/N\epsilon)$ upon Λ^*, reducing experimental data with both sets of parameters. In both cases a significant difference between the two curves is observed (see Figs (4.2) and (4.3).) Similar plots using virial parameters alone have been given by Dobbs and Jones (56) after De Boer (95) and by Boato (57). However, as our zero point values of ϵ and σ were directly calculated from V_o and U_o the curves arising from their use must be considered the most rigerous. In addition they also display

Table 4.1 Characteristic L.J. parameters and zero point properties.

Element.	Experimental zero point data.		Z.pt.params. (graphical)		Z.pt.params. (computed)		Second virial	
	U_o $\frac{cal}{mole}$	V_o $\frac{cc}{mole}$	ϵ/k (^oK)	$N\sigma^3$ $\frac{cc}{mole}$	ϵ/k (^oK)	$N\sigma^3$ $\frac{cc}{mole}$	ϵ/k (^oK)	$N\sigma^3$ $\frac{cc}{mole}$
H_2	183[a]	22.5[a]	32.6	15.64	32.92	15.35	36.7[e]	15.60[e]
"							37.0[f]	15.12[f]
D_2	274[a]	19.5[a]	34.4	15.85	33.70	15.72	35.2[e]	15.50[e]
"							37.0[f]	15.12[f]
^{20}Ne	448[b]	13.39[d]	36.6	12.89	36.31	12.87	33.74[g]	12.61[g]
Ar	1846[c]	22.55[d]	120.8	23.68	120.5	23.64	119.5[h]	23.89[h]

a. Best values of Levelt & Hurst(114)
b. Clusius et al.(115)
c. Morrison et al.(116)
d. Batchelder.(117)
e. Michels et al.(118)
f. Table 1a Ref.35.
g. Nicholson & Schneider.(119)
h. Whalley & Schneider.(120)

The Reduced Zero Point volume as a function of the De Boer parameter.

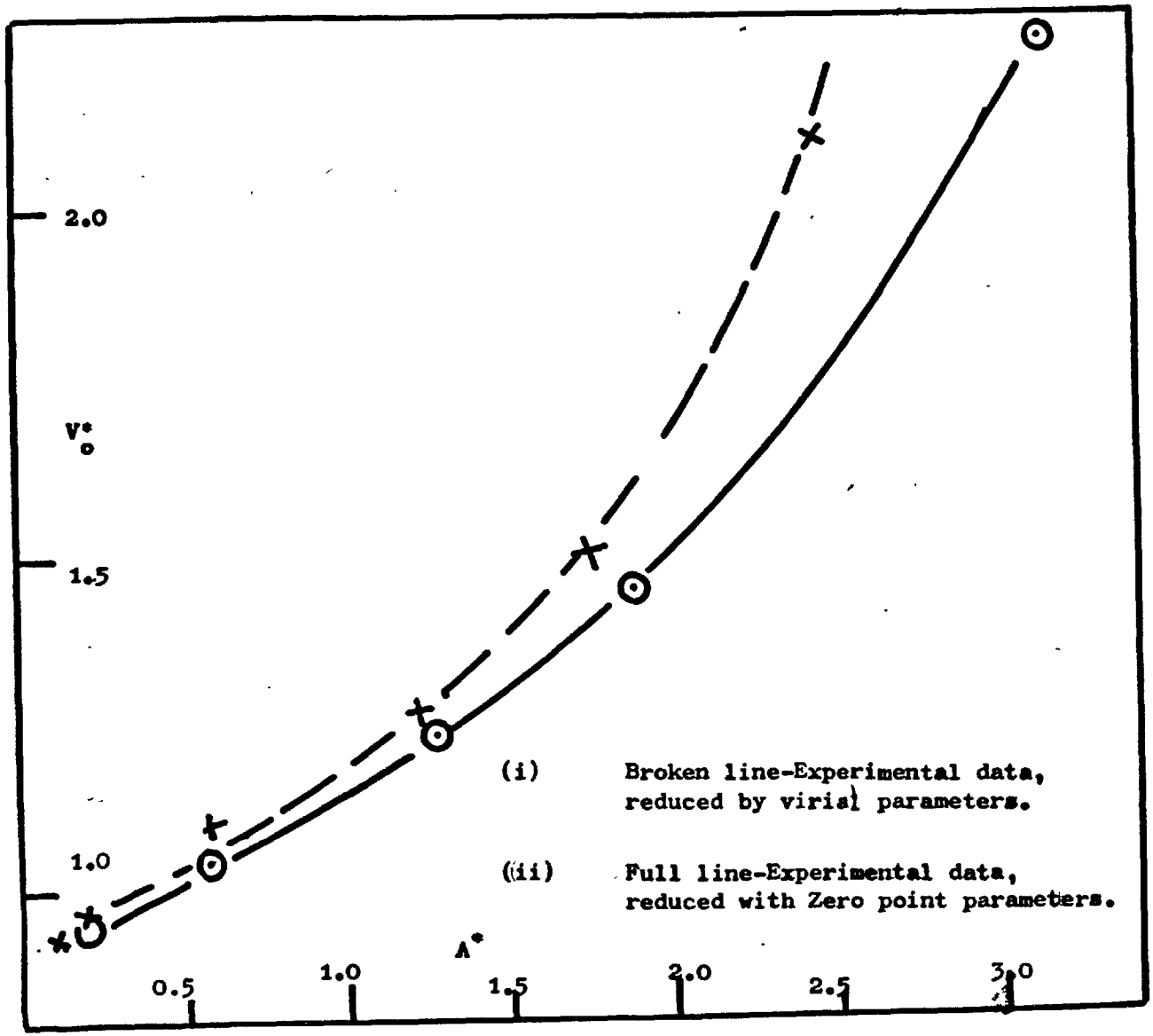

Fig 4.2

Fig 4.3 Reduced total crystal energy as a function of the De Boer parameter.

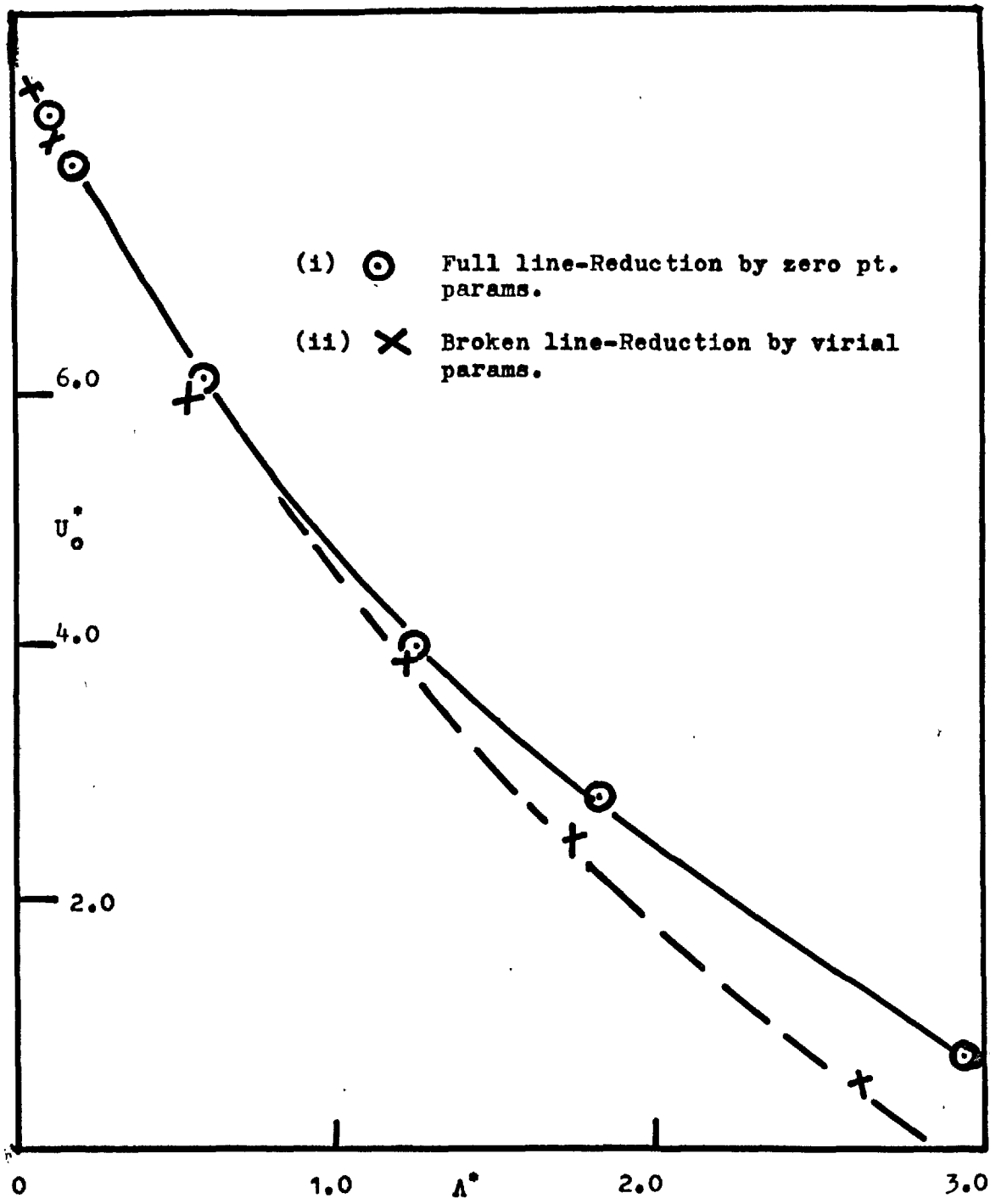

no irregularities unlike the plot of V_o^* vs Λ^* given by Boato (57)

Another point of interest arising from the evaluation of the parameters is that all other attempts to use (4.3.1) and (4.3.2) to characterise the pair potential have made use of the Debye temperature θ_D to give an"experimental" value for λ_o, i.e.

$$U_{o(expt)} = (9/8)R\theta_D + (N/2)W(0) \qquad (4.3.5)$$

$$(d/dr)(NW(0)/2 + (9/8)R\theta_D) = 0 \qquad (4.3.6)$$

where $\underline{r}$ is the nearest neighbour distance. The derivative $d\theta_D/dr$ however, must be calculated theoretically and in general a harmonic oscillator approximation must be made. Such calculations are at best suspect especially for particles lighter than argon.

A comparison of the theoretical values of λ_o^* with the reduced zero point energy may be made by plotting these quantities as a function of Λ^*. This is done in Fig (4.4) from which it can be seen that for $\Lambda^* \geq 0.4$, a marked discrepency between the two quantities occurs.

However on a perfunctory comparison of zero point parameters with those obtained from gas data (Table (4.1)) and on a further examination of Figs (4.2) and (4.3) a casual observer might conclude that although the parameters differ, this difference, on account of its low order of magnitude, should be unimportant. In the study of the high density state this surmise would certainly be false, to what

Fig 4.4 Reduced Zero point energy as a function of the De Boer parameter.

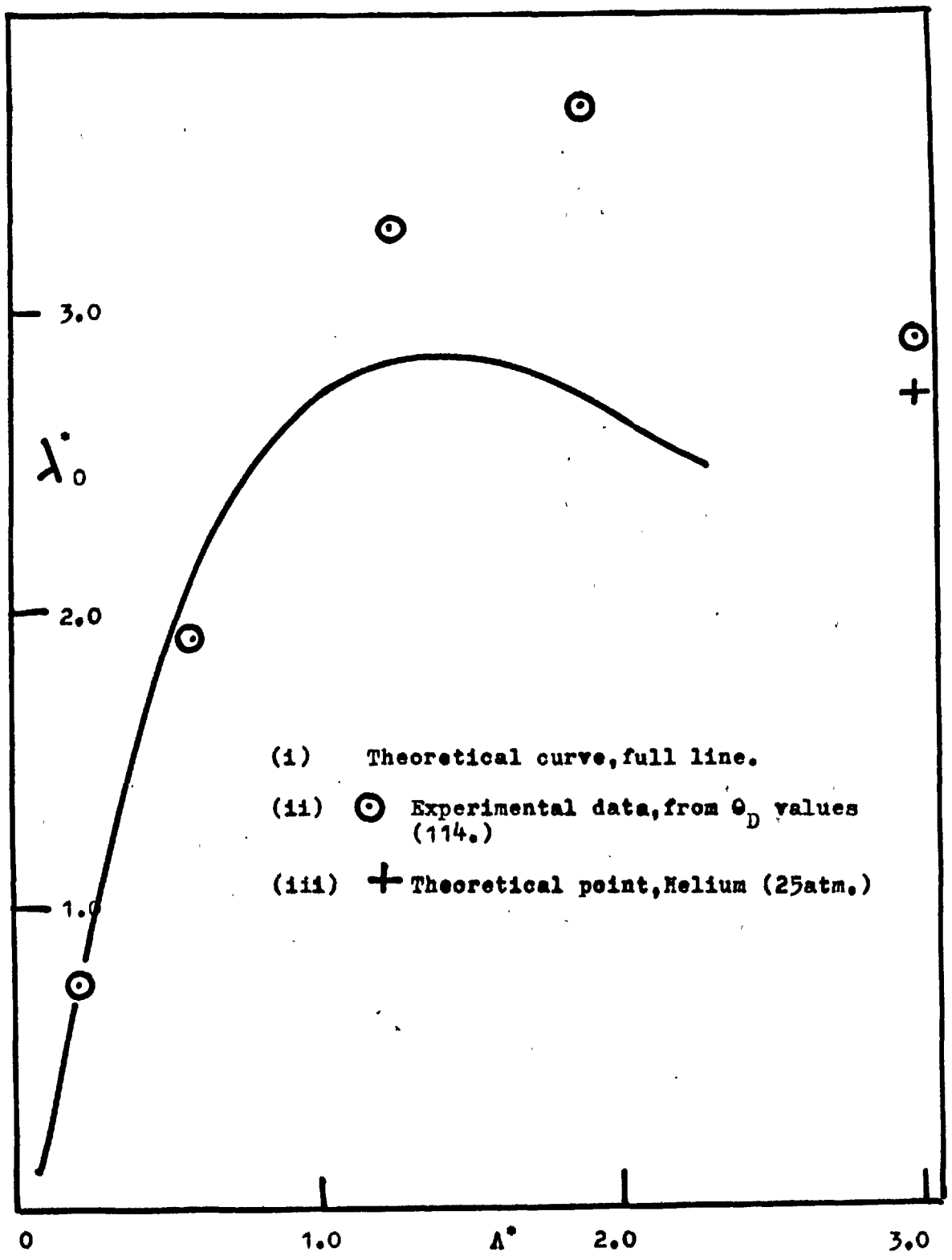

degree will be illustrated in the following sections when we will deal with solid argon (Λ^*=0.185) and the more quantum solid - neon(Λ^*= 0.584).

4.4 Solid Argon.

Of all the inert gases argon lends itself most easily to any theoretical study. The low magnitude of its Λ^* parameter indicates that quantum effects though present do not exert an overbearing effect on its low temperature properties. More important however is the abundance of experimental data available - in particular the recent X ray diffraction measurements of Batchelder (117) together with the heat capacity and vapour pressure values obtained by Morrison et al (116). These latest measurements are assumed to have superceded all others for the relevant properties, further data however may be found in Pollack (58) and in Dobbs and Jones (56).

Most previous theoretical treatments of the solid have been based on the assumption that the particles in the crystal lattice are constrained to their equilibrium positions by harmonic forces. Typical of these are the Einstein model (121), assuming the independent vibration of all particles in the crystal and the Debye model where the system is allowed a distribution of vibrational frequencies (122) More recently Henkel (92) and Zucker (123) have predicted

the thermodynamic properties of argon using an Einstein model but have allowed for anharmonicity in the model by suitably peturbing the basis harmonic potential. The marked improvement at high temperatures brought about by the inclusion of the anharmonic terms lends support to the use of the rigerously anharmonic L.J. cell model.

We have therefore evaluated the thermodynamic properties of argon employing the quantum cell model described in (4.2), normalising our computed data with the appropriate zero point parameters. It is important however to examine how the use of virial parameters would effect our calculations. The virial parameters given in Table (4.1) are far from unique. Using experimental data compiled by Dymond (124) and employing a Newton method (125) we have found the best fit from 200° - 300°K. This is shown in Table (4.2).

Table 4.2 L.J. Parameters for Argon.

Source	ϵ/k (°K.)	$N\sigma^3$ (cc/mole.)
Z.point data	120.8	23.68
200-300°K.[a]	119.8	23.50
323-873°K.[b]	119.9	23.90
85-153°K.[b]	104.9	31.53

[a] Virial parameters calculated from compiled data (124)

[b] " " " by Saville (126)

Also given in the above table are the values of Saville (126) who performed similar calculations over other restricted temperature ranges. An examination of the values in Table (4.2) indicates that the good agreement between the

"best fit" virial values and those obtained from zero point data must be chiefly fortuitous. However, since the best fit values are the closest to the zero point parameters we arbitarily employ them for comparative purposes. Their use should minimise the difference between the predicted properties and act as a test as to the sensitivity of these properties to the nature of the parameters.

Taking argon with the appropriate value of Λ^* (dependent on ϵ and σ) and using the W.K.B. approximation, we calculate PV/NkT (i.e. (4.2.16)) over a range of T* for set V* values. The resulting PV/NkT vs T* plots are typified by Fig (4.5). We are interested in the zero pressure state of argon and hence zero compressibility . From this condition we find unique values of V* and T* which, normalised by the appropriate values of $N\sigma^3$ and ϵ/k respectively, determine the volume-temperature relationship at P=0. This is given in Fig (4.6) - (for data from which this and subsequent plots in (4.4) were developed see Appendix 3), the reduced data being normalised by both zero point and by virial best fit values. The plot is remarkably sensitive to the parameters and the two curves are distinctly different. This difference is also most influenced by the magnitude of $N\sigma^3$ (i.e. a lower value of $\epsilon/k_{z.pt.}$ would make the difference appreciably worse.). The discrepency is only of the order of 0.18 cc/mole, however since graphical and computed values agree to within 0.04 cc/mole we do not attribute this difference to graphical errors

Fig 4.5 Argon, 12-6 potential(Λ=0.186). Compressibility factor as a function of reduced temperature.

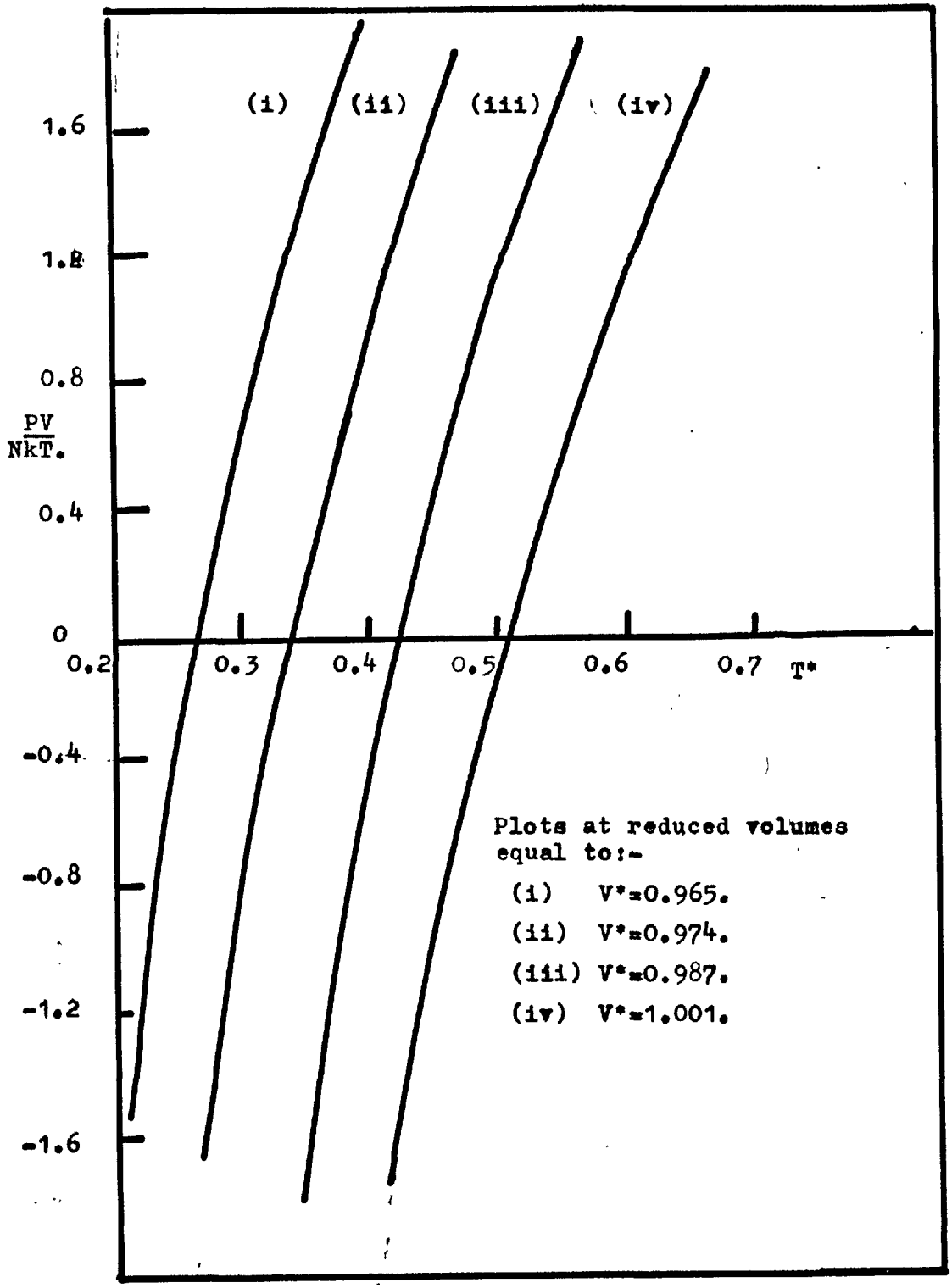

Fig 4.6 Solid Argon:-Molar volume(V, cm^3/molc) vs Temperature.

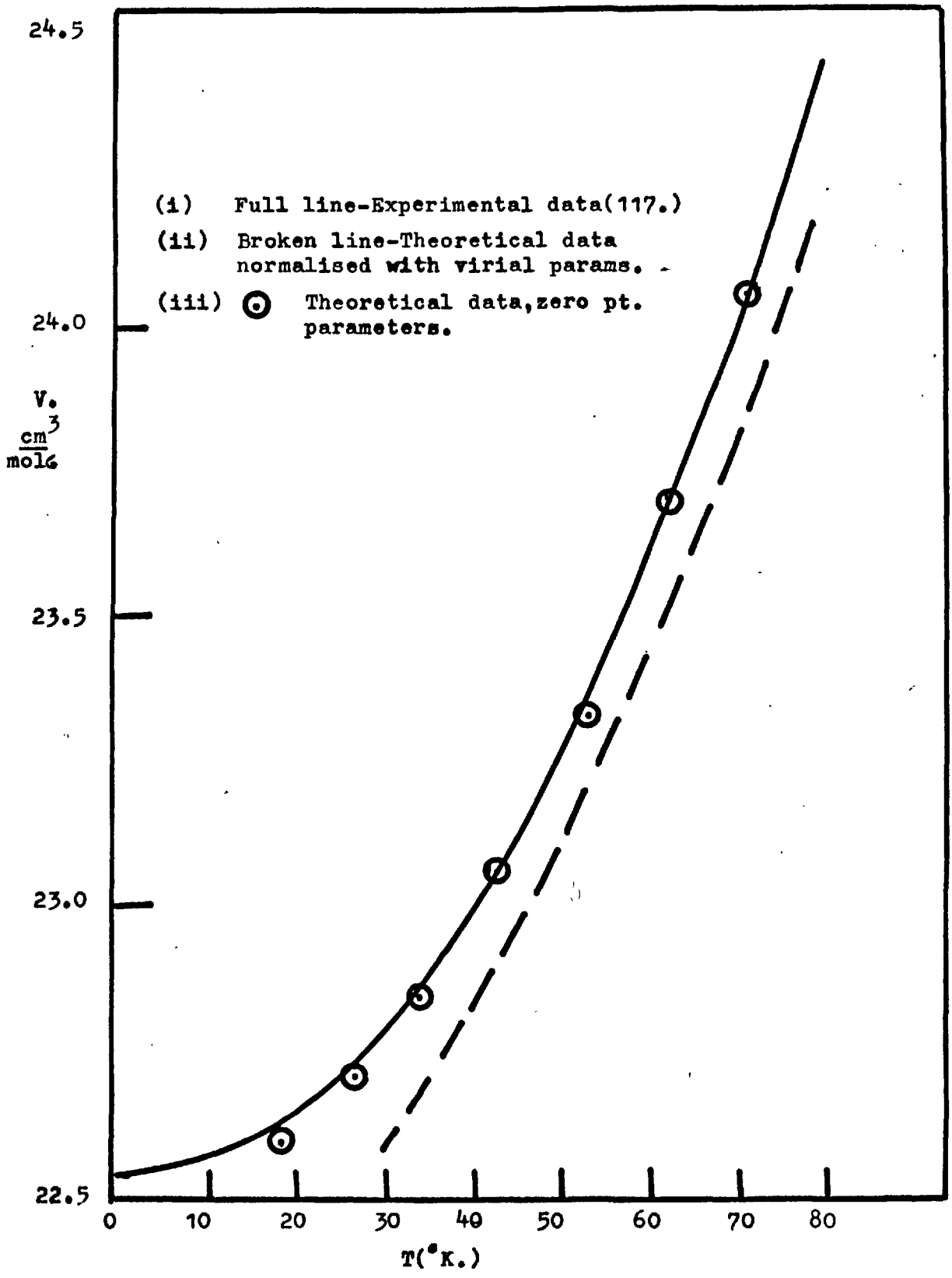

in evaluating our parameters. Attention is drawn to the excellent agreement between theoretical (zero point) and experimental measurements. The experimental data used is that of Batchelder (117), derived from single crystal X ray diffraction measurements, the bulk density values of Dobbs and Jones that we employed in our earlier calculations have been disregarded in favour of these latter results.

In particular we note the good agreement between the theoretical and experimental molar volumes at temperatures below $40^{\circ}K$., This contrasts sharply with the agreement obtained by McGlashan using his "improved" Guggenheim and McGlashan potential (61). He plotted the inter-atomic distance of solid argon (directly related to the molar volume i.e. $r \propto V^{\frac{1}{3}}$) against temperature and explained the discrepencies observed below $40^{\circ}K$. as " in a sense satisfactory because we know that the Einstein approximation must fail progressively at sufficiently low temperatures." He went on to indicate that a correct comparison should involve weighting techniques. This latter statement is substantially true, that the Einstein model fails at low temperatures is also true. However, the degree of this failure is unknown and therefore to dismiss all low temperature discrepencies on these grounds cannot be justified. It is the author's view that discrepencies due to the failure of the Einstein approximation are small, we support this with our results for argon calculated from our anharmonic Einstein model- a more sensitive test will of course

result from the study of solid neon which only exists in this state between 0-25°K.

We now calculate the theoretical heat capacity $C_v(V)$ from (4.2.20) and then compare it to experiment. The experimentally measured quantity however is C_p. This is because measurements of heat capacities are generally made by condensing the gas at a sufficiently low temperature in a suitable container. These measurements give C_s, the heat capacity of the solid in equilibrium with its vapour, but C_s is generally equal to C_p since the vapour pressures are too small to produce appreciable compression effects. Measurements of C_v (the heat capacity at constant volume) are well nigh impossible and this quantity can only be obtained by the use of the coefficients of compressibility and of thermal expansion, through the well known thermodynamic relationship:-

$$C_p - C_v(V) = \alpha^2 TV/\beta \qquad (4.4.1)$$

where α = coefficient of thermal expansion $= (1/V)(dV/dT)_p$

β = isothermal compressibility $= (1/V)(dV/dP)_T$

V = molar volume at T°K.

Theoretical values of α and β may be calculated by fitting a polynomial to the theoretical data. This was done by Hillier (6) and hence the theoretical $C_v(V)$ was converted to a theoretical C_p. The comparison of this with experimental data is shown in Fig (4.7).

It is also possible to convert the experimental C_p to

Fig 4.7 Solid Argon:- Heat capacity(C_p, cal/mole°K.) vs Temperature.

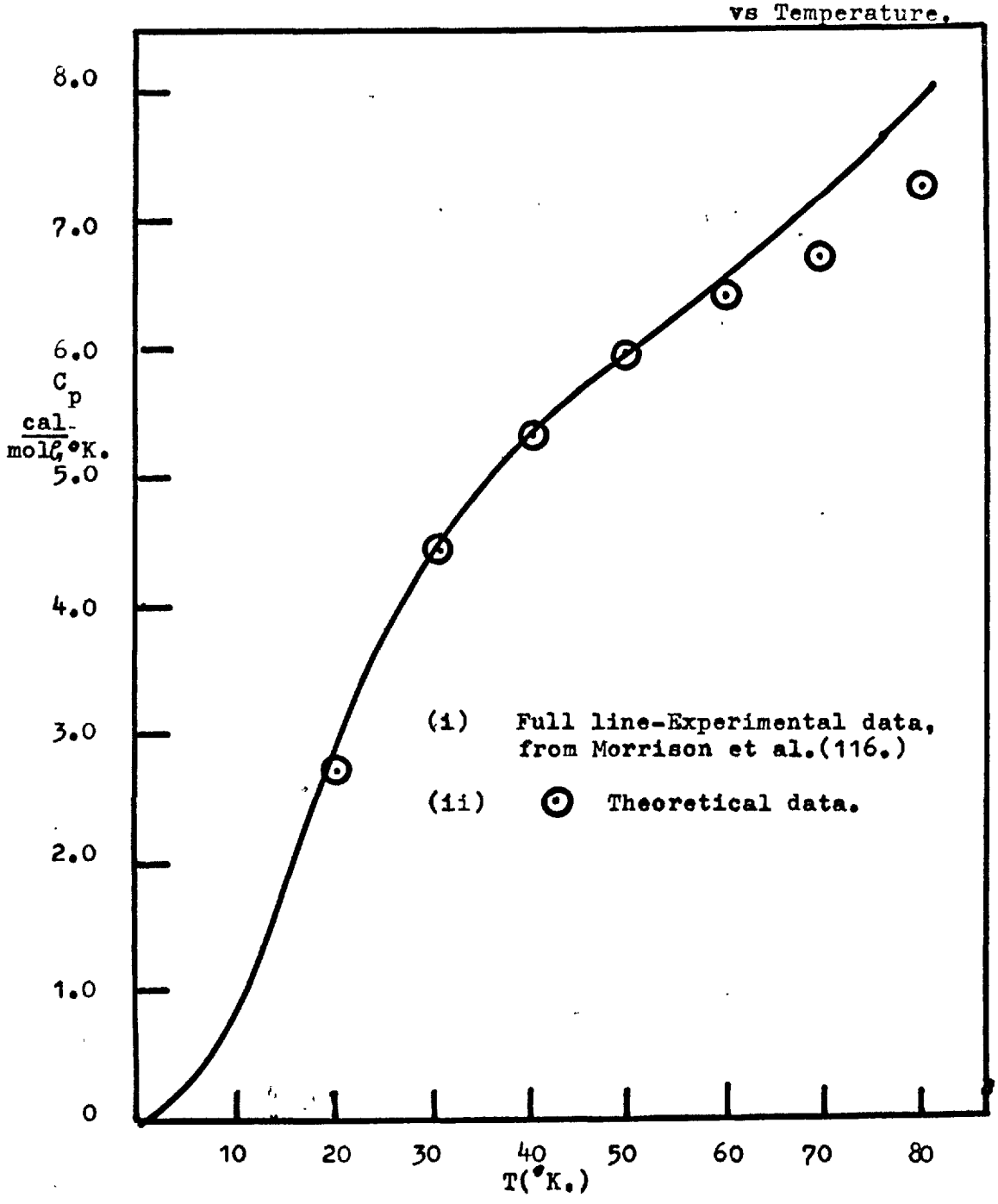

Fig 4.8 Solid Argon:-Heat capacity(C_v, cal/mol$_4$° K.) vs Temperature.

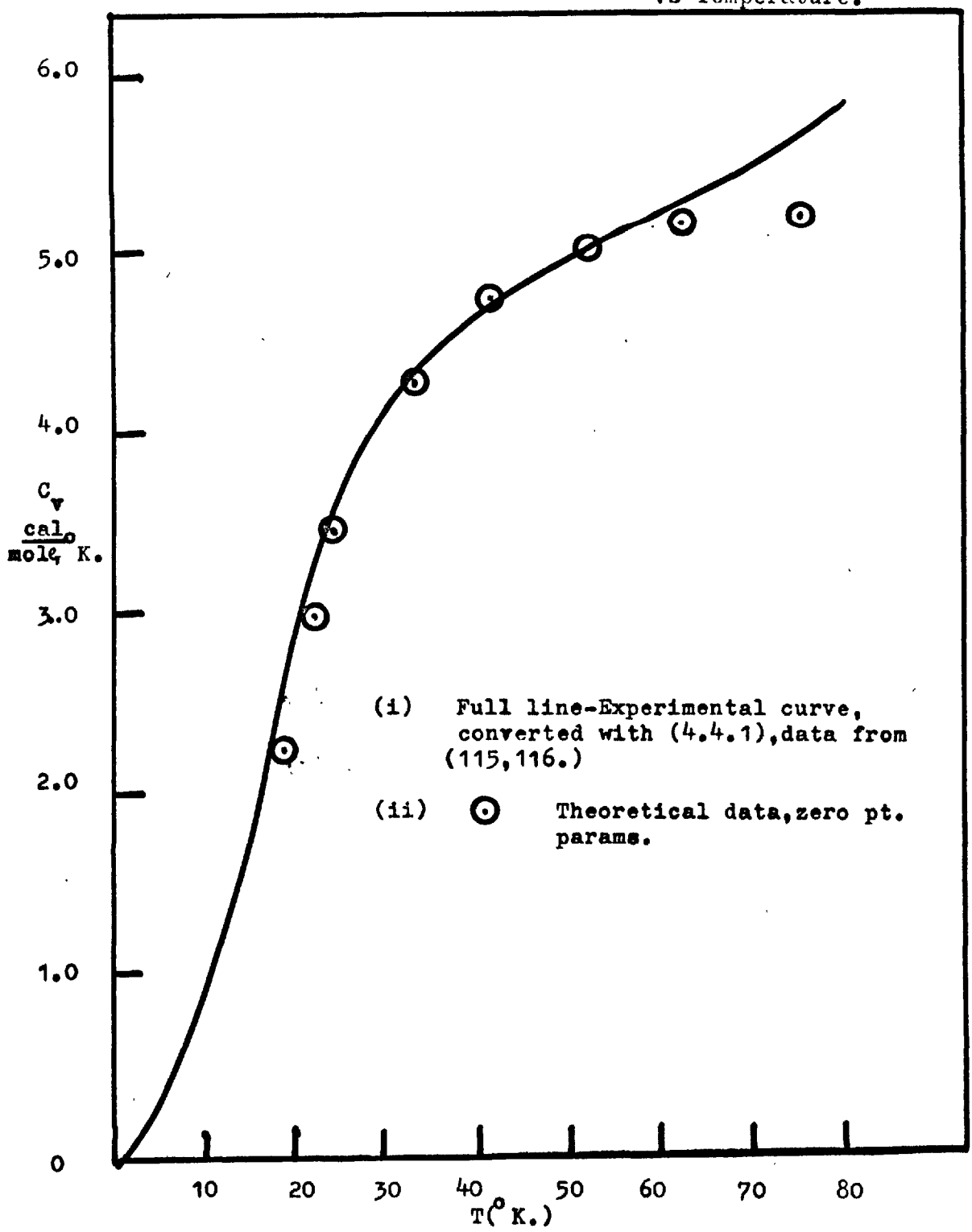

C_v using indirect "experimental" values of α and β . This was done using (4.4.1) and in Fig (4.8) we give a comparison of "experimental" and theoretical C_v, the former being obtained, as were the values of C_p, from the results of Morrison et al (116). In both cases agreement between theory and experiment is again excellent. It should however be noted that these comparisons are sensitive only to the temperature parameter ϵ/k of the potential and therefore either zero point or "best fit " values for argon would give similar results.

An interesting facet of the heat capacity plots is the divergence between the theoretical and experimental curves at high temperatures. One explanation of this is that it is due to thermal vacancies. There are however several objections to this concept which we will discuss in (4.5)

We make a final comparison with experiment by plotting the entropy term as a function of temperature, Fig (4.9). This term may be obtained from the experimental heat capacity data using the relationship -

$$S(T) = \int_0^T (C_p/T)dT \qquad (4.4.2)$$

and the theoretical value directly from theoretical data with the correction for the ideal gas entropy (4.2.19). The agreement is not as good as that observed for other temperature dependent properties. Discussion however is postponed pending the examination of solid neon.

Fig 4.9 Solid Argon:-Entropy(S_T, cal/molℓ°K.) vs Temperature.

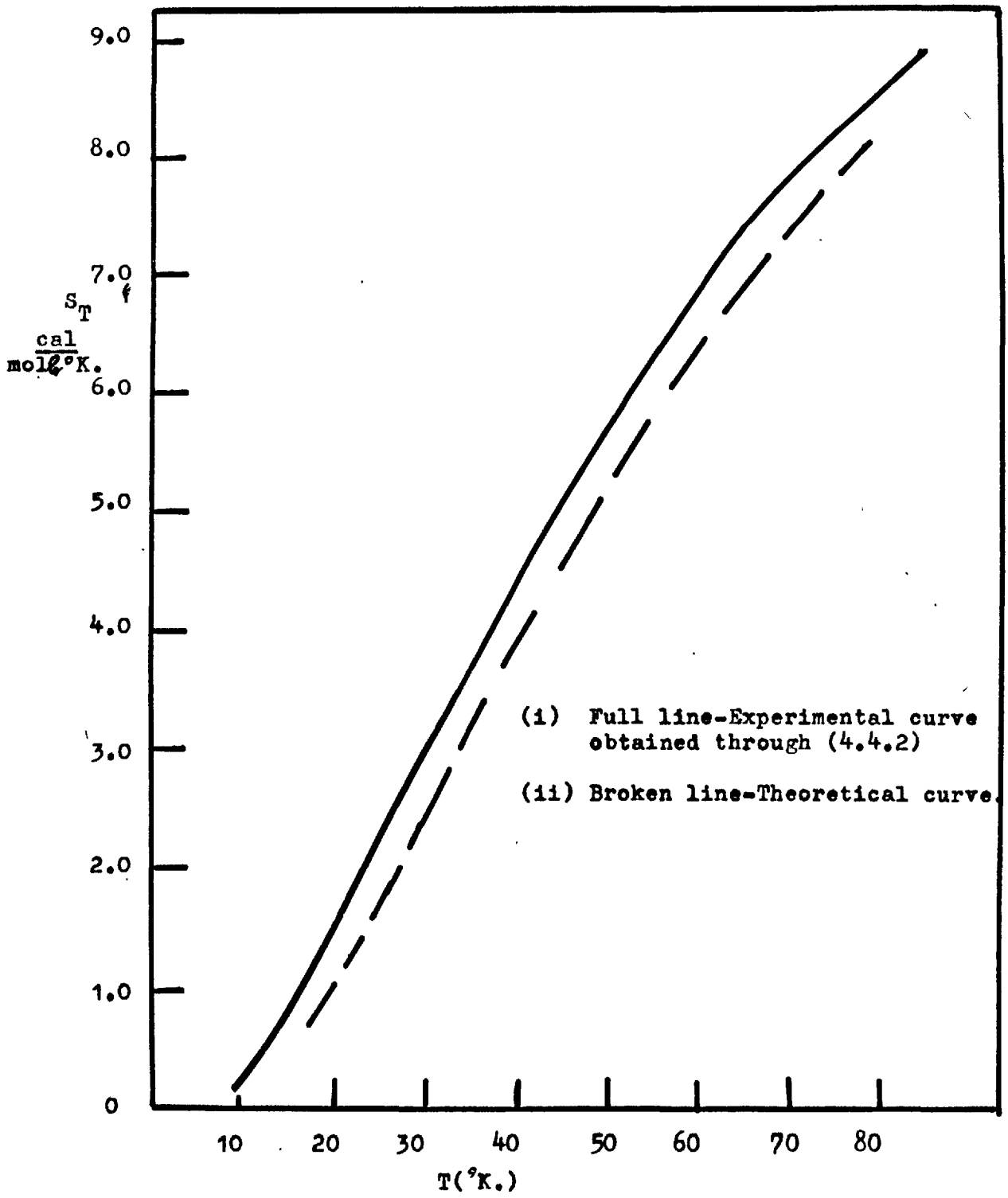

4.5 Thermal Vacancies in solid Argon.

Any consideration of imperfect crystals must consider the problem of vacancies. These are formed at temperatures above $0^{\circ}K.$, and must occur in inert gas solids as in any other crystal. It is probable that vacancies are the only important point defects in pure crystals of the inert gases since the formation energy for interstitials is high compared with that calculated for a vacancy.

Experimental evidence for the presence of vacancies was first given by Martin (127) and later supported by the heat capacity measurements of Morrison et al., as shown in Fig (4.7). The anomolous rise in C_p above $50^{\circ}K.$ is much greater than would be expected from anharmonic effects alone and offers fruitful ground for a theoretical investigation. Two approaches have been applied to this problem; the consideration of vacancy formation purely on energetic grounds, as done by Kanzaki (128), Hall (129) and Nardelli and Chiarotti (130), or a consideration of the lattice in the vacancy (perfect) and no vacancy (imperfect) modes. The latter method was employed by Foreman and Liddard (131) who used a harmonic Einstein model with an anharmonic correction term developed as a classical perturbation and found a clear difference between the vacancy and no vacancy cases for plots of the heat capacity above $50^{\circ}K.$

In this discussion we assume the cell model to represent a no vacancy solid. If the difference in the theoretical

and experimental heat capacity terms is ΔC_p then:-

$$\Delta C_p = \left[d(nh)/dT\right]_V \qquad (4.5.1)$$

where n is the number of vacancies in a crystal of N atoms and h is the enthalpy of vacancy formation.

If we assume that h is independent of T we find:

$$\ln \Delta C_p T^2 = -h/kT + S/k + n(Nh^2/k) \qquad (4.5.2)$$

Measuring the difference ΔC_p from Fig (4.7) the linear plot of $\ln(\Delta C_p T^2)$ against reciprocal temperature can be constructed. This is shown in Fig (4.10) and from its slope the enthalpy of vacancy formation can be calculated as:- h = 1190 cals/mole

This value is in substantial disagreement with the predicted value of 2540 cal/mole given by Nardelli and Chiarotti (130). It is much nearer the value of 1280 cal/mole found by Morrison et al, who estimated the no vacancy heat capacity curve by the extrapolation of low temperature data.

Provided that the quantum cell model is a good representation of the no vacancy case and (assuming that correlated motions do not effect C_p) there is no reason why it should not be, our calculations strongly support the theory of an increase in vacancy concentration above 60°K.

Certain voices have recently been raised against such ideas as those described above and especially we mention those of McGlashan (61) and Batchelder et al (90). McGlashan derived a theoretical expression for C_p that directly fitted the experimental data of Morrison as far as the triple point. He concluded that earlier theoretical

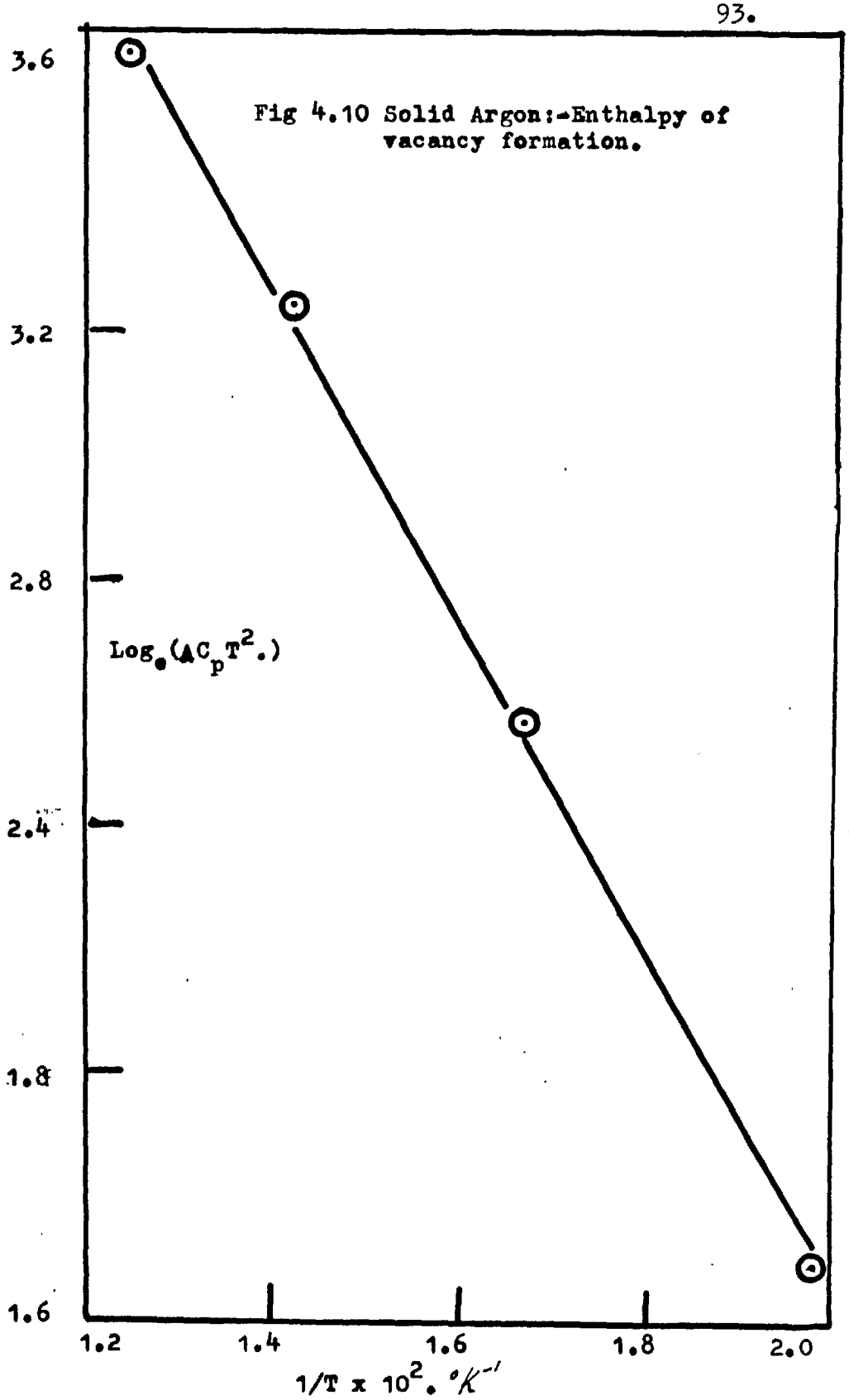

Fig 4.10 Solid Argon:-Enthalpy of vacancy formation.

estimations were in error for in general the experimental specific heat (C_p) was converted to C_v by the use of a "dubious mathematical relationship", and then compared with theoretical predictions. However, this is not true for our treatment (ref. Fig (4.7)), C_p(theory) being derived completely on theoretical grounds and then being compared to C_p(expt.). We further refute the opinion that (4.4.1) is not valid and agree with Zucker (79) that in fact McGlashan has forced correct values onto a model that cannot really cope with them. He has done this by leaning heavily on experimental specific heat data to determine four of his six parameters and the successful prediction of C_p, using these same parameters, must therefore be expected.

However the work of Batchelder et al is more convincing and difficult to disregard. They have performed accurate experiments using single crystal techniques. Adopting these as the "no vacancy" case and using measurements from bulk density work as the vacancy condition they find that the concentration of vacancies appears to decrease with increasing temperature.

These results are considered to raise serious doubts as to whether the presence of vacancies is as important as predicted by Foreman and Liddiard. To resolve this problem direct measurements of the thermal vacancy content and high temperature compressibilities are needed but, at present, little information on these exists.

4.6 Solid Neon

(For theoretical and experimental data used to construct figures in this section see Appendix 4.)

Compared to argon the solid phase of neon has been neglected both experimentally and theoretically. The reason for this must be attributed to the low triple point of the solid (24.55°K.), for with such a narrow range of working temperature experimental problems are substantial. However, experimental data has recently become available and the X ray studies of Batchelder (117) and Bolz and Mauer (132) ably supplemented by the heat capacity measurements of Clusius et al. (115) now provide criteria against which any theory may be compared.

From the theoretical viewpoint solid neon is of much greater interest than the corresponding phase for argon. The quantum effects are substantial (Λ^*=0.584) and anharmonic contrubutions are very large. Leech and Reissland (91) have studied the effects of anharmonicity in the inert gases and have concluded that in the case of neon a harmonic theory could not expect to be realistic. This system therefore acts as a test for the anharmonic nature of our model and in addition of the ability of the quantum cell theory to successfully predict properties for systems displaying large quantum effects.

The earliest attempt to formulate a theory for solid neon might be attributed to Johns (133) who used a Henkel

model (92) to study isotopic differences especially those in the vapour pressure. This model although taking some account of anharmonicity cannot be regarded as a valid approach and any success through its use must be considered fortuitous. Variational calculations have been made by Bernardes (134) and Mullin (135). The former employed a wave function assuming simple spherical symmetry. Mullin extended this technique allowing for some correlation between the atoms by using a Jasrow type wave function and a L.J. potential. He found correlation effects between the molecules to be negligible at $0^{\circ}K.$, and obtained good agreement with experimental data at this temperature by altering the value of his energy parameter.

However, (apart from the data of Leech and Reissland) there has been no extensive work to date on the temperature dependent properties of neon. Once again we have applied our quantum cell model to evaluate these properties. The choice of parameters - already shown to be sensitive for argon - in the case of neon is almost critical. The values of ϵ and σ from various sources together with related data is given in Table 4.3 (see overleaf).

The values of our zero-point parameters $\underline{g}$ and $\underline{h}$ were obtained using the recent X ray diffraction of Bolz and Mauer (132) which together with that of Kogan et al. (139) replaced the earlier data of Smedt, Keesom and Mouay measured in 1930 (140). Bolz and Mauer gave a lattice spacing for ^{20}Ne of 4.462 $\mathring{A}$ at $4.2^{\circ}K.$, the value of Smedt et al. being

Table 4.3. L.J. Parameters for Neon

Source & Ref	$\varepsilon/k(^{\circ}K)$	σ(A)	$N\sigma^3$(cc/mole)	Λ^*	
Nicholson & Schneider(119)	33.74	2.757	12.61	0.608	a
Boato & Casanova(136)	37.10	2.670	11.46	0.596	b
Horton & Leech(137)	35.31	2.699	11.83	0.607	d
Mullin(135)	35.70	2.750	12.52	0.593	c
Bernardes(134)	36.23	2.740	12.38	0.590	e
Brown(138)	35.28	2.774	12.86	0.591	f
Z.point(graph.)	36.60	2.777	12.89	0.580	g
Z.point(comp.)	36.31	2.775	12.87	0.582	h

4.350Å (confirmation of the former value has been communicated to us by Batchelder).

Brown has also used the data of Bolz and Mauer to repeat the calculations of Horton and Leech for neon. His values are given as f (Table 4.3), which closely agree with our zero point (either graphical or numerical) values. As may be seen from the table, parameters from the other sources have a spread of about 10%, a spread that is not negligible when reflected in the thermodynamic properites.

It is considered of interest that the Levelt and Hurst calculations (114) based on virial values give a zero point energy of 136 cal/mole agreeing will with the Domb and Salter approximation i.e. $9R\,\Theta_D/8$, of 139 cal/mole. Our calculations give a value of 142 cal/mole, so this would not

account for the difference in α/k values as calculated by ourselves and Brown. It is possible, but not certain, that these values might arise from the nature of the Horton and Leech calculations themselves. However, the critical test of the parameters lies in their prediction of temperature dependent properties.

In Fig. 4.11 we present a plot of zero point molar volume as f(T). The experimental curve may be constructed from the data of Bolz and Mauer or of Batchelder. The theoretical data normalised by the parameters of Boato and Casanova, by Mullin and by Nicholson and Schneider were rejected. The theoretical zero point parameters give a far better agreement with experiment and the separation of the various plots is an inidcation of the sensitivity of the data to the parameter values.

In Fig. 4.12 we plot lattice constant (a_o) against temperature and compare theory to the latest data of Batchelder. The lattice constant is simply related to the molar volume (V). Hence, for a close packed lattice:-

$$V = N r_o^3 / 2^{\frac{1}{2}} \qquad (4.6.1)$$

where r_o is the interatomic distance;

but $a_o = r_o / 2^{\frac{1}{2}}$

and $a_o = 2^{\frac{1}{2}} \times (2^{\frac{1}{2}} V/N)^{\frac{1}{3}}$ (4.6.2)

$$a_o = 1.879\ V^{\frac{1}{3}}\ (\text{Å}) \qquad (4.6.3)$$

Fig(4.12)is therefore another way of presenting Fig (4.11). However, it is perhaps a better illustration of the predicative value of the theory. The agreement is excellent

Fig 4.11 Solid Neon:- Molar volume(V, cm^3/mol) vs Temperature

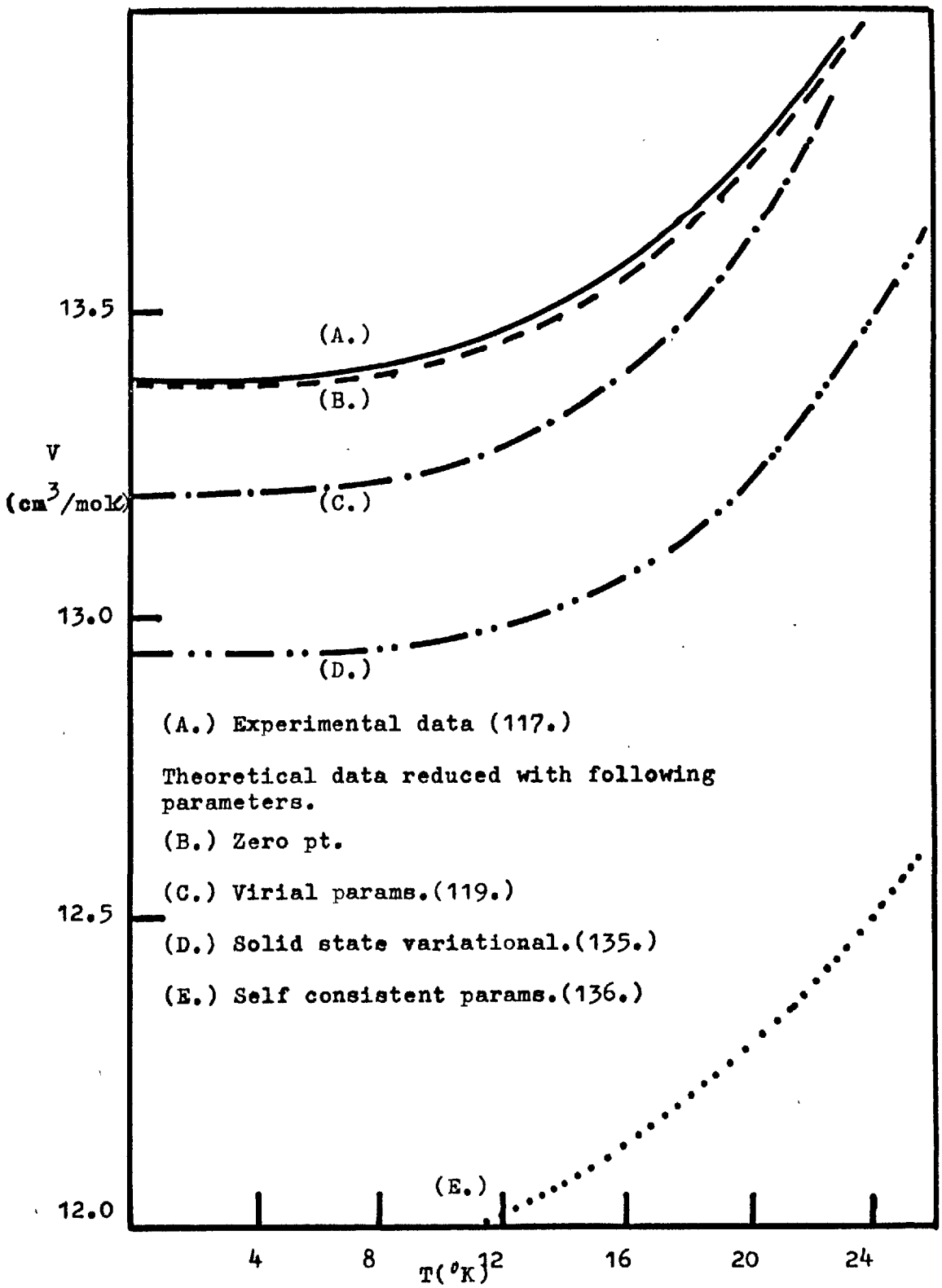

Fig 4.12 Solid Neon:-Lattice constant a(Å) vs Temperature.

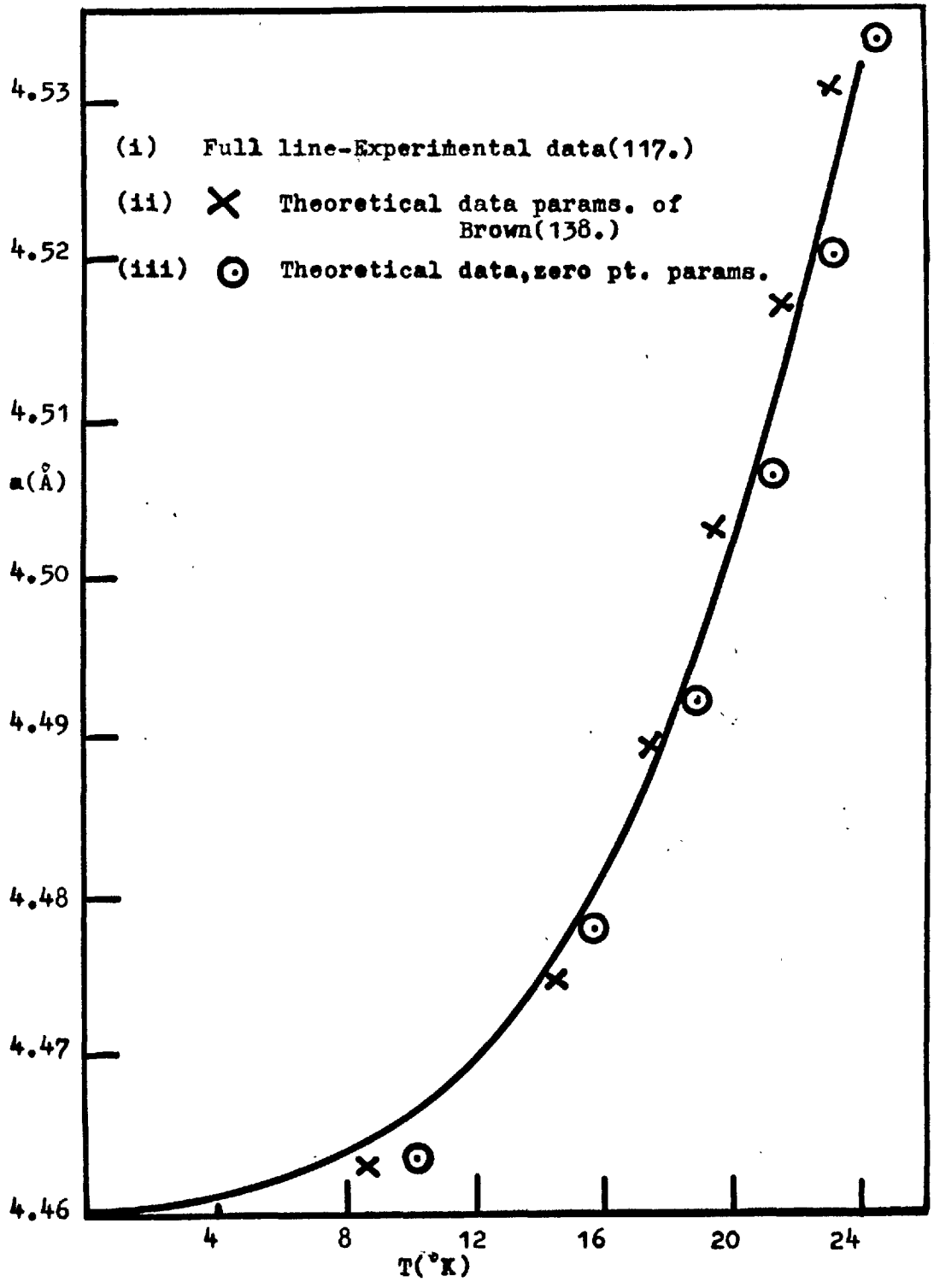

being almost within experimental accuracy ($\pm$0.001 Å). In this plot we also normalise the theoretical data with the parameters of Brown. This, for the sake of clarity was not done in Fig. 4.11. Agreement with experiment is again acceptable.

The heat capacity term $C_v(V)$ is plotted as a f(T) in Fig. 4.13. The experimental data is that of Clusius, which is calculated from C_p using Gruneisen's relationship (142):-

$$C_v = C_p - k_1 C_p^2 T \qquad (4.6.4)$$

where k_1 is a constant.

Although this evaluation can only be regarded as approximate, confirmation of the C_v value is given through the data of Batchelder, using (4.4.1) and values of α and β derived from accurate X ray data.

The comparison of experimental and theoretical values of C_v show that the theoretical data "normalised" by the parameters of Brown gave a slightly better fit with experiment - a direct result of a lower value of ϵ/k.

In Fig. (4.14) we give a plot of C_p against temperature. The theoretically computed $C_v(V)$ are corrected to C_p through the use of (4.4.1), the expansion coefficients being evaluated from theoretical data, utilizing the fact that (4.4.1) reduces to:-

$$C_p - C_v = \alpha^2 VT/\beta = (dV/dT)^2 T/(dV/dP) \qquad (4.6.5)$$

where (dV/dT) and (dV/dP) may be evaluated from computed results.

The agreement between theory and experiment is again

Fig 4.13 Solid Neon:-Heat capacity(C_v cal/mole, °K.) vs Temperature.

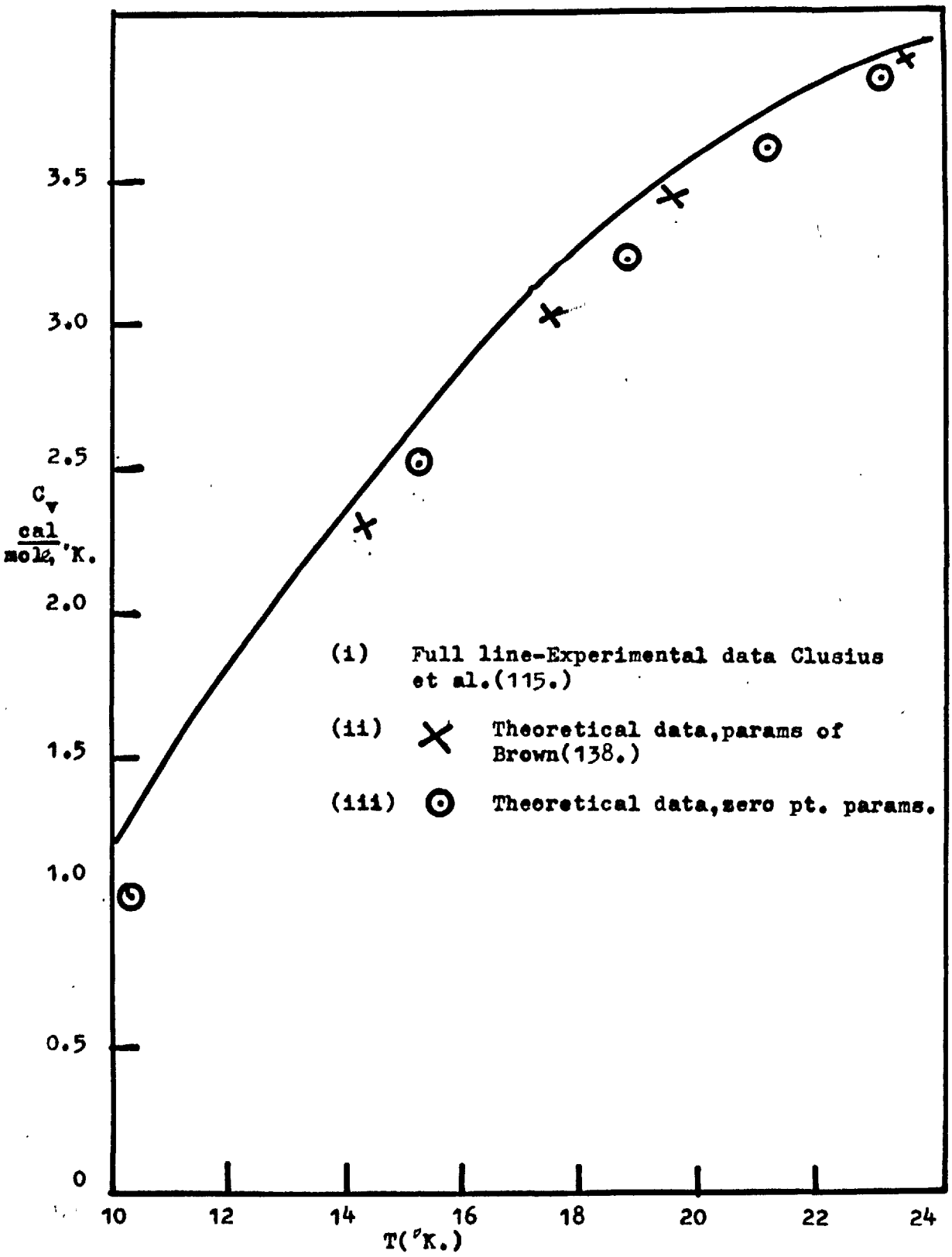

Fig 4.14 Solid Neon:-Heat capacity(C_p, cal/mole°K.) vs Temperature.

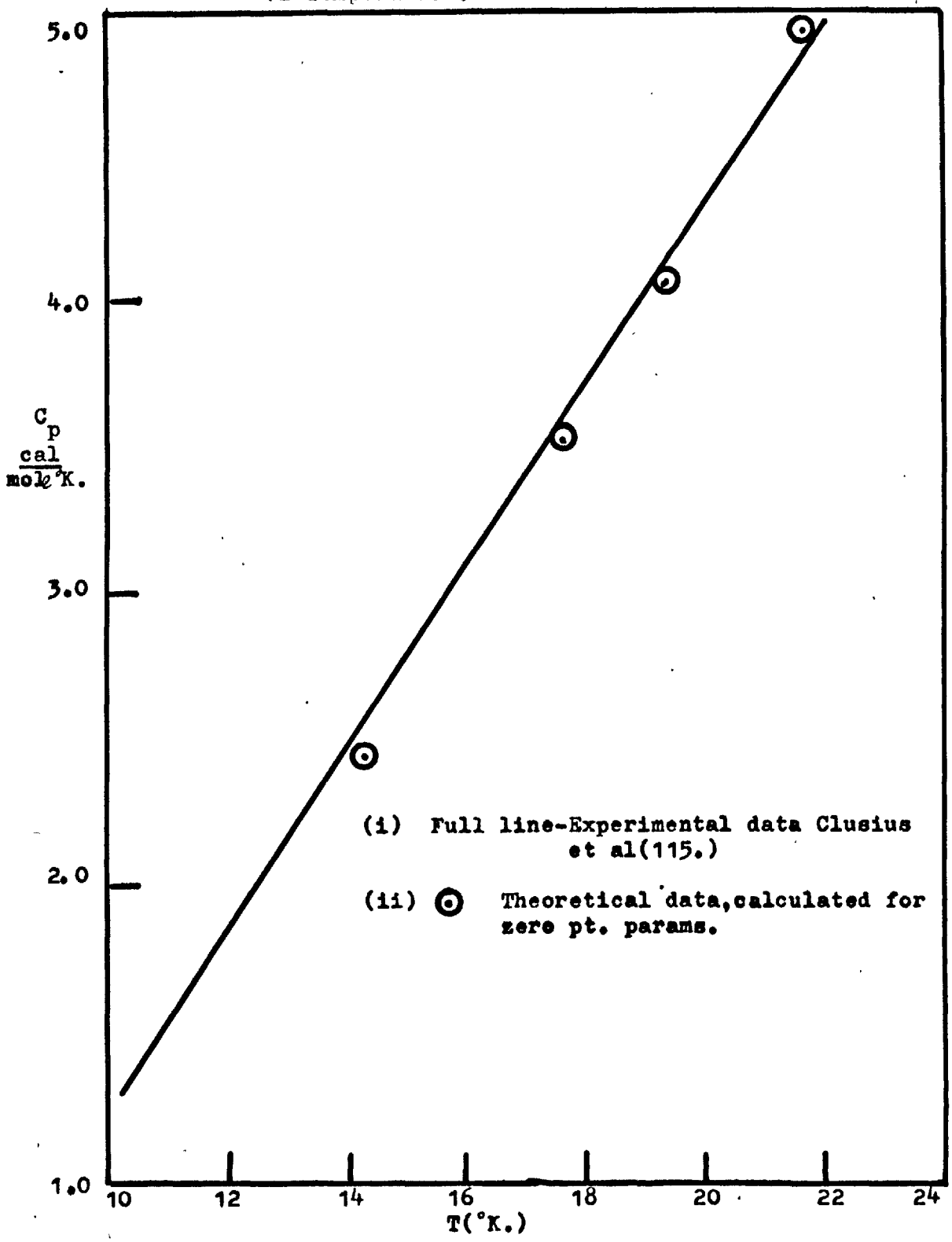

good and in particular no divergence is observed in the pre-melting region. However, since α is by definition $(1/V)(dV/dT)$ and the theoretical and experimental V vs T curves - Fig. (4.11) - are definitely not identical, this agreement may be somewhat fortuitius.

Finally we compare the theoretical and experimental total entropies in Fig. (4.15). As in the case of argon the experimental curve was calculated from heat capacity data using (4.4.2). The agreement is very similar to that found for argon, the theoretical curve exhibiting the lower entropy. It is of interest to observe that for both neon and argon the theoretical and experimental curves are roughly parallel and some 0.4 cal/deg.mole apart. Barker has recently stated that the entropy calculated by an Einstein model should be too low at high temperatures (94). He also mentioned that his calculations for the particular case of a Lennard-Jones potential indicated that the discrepancy was approximately equal to 0.2R (i.e. 0.39 cal/deg. mole). We therefore conclude that this discrepancy in entropy may be in the adoption of the Einstein model, to which, of all thermodynamic properties the entropy is most sensitive.

4.7 Discussion

The success of the cell model in predicting the thermodynamic properties of neon at high densities is unquestionable. Its exact allowance for anharmonicity is markedly superior

Fig 4.15 Solid Neon:-Entropy(S, cal/°K, mole.) vs Temperature.

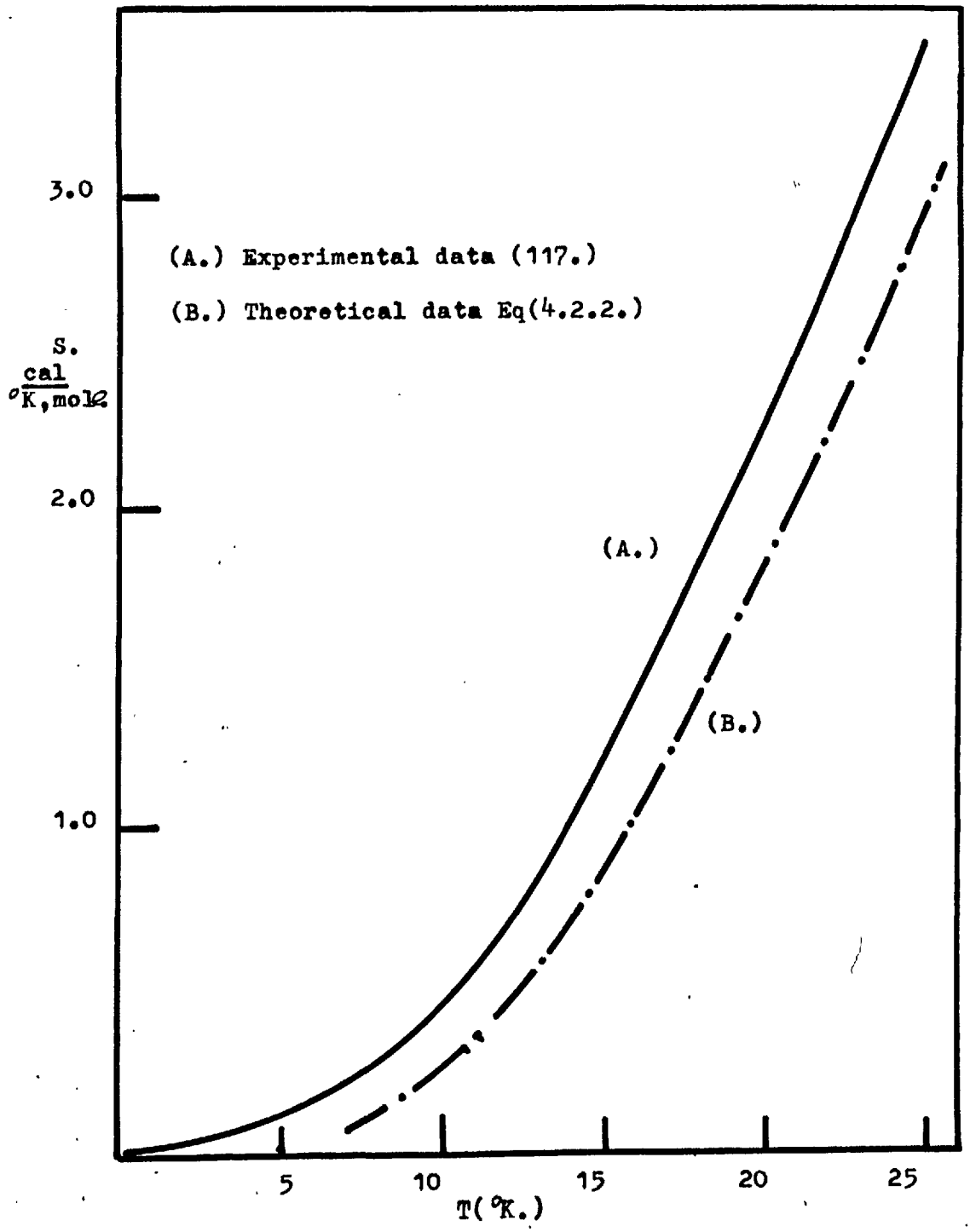

to anharmonic corrections developed for harmonic models. This point is ably illustrated by the results of Leech and Reissland, who, although improving their model, were unable to attain a satisfactory agreement between theory and experiment (for lattice constant as a function of temperature).

Further we might conclude from the results observed for both argon and neon that the 12:6 potential appears to be satisfactory for the prediction of solid state properties. However, when employing this potential at high densities it appears essential to derive the potential parameters from solid state data at $0^{o}K.$, accepting the fact that at these temperatures the second virial appears too insensitive a property for this purpose.

The observed agreement between theoretical and experimental data does not appear to warrant the use of non-additivity corrections, although it is possible that these effects may be adequately accounted for by the characterisation of the cell potential through zero point (multi-particle) data, i.e. instead of a strict pair potential we are in fact employing an "effective potential" that allows for multi-particle interactions.

The cell model employing a 12:6 interaction is therefore a much more versatile medium for investigating the solid inert gases than any method involving multi-parameter potentials, or anharmonic perturbation theories. The excellent prediction of temperature dependent properties argues well for the model, while the W.K.B method provides a rapid

and accurate method of summing the required energy levels and evaluating the compressibilities. The potential is known to be empirical but it is difficult to say whether any noted discrepencies can be directly attributed to this. We will now proceed to investigate the potential in a general n:n form and further to study the effect of the zero point parameters in predicting second virial behaviour.

CHAPTER 5.

The Bi-reciprocal potential and some considerations of The Second Virial Coefficient.

"For up and down and round says he
Go all appointed things
And losses on the roundabouts
Means profits on the swings."

P.R. Chalmers (1872-1940)

5.1 The Bi-reciprocal Potential.

Our investigations in the high density region have invariably used a 12:6 potential in the cell model. It is mathematically convenient and in its own right often more valuable than the rigorous forms described in (3.2). However, if we consider the potential as a general bi-reciprocal form of the n:n type, as originally proposed by Mie, an infinite number of possible n:n combinations exist This number can be rapidly narrowed by assuming the attractive power to be six, as suggested by the London concept (1.2). There can be little doubt that this is the correct asymptotic form. Under certain circumstances, generally at large intermolecular separations, it has been suggested that r^{-6} in the attractive term may be replaced by r^{-7} (143). In sharp contrast for the evidence available for fixing the index of attraction is the way in which the repulsive index is set at twelve (r^{-12}). Its justification has often been simply its mathematical convenience, or that it fits experimental results best, while it is widely held that any value of n between 10 and 14 will give adequate agreement between the calculated and experimental data for low energy properties such as the second virial coefficient. Any alteration of this index is reflected in a change of slope of the repulsive arm of the potential (see Fig (1.1)), and consequently alters the shape of the potential bowl. A lowering of the index "softens" the arm and generally

widens the bowl, while an increase $\underline{n} > 12$ "hardens" the potential making the repulsive arm considerably steeper.

A consideration of the potential in its general n:n form has been the concern of several workers. Their results are varied and their conclusions nebulous. However, these investigations deserve mention if only to indicate the degree of confusion surrounding the topic.

To find an optimum value of $\underline{n}$ Corner (67) employed second virial and Joule Thompson data. The optimum fit was obtained with $\underline{n}=12$, but also little difference was observed in varying $\underline{n}$ over the range mentioned previously ($10 < \underline{n} < 14$). These conclusions were supported in part by Zucker (77), who derived his parameters from solid state data and used them to fit the experimental properties of argon, krypton and neon. He obtained "best fit" values with $\underline{n}=12$ for Ar, Kr but for Ne $\underline{n}=14$.

Kihara and Koba (68) investigating the relative stability of crystal structure for the inert gases found that in order for cubic (f.c.c.) to be of lower energy than hexagonal (h.c.p.) a much broader well than that given by the 12:6 was needed. They examined the 9:6 (first used by Kihara in his study of third virials (86)), 7:6 and 12:6 but experienced little success, since this problem is now generally accepted as one of three body forces (3.3). Epstein and co-workers (144-146) also discussed the 9:6 potential in some length, justifying its use by the findings of Kihara and other investigations current at that time (147).

Their findings, however, did little to advance the cause of r^{-9} as the true repulsive term.

Perhaps the most rigorous investigation as to the value of the repulsive exponent was that of Brown and Rowlinson (148). This involved a thermodynamic discriminant, and evaluated $\underline{n}$ directly from experimental results without the need for statistical calculations. The discriminant, a specific function of pressure, temperature and several thermodynamic properties as well as $\underline{n}$ was shown to satisfy a "Schwarz inequality" at all pressures and temperatures and for all values of $\underline{n}$. This process set a lower bound for $\underline{n}$ such that $n \geqslant 13.3$ for liquid argon near the triple point. Due to quantum effects no test of the potential could be made in the solid region but it was considered that a bi-reciprocal potential should be satisfactory at low temperatures if $n > 13$.

The effect of varying $\underline{n}$ where $10 < n < 14$ was also studied by Horton and Leech (137) as part of a systematic examination of the inert gas solids (Ne, Ar, Kr, Xe), the potential parameters in each case being determined from solid state data. Machine calculations were performed to evaluate the specific heat and Gruneisen's constant "γ" and the temperature variation of these quantities studied. The conclusions drawn from this investigation are many and complex, and in fact almost too complex for a great deal of useful information to be obtained. The comparison of theoretical results with experimental data did, however, lead to the statement

"that no $\underline{m}$=12 calculation comes near experiment", a conclusion not in concordance with our findings for argon and neon (4.4, 4.6).

These arguments for and against various values of $\underline{m}$ do not appear to be in harmony - even in the case of the inert gas solids. It might well be that the often neglected anharmonicity or non-additivity corrections have unduly influenced the final results but the validity of this is difficult to estimate. Moreover, comparisons of predicted and experimental properties using these differing potentials have been generally directed towards second and third virial coefficients and only in the Lattice dynamical calculations of Horton and Leech has the variation of temperature dependent properties with $\underline{m}$ been studied. We therefore consider it of value to examine the effect of varying $\underline{m}$:$\underline{n}$ values in our cell model calculations and hence to ascertain the sensitivity of the predicted properties to this variation.

5.2 The General "n:n" for Solid Argon

We have studied the general $\underline{n}$:$\underline{n}$-model by extending our theoretical calculations for solid argon. The potentials we employed were 9:6, 18:6, 14:7, 28:7 (in addition to 12:6 - (4.4)). The 9:6 potential has already been mentioned; the 18:6 is somewhat more arbitrary but gives us a good indication as to the effect of "hardening" the repulsion with respect to

the 12:6. The 14:7 and the 28:7 are included to investigate the effect of altering the attractive term. They are not suggested as a logical description of the Ar-Ar interaction, and have only been seriously considered elsewhere (149) as approximations for the force field between quasi-spherical molecules. Together these potentials give a spectrum of variables that should indicate the value and sensitivity of the arbitary 12:6.

The general m:n potential may be written as:-

$$W(r) = (n\epsilon/m-n)(m/n)^{n/m-n}\left[(\sigma/r)^m - (\sigma/r)^n\right] \qquad (5.2.1)$$

where $m > n > 0$

This leads to a generalised cell potential which is an extension of (1.4.6). The potential is applied through the W.K.B. method (Appendix 1) and this may be done for any system of m:n values. The calculation of the compressibility for any quantum system however, requires the volume derivative of the static lattice term W*(0) (see (4.2.18)) and this was separately evaluated for each potential. Its calculation considers an infinite crystal and may be written (after Kihara and Koba (68)) as :-

$$W(0) = (N/2)C_{m,n}\epsilon\left\{(1/a^m)\sum_{n=1}^{\infty}(Z_n/N^{n/2}) - (1/a^n)\sum_{n=1}^{\infty}(Z_n/N^{n/2})\right\} \qquad (5.2.2.)$$

where $C_{m,n} = (m/m-n)(n/n)^{n/m-n} = f(m,n)$

Z_n = number of molecules in n^{th} shell.

$a_n = n^{\frac{1}{2}}a$ = distance of n^{th} shell.

Hence writing $V = Na^3/2^{\frac{1}{2}}$; $V_o = N\sigma^3$ and $V^* = V/V_o$

$$W^*(0) = (C_{n,n}/2)\left\{A.(2V^{*2})^{-n/6} - B(2V^{*2})^{-n/6}\right\} \qquad (5.2.3)$$

where $A = \sum_{n=1}^{\infty}(Z_n/N^{n/2})$; $B = \sum_{n=1}^{\infty}(Z_n/N^{n/2})$

therefore

$$V^*/2T^*(dW^*(0)/dV^*) = (C_{n,n}/12T^*)\left\{Bn(2V^{*2})^{-n/6} - An(2V^{*2})^{-n/6}\right\} \qquad (5.2.4)$$

A and B are evaluated by summing to convergence over a cubic close packed lattice giving the results in Table (5.1)

Table 5.1

n	$\sum_{n=1}^{\infty}(Z_n/N^{n/2})$
6	14,4539
7	13.3594
9	12.4920
12	12.1315
14	12.0589
18	12.0130
28	12.0036

The above values agree almost exactly with those obtained by Kihara and Koba who performed a summation and a partial integration.

Any treatment of the potential in its n:n form requires the evaluation of the L.J. parameters ϵ and σ. These were obtained from zero point data using the iterative method of Utting given in Appendix 2. The results are shown in Table (5.2) together with the 12:6 values obtained previously.

It should be noted from these tabulated values that whereas the change in σ is small (the ratio of σ(9:6) to

Table 5.2 Zero pt. parameters for some "m-n" potentials, applied to Argon.

Potential	$\epsilon/k(^{o}K)$	σ (Å)	$N\sigma^3$ cc/mole	Λ^*
9-6	105.2	3.398	23.62	0.199
12-6	120.4	3.398	23.62	0.185
18-6	132.4	3.429	24.27	0.176
14-7	141.0	3.405	23.77	0.177
28-7	156.9	3.479	25.35	0.159

Table 5.3 Virial parameters for some "m-n" potentials, obtained by "fitting" to Argon experimental data (124).

Potential	$\epsilon/k(^{o}K)$	σ(Å)	$N\sigma^3 \frac{cc}{mole}$	Λ^*
12-6	119.8	3.396	23.50	0.186
18-6	160.7	3.249	20.65	0.168
14-7	170.5	3.231	20.50	0.164
28-7	249.0	3.028	16.71	0.145

σ(12:6) is 1.004) the depth of the potential minimum drops sharply as the repulsion "hardens".

It was also considered of interest to calculate ϵ and σ from second virial data for some n:n potentials using the "best fit" method and the data in the same temperature range as studied previously (4,4). These parameters are presented in Table (5.3). The virial values are in complete variance with the zero point parameters. Preliminary calculations indicated that apart from 12:6 they appeared totally unable to interpret theoretical data realistically and they were therefore rejected.

The investigation of the model with a general n:n potential was effected by computing the reduced thermodynamic properties of argon at the Λ^* for each potential and then converting the reduced data to unreduced units by use of the appropriate parameters.

Figs (5.1) and (5.1a) show the results of molar volume V(cc/mole) against temperature for the five potentials. The most significant factor appears to be the increase in ϵ/k by the hardening of the repulsive wall. For the n:6 potential the similarity in σ between the 9:6 and 12:6 is completely overshadowed by this effect, and even with a more marked increase in σ from 12:6 to 18:6 the well depth again appears to be all important. The alteration of the attractive (i.e. r^{-6} to r^{-7}) similarly affects predicted values and this potential suffers in a similar way to the n:6 in going from 14:7 to 28:7.

Fig 5.1a Solid Argon:-Molar volume(V, cm^3/molℓ) vs Temperature, for general "m-n" potentials.

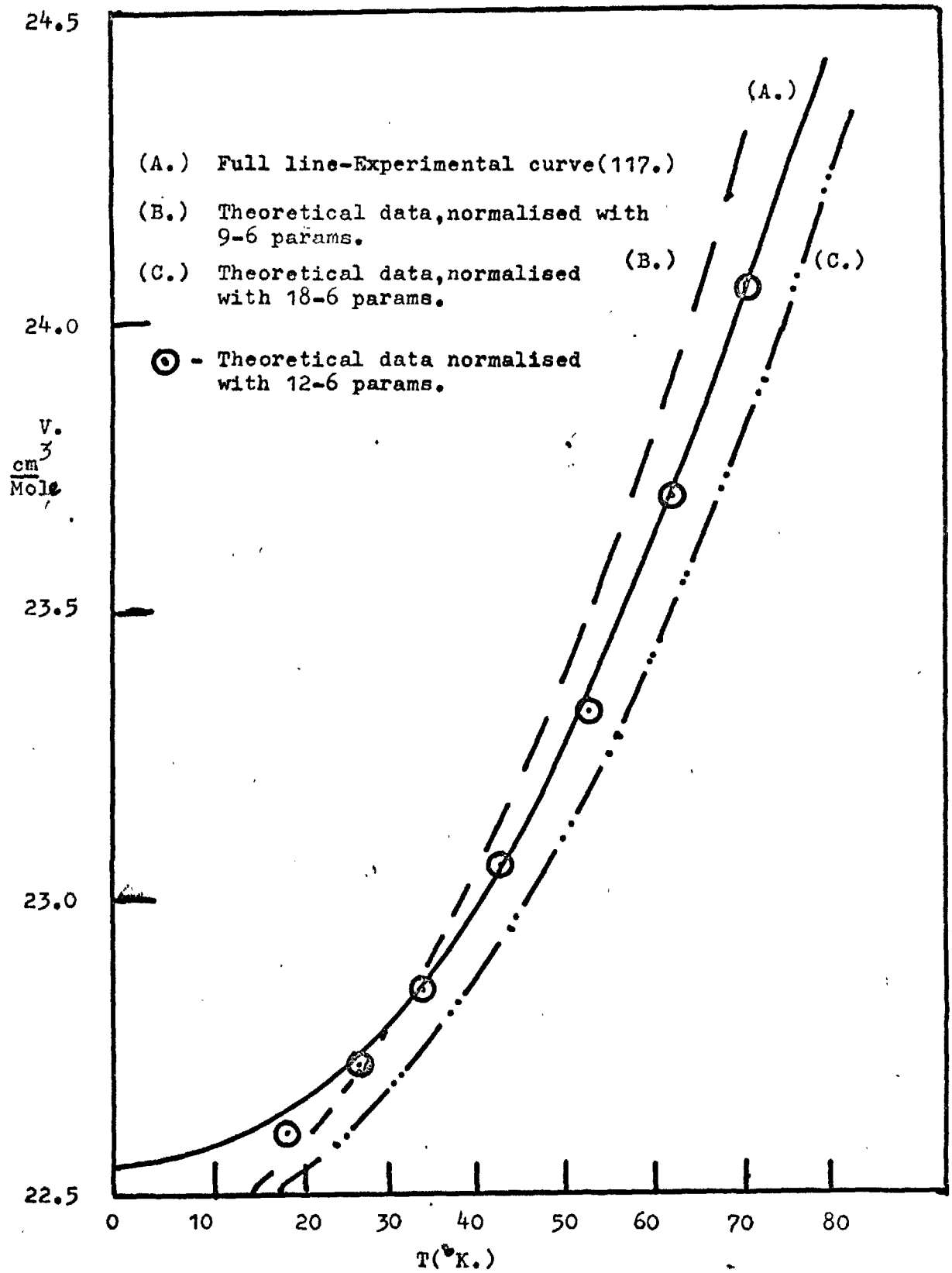

Fig 5.1b Solid Argon:-Molar volume(V, cm^3/mole) vs Temperature, for general "m-n" potentials.

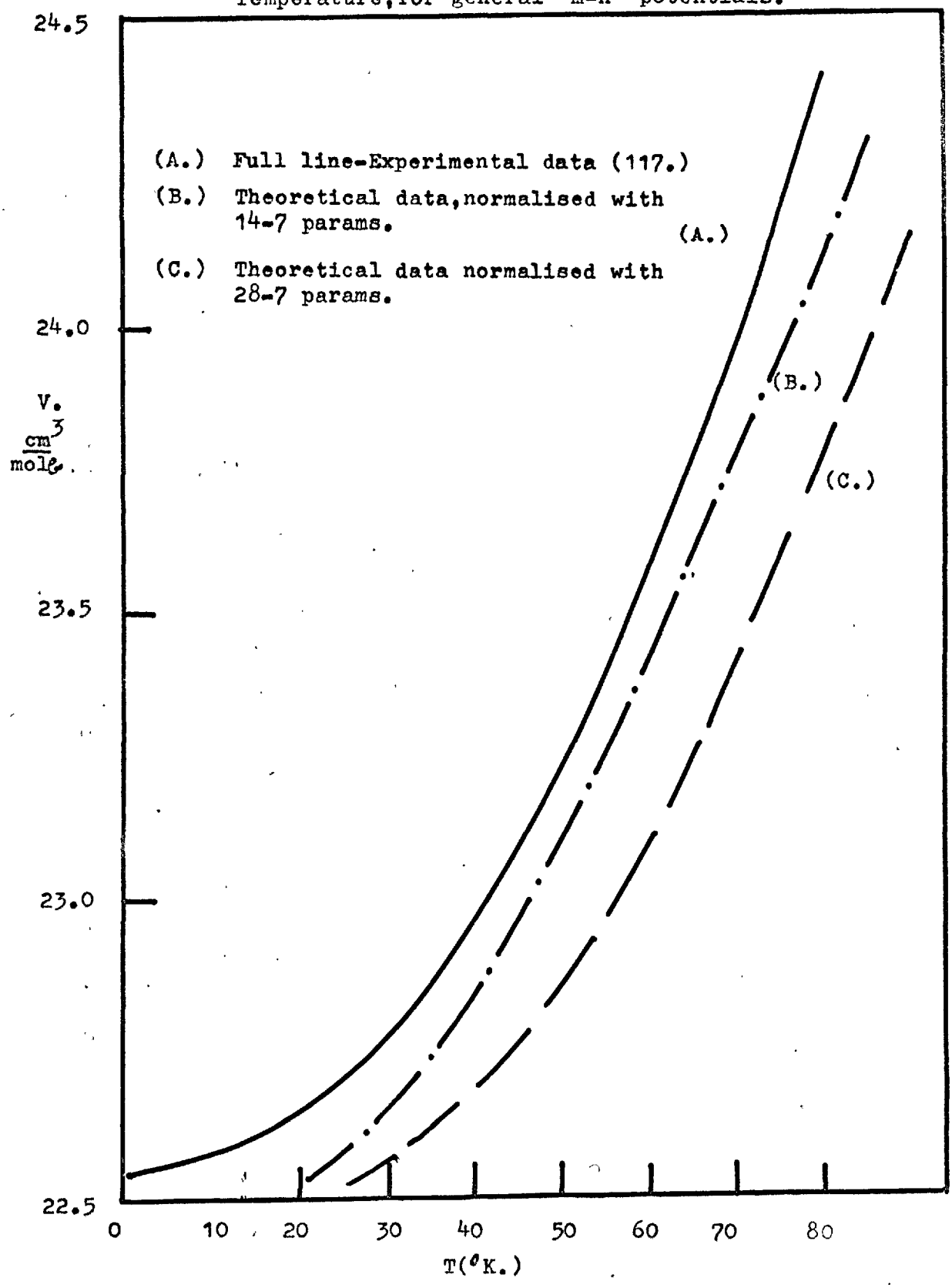

The comparison of the theoretical specific heat C_v with converted experimental data (4.4.1) is shown in Figs (5.2) and (5.2a). Since we are primarily concerned with a comparison of theoretical values, C_v is clearly a better medium than C_p. In this case the theoretical plots are entirely dependent on the ϵ/k values (this is not strictly true since the reduced data depends on Λ^*). Once again the effect noticed in Fig (5.1) is emphasised and each potential provides a unique prediction of experimental data.

In the case of argon it was not felt necessary to pursue this investigation any further. The indications of the molar volume and specific heat vs temperature plots are indisputable. They are that the alteration of the shape of the potential by hardening or softening the repulsive wall, or by making the attraction a shorter range force, drastically affects the predicted properties. Further the 12:6 potential is far and above the best form to predict experimental properties. Other investigations of an n:n potential for neon (113) have resulted in similar conclusions (cf. Zucker (77) n=14).

We therefore underline the points made in (4.7) with the rider that the potential for the anharmonic quantum cell model must be the L.J. 12:6. Further we emphasise that the study of high density phenomena must utilise parameters derived from solid state properties and that for this phase of matter parameters obtained from second virial measurements are of dubious value.

Fig 5.2a Solid Argon:-Heat capacity(C_v,cal/mol°K.) vs Temperature, for general "m-n" potentials.

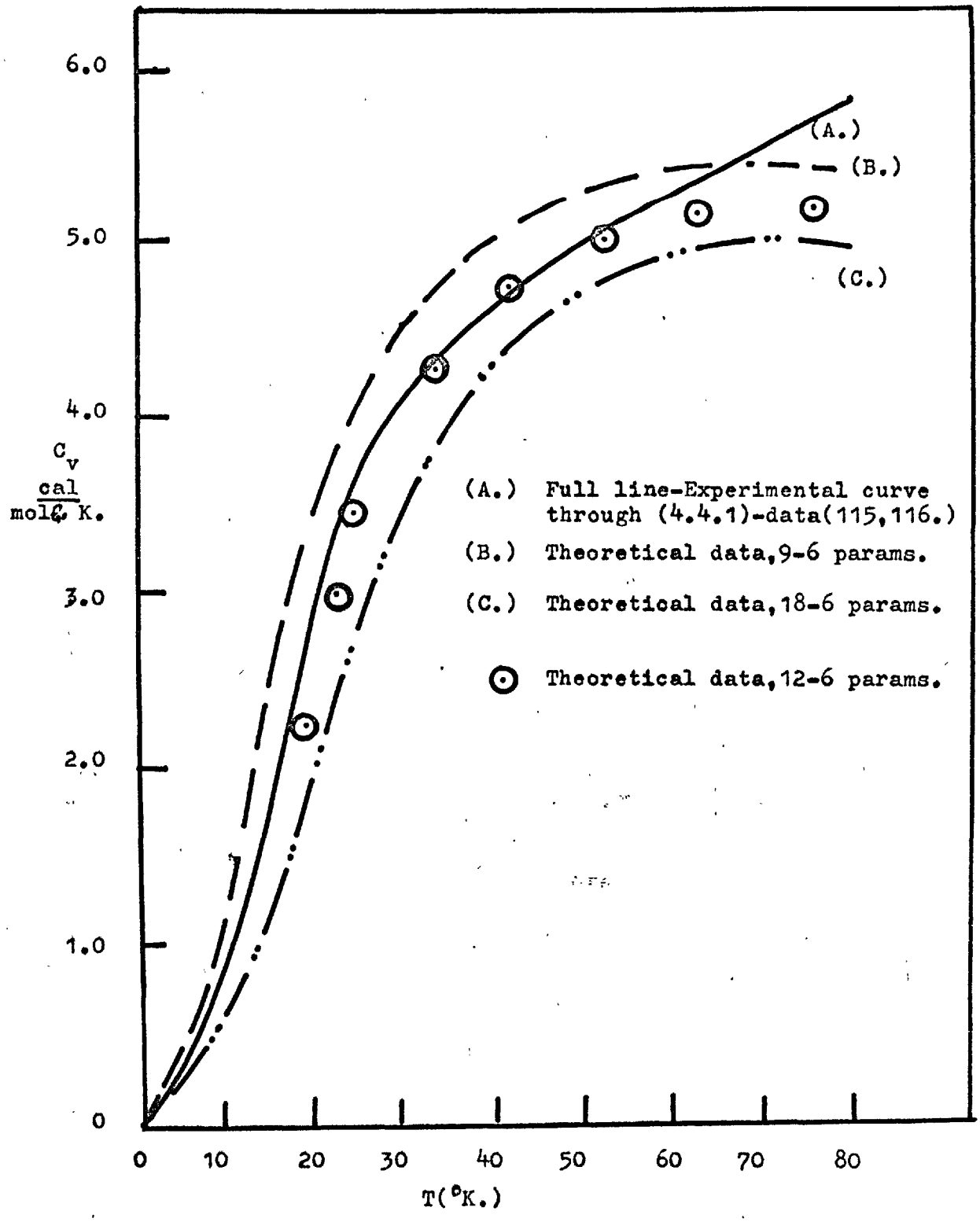

Fig 5.2b Solid Argon:-Heat capacity(C_v,cal/mol$_g$ K.) vs Temperature,for general "m-n" potentials.

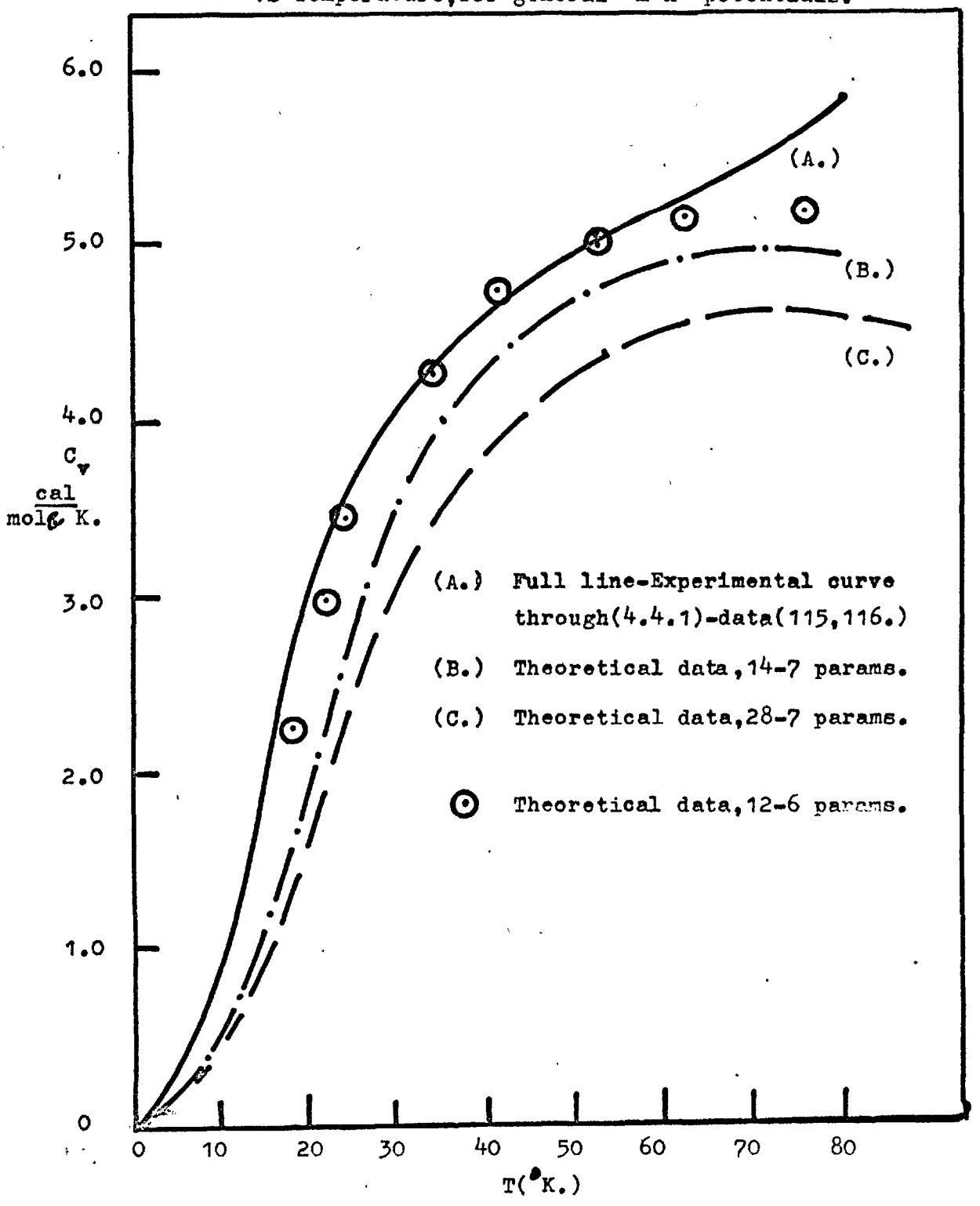

5.3 The Second Virial Coefficient.

In view of the conclusions reached in the previous section and in Chapter 4. it was decided to make a brief but concise examination of second virial coefficient data using zero point parameters and the pair potential. This test of these properties in predicting a two body interaction could yield more information (especially as to the validity of the potential) if the temperature derivative of the second virial and the third virial coefficient were studied. However, the amount of experimental data available especially for the latter property are limited and this investigation is therefore confined to the prediction of reduced second virials.

From the quantum partition function written as the Slater sum for two particles:-

$$Z_{qu}^{(2)} = \int \sum_i \psi_i^* \exp(-\lambda_i/kT)\,\psi_i \, dq^{(2)} \qquad (5.3.1)$$

the second virial coefficient B(T) is developed as:-

$$B(T) = (N/2)\int \{1 - S(q)\}\, dq \qquad (5.3.2)$$

and $$S(q) = \sum_i \psi_i^* \exp(-H_i/kT)\psi_i \qquad (5.3.3)$$

The expansion of (5.3.3) in terms of the pair potential W(r) and the integration of (5.3.2) leads to the series representation of the quantum second virial coefficient:-

$$B(T) = B_{cl}(T) + (h^2/m)B_I(T) + (h^2/m)^2 B_{II}(T) + \ldots . \qquad (5.3.4)$$

where $$B_{cl} = -2\pi N \int_0^\infty \{(\exp(-W(r)/kT) - 1)\} r^2 . dr$$

$$B_I = 2\pi N (48\,\pi^2 k^3 T^3)^{-1} \int_0^\infty \exp(-W(r)/kT)(dW(r)/dr)^2 r^2 dr$$

etc (150)

A further term is included to account for Bose or Fermi statistics obeyed by the quantum gas and the final reduced form may be written as:-

$$B^*(T^*) = (B^*_{cl} + \Lambda^{*2}B^*_{I} + \Lambda^{*4}B^*_{II} + ...) \pm \Lambda^{*3}B_o \quad (5.3.5)$$

where $B^*_i = B_i/b_o$ and $b_o = \frac{2}{3}\pi N\sigma^3$

The values of B^*_{cl}, B^*_I etc have been tabulated (150,151). They may be calculated by numerical integration or by the use of gamma functions, assuming an n:n potential. Hence, knowing Λ^*, the reduced second virial can be obtained for any quantum particle (for a more complete treatment see (150,152).)

Fig (5.3) shows the comparison of the theoretical reduced second virial curve (5.3.5) for argon with the reduced experimental data of Fender and Halsey (64) $< 110^oK$. and of Michels et al (153) $> 110^oK$. The experimental data is reduced both by zero point parameters and by the values of Boato (136). The agreement in the low temperature region $T^* < 1$ is not substantially improved. In Fig (5.4) a similar comparison is made for neon, but over a wider temperature range. The theoretical curve was calculated for $\Lambda^*=0.584$(the zero point value) and the experimental data of Michels and co-workers (154) reduced with zero point parameters and also those calculated by Nicholson and Schneider (see Table 4.3). The change in agreement for the different ϵ and σ values is insignificant (reflected by the change in Λ^*) and although the zero point parameters reduce the data to a slightly better degree, the curve is

Reduced Second virial coefficient of Argon vs Reduced temperature.

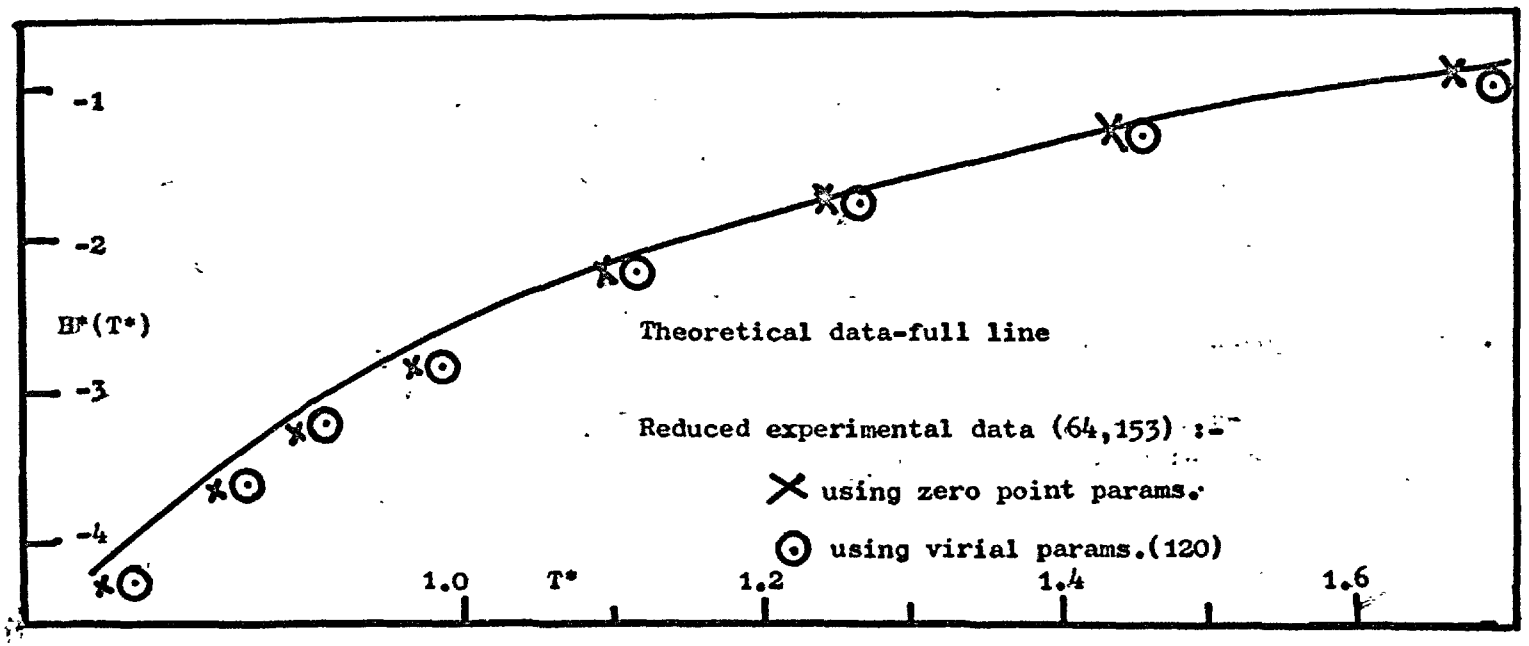

Fig 5.3

Reduced Second virial coefficient of Neon vs Reduced temperature.

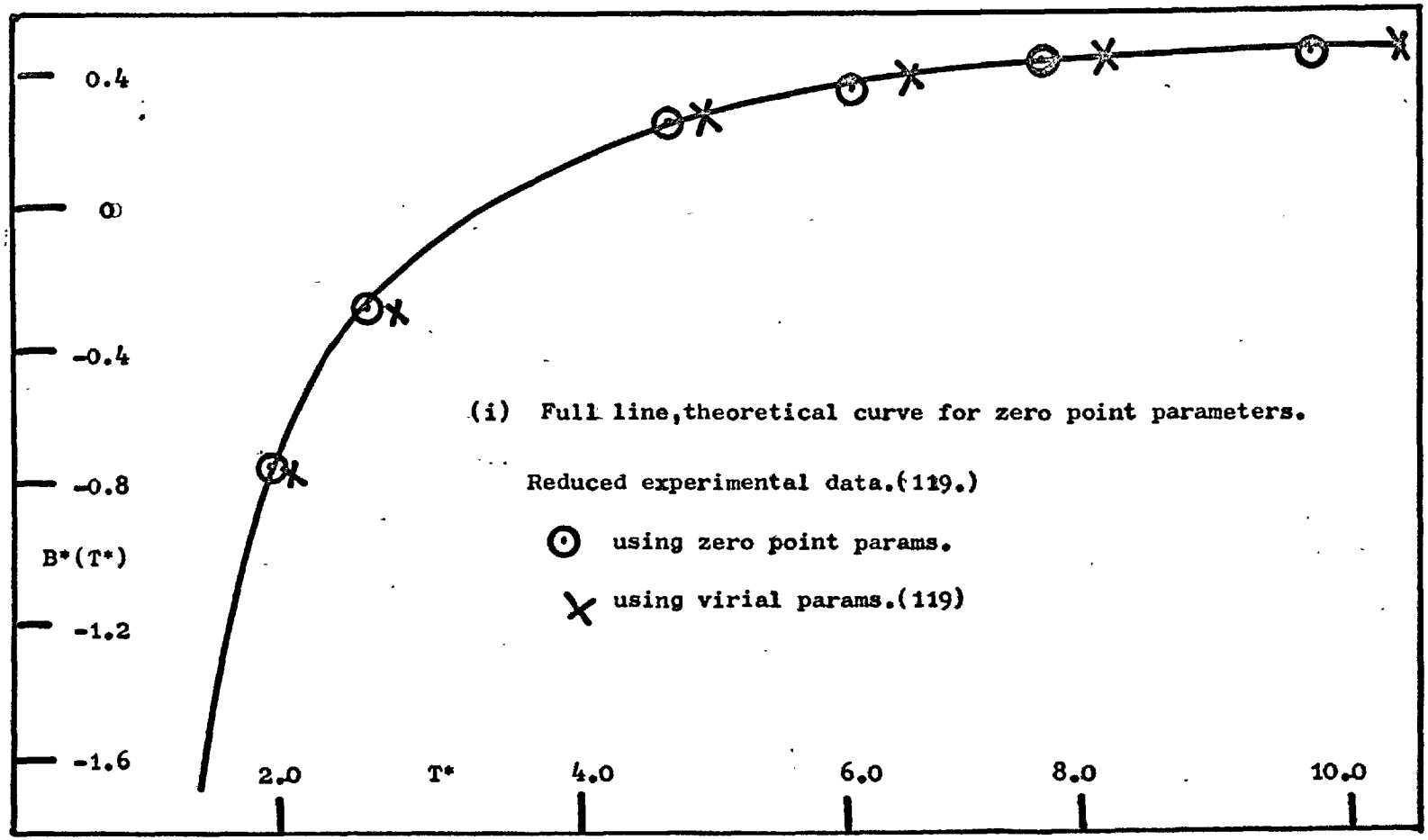

Fig 5.4

relatively insensitive to the alterations in ϵ and σ (especially when the comparisons of 4.4, 4.6 and 5.2 are borne in mind.)

In the case of hydrogen and deuterium, zero point studies yield parameters, markedly different from those obtained from virial data (Table 4.1). It should also be noted that not only were these parameters different but that those for D_2 were smaller than those for H_2, a trend opposite from that found by Michels in his examination of second virial data. In Figs (5.5) & (5.6) the experimental data of Michels et al is reduced with the appropriate zero point parameters and compared with the theoretical curves from (5.3.5) for H_2 and D_2 respectively. Agreement is quite acceptable and tallies reasonably well with that found by Michels who used a more rigorous equation and his own virial parameters.

The results of this section, therefore indicate that parameters derived from zero point data are not invalid in a consideration of the gas phase. However, bearing in mind the insensitivity of the second virial coefficient, a factor ably illustrated in Figs (5.3) & (5.4), it would be fair to say that they do not show a marked improvement over values obtained from virial data itself. The use of the multi-particle situation at $0^{\circ}K$. to characterise parameters for high density work must be beyond dispute. The carrying over of these parameters to describe the fluid and gaseous states is a step that can only be undertaken with caution, and only in the light of more evidence than is at present available.

Reduced Second virial coefficient of Hydrogen vs Reduced temperature.

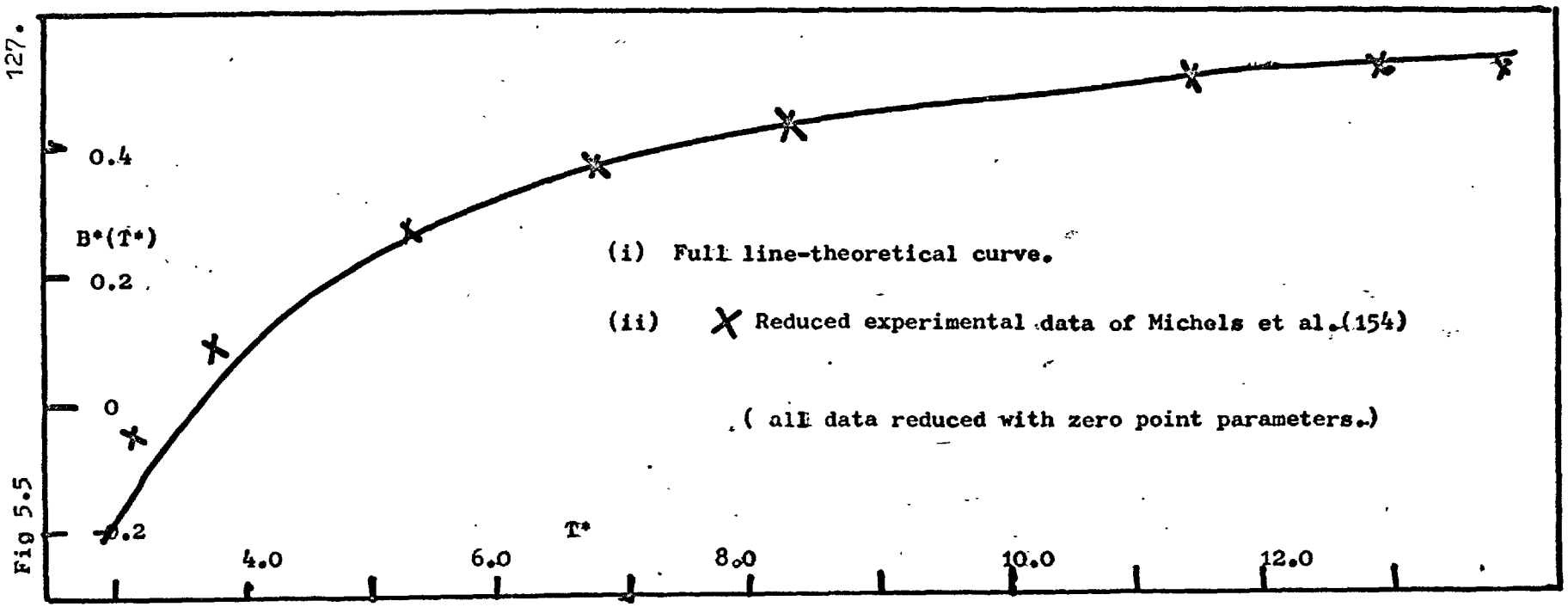

Fig 5.5

Reduced second virial coefficient of Deuterium vs Reduced temperature.

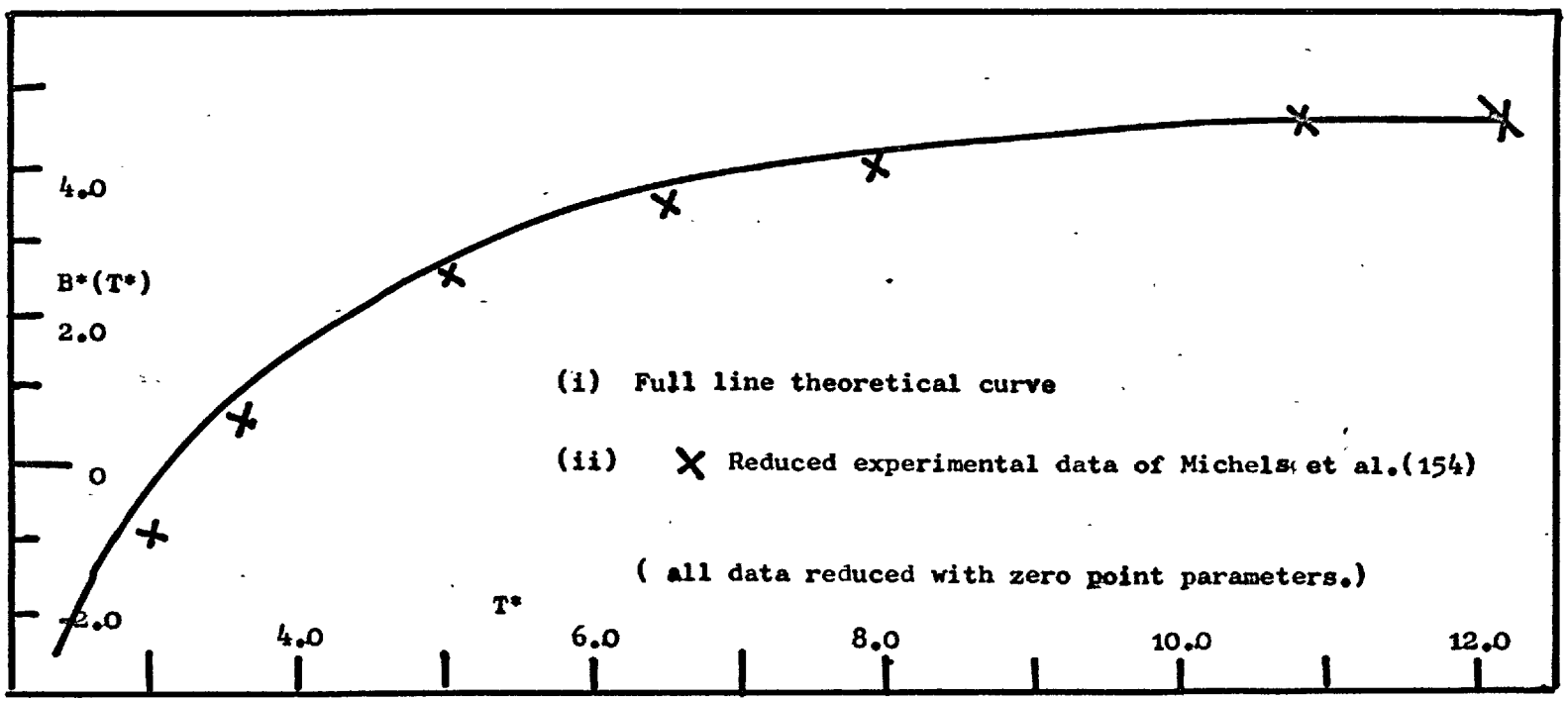

Fig 5.6

CHAPTER 6.

Quantum Corresponding States.

"Oh let us never, never doubt
what nobody is sure about."

Hilaire Belloc (1870-1953)

6.1 The Uniform Potential Model

The success of the cell model for quantum solids at low temperatures and its relative merits in a pair interaction situation cannot and are not carried over into the fluid region. The nemesis that greets any such straightfoward attempt is inherently due to the assumed static lattice structure or to the form of the potential itself. The first pitfall can, as we will show, be avoided under certain circumstances. The second problem, that of the potential, especially that employed in quantum statistics is almost impossible to deal with on a rigorous basis. Any more realistic picture of the pair interaction must complex the mathematics involved, sometimes to an impracticable degree. Our other alternative is to simplify the potential, a process that of necessity must be of an arbitary nature. However, it can enable the wave equation to be solved quickly and easily. One application of this, first proposed by Prigogine and Mathot (156) and developed by Hamann and David (102), is to regard the cell potential as uniform but rising discontinuiously infinate at some displacement r_m from the cell centre.

$$\left.\begin{aligned} \text{i.e}\quad W(r) &= W(0) \qquad r < r_m \\ W(r) &= \infty \qquad\quad r > r_m \end{aligned}\right\} \qquad (6.1.1)$$

This theory was put onto a quantum basis by Hillier and Walkley (157). We will only mention here the parts of this treatment relative to the present discussion, for a more

complete presentation the reader is refered to Appendix 6.

The classical expression for the cell theory configurational integral (1.3.5) leads to the compressibility term.

$$(PV/NkT)_{class.} = (d\ln v_f^*/dV^*) - (V^*/2T^*)(dW^*(0)/dV^*) \qquad (6.1.2)$$

where $v_f^* = v_f/N\sigma^3$ and v_f is given by (1.3.6)

If the limit r_n is chosen as the point at which the potential W(r) is numerically zero, then a simple relationship between y_n^* $(=(r_n/a)^2)$ and the reduced volume is found. We may then write (6.1.2) as:-

$$C_{class} = (1 + 1.5V^*(d\ln y_n^*/dV^*) - (V^*/2T^*)(dW^*(0)/dV^*)) \qquad (6.1.3)$$

where (PV/NkT) = compressibility = C.

When treated on a quantum basis (see A.6) analytical solutions to the spherical cell potential wave equation are possible and the partition function may be developed as:-

$$C = \frac{\sum_l (2l+1)(D^*C_l^*/T^*V^{*\frac{2}{3}}y_n^*)(V^*d\ln y_n^*/dV^* + \frac{2}{3}).\exp(-D^*C_l^*/T^*V^{*\frac{2}{3}}y_n^*)}{\sum_l (2l+1).\exp(-D^*C_l^*/T^*V^{*\frac{2}{3}}y_n^*)} - (V^*/2T^*)(dW^*(0)/dV^*) \qquad (6.1.4)$$

where $D^* = h^2/8m\epsilon\sigma^2 2^{\frac{4}{3}}$ and C_l^* is obtained numerically from the zeros of half integral Bessel functions.

6.2 The Quantum Correction Term.

The uniform potential and quantum cell model (4.2) equations of state are developed through a numerical determination of the eigen values arising from the wave equation. We have mentioned earlier the work of Lunbeck

and De Boer (97) which sprung from ideas by Kirkwood (158) and Uhlenbeck (159). In these the Slater sum (4.1.5) was transformed to the integral over phase space so

$$Z_{qu} = \int_0^\infty S(r).4\pi r^2.dr \qquad (6.2.1)$$

$$\text{where } S(r) = \sum_i |\psi_i|^2 \exp(-\lambda_i/kT) \qquad (6.2.2)$$

$$= \sum_i \psi_i^* \exp(-H_{op}/kT)\,\psi_i \qquad (6.2.3)$$

and terms in $F(r) = \exp(-H_{op}/kT)\,\psi_r$ satisfy the equation

$$H_{op}.F = kT^2(dF/dT) \qquad (6.2.4)$$

By a successive approximation solution and replacement in (6.2.1) followed by partial integration the partition function was expanded to give

$$Z_{qu} = (nkT^2/2\pi h^2) \int \exp(-W(r)/kT).4\pi r^2 dr \left\{ 1 - \frac{h^2 A(r,T)}{nkTr^2} + \frac{h^4 B(r,T)}{n^2 k^2 T^2 r^4} + \ldots\ldots\ldots \right\} \qquad (6.2.5)$$

where $A(r,T) = (rW'/kT)^2/24(2\pi)^2$

$$B(r,T) = \frac{(r^2W''/kT)^2 + 2(rW'/kT)^2 + 10/9(rW'/kT)^3 - 3/56(rW'/kT)^4}{480(2\pi)^4}$$

The development of Z_{qu} is comprehensively described in the references quoted above. Our interest in such an approach is limited to the fact that through it the free energy of the system may be written as a power series in the quantum parameter.

$$F^* = F_o^* + \Lambda^{*2} F_1^* + \Lambda^{*4} F_2^* + \ldots\ldots \qquad (6.2.6)$$

This expansion when applied to systems of high mass reduces to the single classical term F_o^*. The equation of state may be expressed in a similar manner so:-

$$P^* = P_o^* + \Lambda^{*2} P_1^* + \Lambda^{*4} P_2^* + \ldots\ldots \qquad (6.2.7)$$

where $P_i^* = -(dF_i^*/dV^*)_T$

The first term in (6.2.7) is the classical reduced pressure having no Λ^* dependence. The remaining terms in the series represent the "quantum correction" i.e. that pressure in excess of the classical value. We now propose to use this correction term in a corresponding states treatment at fluid densities.

6.3 The Cell theory and Corresponding States.

The problem of a long range order assumption in any fluid theory may now be examined in closer detail. Calculations show that the effect of this lattice array upon the classical equation of state (6.1.2) is such that the inclusion of further neighbours beyond the first shell (at radius $\underline{a}$) has only a minor effect on the free volume integral. The inclusion of further neighbours has however a drastic effect upon the static lattice term and upon its volume derivative dW(0)/dV. It would therefore appear that the effect of a lattice structure upon the equation of state arises almost entirely through the static lattice term. These criticisms apply exactly to the quantum cell model as was illustrated by Hillier and Walkley (106) in their investigation of hydrogen and deuterium and similarly, since it is based on the same model, must also be valid

for any examination of a uniform potential theory.

We now reintroduce the idea first fowarded by Hamann (101,102) that the quantum equation of state may be regarded as a composite term made up of a classical term and a quantum correction term. If this classical term is represented by actual experimental data then the latter quantum correction term may be compounded theoetically from the cell model. Hence if this term is given by P_{theory} then from (6.1.2) and (4.2.12)

$$P_{theory} = T^*(d\ln \sum_i \exp(-\lambda_i / T^*)/dV^* - d\ln v_f^*/dV^*) \qquad (6.3.1)$$

The quantum pressure for any given T^*, V^* and Λ^* is therefore

$$P^*_{quantum} = P^*_{classical} + P^*_{theory} \qquad (6.3.2)$$

As will be seen from (6.3.1) the correction term is completly independent of the static lattice concept and depends solely on the free volume terms that are relatively insensitive to further neighbour contributions. Thus the development of the quantum correction allows a far better investigation of a single particle theory at fluid densities.

We now proceed to apply our "corresponding states" approach to quantum systems. These calculations are carried out in reduced variables and therefore prior to any calculations two decisions are required. Foremost the values of the reduction parameters used on any experimental data must be determined and secondly the choice of a system to represent the experimental classical term in (6.3.2) must be made. The first problem raises several debatable points. To date

the majority of our calculations have employed L.J. parameters derived from zero point data. The use of these multi-particle parameters in fluid state calculations is of interest but also of dubious validity . Another matter that must be considered in this context is that although the P_{expt} and the P_{theory} terms are evaluated at similar T^*, their unreduced values cover widely differing temperature ranges. Because of these arguements it was decided to use virial data to calculate the parameters over the temperature range from which the experimental results were obtained.

The second problem, that of choosing a classical system, was solved by using experimental data for argon (160), since it had previously been observed that this exhibited little departure from classical cell theory data for $T^* > 1$ at fluid densities (106). The choice of parameters to reduce this data was obtained by a Newton fit (identical to that used in (4.4)) which gave $\epsilon/k = 119.8^{\circ}K.$, and $N\sigma^3 = 23.71$ cc/mole.

6.4 Theoretical Results.

(Experimental and theoretical data used to construct relevant figures are given in Appendix 5)

The compressibilities of hydrogen and deuterium at $T^* = 1.748$ were derived by writing (6.3.2) as

$$C_{qu} = C_{argon} + (C_{qu} - C_{class})_{theory} \qquad (6.4.1)$$

Where $C = (PV/NkT)$; C_{argon} is from the data of Levelt (160) and C_{qu} , C_{cl} are derived from (4.2.16) and (4.2.17) for the 12:6 model and from (6.1.4) and (6.1.3) for the U.P. model respectively.

The resulting compressibilities are plotted against V^* in Figs (6.1) and (6.2) and compared to the experimental data of Hamann (102). In both instances the good agreement of the Uniform Potential (henceforth U.P.) approximation against that of the 12:6 isotherm is well illustrated. In Figs (6.3) and (6.4) a comparison is made of the theoretical isotherm using only the U.P. difference at $T^* = 3,32$ with the experimental data of Michels et al (161). Once again good agreement is observed.

A more testing system than hydrogen and deuterium is provided by helium. This exhibits enhanced departure from classical corresponding states, which is demonstrated by its high Λ^* value ($\Lambda^*=2.674$) and its small fundimental parameters. In Fig (6.5) the experimental data of Buchmann (162) for helium at $T^* = 1.996$ is shown as compared to the U.P. and 12:6 correction term isotherms. The data for the U.P. model are again in better agreement than those from the 12:6 calculations but not as good as observed for H_2 and D_2 This increased discrepancy might arise from treating helium by an over-simplified quantum theory. The latter is unable to take account of behaviour other than that of Boltzmann statistics which, in the case of helium, could well be

Fig 6.1 Hydrogen:-Compressibility factor isotherms for $T^*=1.748$.

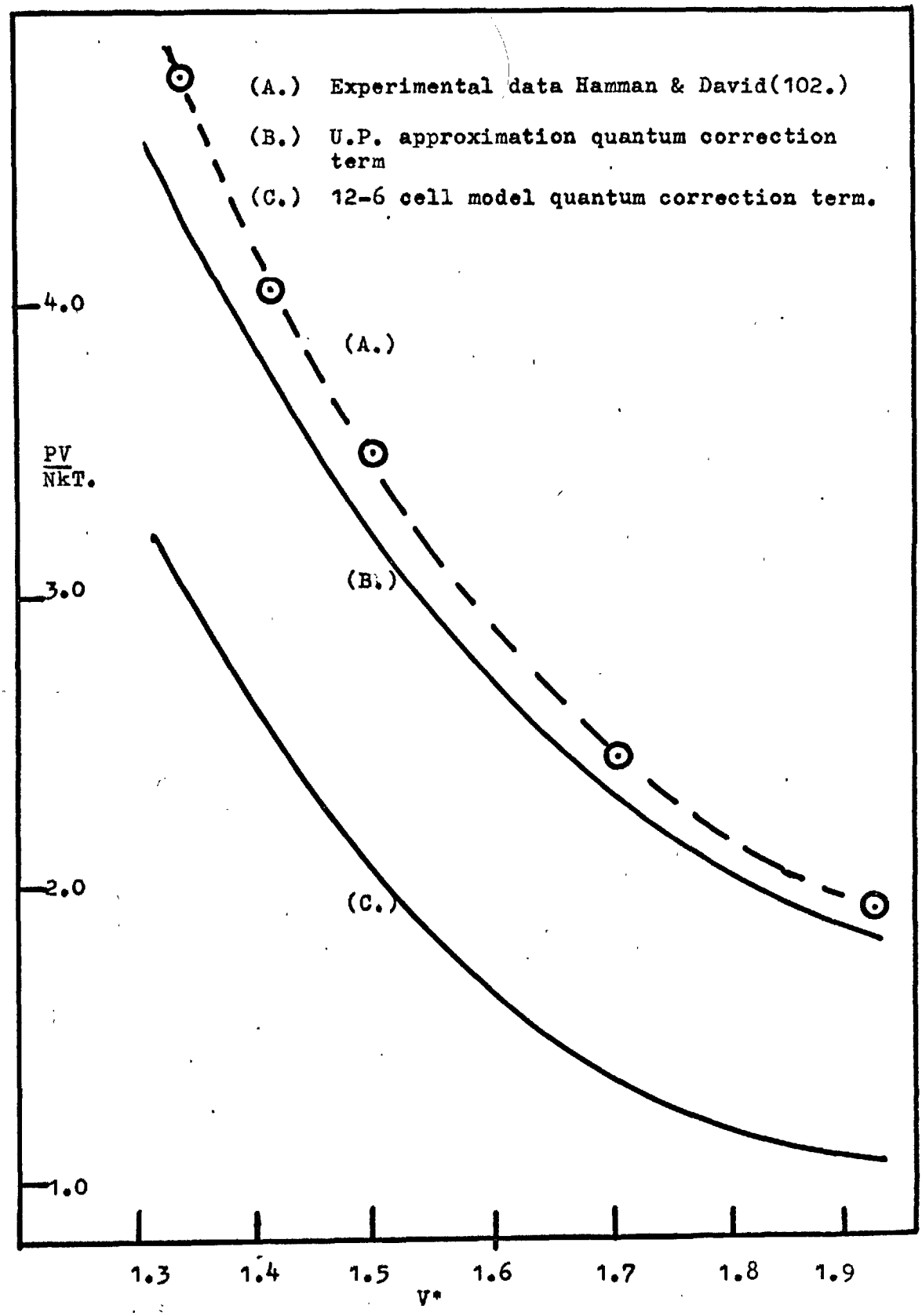

Deuterium Compressibility factor isotherm T* = 1.748.

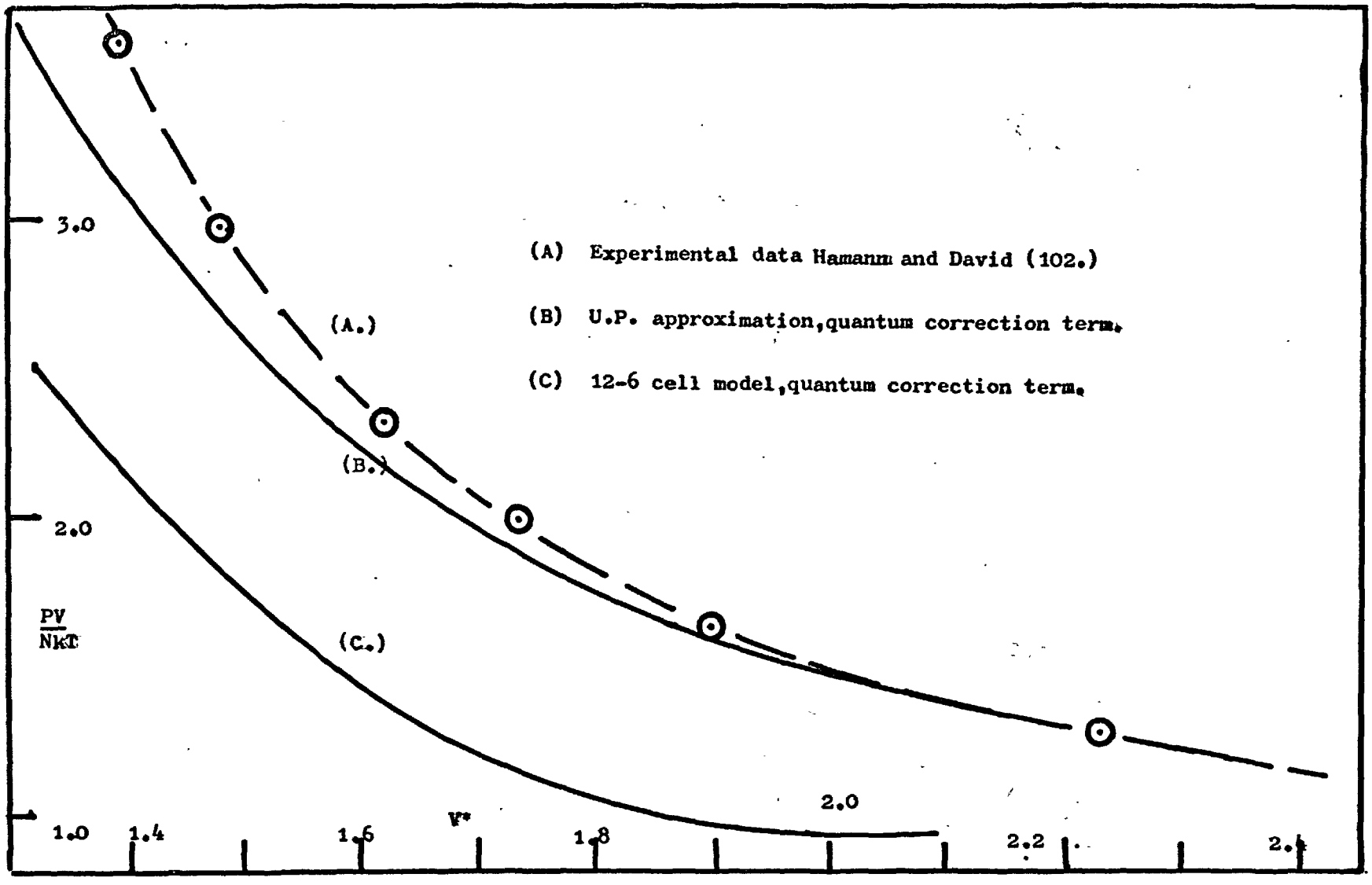

Fig 6.2

Hydrogen -Compressibility factor isotherms, $T^* = 3.32$.

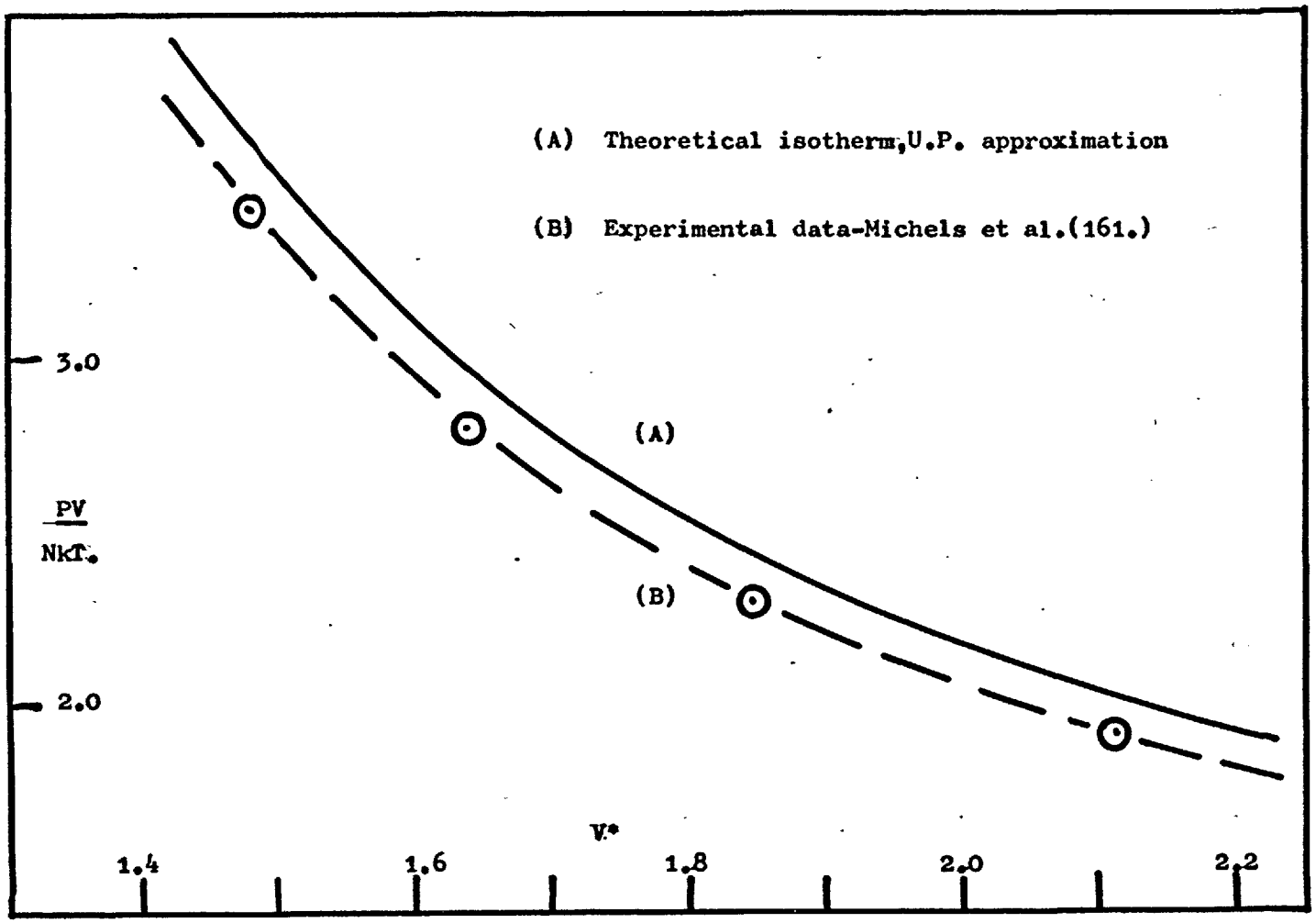

Fig 6.3

Deuterium-Compressibility factor isotherm T*=3.32

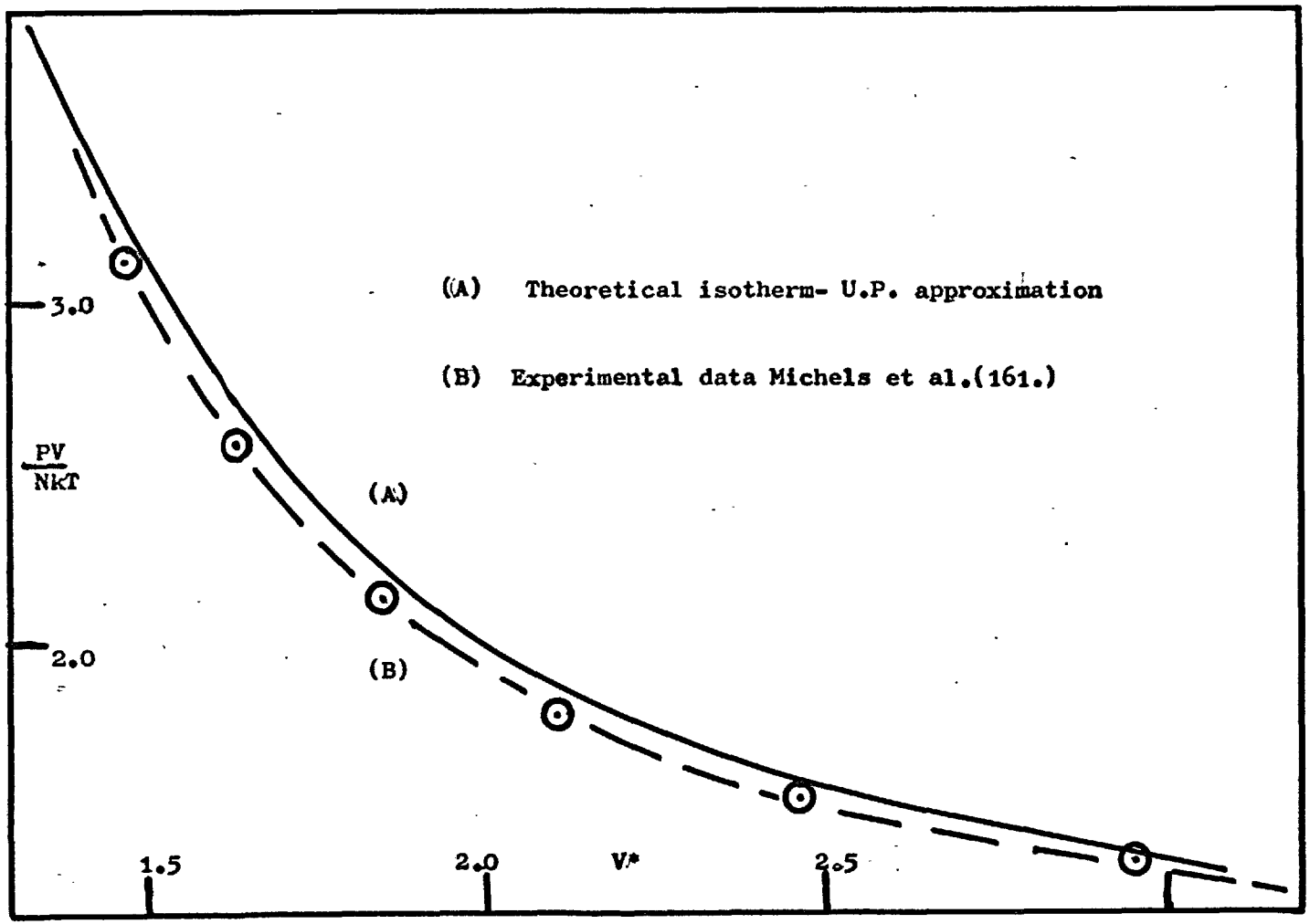

Fig 6.4

Helium compressibility factor isotherm T*= 1.996

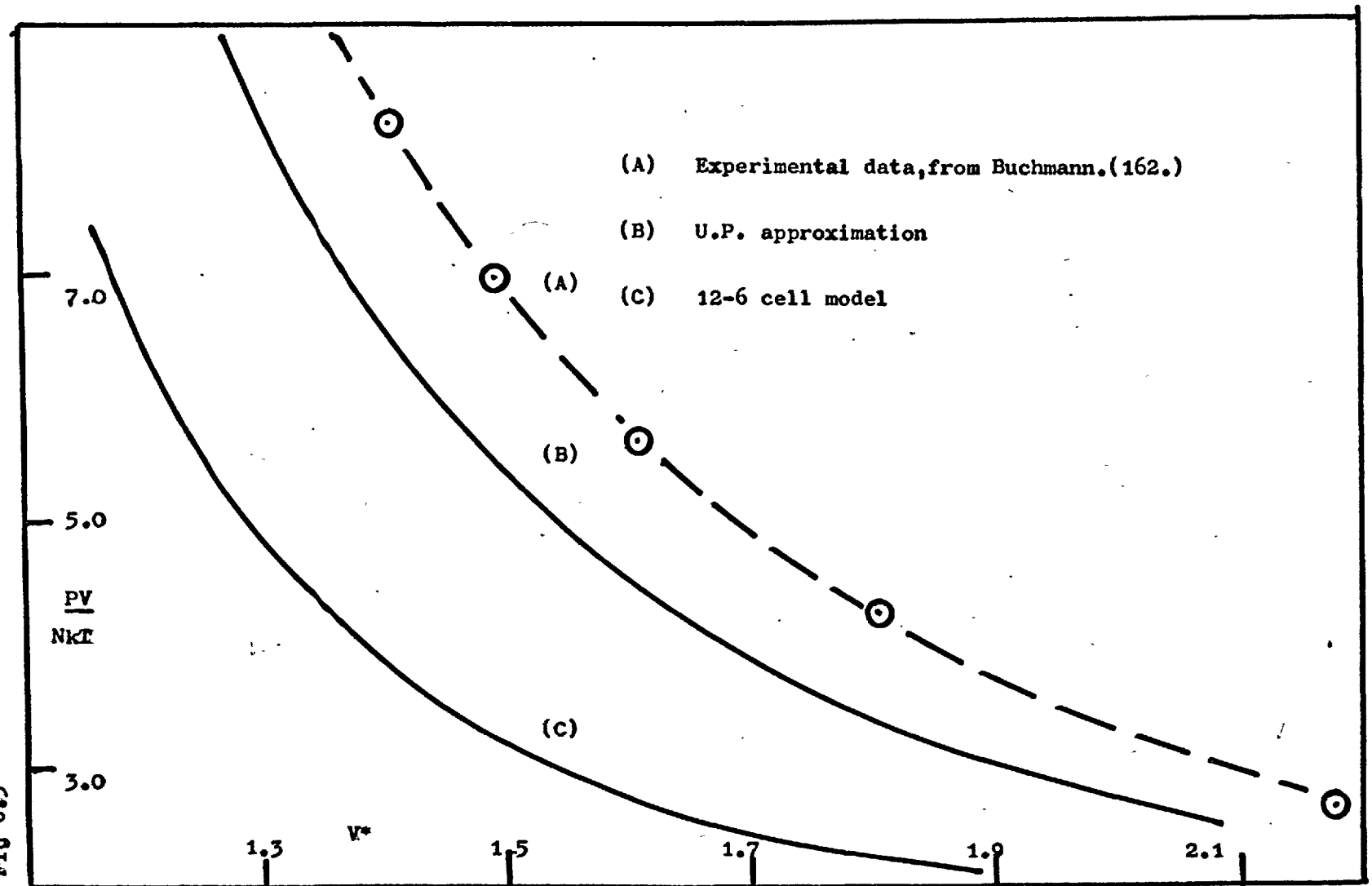

Fig 6.5

inadequate. Another cause for disagreement might be traced to the reduction parameters, to which, in this case, the curves are particularly sensitive. However, we cannot justifiably alter these without invalidating our previous calculations and the discrepancy for helium must therefore remain unexplained.

It is now of interest to delve deeper into a matter that results directly from the formulation of (6.3.2). We have already observed that the low ϵ/k values for the light gases (H_2,D_2,He) compared to the large ϵ/k for argon means that data at the same reduced temperature describes markedly different experimental temperatures. Thus an experimental study of $H_2$and D_2 at room temperatures, i.e. $T^*=8$, is not an unreasonable task. To study argon at a similar T^* would involve measurements around $960^{\circ}K.$, and would present an experimental problem of some magnitude. It is also observed that experimental data for H_2 and D_2 are available up to $T^*=8.73(323^{\circ}K.)$ while none appears for argon above $T^*=3.5(420^{\circ}K.)$. We have therefore reversed our corresponding states procedure and using data for the light isotopes at $T^*= 8.73$, have subtracted the U.P. correction term to give a "theoretical isotherm" for argon at $1048^{\circ}K.$ This is shown in Fig (6,6). The agreement between the two sets of theoretical data is satisfactory. However, in view of the somewhat better prediction of the deuterium isotherm from argon data at lower temperatures, the classical isotherm at this elevated temperature may best be

High Temperature isotherm T*= 8.73,experimental data Michels et al.(161)

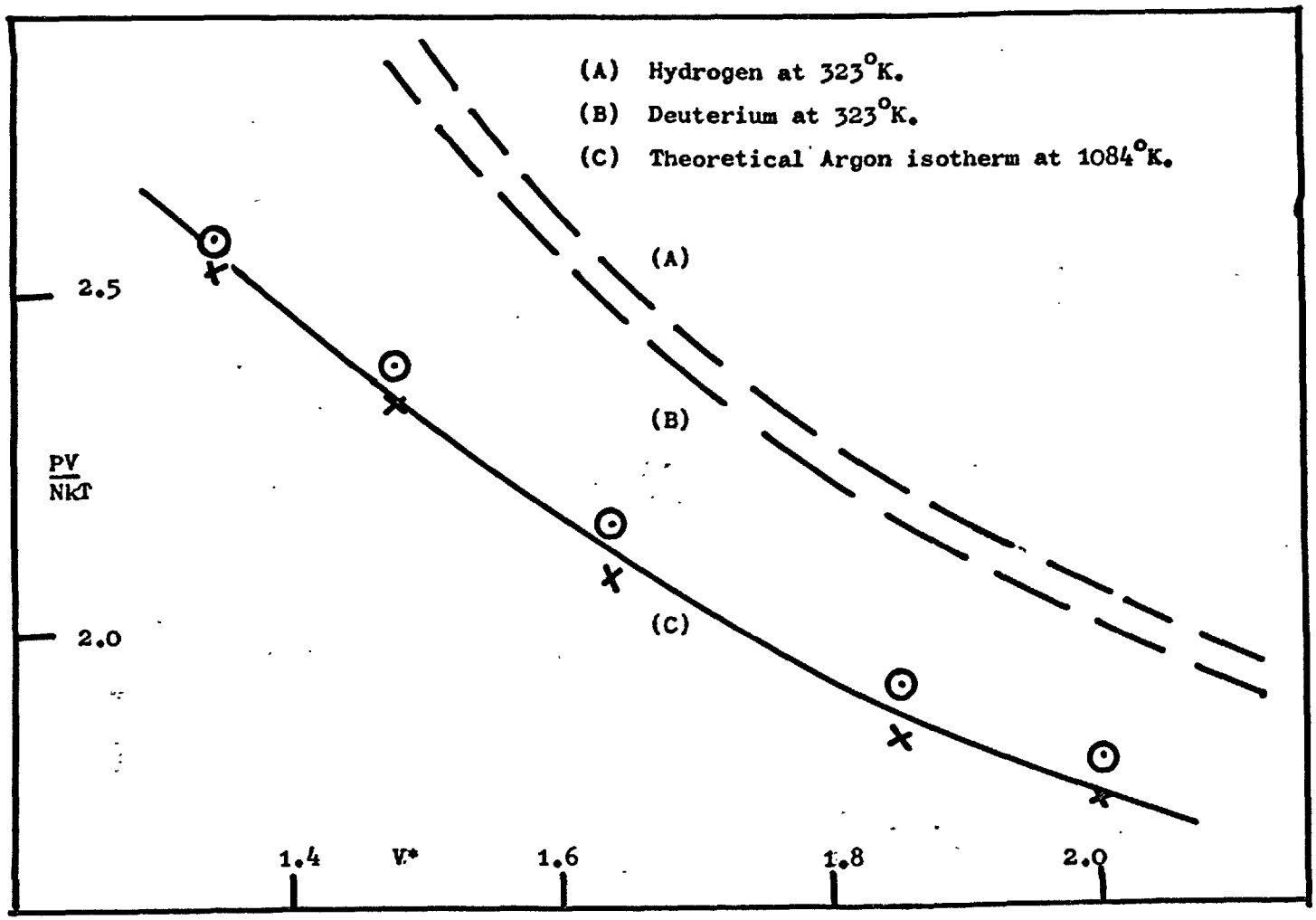

Fig 6.6

considered as given by predictions from D_2 experimental results.

The predicative value of the calculations given in Figs (6.1 - 6.5) can be emphesised by considering the magnitude of the quantum corrections. For H_2 at $T^*=1.748, V^*=1.35$ the experimental compressibility is 1216 atms., and the quantum correction 533 atms. At the same reduced temperature and a $V^*=1.90$ these pressure values are 366 atms. and 175 atms. respectively. The successful prediction of a correction of such magnitude, approximately 45% of the experimental value, must therefore stand as a sensitive test of the theory.

The validity of the adaptation of our treatment at high T^* is, on a single prediction open to question. This region of high temperature is of considerable interest. Plots of the compressibility against reciprocal reduced temperature for H_2 and D_2 are seen to pass through a maximum (Fig (6.7)). This plot also shows a similar curve for argon compounded from experimental data and continued into the region of high T^* by theoretical considerations identical to those employed in forming Fig (6.6). The theoretical plot, constructed from experimental deuterium data, exhibits a maximum comparable to that observed for the H_2 and D_2 curves and therefore provides a rational continuation of experimental data.

From our accurate but perhaps limited application of the corresponding states theory at fluid densities it would appear that the method is capable of a reasonable degree of

Fig 6.7 Compressibility factor as function of reduced temperature at $V^*=1.68$

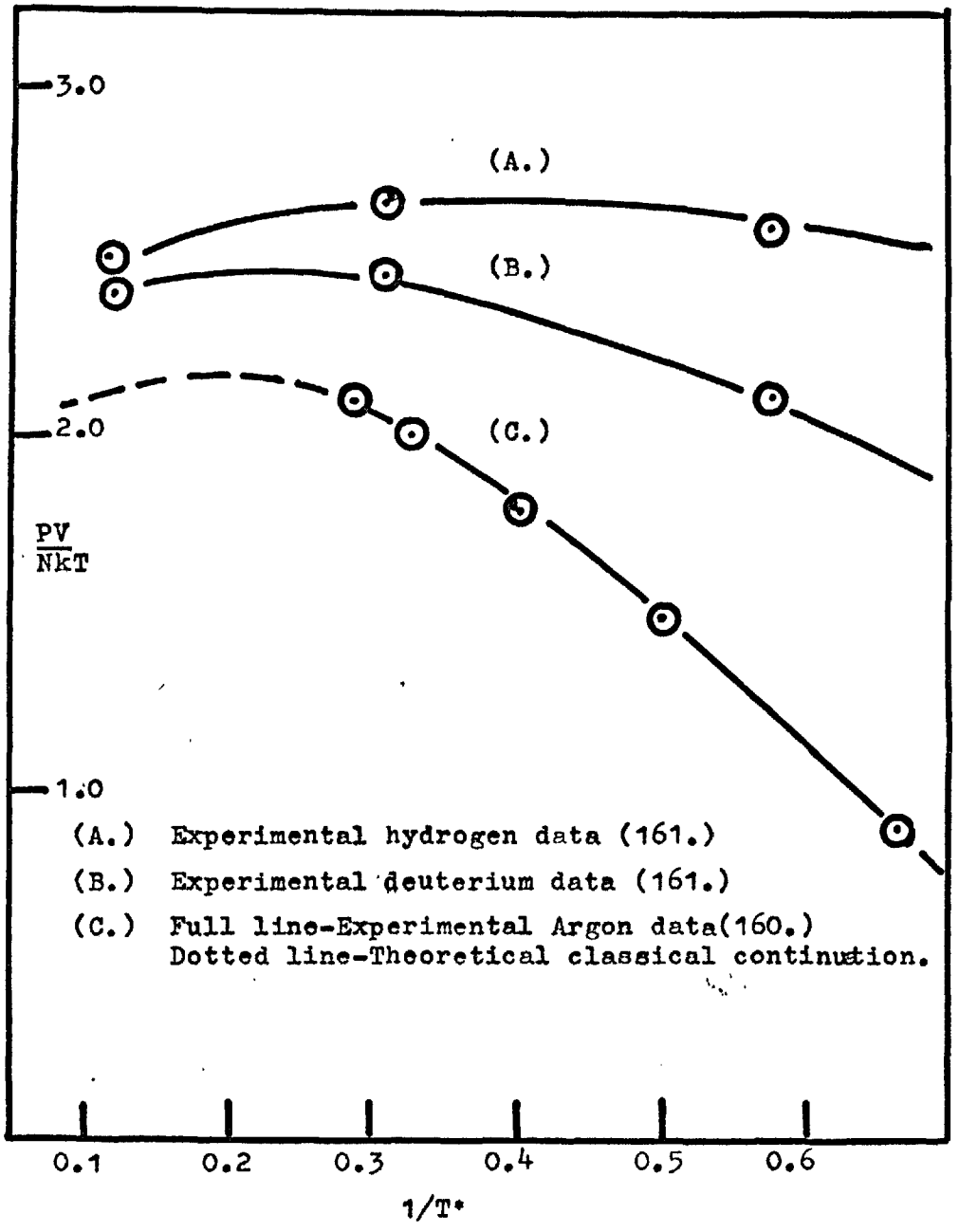

of success, but only through the use of the uniform potential model. The quantum L.J. method, so applicable in the high density state, fails for fluids even in the context of a corresponding states approach. These observations would indicate that the situation at fluid densities is again critical to the nature of the potential. The shape of the potential term is known to be of considerable importance in the solution of the energy eigen value equation and in fact the major reason for the existance of the U.P. model is to make this solution readily available. It is therefore somewhat disturbing to find that an arbitary potential of this type appears so decidly superior to the 12:6 , which although empirical in certain respects is much closer to the true picture of the intermolecular interaction. The success of the U.P. approxmiation may, of course, be considered as fortituous. The same cannot be said for the failure of the L.J. model which, as always, appears to reward the slightest excursion beyond its favoured range of high densities and low temperatures with results that are both unwanted and inexplicable.

CHAPTER 7.

Gas solubility and the Cell theory - an Introduction.

"One may not doubt that somehow good
Shall come of water and of mud
And sure, the reverent eye must see
A purpose in liquidity."

Rupert Brooke (1887-1915)

7. Gas Solubility and the Cell Theory-an Introduction.

Our discussions to date have been confined to a narrow range of physical limits. We now move from these nether regions around absolute zero to the more realistic and more easily approached (at least experimentally) phenomena that are observed at and around room temperature. In particular we are interested in gas solution theory which presents several situations that may possibly be interpreted through the use of a suitable cell model.

Any consideration of solution theory is, by definition, a consideration of solubility and solubility phenomena and similarly any consideration of the work in this field must deal with the work of Hildebrand (10-16, 163-169). Over more than fifty years Hildebrand, together with co-workers has produced a prodigious array of experimental results on the solubilities of solids, liquids and gases in various solvents . From these results has sprung regular solution theory which, as the name implies,,has predicted from experimental observations a regular relationship for many differing solute-solvent systems. These relationships indicate that the entropy of mixing for non polar compact molecules of different species may easily be estimated unless anomolies such as complexing or unorthodox forms of bonding occur. Hildebrand's theories are excellent in that they rationally account for much of the solution behaviour of solid-liquid and liquid-liquid systems but in

the case of gases dissolved in non polar solvents regular solution theory is observed to fail.

Early studies of gas solubility behaviour were limited by the absence of accurate experimental results with which to compare any theory. The work of Horiuti (170) remained for many years the only source of reference, but recently measurements by Reeves (16), Cleaver et al (171-173) and Hiroka (14) have provided a wide and reliable spectrum of solubility data. From these Hildebrand was able to derive solubilities and entropies of solution for many differing systems. On the theoretical level however no explanation was readily obtainable and in most investigations any attempt at a theoretical treatment was either avoided or postponed to an ensuing (but rarely materialising) publication.

The regions for the above measurements were restricted to dilute solutions.which, when considered in terms of the concentration of the solute gas, are,to a good approximation, infinitely dilute. Under these conditions any theoretical treatment of the problem in terms of intermolecular forces may ignore all solute-solute interactions and consider only the forces between solute and solvent molecules.

If we assume the solute gas molecules to be spherical non polar entities the solution process creates a situation which can, quite logically, be described by a cell theory. The use of the word logic in this context is perhaps open to question. Over many years and on many different occasions

Hildebrand has expressed his hardened and clear cut views on such an interpretation of solubility phenomena. "There is no quasi-crystalline or lattice structure, there are no holes of definite size or shape, no discrete molecular frequencies or velocities and no distinguishable gas-like or solid-like molecules." Hildebrand in fact adheres strictly to the concept of maximum randomness in a pure liquid and in mixtures of non polar, non reacting molecular species (174). In such concepts a cell theory obviously has no place but as we have already observed neither are the problems arising from gas solubility satisfactorily explained by regular solution theory.

To return to the cell model picture of the solution process, the introduction of the solute molecule must disturb the molecular arrangement of the solvent. A time averaged approximation therefore pictures the solute as "sitting" at the centre of a spherical cavity which it has dug out for itself in the liquid. This is by no means a new idea, similar suggestions having been made by Eley (175-176) and Uhlig (177), and should be considered with an experimental property not mentioned to date, namely the partial molar volume.

When a solute in any physical form dissolves in a solvent at a constant temperature, a volume expansion of the system directly attributable to this process occurs. This expansion is defined in terms of the partial molar volume (V_2)

i.e. $V_2 = (dV/dN)$ cc/mole.

where the dissolution of dN moles. causes the volume of the system to increase by dV cc. This quantity is a property of the system rather than a property of the solute in that it represents (as do other partial molar quantities) the change occuring in the system on the addition of a differential amount of solute. However, in a gas-liquid system, considered as an infinitely dilute solution the partial molar volume (P.M.V.) may be regarded as the major factor in determining the size of the cavity occupied by the solute molecule.

It might be as well at this point to consider the cell theory approach in a little more detail. In investigations of the inert gas solids the model used was that of L-J.&D. based on a regular lattice structure and on several other doubtful assumptions (doubtful in regard to fluid state situations). In the application of a corresponding states approach to quantum fluids attempts were made to eliminate the effect of the static lattice while a more empirical uniform potential was also studied. It is known that any explanation of liquid phenomena at room temperatures must acknowledge that at best only short range order can be present. A rigorous cell model is therefore unacceptable and the theory must be considered in its simplest form as a free volume type model with a definite but limited degree of imposed order. The potential in the cell and the number of neighbouring solvent molecules surrounding the solute gas are not uniquely defined by the assumptions of the model but are

rather adjustable factors, the true form of which will only be obtained by a thorough "free volume" treatment.

To embark upon any such treatment for a suitable number of differing gas-liquid systems demands numerous and accurate values of the P.M.V. The extent and validity of the data obtained by earlier workers will be described in the next section together with a detailed account of our own experimental measurements for a large number of solute-solvent systems. Subsequent chapters will describe a treatment of these results in terms of varying free volume theories and our attempts through these to come to grips with some of the theoretical problems of gas solubility.

CHAPTER 8.

An experimental determination of some partial molar volumes at 25°C.

"Why think-why not try the experiment?"
John Hunter (1728-1793) in a letter to Edward Jenner.

"The true worth of the experimenter consists in his pursuing not only what he seeks in his experiments but what he did not seek."
Claude Bernard (1813-1878)

8.1. Previous Work

The volume change in a system resulting from gas dissolution can be accurately determined by measuring either the volume increment itself or the accompanying change in density. The former method involves dilatometric techniques while the latter is effected through a pycnometer. For the systems in which we are interested these changes are of a very small order of magnitude and hence extreme accuracy of measurement and a sensitive control of experimental conditions are required. It is possible to achieve this accuracy by the use of either method but in general the measurement of volume expansion using a dilatometer has been found the more convenient. This, in fact, was the conclusion reached by Horiuti (170) who published extensive and accurate data for the P.M.V.'s of various gases in organic solvents.. Unfortunately, from the viewpoint of contemporary investigations, the systems Horiuti studied are, apart from those in two or three solvents, not of a great deal of interest. However, his experimental dilatometric method of measuring the partial molar volume has been adopted with only minor modifications by nearly all later workers.

The method of Horiuti was used by Kritchevsky and Iliinskya (178) who measured the P.M.V.'s of several gases in methanol and water, and by Schumm and Brown (179), in their study of CF_4 and CH_4 in various organic solvents at 27°C. We are specifically interested in systems of the latter

type i.e. non polar gases in non polar solvents. The majority of work on these systems as might well be expected, is due to Hildebrand and co-workers who studied P.M.V.'s as part of their general investigation of solubulity theory. Hildebrand's results are given for systems at 25°C. The earlier work of Horiuti had shown the P.M.V. (V_2) to be temperature dependent but only to a minor extent. For slightly soluble gases in organic solvents Horiuti only published results at 25°C. We have therefore restricted our investigations (both theoretical and experimental) to measurements at this temperature and have not considered the more complex but doubtless more accurate expression for V_2 as f(T).

From the work listed above we have compiled V_2 values for 41 systems of relative interest and these are given in Table(8.1). All values are at 25°C., except for those of Schurm and Brown at 27°C. and all have been obtained through dilatometric measurements. A closer examination of the results indicates the presence of pronounced and indisputable trends in the V_2 values for the various systems. If the non polar gas molecule is treated as a spherical entity (which on the scale we consider is valid for all gases listed) having a collision diameter σ (where σ is the Lennard-Jones constant) then, as might be expected, the value of V_2 increases with molecular size. Further, if the non polar solvents are characterised by the Hildebrand solubility parameter δ, V_2 is generally seen to decrease

Table 8.1 Experimental P.M.V.'s at 25°C., (cc/mole.)

Gas / Solvent	n.C_7H_{16}	iC_8H_{18}	C_6H_{14}	C_7H_{16}	c.C_6H_{12}	CCl_4	C_6H_5-CH_3	C_6H_6	CS_2	$CHBr_3$	c.C_6H_{11}-CF_3	C_6H_{11}-C_2F_5	CCl_2F-$CClF_2$	$(C_4F_9)_3$-N
H_2	54[1] 54.4[2]					37.6[6]	36[1]	35[1] 35.3[2]						
D_2							35[1]	34[1] 32.7[2]						
Ar		50[1]				44[1]	45[1]		45[1]	44[1]	51[1]		51.8[7]	
O_2						45.2[6]		47.7[6]						
N_2	66.1[3]					53.1[6]		52.6[6]					66[7]	
CO						52.4[6]		51.7[6]						
CH_4	68.4[3]	56.6[4]	60[3] 56.8[4]	55.4[4]		52.4[6]		54.8[6]	56.1[3]					
C_2H_6	82.3[3]		69.3[3]						67.4[3]					
CF_4		85.4[4]		86.4[4]		79.7[4]		83.2[4]					87.7[7]	
SF_6		104.2[5]		105.5[5]		104[5]		105.5[5]	126[5]			94[5]	101.4[5]	93.7[7]

1. Jolley and Hildebrand(13); 2. Walkley and Hildebrand(169); 3. Gjeldabeck and Hildebrand(10)

4. Schumm and Brown(179); 5. Hiroka and Hildebrand(168); 6. Horiuti(170); 7. Hiroka and Hildebrand(14)

with increasing δ. These parameters have been extensively used by Hildebrand to predict and interpret solubility in a semi-quantitative manner. They are defined as the square root of the cohesive energy density, viz.

$$\delta = (-E/V_1)^{\frac{1}{2}}$$

where -E, is the cohesive energy density of the liquid, essentially the molar energy of vapourisation for the liquid at zero pressure (i.e. infinite separation of the molecules) and V_1, the molar volume of the liquid. The parameters, which are specific for each solvent, are easily evaluated from experimental data and are usually quoted in units of $(cal/cc)^{\frac{1}{2}}$. Extensive tables of δ values are given in Refs. (163,164).

Another interesting but perhaps not obvious factor arising from Table (8.1) is the relative value of V_2 for H_2 and D_2 in the same solvents. Jolley and Hildebrand (13) found evidence that V_2 for hydrogen was greater than V_2 for deuterium, but within the limits of their experimental measurements were unable to draw any conclusions from this observation. However, later and more accurate work by Walkley and Hildebrand (169) to determine the P.M.V.'s of H_2 and D_2 in benzene, toluene and perfluoro-n-heptane confirmed these earlier findings and indicated that, in benzene, hydrogen occupied a volume larger by 8% than that for deuterium. The only explanation for this phenomenon must lie in a quantum effect, but while this is undoubtedly present for H_2 and D_2 at low temperatures it is scarcely credible that one should exist in the region of 25°C.

We have already mentioned the linearity of P.M.V., values with regard to increasing gas size and perhaps more important decreasing δ. There exists one striking deviation from the latter "rule" - that of the P.M.V.'s of sulphur hexafluoride as measured by Hiroka and Hildebrand (168). The irregularities in these values were linked with the irregular solubility relationships for SF_6 as found by Hildebrand and Archer (12) being attributed to "departures of SF_6 from the geometric mean relation in mixtures with non fluoride solvents". Such a conclusion was inconsistent with other available data. Archer (12) had observed similar irregular solubility behaviour for freon (CF_4). However, the values of V_2 for freon as quoted by Schumm and Brown (179) followed the expected trend, increasing with decreasing δ.

The survey of previous experimental work indicated that substantial gaps still remain in our knowledge of P.M.V's. Many of the quoted values were for uncommon systems (e.g. Hildebrand's numerous values for fluorocarbons) and further several doubtful or curious results stood without experimental confirmation. The most extensive work as listed in Table (8.1) was that of Jolley (13), giving results for eleven systems while the most comprehensively examined solvents were benzene and carbon tetrachloride. We therefore decided to measure the P.M.V.'s for gases of increasing molecular sizes in solvents covering a small but distinct range of solubility parameters. The gases used were Ar, CH_4, CF_4 and SF_6, and the solvents benzene (δ=9.2), cyclohexane (δ=8.2), n-heptane (δ=7.95)

and iso-octane (where δ is usually given as 6.9, but about which value there appears to be some doubt - see (8.8)). To the selected gases hydrogen and deuterium were added giving in all twenty four systems to be studied. It should be noted that not only did these systems extend over a wide spectrum of gas size and δ values but also permitted an examination of several pertinent facts - whether more evidence for a quantum effect at room temperature could be obtained from the measurements involving hydrogen and deuterium - if the values of Schurm and Brown at 27°C. would be identical with measurements for the same systems at 25°C. - and whether a check could be made on the seemingly anomolous data of Hiroka for SF_6. Finally it was considered that several regular systems which had been measured previously would serve as a sensitive test of the accuracy of our experimental method. With these objectives in mind we performed our measurements employing the dilatometric techniques so successfully introduced by Horiuti some thirty years earlier.

8.2 The Dilatometer

The dilatometer used in our experiments is shown in Fig. (8.1). It possesses one innovation when compared to those used previously in that it is in two sections joined by a Quickfit B.19 cone and socket (F). This device enables the otherwise lengthy cleaning procedure to be considerably

Fig 8.1 The Dilatometer.

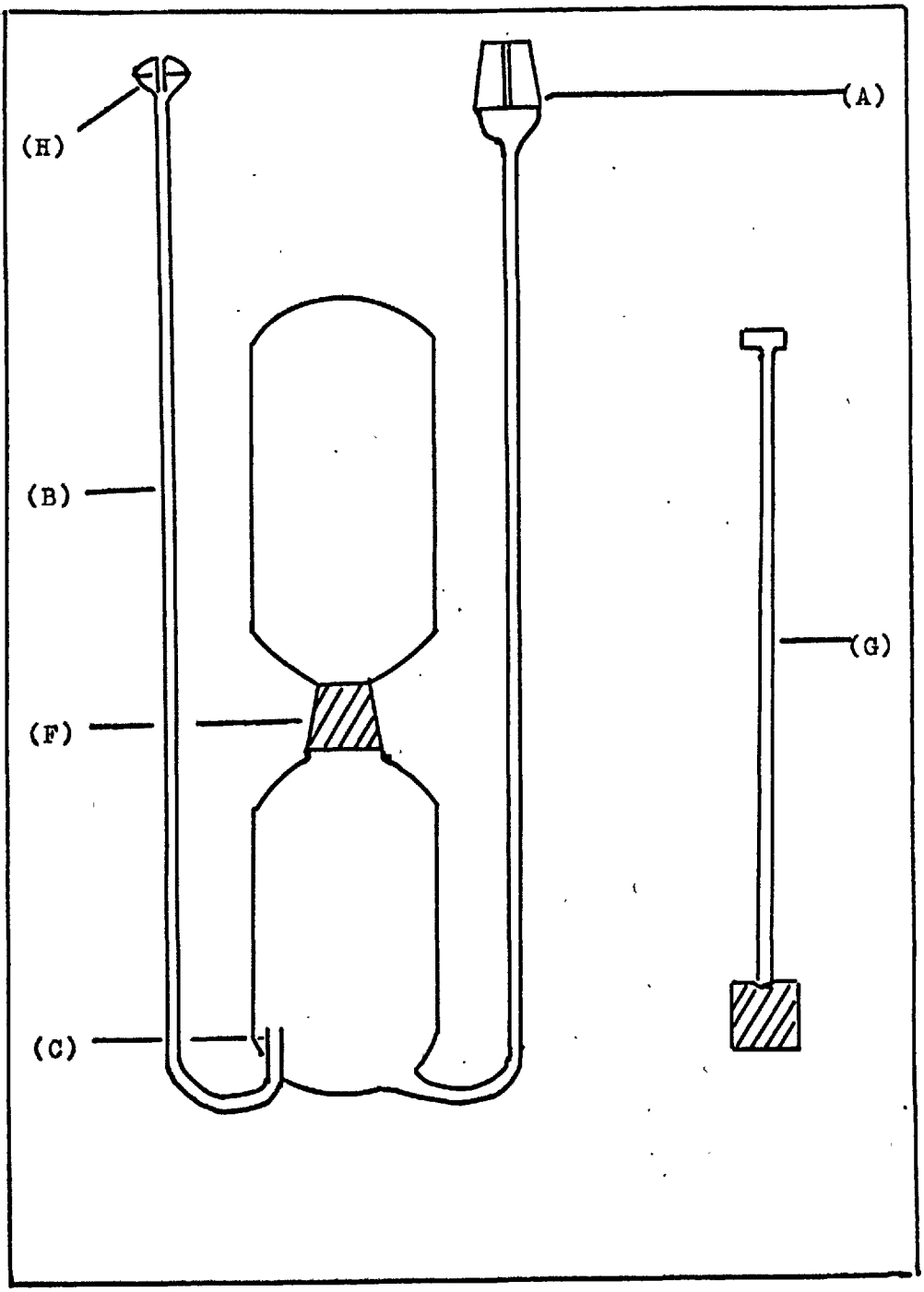

shortened, and provided due care is taken, does not introduce any new source of error into the measurements.

The general dimensions of the dilatometer are considerably larger than any of those previously employed. Its total capacity is approximately 300 cc. (cf. 140 cc. - Jolley (13) and Schumm and Brown (179)) and during any experimental run about 250 cc. of this space is occupied by the solvent. The two capillary arms (A) and (B) are also longer than those used by other workers, being 33 cm. (approx) compared with the 20 cm. arms of the Horiuti dilatometer.

Prior to the construction of the dilatometer these arms, made from precision capillary, were calibrated by the "mercury drop method". A selected length of precision capillary was marked off and a slug of mercury introduced (sufficient to occupy a length of about 6 cm.). This was moved down the capillary and its length at various points carefully measured with a travelling microscope. After 20-25 such readings the mercury was removed and weighed and from the readings the average length of the slug determined. Thus, knowing the density of mercury it was a relatively simple matter to evaluate the radius and hence the area cross section of the capillary. The following results were obtained.

(i) Left hand limb (B)

Radius of capillary (r) = 3.047×10^{-2} cm.

Hence a rise of 1 cm. in the capillary is equal to a volume V, where

$V = \pi r^2 x1 = 2.916 \times 10^{-3}$ cc./cm.

(ii) Right hand limb (A)

Similar to (B) with $r = 3.037 \times 10^{-2}$ cm.

and $V = 2.899 \times 10^{-3}$ cc./cm.

(It should be emphasised that for the above measurements strict precautions were taken that, at all times, both capillary and travelling microscope were in the same plane.)

Returning to Fig. (8.1) we may note two other factors, namely that the left hand limb enters the dilatometer through a nozzle (C) and that the same arm ends in a Quickfit ball joint (H). The nozzle was first introduced by Horiuti (170) and enables gas to be injected directly into the solvent, without adhering to the wall of the vessel. The ball joint owes its origin to experimental convenience since it reduces the tension on the vacuum line and enables the dilatometer to be easily attached to the main rig.

For an experimental run the dilatometer is clamped to a perspex and brass frame while inside it is placed the stirrer, shown as (G) in Fig. (8.1). This was constructed from stainless steel, coated with liquid "Araldite" and fixed to a "Teflon" base. Its length was such that it could easily be agitated by a magnet held just above the top of the dilatometer. This design of stirrer was adopted in preference to a glass (or Teflon) coated metal slug on two counts; first, the difficulty in controlling such a device in our experimental arrangement and secondly the maximum width of any stirrer imposed by the diameter of the cone (F). The stirrer (G)

was found to be efficient and providing that the solvents we used did not affect the Araldite coating (manufacturer's data assured us that they did not) no adverse effects should have been introduced.

8.3 The Vacuum Line

Experimental procedure demands that the dilatometer is placed in a thermostatic tank and attached to the vacuum line at (C) (see Fig.(8.2)). This line consists essentially of two sections; that to the left of the dilatometer that leads to the vacuum pump (A) and that to the right that stores the gas to be used during the run. The gases, which are obtained stored in cylinders are connected to the line at (F) by a Matheson Automatic Regulator No.36. Gas passes through the two way tap (E) and is stored and isolated in the gas burette (G). This burette consists of an inner "U" tube surrounded by an outer jacket through which water is circulated. The left hand limb of the U tube was constructed from a Springham straight bore burette, calibrated from 0-25 cc. with 0.05 cc. direct accuracy. The tube was connected to a mercury reservoir (M) through a spring loaded tap (H) and the reservoir attached to a stand that could be moved in a vertical plane. The contents of the burette were thermostatted by water at 25°C., circulated by a Stuart Turner centrifugal pump No.10. The water was stored in a well stirred, well lagged bath , thermostatic equilibrium

The Vacuum Line.

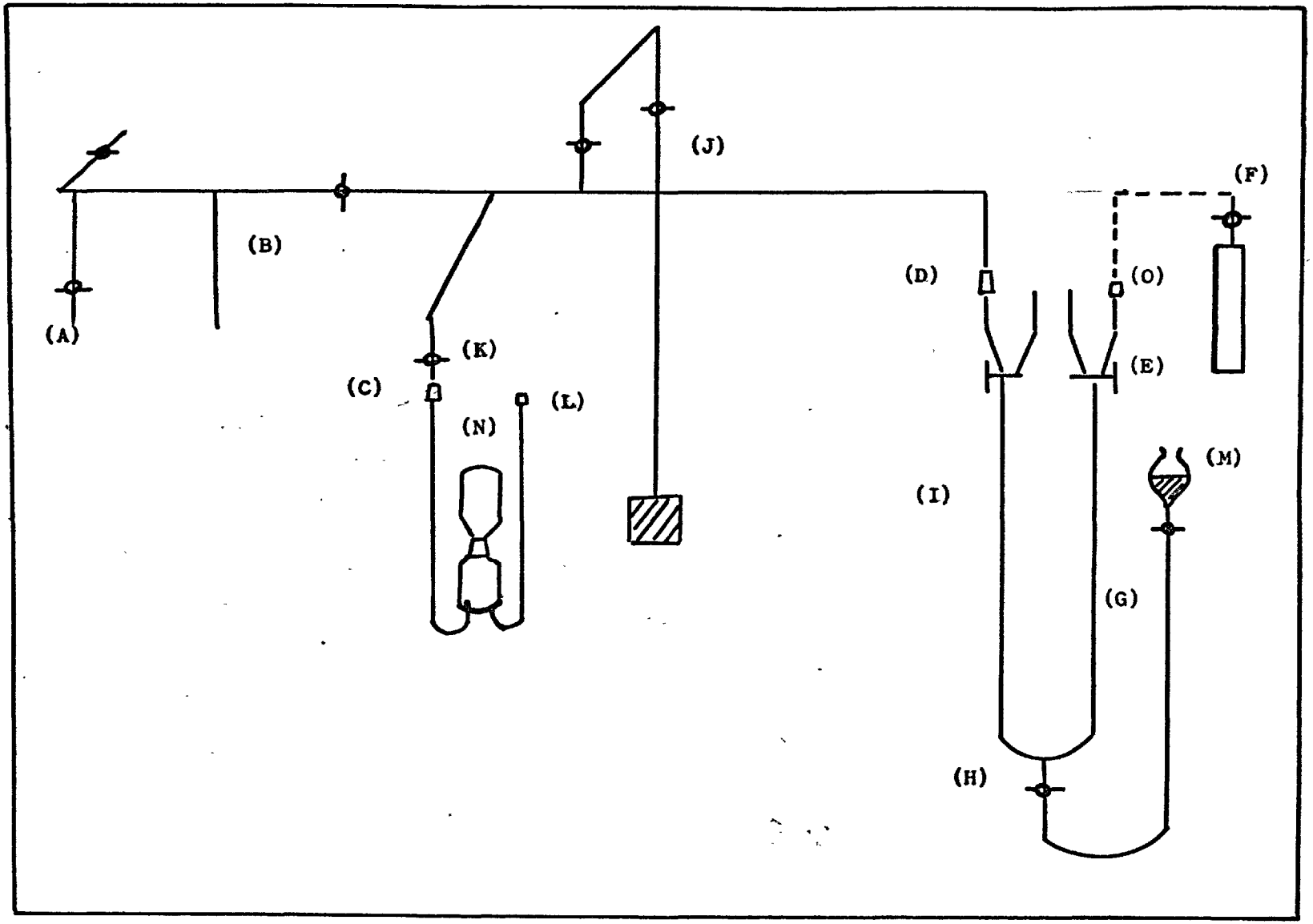

Fig 8.2

being maintained by an Electro methods Ether control relay, which operated a 60 watt lamp and a 30 watt "fish tank" heater. Temperature control was through a contact thermometer made by the Electro Thermometer Co. Ltd., having a range of 20-30°C., and a sensitivity of 5°C.-1 cm.

All taps on the line were greased with Apiezon "N" and the joint (D) was secured with springs. Joints (C) and (F) were made particularly secure and the reliability of the whole line with respect to leaks etc. could be investigated by use of the manometer (J).

8.4 The Thermostatting of the Dilatometer

Perhaps the most important experimental factor to be considered in our measurements is the maintenance of a high consistency of temperature in the neighbourhood of the dilatometer. The volume changes resulting from gas dissolution are small and any temperature fluctuation even in the region of 0.01°C., can affect the accuracy of these measurements to a considerable extent.

The choice of a thermostat vessel, a suitable control system and a sensitive method of detecting temperature fluctuations were all problems that had to be solved before any meaningful results were obtained. These problems (or rather unsatisfactory attempts to by-pass them) caused many delays in the project and in fact the majority of experimental difficulties can be directly or indirectly traced

to lapses in thermostatic control. However, we do not propose to describe the various permutations forwarded as vain solutions but rather the optimum conditions of control and the successful experimental method that evolved from their consideration.

When the dilatometer is attached to the line at (C) (see Fig. (8.2)), it is immersed in a copper thermostat tank. This has the internal dimensions of 32cm.x25cm.x47cm., with a glass window 26cm.x40cm. fitted in the front. The other sides are padded and the top may be covered with a lid. The thermostatic liquid that filled the bath was water and this was vigorously agitated by a stirrer driven by a Griffin and George adjustable speed motor. The motor drove an axial rod which carried five copper paddles each 8.5 cm. in diameter and each being interleaved into eight sections.

Temperature control is achieved via an electronic relay and a contact thermometer which together consiitute a typical "on-off" system. Such a system is in essence an osdillatory circuit in which temperature control is enhanced by (i) increasing frequency, (ii) decreasing amplitude.

An increase of frequency is obtained by increasing the sensitivity of the control and minimising the inertia of the thermal load (where in our case the load is the heat capacity of the heater and contact thermometer). The frequency may also be increased by decreasing temperature lags, consequently making it easier to attenuate oscillations by filtering.

To decrease the amplitude, factors such as efficient stirring must be considered. This is requisite in order to remove "temperature pockets" in the liquid and hence minimise irregularities due to localised heating.

These objectives were achieved, in part, by using a contact thermometer of the gas sealed "metastatic" type supplied by the Electrical Thermometer Co. Its adjustment was 1cm/1°C., and it gave a differential of 0.001°C with negligable lags over the range 20° -30°C. Also attached to the relay was a heater of nichrome wire, wound on a glass frame. The power for the heater was obtained by reducing mains voltage through a Douglas MT 3AT transformer, which took 30 volts D.C. off the A.C. mains. The input of this voltage was further monitored by a variac transformer (Zenith Elect. Co. Variac Duratrak) which provided a sensitive control over heater current. As was stated above this heater was connected to the relay - an identical heater operated in a similar manner was placed in the bath to act as a permanent heating source. This enabled the temperature differential to be kept to a minimum (fast response) and also if thermostatting control was lost due to large alterations in room temperature, enabled the balance to be restored without any adjustment of the sensitive relay circuit.

Bearing in mind the minimisation of lags, fast response to temperature changes, elimination of temperature pockets by stirring etc., there exists one factor which, though

important, owes its solution chiefly to trial and error methods. This is the best relative position in the bath of the heaters (both switching and permanent), contact thermometer and stirrer, the most favourable arrangement being of course that where temperature variations are smallest. To find this position we must be able to detect these fluctuations, a technique that demands an accurate temperature measuring device, and moreover one that responds rapidly to small temperature changes. The Beckmann thermometer, used in these investigations, is not ideal for such a task. Its accuracy was quoted as 0.001°C. but it also possesses a large thermal lag (slow response) and is not adverse to "sticking". We therefore searched for an additional and more sensitive medium which we found in the shape of a thermistor.

A thermistor is a sensitive resistor (made from semiconducting materials) whose temperature coefficient of resistance is negative and many times that of ordinary metals at room temperature. A change in temperature of the surroundings therefore produces a change in resistance of the thermistor which, using a simple bridge circuit can be easily evaluated.

We have used a Standard Telephone and Cables F22 thermistor (with a temperature coefficient of -2.8% at 20°C.) and the Wheatstone bridge circuit shown in Fig (8.3). Balancing the circuit in the thermostatic bath (i.e. finding the resistance of the thermistor at bath temperature) it was

Fig 8.3 Thermistor & Thermistor circuit.

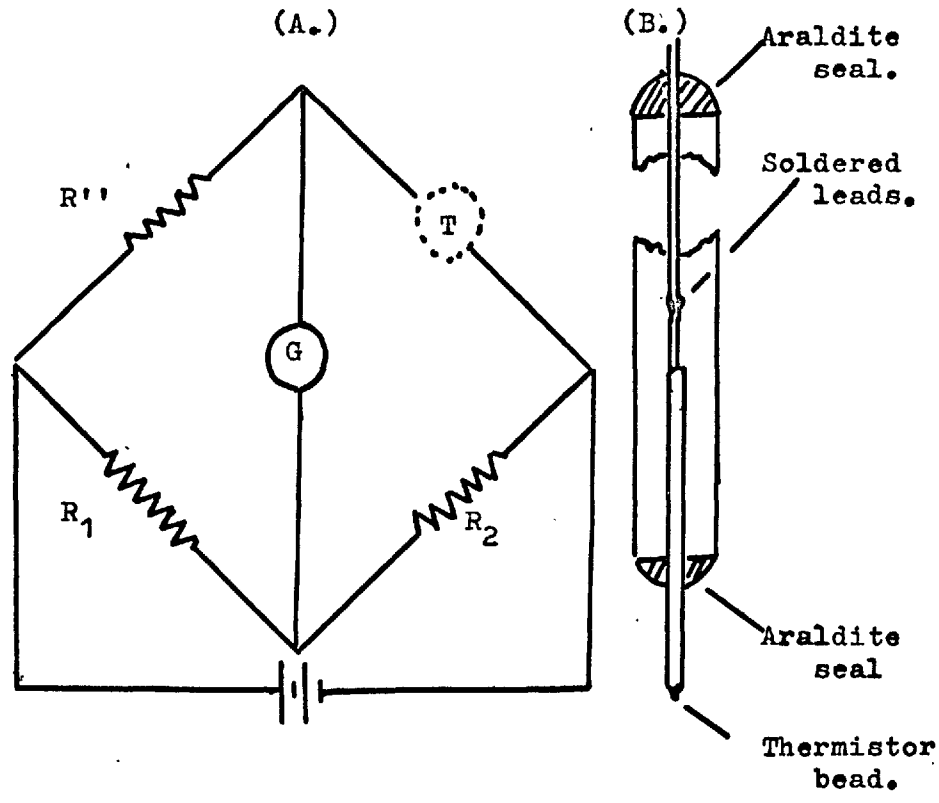

(A.) Thermistor circuit:-

G, scalar galvanometer.

R_1, R_2 arms of Decade box in 10:1 ratio.

R'', variable resistance in form of decade box.

T, Thermistor (S.T.& C.-Type F22.),

(B.) Thermistor-"exploded" diagramn.

possible to calculate the change in resistance for a change of $1^{o}C.$ and from this the fluctuations in temperature for a unit deflection on the galvanometer scale. This calculation indicated that 1mm. on the scale $=0.5 \times 10^{-3o}C.$ (sending 4 volts through the bridge circuit). Hence, making the reasonable assumptions that heating effects due to the thermistor were negligable and that its response time was no more than 15 secs we were able, accurately and easily, to follow temperature changes in the bath.

It might be justifiably stated that for a claim of accurate thermostatting the bath should be "mapped" (i.e. observations should be taken at a variety of different points rather than temperature changes at a fixed position be continually observed). Such a task however presents serious problems and it was felt that a reasonable oscillation on the galvanometer scale supported by a stationary Beckmann gave an accurate indication of good thermostatting. Perhaps more important however, is that the capillary levels of the dilatometer do not change. Because of its large thermal mass, the dilatometer is more sensitive to temperature drifts than to fluctuations, the former being clearly shown by a rise (or fall) in the mercury levels. For the dilatometer to be at equilibrium its levels must be completely stationary. Throughout our experimental measurements we were able to achieve this. When for some reason or other we were not it was nearly always necessary to abandon the relevant run. Temperature control was not

claimed to be better than $0.002^{\circ}C.$, but it may be stated that within our degree of accuracy all volume changes were due to gas dissolution and not to spurious temperature effects.

8.5 A Typical Run.

We will now describe in some detail an experimental run typical of any solute-solvent system investigated.

Triple distilled mercury was first introduced into the open dilatometer so that the mercury level was slightly higher than that of the nozzle (C) - Fig (8.1). The stirrer was next placed in position and the top half of the dilatometer sealed on by the use of Edwards "E" wax. Only a little of this wax was used, just enough to give a clear transparent seal to the joint (F).

During this period about 500cc of the solvent were degassed by boiling under reduced pressure. This was continued for 2-3 hours until the solvent was considered free of all traces of air. The dilatometer was then carefully inverted, attached to the degassing apparatus as shown in Fig (8.4) and evacuated via attachment (R). On completion of this tap (S) was closed and tap (T) opened. It should be noted that a warm solvent would undoubtedly dissolve traces of tap grease. To minimise this we introduced at (T) a spring loaded tap of glass impregnated teflon

Fig 8.4 Filling of Dilatometer.

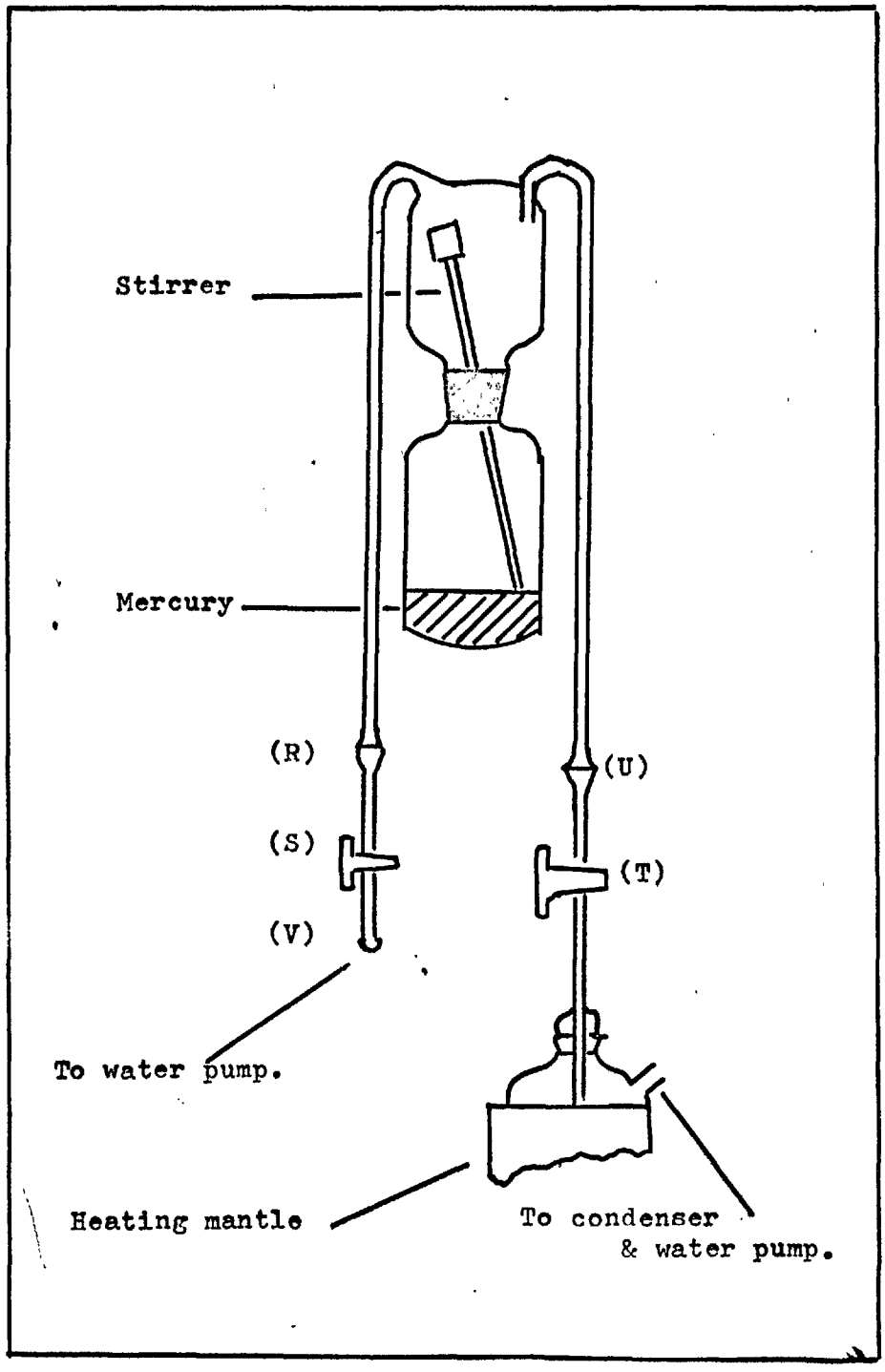

(which of course needs no grease), and only lightly greased the joint (U). The solvent was initially forced into the evacuated dilatometer in small doses ,until it was certain that all air had been removed from the latter. (S) was then closed and (T) left open, enabling the solvent to rapidly fill the dilatometer. When the filling process was complete (T) was shut, The dilatometer removed at (U) and (V) and quickly inverted, extreme care being taken not to introduce any air bubbles into the solvent.

In its normal position the dilatometer now stands, filled with solvent which is isolated from the atmosphere by a lower layer of mercury. However, the filling process results in traces of solvent remaining in the side arms. These traces were removed by warming the dilatometer with an Infra Red Mercury lamp and taking off the excess liquid with "Kleenex". The process of warming and cooling was continued until all traces of solvent had disappeared from the capillaries and the mercury columns moved smoothly without displaying any apparant fracture.

The filled dilatometer was then placed in the thermostat tank and attached to the vacuum line at (C) (this, as all refs. in the following paragraphs, refer to Fig (8.2)), particular care being taken that the frame was fixed in a vertical plane and that the capillaries were in plumb(i.e. not forced out of the vertical by a bad joint). The line was evacuated from (A) as far as the gas regulator (F) and by carefully adjusting (K) the last traces of air above the

dilatometer were removed. This procedure, of course, pulled the mercury level in the left hand limb up to (K) and to avoid air being drawn in through the open capillary excess mercury was added at (L).

All air having been removed, the dilatometer was isolated at (K) and the line flushed several times with the gas under study. The line between (K) and (F) was next filled with gas and the burette isolated by closing (E). The mercury which was held at (H) was forced into the burette in such a manner as to give a head in both arms. The line between (K) and the mercury level in (I) therefore contained solute gas, while atmospheric pressure was applied to the limb (G) by opening tap (E).

Through several adjustments the two arms of the burette were levelled and the dilatometer opened to gas pressure. This pressure forced down the mercury in the closed limb, an effect counteracted by removing the excess from the other arm at (L). By adjusting the pressure through the reservoir (M) it was possible to remove enough mercury from the dilatometer so that the equilibrium position of the capillary levels was approximately half way down the dilatometer arms. However, for a run of four or more doses, a much lower initial level of the capillaries was needed. This could only be achieved by a rather drastic but successful procedure. The thermostatting of the bath was disturbed by heating the contents for a short time with a 300 watt red rod heater. This enabled further mercury to be removed from (L) with a

capillary dropper. Having achieved this the bath was quickly cooled by the addition of ice, the capillary levels falling rapidly. Observations over a substantial number of occasions indicated that the levels continued to fall slowly for 2-3 hours and did not achieve equilibrium much before a 4-5 hour period. Considering the severe heating and cooling conditions employed this was not unexpected and therefore for each run the system was at this juncture left overnight to reach equilibrium. It was considered that a period of 10-12 hours should be quite sufficent for this to be effected and it is emphasised that no measurements whatsoever were taken up to this point.

After the lapse of this period of equilibration the stability of the system was checked by ensuring that the mercury levels in the dilatometer were steady. We did this by observing them through a cathetometer telescope (Precision Instruments Ltd.) over a period of 15-20 mins. If there was no measurable motion during this time, temperature equilibrium of the dilatometer and contents were assumed and the run proceeded with.

The atmospheric pressure was noted, the tap above the gas burette closed and by adjusting the reservoir (M) five or six readings of the pressure and volume of the gas obtained. Burette readings and mercury levels were observed through a Griffin and George cathetometer, enabling gas volume to be read to $\pm$ 0.02 cc., and mercury heights to $\pm$ 0.002 cms. On completion of these measurements the burette

was returned to atmospheric pressure (i.e. the height of both arms equal) and the tap connecting the burette to the dilatometer reopened.

Preliminary readings of the dilatometer levels were taken, being over a period of 15 mins.(again to ensure equilibrium). Next a dose of gas was passed by closing (E) and raising the reservoir (M). Gas passed down the closed arm of the dilatometer and bubbled through the nozzel into the solvent, at the same time forcing the mercury up into (L). Having sent over a dose of 1-3 cc., the burette was returned to equilibrium. The capillary levels took up a much higher position than before and the gas dose (or that part of it undissolved) was visible as a bubble in the top half of the dilatometer at (N). Complete dissolution was achieved by agitating the stirrer with a magnet. The period of dissolution varied with the system under study. Thus at the lowest it was ten minutes while for H_2 or D_2 in benzene periods of over $1\frac{1}{2}$ hours were not uncommon. When no further trace of the gas bubble remained in the dilatometer the system was left for 30-45 mins. to equilibrate.

Observations of galvanometer and Beckmann readings enabled us to check that the dissolution process had not altered the thermostatting temperature. The new levels of the mercury in the capillary arms therefore represented the increase in volume of the system due to the dose of gas. These levels were taken (again measurements being spread

over a sufficient period as to ensure consistancy). However, the volume increase as indicated by these readings is not the true volume increase, since due to the rise in the levels of the mercury in the capillaries the liquid in the dilatometer will be under a higher pressure after dissolution than before the gas dose was passed. This necessitates a " compressibility correction" typical of which are those made by Horiuti (170) and by Kritchevsky and Iliinsyka (178). Such a correction introduces several unwanted inaccuracies into the measurements and may be directly avoided by using an experimental "constant pressure" technique devised by Walkley and Hildebrand (169). The dilatometer is isolated at (K) and a negative pressure applied to the open capillary arm. This pressure must be sufficient to pull the level in the closed arm down to the original position it held before the gas dosage. The extension in the open arm will then represent the "true " expansion due to gas dissolution and may be directly measured.

This technique was employed by us for all doses. A slight negative pressure was applied at (L) through a tube attached to a 50 ml. glass syringe. When the level in the closed arm reached its original position, a clip was fixed to the syringe tube to hold the pressure. It was found that this device enabled the mercury level to be held exactly at the required position ($\pm$0.002 cm.). When more than one dose of solvent gas has been passed, there are in fact two positions that are of interest. The one described above,

where each dose acts as an individual measurement of the volume expansion or the consideration of each dose in the context of previous doses. To effect the latter the level in the closed arm is pulled down to the position it occupied in the first instance before any gas was introduced into the system. The expansion in the open arm therefore represents the total expansion in the system due to the cumulative effect of all doses passed, and by averaging and decreasing errors gives a more valid representation of the volume expansion.

To obtain a consistent value for the true expansion pressure was applied and removed on about six occasions over 12-20 mins., in each instance a separate reading being taken. If two reference marks were being used (i.e. the individual dose and the total expansion due to several doses) this procedure was repeated.

On the completion of the above operations atmospheric pressure was again taken, the burette isolated and pressure-volume measurements made to determine the amount of gas remaining after dosage.

Further doses were then passed, the process just described being repeated identically. A run generally consisted of 4-5 doses taking between 8-11 hours. On completion of a run the dilatometer was removed at (C) and emptied by applying a partial vacuum at (L) via a water pump. The two halves of the dilatometer were separated by heating the waxed joint and after cooling all traces of wax were removed.

Preliminary cleaning of the bottom half of the dilatometer was effected by washing with acetone and water. The apparatus was then filled with chromic nitric acid and left standing for 6-8 hours (generally overnight). This process was considered rigerous enough to ensure all grease etc., was removed from the capillaries. After standing, it was washed with distilled water and dried for 3-5 hours in an oven at 150°C. The top bulb was similarly, but not as violently treated being cleaned with acetone, water and chromic sulphuric acid before being dried at 150°C. for 3-5 hours.

The dilatometer could then be reassembled and another run started. Under optimum conditions the process of cleaning filling and performing a run was refined to a two day cycle. The possibility of using two dilatometers was considered but rejected since it appeared to offer little or no saving of labour or time.

8.6 Calculation of Experimental Results.

The procedure of (8.5) was employed for over thirty runs involving approximately 140 doses of the various gases. These gases, obtained from the Matheson Co. Ltd., were quoted to the following minimum degrees of purity, argon (99.998%), methane (99%), sulphur hexafluoride (98%), carbon tetrafluoride or "freon-14" (96%), hydrogen (99.95%) and

deuterium (99.5%). It was considered that these levels of purity made further techniques such as multiple trap sublimation (15) etc. unnecessary and all were used directly from their cylinders.

With regard to the solvents, iso-octane and cyclohexane were "spectro-analytical" reagents supplied by Hopkin and Williams Ltd., and were judged to be acceptable without any further purification. The benzene, obtained "thiopane free" from M.& B.Ltd., was dried and fractionally distilled B.pt. 79.5-80.5°C. The n-heptane, a Hopkin and Williams product conforming to I.P. specification, was similarly treated being dried and fractionated B.pt. 97.5-98.5°C.

Of the runs made certain were rejected due to breakdowns in experimental procedure, or due to inconsistencies in results for successive doses. The errors that may occur in the experimental process will be considered later. We now content ourselves with an examination of the successful results for the 24 systems under study. We do this by giving our complete experimental data for one system and presenting the others in a somewhat abbreviated form.

The system chosen for detailed study is that of deuterium in cyclohexane, for which four doses of gas were used.

The pressure volume data before and after each dose is given in Appendix 7, where it can be observed that the atmospheric pressure changes little during the course of a run. The volume readings are taken directly from the gas burette, while the pressure is calculated by adding the

the difference in the mercury levels (h_2-h_1) to the atmospheric pressure to give the total pressure (P_T). Plots of the volume of gas (V) vs $1/P_T$ are constructed (see Fig (8.5)) and to eliminate errors due to changing atmospheric pressure etc., the resulting straight lines are produced back to P_T =760mm.Hg from which the volume of gas before and after each dose can be easily obtained.

Also given in Appendix 7 are the comprehensive data for the four doses. Attention is drawn to the consistancy in the height of the capillary levels - even under negative pressure conditions, the very small oscillation of the galvanometer scaler and the rock-like steadiness of the Beckmann (which was frequently tapped to avoid sticking). From these results the P.M.V. of deuterium in cyclohexane is readily evaluated, the calculations for the first dose being described below.

Dose I.

(Gas volumes from Fig(8.5), dilatometer levels averaged from results in Appendix 7.)

Vol. of gas before dose = 23.36 cc.
" " " after " = 20.86 cc.
} at 760mm.Hg.

Dose = 2.50 cc.

Dose may be expressed in mols (N), where N =2.50/RT, with R, the gas constant(=82.07 atm.cc./ deg.mole.) and T, experimental temperature(=298.36°K.,or 25°C.)

Hence N = 2.50/82.07 x 298.36 = $\underline{1.021 \times 10^{-4}}$ moles.

Fig 8.5 Deuterium in cyclohexane, P-V isotherms at 25 C.
Volume(cc.)-from gas burette vs Total pressure.

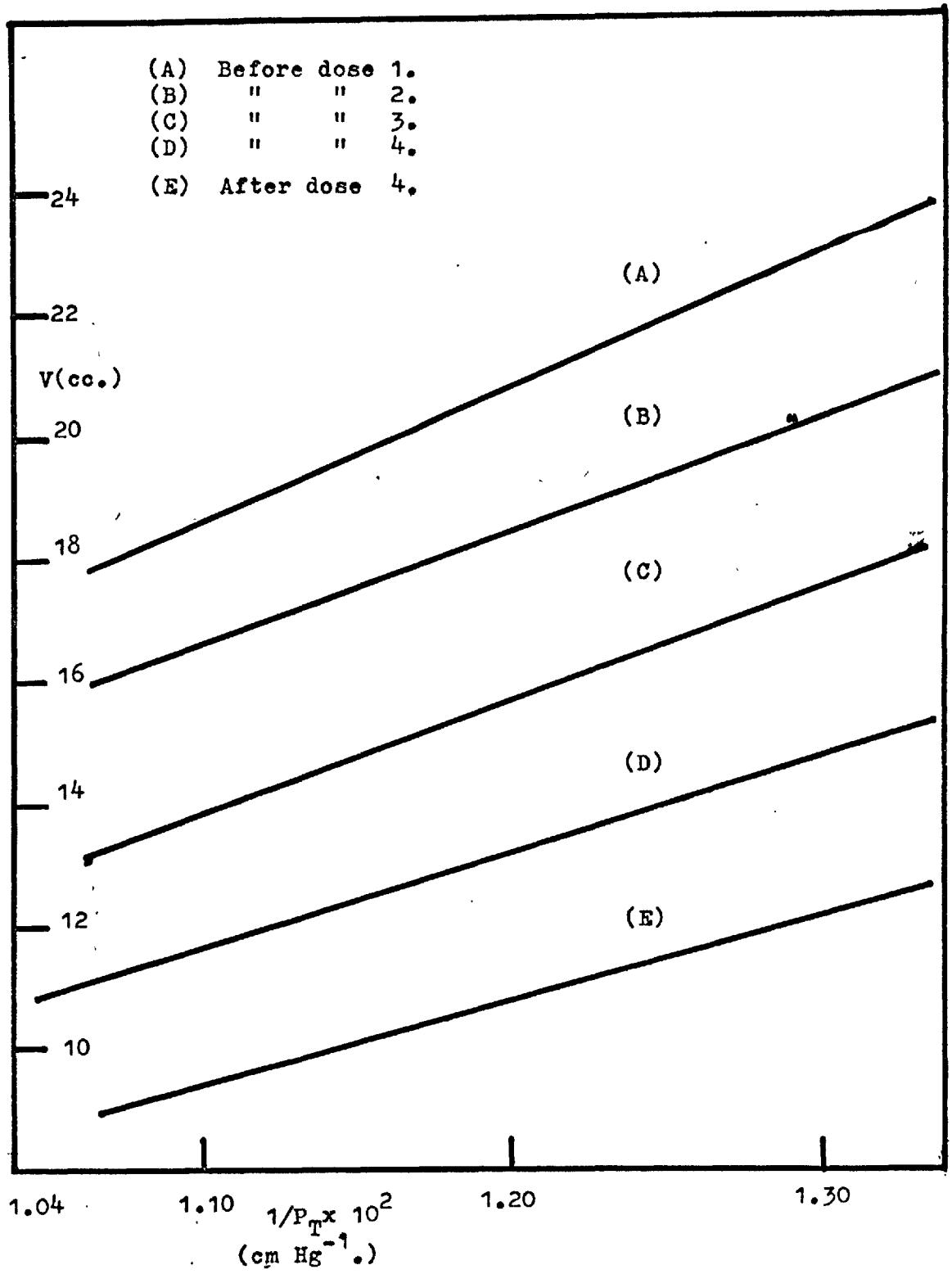

Dilatometer levels-

L.H.Arm(after dose) =36.691 cms; R.H.Arm(after dose) =36.973cms.

" " " (before ") =35.917 cms; " " " (before ") =36.452cms

dl_1 = 0.774 cms dl_2 = 0.521cms

with negative pressure applied-

R.H.Arm(after dose) = 37.888 cms

" " " (before ") = 36.452 cms

dl_3= 1.436 cms.

Calculation of V_2

(a) From negative pressure result("true" expansion)

$$V_2 = dV/dN = \frac{\text{Vol expansion of system in cc.}}{\text{No. of moles of gas passed}}$$

$$= 1.436 \times 2.899 \times 10^{-3} / 1.021 \times 10^{-4} \text{ cc/mole.}$$

(where expansion of 1 cm in L.H. capillary is equal to a volume change of 2.899×10^{-3} cc.-sec (8.2))

Hence

V_2 = 40.77 cc/mole

(b) It is possible to obtain a value of V_2, from the expansion without any application of a negative pressure using a compressibility correction introduced by Kritchevsky and Iliinskya (178). Thus if the apparent volume expansion is V_a, the true volume expansion V_t is greater by a correction term V_c, where

$V_c = \beta V.dP$

and β is the isothermal compressibility of the solvent occupying a volume V, under an excess pressure dP.

For this dose of deuterium in cyclohexane-

$$V_c = 1.08 \times 10^{-4} \times 250 \times (dl_1 + dl_2)/P_A \text{ cc.}$$

where $P_A = 76$ cms.Hg.

hence $\underline{V_c = 0.490 \times 10^{-3} \text{cc.}}$

and $V_2 = (0.774 \times 2.916 + 0.521 \times 2.899) \times 10^{-3} \text{cc.}$

$= \underline{3.767 \times 10^{-3} \text{cc.}}$

From above $V_t = V_a + V_c = 4.257 \times 10^{-3} \text{cc.}$

and $V_2 = 4.257 \times 10^{-3}/1.021 \times 10^{-4} \text{cc/mole.}$

$= \underline{41.69 \text{ cc/mole}}$

For the subsequent three doses the results may be calculated in an identical manner with the extension that using the original position of the left hand meniscus as a reference mark two estimations of V_2 are dtained from the application of a negative pressure to the right hand limb. These results are best drawn up in the form of a table (see Table (8.2))

This shows that it is possible to calculate a value of V_2 for individual doses by three different methods. However, in our evaluation of V_2 for each system we did not employ these methods, or at least not in the form given above. We instead plotted the total extension given by l^b in Table (8.2) against the total volume of gas added (B)- from the same table. The result, which should be a straight line through the origin is shown in Fig (8.6). The points lie on an unique line with a very small scatter and from the slope of this line V_2 may easily be calculated.

Table 8.2 Experimental data and V_2 values for Deuterium in Cyclohexane at 25°C.

Dose.	(A) V. (cc.)	(B) V. (tot)	(C) N x10^4 (moles)	(D) N x10^4 (tot)	l^a (cms)	l^b (cms)	l^c (cms)	(E) V_2^a	(F) V_2^b	(G) V_2^c
I	2.50	(2.50)	1.021	(1.021)	1.436	(1.430)	1.295	40.8	(40.8)	41.7
II	3.01	5.51	1.229	2.250	1.624	3.052	1.506	38.3	39.3	40.2
III	2.80	8.31	1.143	3.393	1.550	4.546	1.472	39.3	38.8	42.3
IV	2.60	10.91	1.062	4.555	1.451	5.997	1.341	33.8	39.0	41.5

A(or-C)= Vol of gas passed for each dose in cc.(or-moles)
B(or-D)= Total volume of gas passed during run in cc(or-moles)

l^a = Extension refered to reference mark before that dose.
l^b = Total extension refered to reference mark before Dose I.
l^c = Combined extension (dl_1+dl_2), both arms.

E= V_2^a, P.M.V. calculated from l^a and A.

F= V_2^b, P.M.V. " " l^b and B,

G= V_2^c, P.M.V. " " l^c and A with compressibility correction.

Deuterium in Cyclohexane at 25°C., Extension (cms.) vs Gas Passed(cc.)

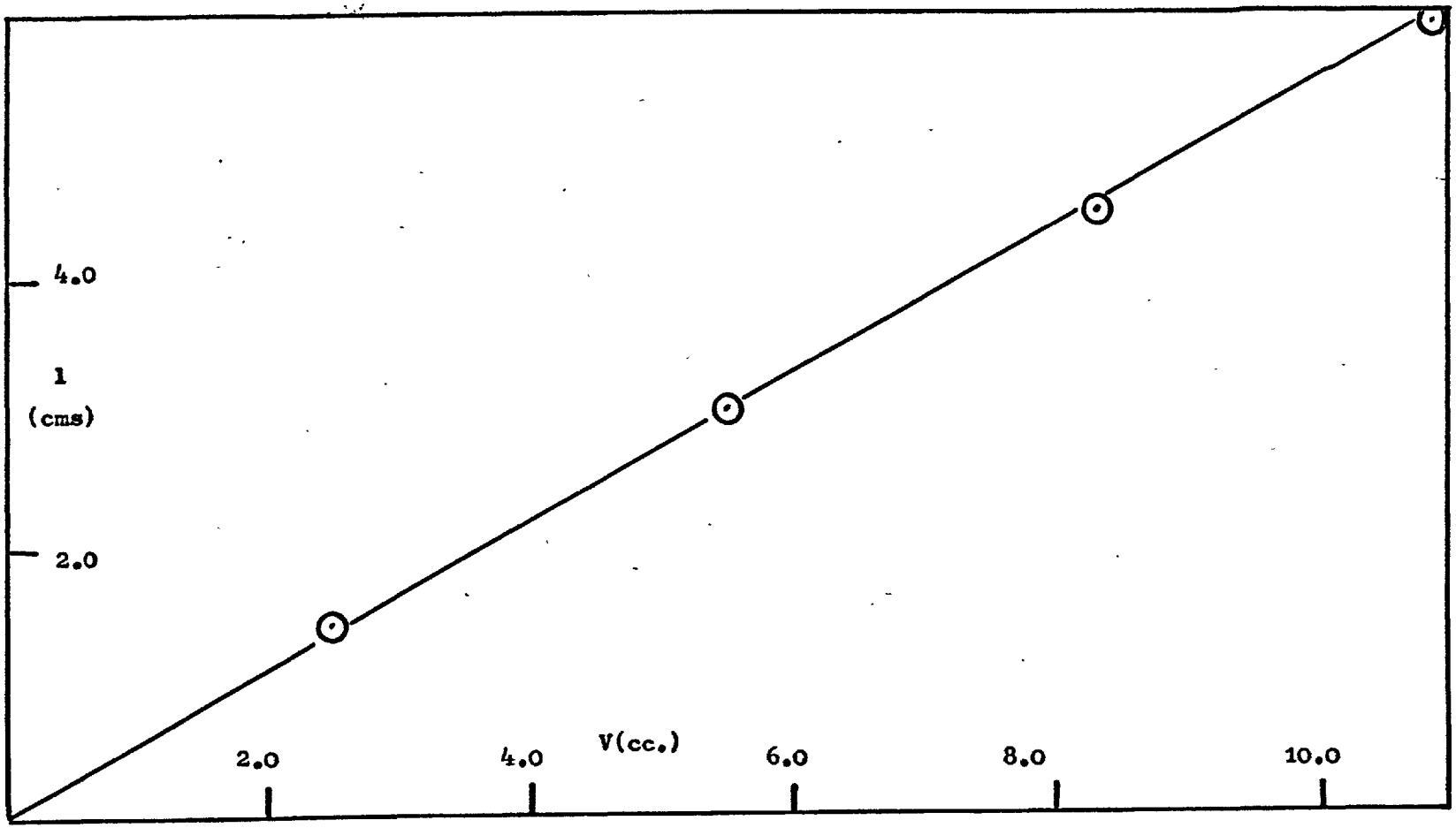

Fig 8.6

Hence for D_2 - Cyclohexane at 25°C.

$V_2 = (dl/dV)_{slope} \times 298.36 \times 82.07 \times 2.899 \times 10^{-3}$ cc/mole.

$= \quad " \quad \times 70.986$ cc/mole.

$= 5.54/10.00 \quad \times \quad " \quad "$

$V_2 = 39.33$ cc/mole.

The calculation of the P.M.V. by this method yields a result that is dependent on the run as a whole and not on separate doses. It therefore averages certain errors and can withstand the effect of slightly spurious expansions. The values of V_2 given in (F) - see Table (8.2), which gives results for each original dose are much more sensitive and, since they deal with smaller extensions and gas doses, are more liable to errors. The use of the compressibility correction to give the results in (G) is of very dubious merit; values of β and V are uncertain and the mathematical formulation of the correction term is itself open to criticism. For certain systems it yielded results in close agreement with those obtained directly from the "true" expansion but for others agreement was at the best poor. For subsequent tables results obtained by the use of this correction term have not been included, emphesis instead being placed on the more meaningful values obtained from the volume expansions that resulted from the application of a negative pressure.

The results from the other 23 systems studied were treated in an identical manner (considering the above arguements) as those of the deuterium-cyclohexane system.

These results are presented tabularly in Appendix 8, together with the plots of length (volume expansion) against total volume of gas passed, from which the required values of V_2 at 25°C., are readily obtainable.

8.7 Errors and Difficulties of Operation.

In this section we consider not only errors of measurement likely to effect the accuracy of our V_2 values but perhaps the more important effects that cannot be represented numerically. These when present may result in such gross disturbances as to cause the experimental run to be abandoned or more dangerously, may effect the final results to an unknown degree.

The process of filling the dilatometer can introduce several such factors, the most difficult to eliminate being small solvent traces in the capillaries and fractures of the mercury columns in the semi-visible part where the capillary joins the dilatometer. The latter effect is also very difficult to detect and several anomolous runs were traced to this cause. Linked with this is capillary blockage caused by dust or other foreign matter in the arms. In spite of our extreme care in cleaning and filling, and also in the use of freshly distilled mercury for each run small blockages sometimes appeared and in the case of certain solvents a slight tailing effect for the mercury

was noted. In fact, after thermostatting, capillary behaviour gave most experimental trouble, but unlike spurious temperature fluctuations which we were rapidly able to pick up, these errors often managed to escape notice for some little while.

Another not infrequent but fortunately easily detected fault was that of a gas leak between the dilatometer and the burette. The causes of these were uncertain i.e. faulty taps, loose joints etc., but the effects were generally mirrored in the unexpected movements of the burette levels and in these cases the run was usually abandoned.

There are many other small errors likely to occur during the course of a run which are too indeterminate to be mentioned here. However, it should be clear that an individual gas dose is much more likely to suffer from these (and the errors already mentioned) than the overall run spread over 4-5 doses and a proportionately longer period. This is one of the major reasons for our method of calculating the P.M.V.'s. We consider at all times the expansion caused by the total volume of gas passed during the run, spurious effects such as capillary blockage can generally be detected, while from a numerical viewpoint we are continually dealing with larger quantities so the errors in their measurement, assumed constant, become proportionally smaller.

To attach a definite accuracy to the numerical value of the experimental results we adopt a straightfoward, rather

than complex evaluation of errors. These may arise directly from two sources; the measurement of gas volume and that of capillary height. If we assume the plots such as Fig (8.5) to be accurate, the error in the gas volume should not be more than $\pm$ 0.05 cc. Similarly if the dilatometer levels are consistant the error in their heights should not be more than $\pm$ 0.020 cms. Substituting these values into our calculations and using normal error techniques we find a maximum error in V_2 of 1.4% - 1.8%. It is stressed that this figure does not take into account errors in graphical methods or other uncertain experimental factors, but within these limits it is a maximum rather than a minimum figure. However, we consider the claim of Hiroka (168) to an accuracy of 0.8% in V_2 values, measured in a similar fashion to ours impossible and further state that quoting the P.M.V. to even the first decimal place is somewhat optimistic.

8.8 Discussion and Comparison of Experimental results.

From the experimental data in Appendix 8. we were able to calculate the P.M.V.'s at 25°C., which are shown in Table (8.3) together with where relevant (and where available) results of earlier workers for the same systems. We believe our accuracy comparable with most data previously quoted. This may be verified by an examination of the tables in A.8. From these it is clearly seen that while the

Table 8.3 Partial Molar Volumes at 25°C.(cc/mol)

Gas / Solvent	Ar.	CH_4	CF_4	SF_6	N_2	D_2
C_6H_6 δ=9.2	44.6	53.3 (54.8)	82.3 (83.2)	97.1 (105.5)	35.4 (35.3)	32.7 (32.7)
c-C_6H_{12} δ=8.2	47.6	55.0	87.4	101.4	41.0	39.4
n-C_6H_{14} δ=7.45	48.3	59.6 (55.4)	88.6 (86.4)	102.6 (105.8)	43.2	41.2
i-C_8H_{18} δ=6.9	49.6 (50.0)	56.6 (56.6)	86.7 (85.4)	103.3 (104.2)	46.2	43.1

( ) = Results of previous workers, see Table 8.1

data for individual doses may show some discrepency, that from which the graphical plots of expansion vs gas volume were constructed have a significantly smaller spread. A noticable exception to this perhaps is the plot for freon in n-heptane. In all four runs were made on this system and in each case the data demonstrated wide and sometimes startling inconsistancies. We can offer no explanation for this anomalous behaviour and foward our value of V_2 = 88.6 cc/mole, subject to a larger degree of error than our other results.

The overall pattern of the P.M.V.'s follows the lines already discussed in (8.1) - increasing with increasing molecular size of solute gas and decreasing with increasing δ for the solvent. Comparing our values with those obtained by previous workers we exactly agree with Jolley (13) for argon in iso-octane and within experimental accuracy with Horiuti (170) for the methane-benzene result. However, our results for SF_6 in all solvents show a total disagreement with those of Hiroka (168). The most striking of these is for the SF_6-benzene system. Our value differs from that previously measured by nearly 8.5 cc/mole. To check this we quote two runs totalling nine doses (see A.8.). The experimental result shown in Table (8.3) is from the first of these.. The second run gives data with a slightly higher spread but a smaller V_2 value and in not one instance on our graphs do we have an experimental point in excess of 100 cc/mole. The remaining comparison

of P.M.V.'s for sulphur hexafluoride do not yield such striking discrepencies but whereas Hiroka's values for different systems were almost identical, ours show a small but definite tendency to behave "normally" in that they increase with decreasing δ.

With regard to the results of Schumm and Brown (179) no firm conclusion may be reached. We agree with their value for freon in benzene, but disagree outside the limits of permitted accuracy for methane in n-heptane. Moving to iso-octane as the solvent medium we again agree with their results for methane (exactly) and for freon (within limits). However, these are against the predicted trend i.e. we would expect larger P.M.V.'s on going from n-heptane to iso-octane. We can only attempt to explain this by refering to the work of Fujishiro et al (180) on liquid-liquid mixtures. In this, anomalous behaviour for iso-octane was again observed and was attributed to "loose structure". Further it was suggested that to fit experimental data the solubility parameter of the solvent should be altered from δ=6.85 to 7.7-7.9. A step of this nature would not help us particularly since although explaining the low values of the P.M.V.'s for methane and freon it would make the Ar, SF_6, H_2 and D_2 results irregular. We must therefore conclude that in certain situations iso-octane exhibits anomalies. These may well be due to its branched structure but to put a numerical estimate on this effect is beyond our scope.

Finally we draw attention to the results observed for hydrogen and deuterium. In each solvent a distinct "quantum difference " is noted, slightly dubious perhaps for cyclohexane but clearly outside the range of experimental uncertainty in all other cases. Further the results in benzene agree exactly (but probably fortuitously) with the results of Walkley and Hildebrand (166). The origin of this quantum difference is thought to lie in the fact that the solvent exerts an internal pressure of a considerable magnitude (3000 atm. - approx.). Under such conditions the dissolved molecule of hydrogen or deuterium acquires a zero point energy well in excess of its classical energy, and this, even at 25°C. is responsible for a quantum effect. Any theoretical treatment of such behaviour therefore requires a consideration of quantum statistics, the success (or failure) of which will act as a test both for any model and for the explanation of the P.M.V. difference as voiced above.

CHAPTER 9.

The Hard Sphere theory and Partial molar volumes.

"How often have I said to you that when we have eliminated the impossible whatever remains however improbable, must be the truth."

Sir Arthur Conan Doyle (1859-1930)

- from "The Sign of Four."

9.1 Regular Solution Theory.

A theoretical prediction of P.M.V.'s from regular solution theory may be developed through a consideration of the excess volume V^E i.e. the volume change resulting from mixing (and in the cases that we consider mixing at constant pressure.). This term was given by Hildebrand as-

$$V^E = n \beta F^E \qquad (9.1.1)$$

n, being the ratio of internal pressure to the cohesive energy density ($= (dE/dV)_T/(E/V)$) , β the isothermal compressibility, while F^E is the excess free energy developed by the process of solution.

In the specific case of highly dilute solutions (9.1.1) may be differentiated in the limit $x_2 \longrightarrow 0$ (where x_2 is the mole. fraction of the solvent) to yield an equation for the P.M.V.

$$V_2^E = V_2 - V_2^o = n_1 \beta_1 RT \ln \gamma_2 \qquad (9.1.2)$$

In the above, V_2^o is the molar volume of the solute in its reference state, n_1 and β_1 are defined as properties of the solvent, while γ_2, the activity coefficient of the solute is given as

$$RT \ln \gamma_2 = \phi_1^2 V_2^o (\delta_1 - \delta_2)^2 \qquad (9.1.3)$$

where ϕ_1 is the volume fraction of the solute and δ_1 and δ_2 the solubility parameters of the solute and solvent respectively. (9.1.2) and (9.1.3) can therefore be combined so that

$$V_2 - V_2^o = n_1 \beta_1 \phi_1^2 V_2^o (\delta_1 - \delta_2)^2 \qquad (9.1.4)$$

The partial molar volumes of iodine and bromine in perfluoro-n-heptane, as measured by Glew (11) and Reeves (182) respectively were tested against theoretical values from (9.1.4). Here $\beta_1 = 2.34 \times 10^{-4}$ atm^{-1} and $n_1 = 1.49$. Good agreement was found for bromine (i.e. 72.5 cc/mole experiment against 75.7 cc/mole from (9.1.4)) but for iodine a larger discrepancy was observed.

Further successful predictions of P.M.V.'s for solid and liquid solutes were made by Smith and Walkley (17). In all cases they employed (9.1.4) with $n_1 = 1$ (an approximation valid for the majority of non polar liquids) and with V_2^o given by the molar volume of the solute, which in the case of a liquid was obtained by extrapolating from the melting point to the reference temperature (generally 25°C.)

The success of this treatment could not be carried over into gas solvent systems. One major difficulty was the determination of a solubility parameter for the solute gas (δ_2). However, values of δ_2 were indirectly evaluated by Clever et al (171-173) and Gjaldebeck (183-184). Using these values Smith and Walkley applied (9.1.4) to calculate gas P.M.V.'s. The results obtained were completely anomalous. The predicted values of the same gas in differing solvents showed little if any change with δ_1, and in general this approach within the limits of gas liquid systems was proved both insensitive and inaccurate.

Such observations forced Smith and Walkley to look outside the boundaries of regular solution behaviour for an explanation of this phenomenon and led them to formulate a simple but effective hard sphere "free volume" theory. In the following sections we describe the development of this theory and its extensions into the limits of quantum behaviour.

9.2 A Classical Hard Sphere Treatment.

The hard sphere theory follows, to some extent, the earlier ideas of Uhlig (177) and Eley (175,176). It pictures the molecule as occupying a spherical cavity in the solution being surrounded at the boundaries of this cavity by the neighbouring solvent molecules. The simplest theoretical approach is to consider the solute as a hard sphere molecule of diameter σ, (i.e. an entity capable of exerting only a repulsive potential). This molecule positioned at the centre of its cell will therefore generate a pressure (obtainable from the hard sphere equation of state) which, to maintain equilibrium, is balanced by an equal and opposite pressure from the solvent, the latter being defined as the "internal pressure". The mixing process is considered to be such that, having attained this equilibrium, mixing occurs without any further volume change and therefore the molecular volume of the solute

in the hypothetical liquid state must be identical with the partial molar volume of the solute in the final solution. Putting this concept on a somewhat simpler basis, before solution the gas consists of a system of hard spheres at atmospheric pressure, the volume occupied by this system being given by the hard sphere equation of state. For mixing to occur the gas must be drastically compressed until its pressure is equal to the mixing pressure (given by the internal pressure of the solvent). At this pressure isothermal and isometric mixing take place, while also at this pressure the volume occupied by the gas is equal to its P.M.V. in solution.

The internal pressure of a solvent is given as

$$(dE/dV)_T = T(dP/dT)_V - P \qquad (9.2.1)$$

Since P is generally one atmosphere it may be ignored in comparison with $T(dP/dT)_V$ which is in the region of 2000-3000 atms.

The free volume of a system of hard spheres is readily evaluated

$$V_f = \int_0^{a-\sigma} 4\pi r^2 dr = (4/3)\pi(a - \sigma)^3 \qquad (9.2.2)$$

where a is nearest neighbour distance.

Substitution of (9.2.2) in the classical partition function leads to the classical expression for the pressure of a system of hard spheres

$$P = (RT/V)(1 - \sigma/a)^{-1} \qquad (9.2.3)$$

Now by definition (9.2.3) must be equal to the internal pressure of the liquid, so equating (9.2.1) and (9.2.3)

gives:-

$$(dP/dT)_V = (R/V)(1 - \sigma/a)^{-1} \qquad (9.2.4)$$

We define $V_o = \gamma No^3$ and $V = \gamma Na^3$, where γ is a constant dependent on the geometry of the lattice and set V_o equal to the volume of the gas at 0^oK. Further we assume that when this equilibrium is effective $V=V_2$. (9.1.4) therefore becomes:-

$$(dP/dT)_V = (R/V_2)\left[1-(V_o/V_2)^{\frac{1}{3}}\right]^{-1} \qquad (9.2.5)$$

or

$$V_o = V_2\left[1-(R/V_2)(dP/dT)_V^{-1}\right]^3 \qquad (9.2.6)$$

Hence knowing the collision diameter of the gas (σ) and the value of $(dP/dT)_V$ for the solvent, a value of the P.M.V. may be obtained for any gas-solvent system. Several assumptions must now be made to develop these equations. First the packing parameter γ, is assumed to be unity. This might appear somewhat arbitrary but, like the L-J theory, the lattice concept is only introduced to link nearest neighbour distance and density. This concept has no further part in the calculations, and a packing parameter of $\gamma = 1$ is perhaps as justified as any other assumption. The choice of a value for σ raises somewhat greater problems. It was in fact assumed to be given by the L.J. collision diameter. This parameter can therefore be obtained either from a choice of gas (second virial or transport) data or from solid state properties as characterised by the zero point parameters (4.3). In this treatment, however, we are dealing with gas molecules at room temperature and

and therefore gas imperfection data would appear the obvious choice. This was the procedure employed by Smith and Walkley for Ar, N_2, CO, and CH_4, although they did use solid state data for hydrogen and deuterium. In all our calculations we used the normal σ values derived from second virials, the only exception being the value for sulphur hexafluoride which we later discuss in some detail. Hydrogen and deuterium present a special case and they are treated in (9.3).

The values of $(dP/dT)_V$ for various solvents were, if possible, taken from direct experimental measurements. Failing this they may be obtained to a good approximation from the relationship:-

$$(dP/dT)_V = (\alpha/\beta) \qquad (9.2.7)$$

where α = coefficient of linear expansion and β is the isothermal compressibility of the solvent (185).

The solution of (9.2.6) is effected by writing it generally as:-

$$V_o = f(V) \qquad (9.2.8)$$

For any solvent knowing $(dP/dT)_V$, f(V) may be evaluated over a range of volumes and plotted as V against f(V). Now by definition each gas in this solvent has a unique value of V_o such that $V_o = f(V)$ when $V=V_2$, and hence for each gas-solvent system the value of $\left[f(V)\right]_{V=V_o}$ gives a corresponding value of $\left[V\right]_{V=V_2}$.

The plot of f(V) vs. V for benzene ($(dP/dT)_V$=12.3 atm/deg.) is given in Fig. (9.1) and an abbreviated list of data used to construct it in Table (9.1).

Fig 9.1 Classical Hard Sphere for Benzene, Eq 9.2.8.
$V_o = f(V)$, $(dP/dT)_V = 12.10$ atm/deg

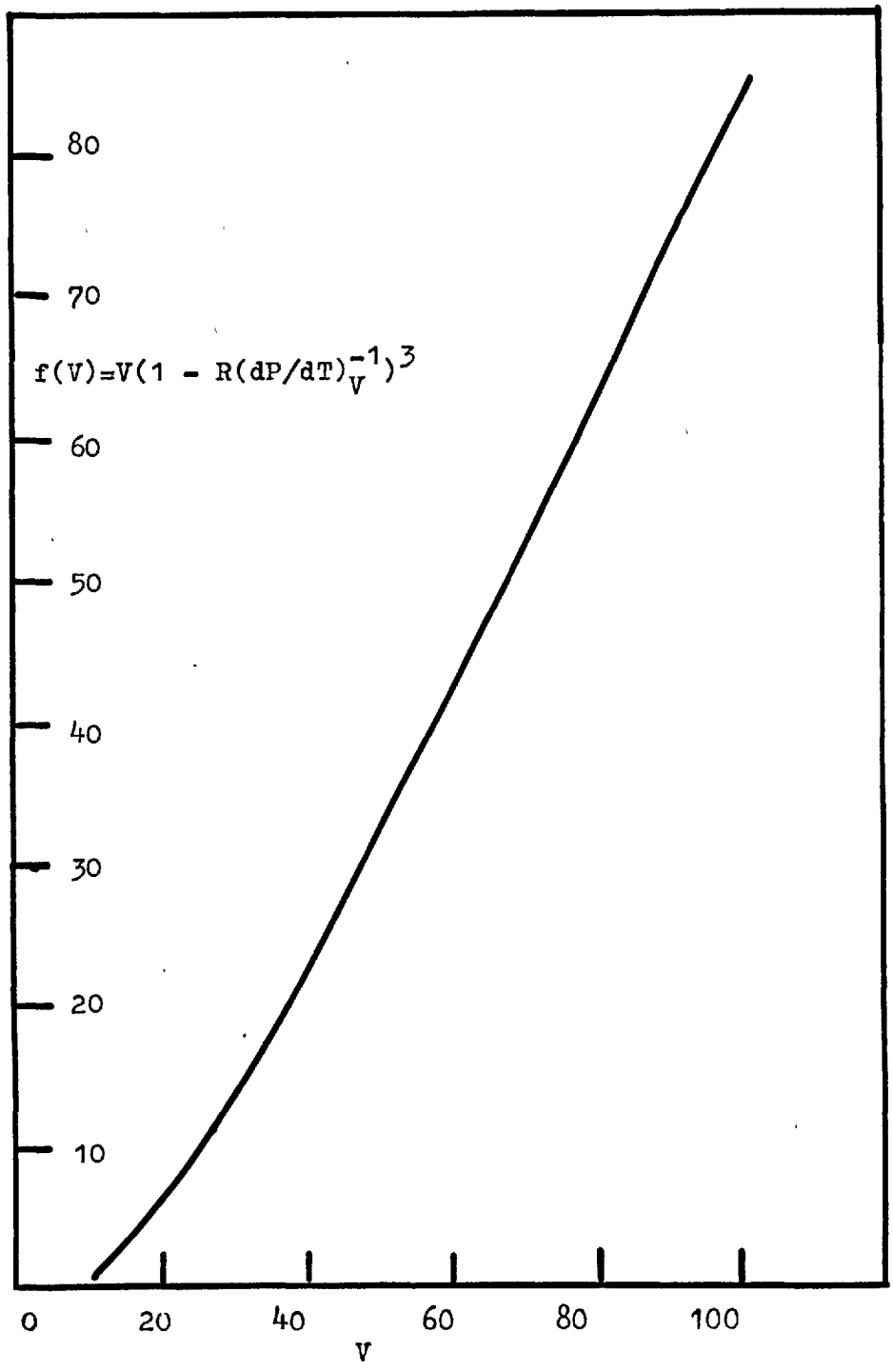

Table 9.1 V vs f(V) for Benzene at 25°C, after Eq 9.2.6

$(dP/dT) = 12.60$ atm/deg, $R = 82.07$ cc, atm/°K, mole

V	$\frac{R}{V}$	$\frac{R}{V}\left(\frac{dP}{dT}_V\right)^{-1}$	$1 - \frac{R}{V}\left(\frac{dP}{dT}_V\right)^{-1}$	$(1- \frac{R}{V}\left(\frac{dP}{dT}_V\right)^{-1})^3$	$V(1- \frac{R}{V}\left(\frac{dP}{dT}_V\right)^{-1})^3$
10	8.207	0.667	0.333	0.037	0.370
20	4.104	0.534	0.666	0.295	5.900
30	2.735	0.222	0.778	0.471	14.130
40	2.052	0.167	0.833	0.578	23.120
50	1.641	0.133	0.867	0.652	32.600
60	1.368	0.111	0.889	0.703	42.180
70	1.173	0.095	0.905	0.741	51.870
80	1.026	0.083	0.917	0.771	61.680
90	0.912	0.074	0.926	0.794	71.460
100	0.821	0.067	0.933	0.812	81.200

Table 9.2 Experimental P.M.V.'s at 25°C, compared with values from the hard sphere theory(from 9.2.8)

Gas / Solvent.	Ar. $N\sigma^3=25$	CH_4 $N\sigma^3=35$	CF_4 $N\sigma^3=63$	SF_6 $N\sigma^3=77$
C_6H_6 $(dP/dT)_V=12.3$	44.6 (42)	53.3 (53)	82.3 (81)	97.1 (96)
c-C_6H_{12} $(dP/dT)_V=10.5$	47.6 (45)	55.0 (55)	87.4 (84)	101.4 (99)
n-C_7H_{16} $(dP/dT)_V=8.4$	48.3 (48)	59.6 (60)	88.6 (89)	102.6 (103)
i-C_8H_{18} $(dP/dT)_V=7.6$	49.6 (51)	56.6 (62)	86.7 (92)	103.3 (106)
CCl_4 $(dP/dT)_V=11.2$	45 (44)	52 (54)	80 (83)	104 (97)

( ) values calculated from H.S. theory (9.2.6) and (9.2.8)

We formulated similar plots for cyclohexane, iso-octane, n-heptane and carbon tetrachloride, and using values of $N\sigma^3$ from second virial data obtained theoretical P.M.V.'s for Ar, CH_4 and CF_4. Preliminary calculations for SF_6 however indicated that any theoretical results would be anomalously high. The value initially used for $N\sigma^3$ was 100.7 cc/mole, being derived from the σ value (=5.51Å) given by MacCormack and Schneider (186). These workers were also responsible for parameters for CF_4 which appeared to give orthodox results. However, a close study of their work indicated that their fitting procedure for SF_6 was most unsatisfactory. Indeed the authors themselves state that "an exact determination of the parameters for SF_6 was not possible". These parameters were of course derived on the assumption of a L.J. 12:6 interaction. However, for some little time there have been definite suggestions that large quasi spherical molecules such as SF_6 might be better described by a 28:7 potential. Values of ϵ/k and σ for such molecules were given by Hamann and Lambert (149) who derived their parameters from collision integrals in combination with existing second virial coefficient data. Hamann's value for $N\sigma^3$=76.61 cc/mole (σ=5.05Å) was much more reasonable than that given by MacCormack, but if a 28:7 interaction is assumed for SF_6 why not for CF_4? To answer this we quote the work of McCoubrey and Sing (187) who investigated intermolecular forces in quasi spherical molecules. Their investigations showed that whereas Xe, CH_4 and CF_4 were adequately described

by a 12:6 potential, SF_6 and SiF_4 were better accounted for with a 28:7 potential. In our calculations we therefore use $N\sigma^3$ for SF_6 from Hamann data. The other gases are all considered to be adequately described by the normal L.J. σ's.

The theoretical results from (9.2.8) are shown in Table (9.2) and are compared with the experimental values from 8.8. The agreement between measured and calculated values is often within experimental error and in only two cases, the "anomalous" iso-octane results for methane and freon (see 8.8), are large discrepancies observed. In particular we note the excellent correspondence between the predicted values for SF_6 and experimental data. For interest we have indicated theoretical values for carbon tetrachlordde which are compared with the experimental results of other workers from Table (8.1). Once again good agreement is observed, apart from the SF_6 value of Hiroka. The fact that the theoretical P.M.V.'s follow the trend of decreasing with increasing δ parameter is not surprising since for any solvent $\delta \propto (dP/dT)_V$ but nevertheless the utility of (9.2.6) must be beyond question. A comparison of values derived from it compared with other more "rigorous" expressions is postponed until later (9.4).

9.3 The Quantum Hard Sphere Equation of State

A close examination of Table (9.2) will reveal no mention of V_2 values, either experimental or theoretical for hydrogen or deuterium. These can be obtained through (9.2.6) and in fact this was done by Smith and Walkley. They assumed V_o values from the volume of the low temperature solid and using these calculated results that were grossly above the experimentally measured data (see Tables (9.3) and (9.4)). The cause of this "failure" of the theory must be in the use of (9.2.3) to give the pressure of the gas. If hydrogen and deuterium indeed display a quantum effect at room temperatures, and the evidence is heavily biased to support this, their pressure and equation of state can only be derived through quantum statistics and hence a quantum hard sphere equation of state.

Such an equation was developed by Hillier and Walkley (157), who then adopted it to evaluate the quantum V_2 values for hydrogen and deuterium in benzene and perfluoro-n-heptane (188), achieving a reasonable agreement with experimental data. For the latter investigation they used an approximation which replaced the spherical cavity by a cubical cell of equivalent free volume. This step was taken chiefly to ease mathematical computation. In our present treatment we use the more accurate spherical cavity method developed by Utting (71) from the work of Hillier and slightly amended by the author. It is in many respects identical to the uniform potential treatment given in

Appendix 6, and is therefore only briefly described here.

The hard sphere potential is given by:-

$$W(r)=0 \quad 0<r<(a-\sigma)$$
$$W(r)=\infty \quad r>(a-\sigma) \qquad (9.3.1)$$

The free volume integral in (9.2.2) is, as is usual in any quantum treatment, replaced by the Slater sum. The resulting Schroedinger wave equation is for one particle in a spherical cell and, for the hard sphere potential, may be solved by transforming to polar co-ordinates (see A6.).

The energy levels are given by:-

$$E = (h^2 C_l^*/8mR^2) \qquad (9.3.2)$$

where R is the radius of the effective cavity and C_l^* is obtained from the zeros of the half integral Bessel functions.

From these arguements, the equation of state may finally be written in reduced units as:

$$(PV/NkT) = f(V^*,T^*) \qquad (9.3.3)$$

where

$$f(V^*,T^*)= \frac{\sum_l (2l+1)(D^*C_l^*/T^*)(V^{*-\frac{1}{3}}-1)V^{*-\frac{1}{3}}\exp(-D^*C_l^*/T^*(V^{*-\frac{1}{3}}-1)^2)}{\sum_l (2l+1)\exp(-D^*C_l^*/T^*(V^{*-\frac{1}{3}}-1)^2)}$$

and $D^* = (h^2/8m\epsilon)V_o^{-\frac{2}{3}} = \Lambda^{*2}/8$ with Λ^* the De Boer parameter.

For our calculations we require, not the compressibility of the system as given above, but the pressure where:-

$$P=(RT/V^*V_o)f(V^*,T^*) \qquad (9.3.4)$$

since $V^*=V/V_o$

which may be equated to (9.2.1) such that:-

$$(V_o/R)(dP/dT)_V=f(V^*,T^*)/V^* \qquad (9.3.5)$$

Hence knowing the L.J. parameters for the system (9.3.5) may be solved in a similar manner to (9.2.6). This is done by computing $f(V^*,T^*)/V^*$ over a range of V^* values with $\Lambda^*=1.729$ (hydrogen) or $\Lambda^*=1.223$ (deuterium). It is necessary to evaluate the function at a reduced temperature T^* such that $T^*=298/(\epsilon/k)$ - i.e. at 25°C. We then plot graphically $f(V^*,T^*)/V^*$ against V^*, for the appropriate quantum gas (the plot for H_2 being given in Fig. (9.2)). Consequently knowing $(dP/dT)_V$ for each solvent we may calculate $(V_o/R)(dP/dT)_V$ for a given gas-solvent system and from the equality of (9.3.5) immediately derive an equivalent V^*. This latter quantity is tabulated and readily normalised (through $N\sigma^3$) to give the V_2 value for the system.

In Tables (9.3) and (9.4) we give the theoretical and experimental data for hydrogen and deuterium. The reduction parameters used in our calculations being those of Michels (118) i.e. H_2 ($N\sigma^3=15.60$ cc/mole; $\epsilon/k=36.7$°K.), D_2 ($N\sigma^3=15.50$ cc/mole; $\epsilon/k=35.2$°K.).

The theoretical results derived from (9.3.5) and listed in these tables again show good agreement with experimental data. A marked exception to this perhaps are the results in cyclo-hexane but the other predicted values although not yielding such close agreement as measurements in Table (9.2) all lie within or just outside the range of experimental error. The difference between theoretical V_2's for hydrogen and deuterium in the same solvent is small and constant (approx. 1.3 cc/mole). We performed other calculations

Fig 9.2 Quantum Hard Sphere for Hydrogen $f(V^*,T^*)/V^*$ vs V^* at $T^* = 8.02$ (i.e. $298^{\circ}K$)

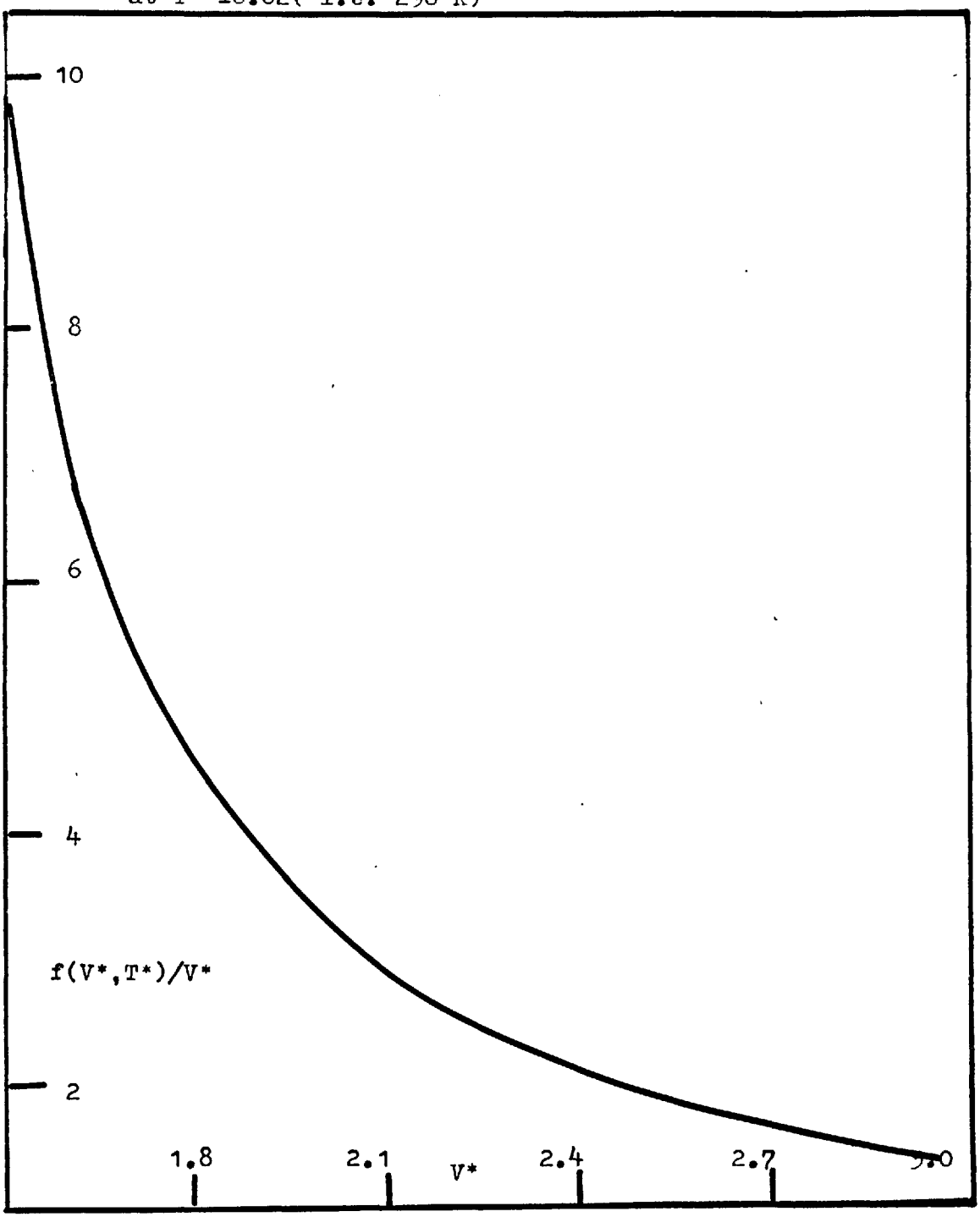

Table 9.3 Hydrogen, theoretical P.M.V.'s from Q.H.S. equation of state($N\sigma^3$ =15.60 cc/mol, Λ^* = 1.729)

Solvent	$(dP/dT)_V$ atm/deg	$V_o\left(\frac{dP}{dT}\right)_V$	$\frac{V_o}{R}\left(\frac{dP}{dT}\right)_V$	V^*	V_2 Theory	V_2 Expt	V_2 (9.2.6)
C_6H_6	12.30	191.9	2.238	2.264	35.3	35.4	39.8
$c\text{-}C_6H_{12}$	10.50	163.8	1.996	2.415	37.7	40.0	42.5
$n\text{-}C_7H_{16}$	8.40	131.0	1.597	2.677	41.8	43.2	46.6
$i\text{-}C_8H_{18}$	7.60	118.6	1.445	2.808	43.8	46.2	49.9

Table 9.4 Deuterium, theoretical P.M.V.'s from Q.H.S. equation of state($N\sigma^3$ =15.50 cc/mole Λ^* =1.223)

Solvent	$(dP/dT)_V$ atm/deg	$V_o\left(\frac{dP}{dT}\right)_V$	$\frac{V_o}{R}\left(\frac{dP}{dT}\right)_V$	V^*	V_2 Theory	V_2 Expt	V_2 (9.2.6)
C_6H_6	12.30	190.6	2.323	2.188	33.9	32.7	36.5
$c\text{-}C_6H_{12}$	10.50	162.8	1.983	2.350	36.4	39.4	39.3
$n\text{-}C_7H_{16}$	8.40	130.2	1.586	2.613	40.5	41.2	43.3
$i\text{-}C_8H_{18}$	7.60	117.8	1.435	2.740	42.5	43.1	45.5

with the parameters given by Hirschfelder et al. (189), which were used in the earlier work of Walkley and Hillier (188). No significant improvement in theoretical values was observed.

The calculations just described in common with other expresssions in reduced variables must be extremely sensitive to the parameters employed in any "normalisation" procedure. In view of this, agreement of theory with experiment must be classed as excellent, especially when one considers the anomalously high values of V_2 for hydrogen and deuterium as derived from (9.2.6) and as shown in the final column of Tables (9.3) and (9.4). The relative success of the quantum cell model must also emphasise two distinct facts. First that the differences in solution properties of H_2 and D_2 at room temperature must, beyond all doubt, be attributed to quantum effects and secondly that even in complex situations the empirical but simple hard sphere theory retains a remarkable predicative value.

9.4 Discussion

We conclude this chapter by comparing the relative merits of the hard sphere "free volume" theory with other methods used to predict P.M.V.'s. Smith and Walkley conclusively demonstrated the inadequacy of regular solution theory (9.1) and also revealed the limitations of the Prigogine-Scott (190) model, which, depending on the thermodynamic properties

of both gas and solvent in their pure states, formulated equations which exhibited minimum dependence on a cell model.

Since then another method of predicting V_2 values, given by Pierotti (191,192) and based on a hard sphere theory theory of fluids developed by Reiss et al (193-195) has been forwarded. Pierotti's approach considers the solution process in much the same way as the work of Eley (175-6) in that two distinct steps are postulated. These are the creation of a cavity to accomodate the solute molecule and the introduction of the molecule into this cavity. From this the expression for V_2 is given as:

$$V_2 = V_i + V_c + \beta RT \qquad (9.4.1)$$

where V_c is the volume change on cavity formation, V_i the change on introducing the solute molecule and β the isothermal compressibility of the solvent. V_i is assumed negative but so small as to be unimportant, V_c is calculated through the equations of Reiss. In Table (9.5) we compare the theoretical V_2 values of Pierotti in benzene at 298°K., with experimental values and our own theoretical calculations from the hard sphere theory. (For Table see overleaf.)

Similar results to those given in Table (9.5) are observed for carbon tetrachloride. Pierotti claims the agreement using (9.4.1) to be good and further states that the discrepancies are " ...what one would expect by ignoring V_i.....". With regard to this statement all

Table 9.5 Theoretical and experimental P.M.V.'s for some gases in benzene at 25°C. (cc/mole.)

Gas	V_2 [a]	V_2(expt.)	V_2 [b]
Ar	52	45	42
N_2	61	53	50
CH_4	65	53	53
H_2	38	35	35

a Values of Pierotti from (9.4.1)

b Our values from (9.2.6.) and (9.3.5)

****

comment is superfluous, while Pierotti's further attempts to use this " evidence " as a basis for dismissing free volume theories out of hand can only be regarded with astonishment.

In fairness to the Pierotti approach however, it must be stated that it is a versatile method in that it allows the prediction of solubilities (via the Henry coefficient) and other thermodynamic solution properties. In this context our model with the hard sphere pressure being balanced by the solvent pressure is strictly limited. We have attempted to extend it to predict the solubilities and entropies of solution using the methods of Eley (175) and the more recent approach of Prausnitz (196) but have not achieved any notable degree of success.

Acknowledging this failure to extend the model to solution properties, we also observe that it can have other and perhaps more unexpected uses. We rewrite the classical

equation (9.2.6) as:

$$V_2^{\frac{1}{3}} - V_o^{\frac{1}{3}} - R(dP/dT)_V^{-1} V_2^{-\frac{2}{3}} = 0 \qquad (9.4.2)$$

or $$V_2 - V_o^{\frac{1}{3}} V_2^{\frac{2}{3}} - R(dP/dT)_V^{-1} = 0 \qquad (9.4.3)$$

(9.4.3) is a cubic equation in $V_2^{\frac{1}{3}}$ and similar to (9.2.6) may be solved graphically, knowing $N\sigma^3$ for the gas and $(dP/dT)_V$ for the solvent. It is specific for any gas-solvent system and in Fig (9.3) we show the relevant curves for argon in benzene and iso-octane and for freon in benzene. These perhaps represent the limits with regard to the gas-solvent systems studied experimentally. It is known that the V_2 values for the same gas in different solvents alter only slightly. This is clear from an examination of (9.4.3) and Fig (9.3). The only term to change is the $(dP/dT)_V$ for the solvent. This results in the iso-octane curve being almost identical to the benzene one but with a lower minimum and with a fractionally larger zeroth intercept ($f(V_2^{\frac{1}{3}})=0$). For different gases in the same solvent the size effect (i.e. V_o) is of much greater importance. This is reflected in the behaviour of (9.4.3) for the freon-benzene curve which is totally different from that of argon in the same solvent.

Throughout this chapter we have continually used the model to predict P.M.V. values. We now reverse the process and assuming a knowledge of V_2 take a further look at (9.4.3). If we know V_2 an experimental solution property, and V_o an empirical gas relationship, we may solve (9.4.3) to find $(dP/dT)_V$ which is a property of the pure solvent.

Fig 9.3 Plot of Eq 9.4.3 for three gas-solvent systems.

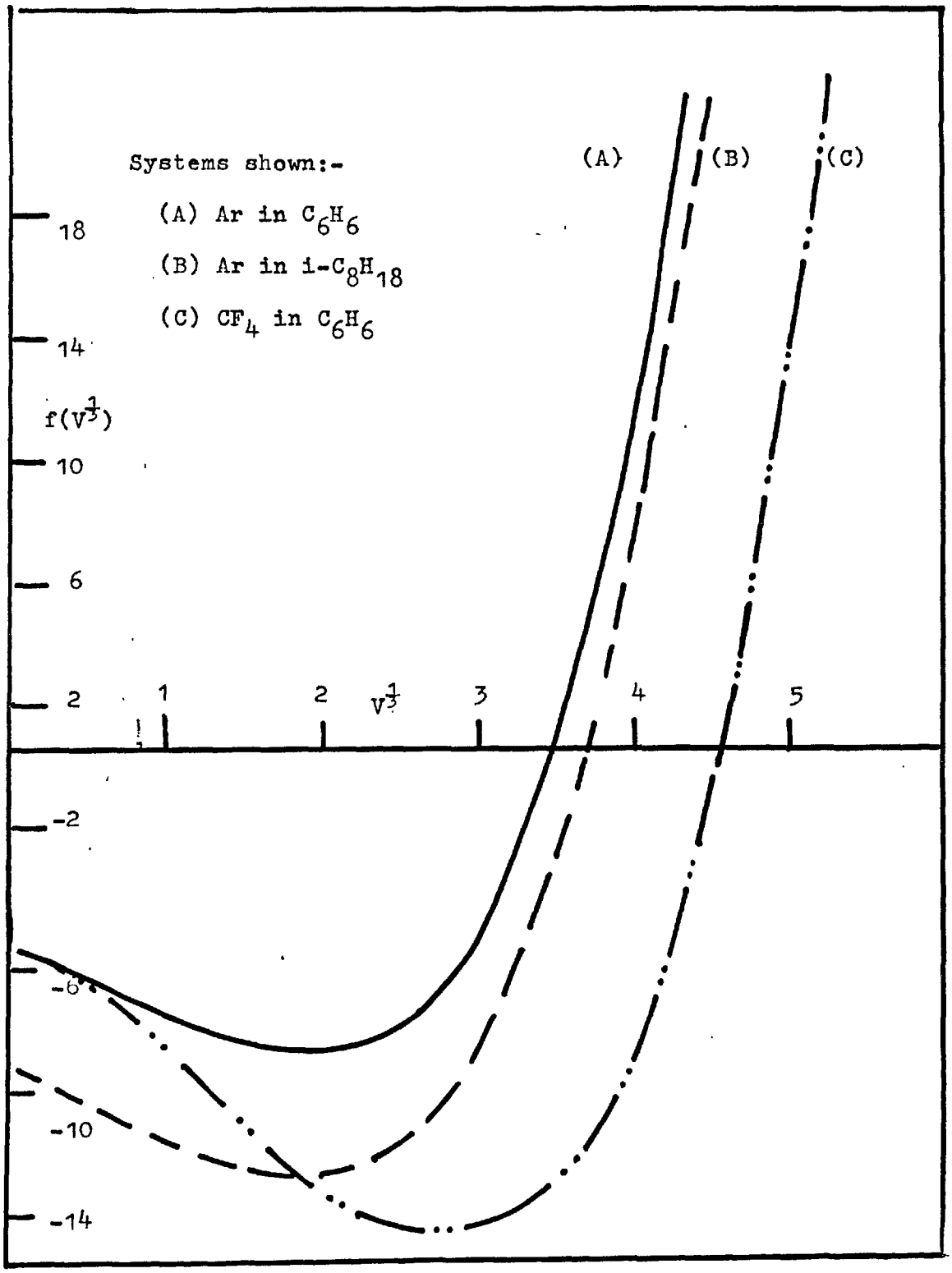

As we have already stated, this may be directly measured or indirectly calculated (9.2.7). Its derivation through (9.4.3) is possibly of questionable value.

We now move to the third and perhaps most surprising corollary of (9.4.3) in that measuring V_2 and $(dP/dT)_V$ experimentally we may proceed through (9.4.3) to evaluate V_o and consequently σ, the Lennard-Jones force constant for the gas. This quantity, normally derived from second virial or transport data, assuming an L.J. 12:6 interaction is specifically a gas property. Can it be successfully evaluated from experimental solution and solvent data? To answer this question we proceed in a somewhat unorthodox manner, by considering the P.M.V.'s of iodine and bromine in perfluoro-n-heptane. These constitute a solid-liquid and liquid-liquid system respectively and were of course used by Hildebrand (9.1) as a sensitive test of regular solution theory. Outside the solutions, there can be no accountable reason to consider either solute as a hard sphere gas. However, the solution process itself and the situation directly resulting from it may, to a good approximation be described by a hard sphere theory.

Therefore using the experimental V_2 values of Hildebrand and co-workers and the $(dP/dT)_V$ for perfluoro-n-heptane measured by Smith (167) we have used (9.4.3) to predict σ values for iodine and bromine which are shown in Table (9.6.)

Table 9.6 σ parameters from V_2 values in n-C_7F_{16} at 25°C.

$((dP/dT)_V = 7.10$ atm./deg.)

Solute	V_2 [a]	σ(Å) [b]	σ(Å) [c]
I_2	100	4.862	4.982
Br_2	73	4.166	4.268

a From Ref (163) p110- values in cc/mole.

b Theoretical values from (9.4.3)

c Experimental values derived from viscosity data (189)

The theoretical values are compared with those obtained from gas viscosity data (189). Even bearing in mind the frequent unreliability (i.e. non uniqueness) of values obtained from transport properties, and in addition the somewhat dated experimental results from which they were derived, the correspondence remains remarkable and must lead to several possible conclusions. The first of these is that (9.4.3) must be insensitive, especially with regard to σ, but this is not supported by our earlier evidence (see Fig (9.3)). The second and, we think, more plausible conclusion is that for solution behaviour directly related to the volume expansion of mixing and involving either gas, liquid or solid solutes the hard sphere theory of Smith and Walkley, used as a simple predicative medium remains without equal. Its theoretical justification is (as we have seen) somewhat nebulous and we offer no rigerous explanation for it. Instead (and here we paraphrase Hildebrand) we must provisionally content ourselves with this presentation and offer the relationships described above as a suggestive model for further theoretical treatments.

CHAPTER 10

A modified Cell theory.

"It is a capital thing to theorise
before one has data."
Sir Arthur Conan Doyle (1859-1930)
from "Scandal in Bohemia."

10.1 The Model

The picture of gas solubility as given by the hard sphere treatment, although attractive, is rather grossly over simplified. We have therefore attempted to extend our approach by utilising the ideas of Kobatake and Alder (19) and Walkley (199). These, while admitting the failure of a lattice model to act as an adequate theory of fluids, especially with regard to the communal entropy problem, (i.e. higher order correlations) emphasise that one particle theories may provide one of the few methods through which meaningful results can be obtained.

In the treatment of either a liquid in its pure state or a liquid gas mixture, a one particle theory pictures each molecule as confined to a cell. To date, in this discussion, such a theory has automatically involved the parallel assumption of a virtual lattice, which is needed to define the cell dimensions. However, we now follow Kobatake and Alder (K.&A.) in rejecting this concept and instead determine the size of the cell from the thermodynamic properties of the system. We therefore picture the representative particle as confined to a spherical cell, not part of a lattice, whose size and whose number of surrounding neighbours are determined by forcing agreement on two thermodynamic properties, the resulting cell parameters being known as "effective" parameters, since they reflect higher order correlations. In any consideration of pure

liquids we have a relatively simple situation, composed of an "array" of identical cells. However, moving to dilute gas solutions the position rapidly complexes. The introduction of the solute molecule is accompanied by cavity formation, which disturbs the uniform nature of the solvent and creates a situation where several different types of cell may exist. The extent and degree of this disturbance is therefore one factor that should be predictable from any rigorous treatment.

To simplify the theoretical model we adopt the assumptions of earlier workers (19,199) with regard to the size of the cell. In pure systems the cell length parameter is determined from the volume per particle, its nearest neighbours being smoothed at a distance equal to $\sigma/2$ (σ is the L.J. parameter). At this latter point the force between two molecules is, by definition, highly repulsive and to a good approximation the wandering molecule may be regarded as being confined to the particle volume. In the case of gas solutions the treatment is similar but the volume per particle is replaced by the P.M.V. for the system and the resulting length used, in conjunction with the radius of the pure solvent, to evaluate the nearest neighbour distance.

Any cell theory, requires the cell potential $W(r)$ as a definite function of volume, temperature and $\underline{r}$ (where $\underline{r}$ is the distance of the "wanderer" from the centre of the cell). K.&A. adopted the Lennard-Jones potential, primarily for the convenience of tabulated integrals (48). We do

likewise but instead use our classical approach that enables us to quickly and readily compute properties over a wide spectrum of "theoretically imposed" conditions. This adaptation of the L-J potential introduces the parameters ϵ and σ which become the "effective" parameters mentioned above. The σ parameter has already been defined, being obtainable from the size of the cell. The energy parameter however, involves not ϵ alone but $Z\epsilon$, where Z is the number of nearest neighbours. From a rigorous cell theory Z=12 but in structures that we consider it varies with volume and temperature. Such a factor should strictly be considered in any manipulation (e.g differentiation) of functions developed from the potential. However, this would introduce complexities into the mathematical process and is therefore arbitrarily ignored.

Calculations using this modified theory are usually made in reduced variables. These differ from the reduced quantities previously defined (1.4) to a considerable extent. Thus reduced temperature (T^*) is replaced by the "effective" reduced temperature (T_e^*) so:-

$$T_e^* = (12/Z)(kT/\epsilon) \qquad (10.1.1)$$

while V_e^*, the effective volume is given as:-

$$V_e^* = a^3/(2^{\frac{1}{2}}\sigma^3) \qquad (10.1.2)$$

$\underline{a}$ being the nearest neighbour distance, σ as above (dependent on the system) while $2^{\frac{1}{2}}$ is not a packing factor but rather a normalisation to allow comparison with previous results. A more exact formulation of (10.1.1) and (10.1.2) is highly

dependent on whether we are studying a one or two component system and the full treatment is therefore postponed until later in this chapter. At this point, however, it is pertinent to remark that in the case of a gas-liquid system the "effective" parameters, if determined through experiment, can be used to obtain information on the arrangement of solvent molecules around each gas-solute. Thus, providing the energy parameter is assumed, the effective temperature can be used to calculate the number of nearest neighbours, while it should be possible, knowing σ, to investigate the geometric distribution of these neighbours around the cell boundary.

The idea of a decreased co-ordination number has previously been examined in the application of the "L-J" to liquid argon (46). In this context its validity must be doubtful. In the field of gas solubility, however, geometrical factors alone make such a concept more probable. An examination of this through (10.1.1) yields information that is confined only to nearest neighbours. However, the arrangement of further neighbours must also be altered and should be reflected in their contribution to W(r). But, as before, a direct evaluation for an effect of this kind is difficult, and to a good approximation it may be assumed that the number of further neighbours changes in the same proportion as the nearest neighbours deviate from 12 in a close packed structure.

Therefore, utilising the above assumptions we have

performed a limited examination (for some of the systems studied in Chapter 8) on the disorder introduced into a solvent by gas dissolution. Other authors have extended this treatment to predict other solution properties. A closer perusal of these extensions, however, reveals them to be based on foundations that even the most optimistic theoretician must regard as shaky. These will be discussed later.

We now apply our effective theory to a consideration of pure liquids.

10.2 Pure Liquids

A liquid may be regarded as a classical system, the partition function of which is given by (1.3.7), and having a Gibbs free energy (A_L) such that:-

$$A_L = \frac{3}{2}RT \ln\lambda - RT \ln v_f + \frac{Nw(0)}{2} \quad (10.2.1)$$

where $\lambda=(h^2/2\pi mkT)$

The corresponding free energy in the gas phase (A_G) is:-

$$A_G = \frac{3}{2}RT \ln\lambda - RT \ln\left(\frac{V}{N}\right) - RT \quad (10.2.2)$$

Assuming the gas to be ideal, (10.2.1) and (10.2.2) balance at a pressure equal to the vapour pressure of the liquid, hence:-

$$\ln v_f - \frac{w(0)}{2kT} = \ln\left(\frac{V}{N}\right) + 1. \quad (10.2.3)$$

From (1.3.7) we may also develop a term for the entropy of vapourisation S^v, which is the excess entropy of the liquid over the ideal gas.

$$S_v^* = \frac{S_v}{Nk} = \frac{3}{2}\ln\lambda + \ln V_f + \frac{d\ln V_f}{d\ln T} + \frac{3}{2} - S_{IDEAL\ GAS} \qquad (10.2.4)$$

$$= \ln V_f + \frac{\partial \ln V_f}{\partial \ln T} - \ln\frac{V}{N} - 1 \qquad (10.2.5)$$

Substituting (10.2.3) in (10.2.5)

$$S_v/Nk = \left(\frac{\partial \ln V_f}{\partial \ln T}\right) + \frac{\omega(0)}{2kT} \qquad (10.2.6)$$

We apply the classical "L-J" cell model as developed in (1.3) to evaluate (10.2.6), together with the compressibility as given by (4.2.7). Calculations of this type must take account of distant neighbours (i.e. those outside the first shell). K.&A. did this by assuming them to be distributed "at the uniform density of the fluid, starting at a distance from the central molecule such that when the nearest neighbour distance corresponds to that of a face centred lattice (a_o) the same results are obtained as for the lattice....". The Kobatake and Alder calculation was therefore almost identical to that normally made in the L.J. treatment and in fact it was stated that the assumption of further neighbours contributing as if they were in a lattice structure would not significantly affect the final results. Our calculations were therefore made on the latter assumption. However, we emphasise that the contribution is so small as to not invalidate our earlier ideas.

For a pure liquid (PV/NkT) is to a good approximation zero and by performing calculations over a range of V_e^* and T_e^* it was possible to obtain the relationship between these two "effective" reduced quantities at zero compressibility. This is shown in Fig.(10.1) while Fig.(10.2) gives a

Fig 10.1 V_e^* vs T_e^* for zero compressibility using a Classical L.J. potential

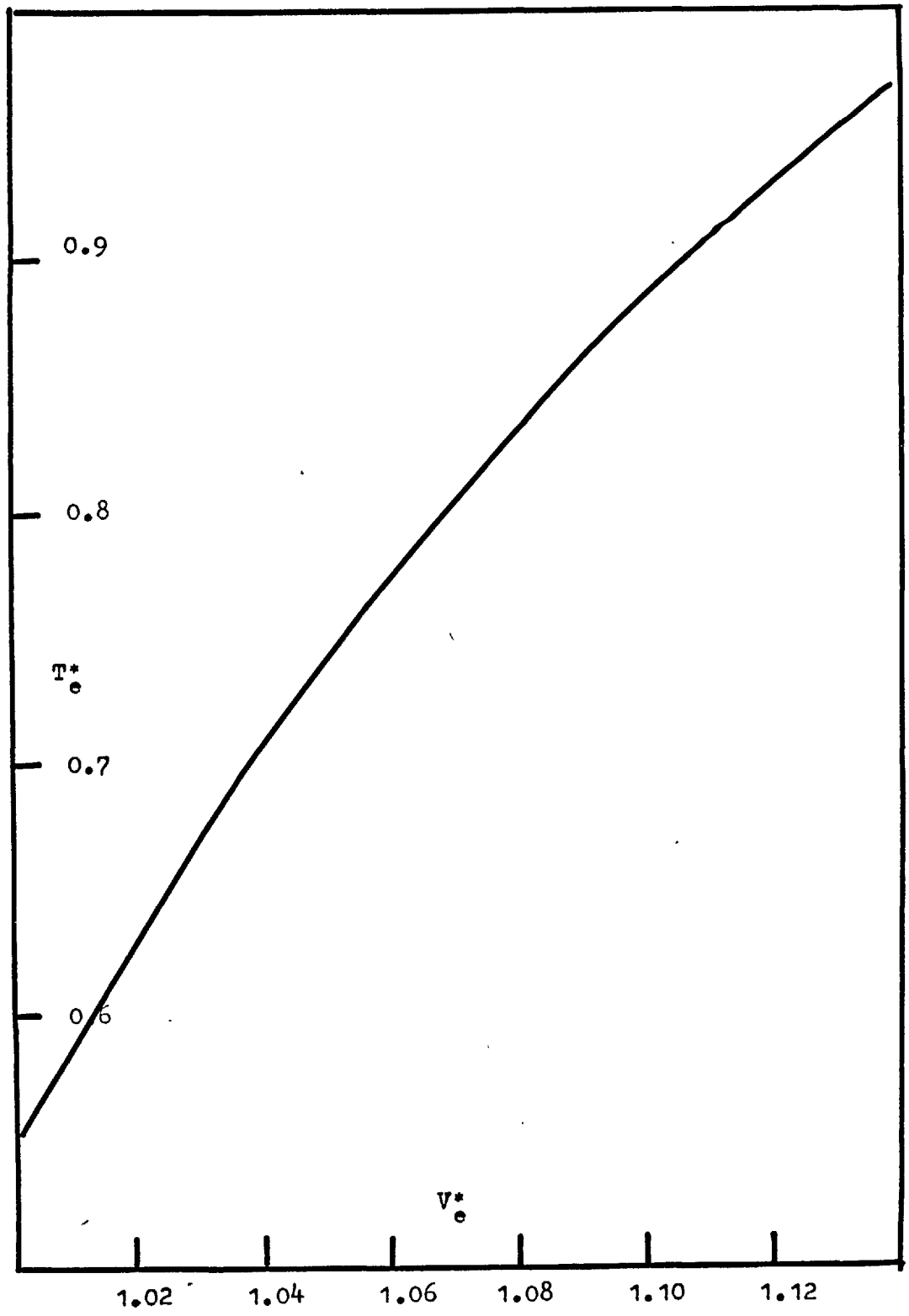

Fig 10.2 Entropy of Vapourisation vs Effective Reduced Volume for zero compressibility using an L.J.potential

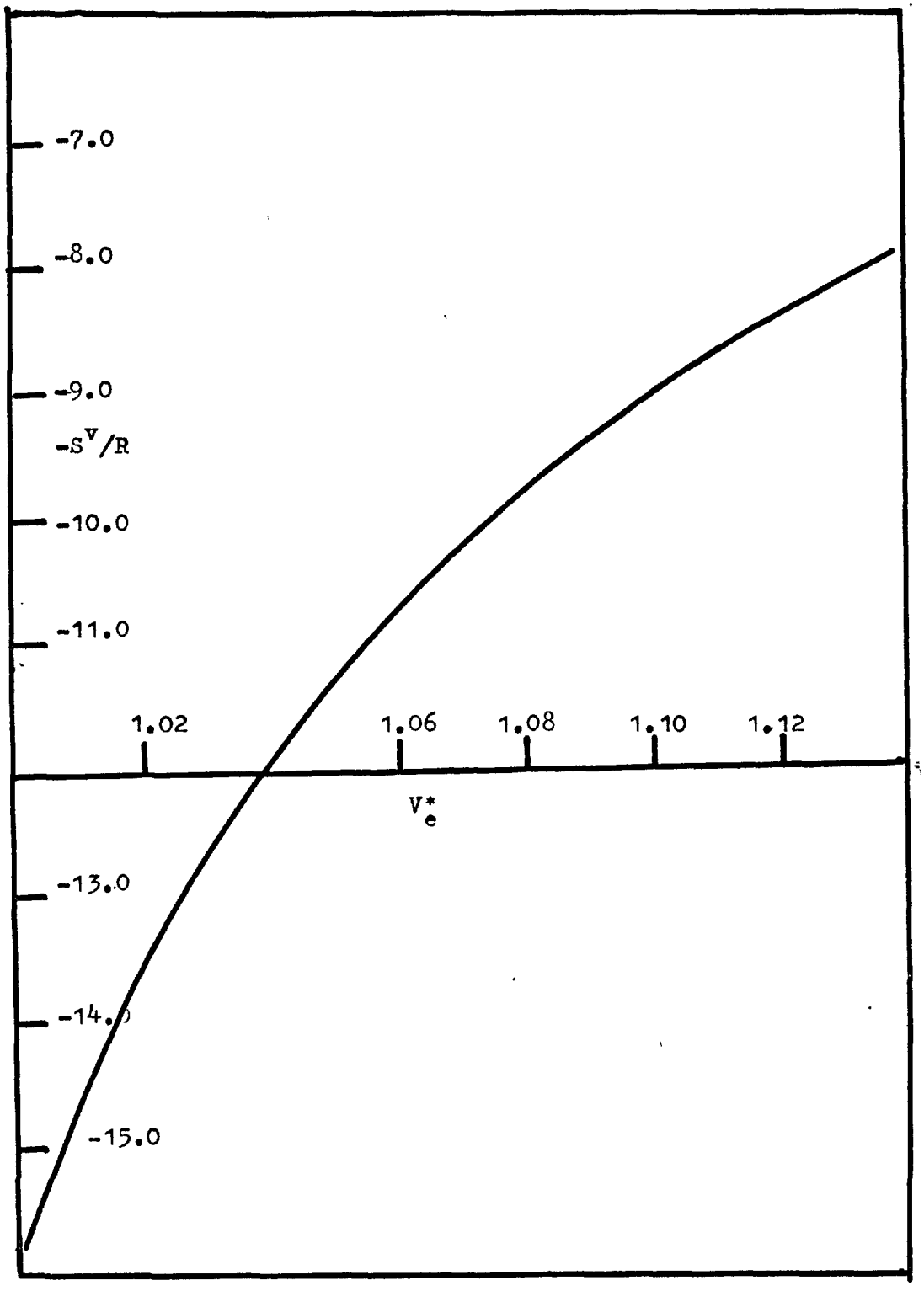

similar relationship between V_e^* and the computed entropy of vapourisation (from (10.2.6)).

Thus, through an experimental value of S^v, an effective reduced volume for the liquid can be found and from this and Fig.(10.1) an effective reduced temperature.

For a pure liquid (10.1.2) may be defined more explicitly as:-

$$V_E^* = a^3/2^{1/2}\sigma_{22}^3 \qquad (10.2.7)$$

where σ_{22} is the distance parameter for the solvent, and $\underline{a}$ is given by the volume per particle, so:-

$$\frac{4}{3}\pi a^3 = \left(\frac{V}{N}\right) \qquad (10.2.8)$$

with V=molar volume of the liquid.

For carbon tetrachloride at 25°C., the heat of vapourisation is given as 7.83 kcal/mole (200). Since $S^v=H^v/T$, the entropy of vapourisation may immediately be calculated as $S^v/R=-13.23$. From Fig. (10.1) we find a corresponding V_e^* such that $V_e^*=1.0232$, and through (10.2.8) and (10.2.7) a σ value of 5.338Å. From Fig.(10.2) we also obtain $T_e^*=0.638$. To evaluate ϵ/k we need to know the number of nearest neighbours, Z. For a pure liquid it is difficult to justify anything other than Z=12, another arbitrary factor but one which serves as a lower limit for the ensuing calculations on gas-liquid systems.

The pair potential parameters for various solvents are given in Table (10.1) and may be compared with those obtained by Kobatake and Alder, using an almost identical procedure and with values quoted from other sources. This is done

Table 10.1 Calculated pair potential parameters for organic solvents.

Solvent	$-S^v/R$ [A]	Mol. Vol.	V_e^* Fig10.2	T_e^* Fig10.1	ϵ/k(°K) (10.1.1)	σ(Å) (10.2.7)
CCl_4	13.23	96.5	1.0232	0.638	467	5.34
C_6H_6	13.69	88.8	1.0183	0.619	481	5.24
$n.C_7H_{16}$	14.78	146.5	1.0084	0.576	516	6.16
$c.C_6H_{12}$	13.37	108	1.0217	0.633	472	5.55
$i.C_8H_{18}$	14.19	165.1	1.0137	0.600	497	6.42

A From Ref. 200.

Table 10.2 Calculated parameters, compared with those from other sources.

Solvent	σ [a] (Å)	σ [b] (Å)	σ [c] (Å)	σ [d] (Å)	ϵ/k [a] (°K)	ϵ/k [b] (°K)	ϵ/k [c] (°K)	ϵ/k [d] (°K)
CCl_4	5.34	5.35	5.88	5.41	467	493	327	486
C_6H_6	5.24	5.22	5.27	5.26	481	504	440	494

a From Table 10.1; b From Kobatake & Alder(19); c From viscosity or second virial measurements(189); From cell theory of Salsberg & Kirkwood(201)

for CCl_4 and benzene in Table (10.2). As might be expected, our values are in general almost indentical with the results of K.&A. but are perhaps a little closer to those obtained from the cell theory of Salsberg and Kirkwood (201). All values differ grossly from those obtained from gas imperfection data. Other workers namely Bird et al. (202) and David, Hamann and Thomas (203) have found it impossible to fit second virial or organic molecules and in particular benzene and cyclohexane. As a test of this we employed our fitting procedure (4.4) together with the data compiled by Dymond (124) for C_6H_6, $c\text{-}C_6H_{12}$ and n-heptane. The results obtained were completely anomalous, σ values in some cases $>10.0\text{Å}$. It would therefore appear that parameters for the liquids are best obtained from liquid state properties (cf. low temperature solids). This conclusion is at least justified on the grounds of finding an unique value. However, a study of these parameters must cause a little uneasiness. The ϵ/k values are much larger than any previously encountered and their adoption assumes that the organic molecule is adequately described by a 12:6 potential - a fact which on available evidence must be under some shadow of doubt.

10.3 Gas-Liquid Systems and The Combining Rules

We now move from pure liquids to solvent-gas systems, infinitely dilute with respect to the concentration of the latter. We assume that the solute is surrounded only by solvent molecules and that beyond a few shells of neighbours the presence of this solute molecule does not affect the solvent medium. We have therefore defined a two component fluid, which must involve composition dependent averages of the interaction constants ϵ and σ such that the "effective" temperature and "effective" volume are given by:-

$$T_E^* = \frac{12}{z} \frac{kT}{\epsilon_{12}} \qquad (10.3.1)$$

$$V_E^* = a^3/2^{1/2}\,\sigma_{12} \qquad (10.3.2)$$

where ϵ_{12}, σ_{12} are the parameters for the solute-solvent interaction. To obtain these, one must apply combining rules. The simplest of which are:-

$$\sigma_{12} = (\sigma_{11} + \sigma_{22}/2) \qquad (10.3.3)$$

$$\epsilon_{12} = (\epsilon_{11}\epsilon_{22})^{1/2} \qquad (10.3.4)$$

where ϵ_{11}, σ_{11}; ϵ_{22}, σ_{22} are the force constants of solute and solvent respectively. As was stated above, these relationships are the simplest available and in fact the arithmetic mean law for the collision diameter (10.3.3) is extremely difficult to improve on. However, there have been several attempts to alter the geometric mean rule (10.3.4) notably by Fender and Halsey (64), who adapted the Kirkwood-Muller formula, and by Hudson and McCoubrey (204) who developed an expression from the London theory of dispersion forces.

In its final form this may be written:-

$$\epsilon_{12} = \left\{ \frac{2\,(I_1 I_2)^{\frac{1}{2}}}{I_1 + I_2} \right\} \left\{ \frac{2^6 \sigma_{11}^3 \sigma_{22}^3}{(\sigma_{11}+\sigma_{22})^6} \right\} \left\{ \epsilon_{11}\epsilon_{22} \right\}^{\frac{1}{2}} \qquad (10.3.5)$$

where I_1, I_2 are the ionisation potentials of the two components and the other quantities are as previously defined. It is seen that for molecules of identical ionisation potentials ($I_1=I_2$) and similar size ($\sigma_{11}=\sigma_{22}$) (10.3.5) reduces to (10.3.4).

For the systems in which we are interested the σ_{22} values (given in 10.2) are all in the region of 5-6 Å, and the values of σ_{11} for the solute gases vary from argon (3.4Å) to SF_6 (5.03Å). (In this context it should be noted that we use σ_{22} values from gas imperfection data, previous calculations having indicated little difference between these and values from S^v and the equation of state data).

It would, therefore seem clear that for these systems the combining rule in the form of (10.3.4) is not rigorous enough. On closer examination the ionisation potentials are also non identical though perhaps not as seriously different as the σ values. We therefore, have three possible ways of applying the geometric mean rule - in its simplest form, by allowing for size effects and rigorously as in (10.3.5) - each of which enables an ϵ_{12} to be formulated. Using this value and knowing the experimental temperature, a T_e^*, which is a strictly theoretical value, may be calculated.

In addition through the cell model, and using an experimental P.M.V. another value of T_e^* may be obtained. Thus, knowing V_2, we may evaluate R_c and the nearest neighbour distance of the system is given by:-

$$a = \left(R_c + \frac{\sigma_{12}}{2}\right) \qquad (10.3.6)$$

with:-

$$V_2 = \frac{4}{3}\pi N R_c^3 \qquad (10.3.7)$$

We may through (10.3.3) and (10.3.2) obtain a V_e^* (expt) and balancing the compressibility equation at unit atmospheric pressure find the corresponding T_e^* (expt). This effective parameter should reflect any alteration in the co-ordination number due to the solution process and is related to T_e^* (theory) by:-

$$T_e^{*}(\text{THEORY}) \times \frac{12}{Z} = T_e^{*}(\text{EXPT}). \qquad (10.3.8)$$

The calculation of T_e^* (theory) may of course be performed in either of three ways, depending on which form of the geometric mean rule we adopt. In Tables (10.3) and (10.4) we present the results for argon and methane in various solvents. Striking anomalies are immediately obvious since for the majority of systems the use of anything more rigorous than (10.3.4) to evaluate ϵ_{12} leads to co-ordination numbers in excess of 12, which are basically unacceptable. Kobatake and Alder using only the geometric mean rule appear to obtain lower Z values than those we have calculated. Thus for $Ar\text{-}C_6H_6$ they find Z=6.3 which even allowing for geometric effects is drastically low. A value of Z of 8-10 is more reasonable, which is in the region of that determined using the simple combining rules. K.&A. further proceed with a

Table 10.3 Co-ordination number for Argon in various solvents at 25°C.

Solvent	V_e^* 10.3.2	T_e^*	T^{*a} theory	Z^a	T^{*b} theory	Z^b	T^{*c} theory	Z^c
C_6H_6	1.246	1.544	1.240	9.6	1.427	11.1	1.479	11.5
$c.C_6H_{12}$	1.261	1.395	1.252	10.8	1.494	>12	1.522	>12
$n.C_7H_{16}$	1.225	1.360	1.220	9.7	1.516	>12	1.548	>12
$i.C_8H_{18}$	1.222	1.533	1.259	9.8	1.636	>12	1.672	>12

a From geometric mean rule(10.3.4); b From (10.3.5) if $I_1=I_2$
c From (10.3.5)

Table 10.4 Co-ordination number for Methane in various solvents at 25°C.

Solvent	V_e^* 10.3.2	T_e^*	T^{*a} theory	Z^a	T^{*b} theory	Z^b	T^{*c} theory	Z^c
C_6H_6	1.191	1.329	1.117	10.1	1.203	10.9	1.222	11.0
$c.C_6H_{12}$	1.188	1.220	1.127	11.1	1.251	>12	1.297	>12
$n.C_7H_{16}$	1.236	1.275	1.078	10.1	1.278	>12	1.325	>12
$i.C_8H_{18}$	1.214	1.250	1.099	10.6	1.341	>12	1.391	>12

a,b and c as for Table 10.3

detailed examination of the solute-solvent system in terms of solubility and entropy, assigning entropy contributions to various shells of solvent molecules. Their treatment, however, appears over optimised and this is exemplified in their evaluation of the solvent contribution to the entropy. They write:-

$$S_E/Nk^{(EXPT)} = S_G/Nk^{(THEORY)} + S_S/Nk \qquad (10.3.9)$$

S_G (theory) is evaluated as in (10.2.6). An expression is given for S_S but it is not calculated; instead the S_G (theory) value is subtracted from S_G (expt.) and the difference attributed to the solvent. This step must be viewed with some suspicion, especially if one considers the relative insensitivity of S_G (expt.) (205). In addition the step is justified through the thermodynamic identity:-

$$\left(\partial S/\partial V\right)_T = \left(\partial P/\partial T\right)_V \qquad (10.3.10)$$

which they simplify to:-

$$\partial S)_{SOLV} = \left(\partial P/\partial T\right)_V V_2 \qquad (10.3.11)$$

i.e."that the entropy contribution of the solvent can be calculated as if the solvent were expanded uniformly by the P.M.V..." However, (10.3.11) is not the usual expression for the entropy of expansion (206) nor is the development of (10.3.11) from (10.3.10) very logical.

The above examples are held out not so much in destructive criticism but rather to drive home the point that it is relatively futile to proceed to situations such as entropy and solubility without first solving the preliminary problems. The results such as those given in Tables (10.3)

and (10.4) and as calculated for other systems are disappointing in that any move towards a more rigorous treatment does not appear to be favoured. At present calculations are being made by altering the structure of "L-J" static lattice term. To expand on this topic we are essentially considering the "cell" and the perturbed shells up to a maximum of three at an effective volume V_e^* (as given in (10.3.2)). The rest of the solvent is presumed uninfluenced by the solute existing with shells numerically unaltered at a pure solvent V* as given by (10.2.7). To date only preliminary results are available and these tend to support high co-ordination values for the first shell ($Z \simeq 10$), similar to those given through (10.3.8)

Considering what has been said in the last few sections and bearing in mind present calculations, it would be fair to say that for this part of our work the picture is far from clear. The reasons for this are reasons that we have dealt with over the preceding chapters, and which one must deal with in any calculations involving potentials of the Lennard-Jones type, namely the sensitivity of the calculated results to the empirical potential parameters. In the present case we are faced not only with the problem of evaluating the parameters but also with that of combining them. It has already been noted (cf. SF_6 in Chapter 8) that the larger the gas molecules become the more difficult it was to adequately describe them by an "L-J" potential. A large ellipsoidal organic molecule which typifies the

the solvents under study, is hardly the ideal medium for such a treatment. The simple combining rules have been encountered elsewhere, in the application of the quantum cell model to argon trapped in a β-quinol clathrate (6). The theoretical data obtained showed wide divergences from experiment and once again exemplify the complications encountered in a two component system. We therefore conclude that in such systems and particularly in gas-liquid mixtures the cell theory can undisputably be manipulated to give detailed information on the thermodynamic behaviour of the system. However, for such information to be meaningful, some of the inherent assumptions must be removed and the model placed on a sounder theoretical basis.

Conclusion

The objective of this investigation as set out in the Introduction, was an examination of the defects and merits of the cell model under various sets of physical conditions. Throughout the text we have discussed in some detail the reasons for the relative successes and failures of this model and consequently do not propose to repeat them here other than underlining a few salient points.

The first and most general of these is whether, in the situations we have studied (most of which are rife with semantics) the ultimate criterion of success is the correct prediction of experimental data through a theoretical model? This is possibly too arbitary a demand but is one that must at least be met in part by any meaningful theory. Bearing this in mind our investigations indicate time and time again that a simple and often arbitary approach appears to yield more exact results than any more rigorous method. This fact is clear and indisputable, the reasons for it are somewhat more diffuse.

In the consideration of the inert gas solids the Lennard-Jones model finds itself in a situation which is ideal. The errors of its basic assumptions are minimised, it deals exactly with anharmonicity and "effectively allows for many body forces by using solid state data to determine its parameters. In contrast the discipline of lattice

dynamics, admitedly complex but perhaps more correct for this phase of matter encounters greater difficulty in allowing for anharmonicity and even when this has been achieved does not appear to give as successful predictions as the simple theory already mentioned.

From our consideration of quantum fluids through a Corresponding States approach another factor emerges in that the Uniform Potential approximation gives markedly superior results to those obtained from the L.J. model. Does this mean that the former empirical model gives a more correct picture of the intermolecular potential at fliud densities? This is hardly likely but might augur well for the amendment of the bi-reciprocal form in such situations

Finally examining gas solubility we find that our accurate experimental results are best interpreted by the empirical hard sphere theory. What is the explanation of this - does it lie in the behaviour of the solute after solution has been effected or does it lie in the nature of the internal pressure of the solvent? The latter line of investigation would seem the more profitable for it has already been demonstrated that in this pressure lies the reason for quantum behaviour in solutions at room temperatures

We have therefore used a cell model to obtain favourable results (when compared to experiment) in several differing situations. We admit that in these cases the word "success" is often linked closely with the words "arbitary" or

"empirical" but accepting these limitations the model generally appears decidedly superior to any alternative.

* * * * *

The author acknowledges the award of a grant from The Science Research Council that enabled this research to be completed and thanks The University of London Institute of Computing Science for extensive use of its facilities and of computer time.

REFERENCES

1. H.Eyring, D.Henderson, B.J.Stover & E.M.Eyring "Statistical Mechanics and Dynamics" (J.Wiley & Son Ltd. 1964.)
2. J.E.Lennard-Jones & A.F.Devonshire Proc.Roy.Soc.163A,53,(1937)
3. " " " " " " 165A,1,(1938)
4. " " " " " " 169A,317,(1938)
5. " " " " " "170A,469,(1939)
6. I.Hillier & J.Walkley J.Chem.Phys.43,3713,(1965)
7. W.I.Jenkins & J.Walkley J.Chem.Phys.43,3721,(1965)
8. I.H.Hillier, W.I.Jenkins & J.Walkley unpublished data
9. " " " " J.Chem.Phys.42,3413, (1965)
10. J.C.Gjaldabeck & J.H.Hildebrand J.Am.Chem.Soc.72,1078,(1950)
11. D.N.Glew " " J.Phys.Chem.60,616,(1956)
12. G.Archer " " J.Phys.Chem.67,1830,(1963)
13. J.E.Jolley " " J.Am.Chem.Soc.80,1050,(1957)
14. H.Hiroka " " J.Phys.Chem.68,213,(1964)
15. Y.Kobatake " " J.Phys.Chem.65,331,(1961)
16. L.W.Reeves " " J.Phys.Chem.67,1918,(1963)
17. E.B.Smith &J.Walkley J.Phys.Chem.66,597,(1962)
18. I.H.Hillier & J.Walkley Nature 198,257,(1963)
19. Y.Kobatake & B.J.Alder J.Phys.Chem.66,597,(1962)
20. J.Barker "Lattice theories of the liquid state" (Pergammon Press Ltd. 1963)
21. A.Eisenstein & N.S.Gringrich Phys.Rev.62,261,(1942)
22. D.Henshaw Phys.Rev.105,976,(1957)

23. T.W.Wainwright & B.J.Alder Nuovo.Cim.9,Supp.1,116,(1958)

24. H.Eyring J.Chem.Phys.4,283,(1936)

25. " & J.O.Hirschfelder J.Phys.Chem.41,249,(1937)

26. " " J.F.Kincaid J.Chem.Phys.5,587,(1937)

27. J.A.Rowlinson & C.F.Curtiss J.Chem.Phys.19,1519,(1951)

28. H.S.Chung & J.S.Dahler J.Chem.Phys.40,2868,(1964)

29. G.Mie Ann.Phys.(Leipzig) 11,657,(1903)

30. W.H.Keesom Comm.Phys.Leiden Supp.24B,32,(1912)

31. P.Debye Z.Physik.21,178,(1920)

32. F.London Z.Physik.Chem.B11,222,(1930)

33. R.Fowler "Statistical Mechanics" (Cambridge 1936) p236

34. J.E.Lennard-Jones Proc.Phys.Soc.43,461,(1931)

35. J.O.Hirschfelder, C.F.Curtiss & R.B.Bird "Molecular Theory of Gases and Liquids" (J.Wiley and Sons Inc.1954)

36. B.Axilrod & E.Teller J.Chem.Phys.11,229,(1943)

37. Faraday Society Discussions 40, "Intermolecular Forces" (1965)

38. J.E.Lennard-Jones Proc.Roy.Soc.A106,463,(1924)

39. I.Prigogine & S.Raulier Physica 9,396,(1942)

40. R.H.Wentorf, R.J.Beuhler, J.O.Hirschfelder & C.F.Curtiss J.Chem.Phys.18,1484,(1950)

41. I.Prigogine & G.Garikian J.Chim.Phys.45,273,(1948)

42. Z.W.Salsburg & G.W.Kirkwood J.Chem.Phys.21,2169,(1953)

43. B.J.Alder ~~J.Chem.~~Phys. ~~31,1666,(1959)~~ Rev, 157, 359 (1962).

44. W.Fickett & W.W.Wood J.Chem.Phys.20,1624,(1954)

45. I.Prigogine "Molecular Theory of Solutions" (N.Holland. Amsterdam 1957)

46. J.De Boer Proc.Roy.Soc.A215,4,(1952)

47. W.W.Wood & F.R.Parker J.Chem.Phys.27,720,(1957)

48. R.H.Beuhler, R.H.Wentorf, J.O.Hirschfelder & C.F.Curtiss J.Chem.Phys.19,61,(1951)

49. J.A.Barker Proc.Roy.Soc.A230,390,(1955)

50. " " " " A237,63,(1956)

51. " " " " A240,265,(1957)

52. J.A.Pople Phil.Mag.42,459,(1951)

53. P.Janessens & I.Prigogine Physica 16,895,(1950)

54. A.F.Devonshire Proc.Roy.Soc.A174,102,(1940)

55. J.Corner & J.E.Lennard-Jones Proc.Roy.Soc. A178,401,(1941)

56. E.R.Dobbs & G.Jones Repts.Progr.Phys.20,516,(1957)

57. G.Boato Cryogenics 4,65,(1964)

58. G.L.Pollack Rev.Mod.Phys.36,748,(1964)

59. A.C.Hollis Hallet "Argon, Helium & the Rare Gases", edited by G.A.Cook (Interscience 1961) pp313-85

60. J.H.Dymond, M.Rigby & E.B.Smith J.Chem.Phys.42,2801,(1965)

61. M.L.McGlashan Disc. Farad.Soc.40,59,(1965)

62. R.J.Munn J.Chem.Phys.40,1439,(1964)

63. J.C.Rossi & F.Danon Disc.Farad,Soc.40.97,(1965)

64. B.E.F.Fender & G.D.Halsey J.Chem.Phys.36,1881,(1962)

65. Ref.35, pp165-168

66. G.Staveley Private communication

67. J.Corner Trans.Farad.Soc.44,914,(1948)

68. T.Kihara & S.Koba J.Phys.Soc.Japan 7,348,(1952)

69. E.A.Mason & W.E.Rice J.Chem.Phys.22,843,(1954)

70. A.K.Barua J.Chem.Phys.31,957,(1959)

71. B.D.Utting Unpublished data.

72. O.K.Rice J.Am.Chem.Soc.63,3,(1941)

75. E.A.Guggenheim & M.L.McGlashan Proc.Roy.Soc.A255,456, (1960)

76. C.Domb & I.J.Zucker Nature 178,484,(1956)

77. I.J.Zucker J.Chem.Phys.25,915,(1956)

78. B.E.F.Fender & G.D.Halsey J.Chem.Phys.36,1881,(1962)

79. I.J.Zucker Disc.Farad.Soc.40,117,(1965)

80. E.A.Guggenheim & M.L.McGlashan Mol.Phys.3,563,(1960)

81. T.H.K.Barron & C.Domb Proc.Roy.Soc.A227,447,(1955)

82. B.M.Axilrod J.Chem.Phys.19,719,(1951)

83. L.Jansen & J.M.Dawson J.Chem.Phys.23,482,(1955)

84. L.Jansen Physics Letters 4,91,(1963)

85. L.Jansen & S.Zimering Physics Letters 4,95,(1963)

86. T.Kihara Adv.Chem.Phys.1,267,(1958)

87. A.E.Sherwood & J.M.Prausnitz J.Chem.Phys.41,429,(1964)

88. J.Rowlinson & G.Staveley Unpublished results.

89. T.Kihara Rev.Mod.Phys.25,831,(1953)

90. D.N.Batchelder, O.G.Peterson & R.O.Simmons Phil.Mag. 12,1193,(1965)

91. J.W.Leech & J.A.Reissland Private Communication.

92. J.H.Henkel J,Chem.Phys.23,681,(1955)

93. R.O.Davies & S.Parke Phil.Mag.4,341,(1959)

94. J.A.Barker Disc.Farad.Soc.40,117,(1965)

95. J.De Boer Physica, 14,139,(1948)

96. Ref.58 p771.

97. R.J.Lunbeck & J.De Boer Physica 14,520,(1948)

98. I.Prigogine & J.Philpot Physica 18,729,(1952)

99. D.Henderson, S.Kim & H.Eyring Proc.Nat.Acad.Sci.U.S. 48,1753,(1962)

100. D.Henderson Proc.Nat.Acad.Sci.U.S, 49,487,(1963)

101. S.D.Hamann Trans.Farad.Soc.48,303,(1952)

102. " & H.David Trans.Farad.Soc.49,711,(1953)

103. " J.Am.Chem.Soc.76,4244,(1954)

104. J.M.H.Levelt & R.P.Hurst J.Chem.Phys.32,96,(1960)

105. D.Henderson & R.Reed J.Chem.Phys.40,975,(1964)

106. I.H.Hillier & J.Walkley J.Chem.Phys.41,2168,(1964)

107. H.Margenau & G.H.Murphy "Mathematics of Physics and Chemistry" (D.Van Norstand 1956) p364

108. I.H.Hillier, M.S.Islam & J.Walkley J.Chem.Phys.43,3705, (1965)

109. D.Bohm "Quantum Theory" (Prentice Hall 1951) p264

110. R.E.Langer Phys.Rev.51,669,(1937)

111. L.I.Schiff "Quantum Mechanics" (McGraw Hill 1955) p.188

112. R.Kramers Z.Physik.39,836,(1926)

113. M.S.Islam Ph.D. Thesis,Univ.of London 1966.

114. J.M.H.Levelt & R.P.Hurst J.Chem.Phys.34,54,(1961)

115. K.Clusius, P.Flubacher, K.Schleich & A.Sperandio Z.Naturforsch.15,1,(1960)

116. P.Flubacher, A.J.Leadbetter, & A.J.Morrison Proc. Phys.Soc.78,1449,(1961)

117. D.N.Batchelder Private Communication.

118. A.Michels, J.C.Abels, C.A.Teu Seldam & W.De Graaf Physica 26,381,(1960)

119. G.A.Nicholson & W.G.Scneider Can.J.Chem.33,589,(1955)

120. E.Whalley & W.G.Schneider J.Chem.Phys.23,1644,(1955)

121. J.Corner Trans.Farad.Soc.35m711,(1939)

122. K.Herzfeld & M.Goppert-Mayer Phys.Rev.46,995,(1934)

123. I.J.Zucker Phil.Mag.3,987,(1958)

124. J.H.Dymond Private Communication.

125. Ref.35 p166.

126. G.Saville Private Communication.

127. D.L.Martin Rept.2nd.Symp.N.R.C. Canada,(Ottawa 1957)

128. M.J.Kanzaki J.Phys.Chem.Solids 2, 24,(1957)

129. G.L.Hall J.Phys.Chem.Solids 3,210,(1957)

130. G.F.Nardelli & A.Repani Chiarotti Nuovo.Cim.18,1053, (1960)

131. A.J.E.Foreman & A.Lidiard Phil.Mag.8,97,(1963)

132. L.H.Bolz & F.A.Mauer "Advances in X Ray Analysis" (Plenum,New York,1963) pp242-249.

133. T.F.Johns Phil.Mag.27,229,(1958)

134. N.Bernardes Phys.Rev.120,807,(1960)

135. W.J.Mullin Phys.Rev.134,1249,(1964)

136. G.Boato & G.Casanova Physica 27,571,(1961)

137. G.K.Horton & J.W.Leech Proc.Phys.Soc.82,816,(1963)

138. J.S.Brown Proc.Phys.Soc.85,394,(1965)

139. V.S.Kogan, B.G.Lazarev & R.F.Bulatova Soviet Phys. -J.ETP.13,19,(1961)

140. J.De Smedt, W.H.Keesom & Mooy Commun.Phys.Lab.(Leiden) 203e,41,(1930)

141. C.Domb & L.Salter Phil.Mag.43,1083,(1952)

142. E.Gruneisen "Handbuch der Physik" (Springer-Verlag 1960) Vol.10,p1.

143. B.J.Alder Ann.Rev.Phys.Chem.12,195,(1961)

144. L.F.Epstein & C.J.Hibbert J.Chem.Phys.20,752,(1952)

145. " , G.M.Roe & M.D.Powers J.Chem.Phys.20,1665,(1952)

146. " , " , " ,& C.J.Hibbert J.Chem.Phys.22,464,(1954)

147. E.A.Moelwyn-Hughes J.Phys.Colloid.Chem.55,1246,(1951)

148. W.B.Brown & J.S.Rowlinson Mol.Phys.3,35,(1960)

149. S.D.Hamann & J.A.Lambert Aust.J.Chem.7,1,(1954)

150. Ref.35 p420 and following.

151. J.Dymond, M.Rigby & E.B.Smith Private Communication.

152. R.Lunbeck Doctoral Dissertation, Amsterdam (1951)

153. A.Michels, J.M.H.Levelt & W.De Graaf Physica 24,659, (1958)

154. A.Michels, T.Wassenaar & P.Louwerse Physica 26,539 (1960)

155. A.Michels, W.De Graaf & C.A.Teu Seldam Physica 26,393, (1960)

156. I.Prigogine & V.Mathot J.Chem.Phys.20,49,(1952)

157. I.H.Hillier & J.Walkley J.Chem.Phys.41,3205,(1964)

158. J.Kirkwood Phys.Rev.44,31,(1931)

159. E.Uhlenbeck & E.Beth Physica 3,729,(1936)

160. J.M.H.Levelt Physica 26,361,(1960)

161. A.Michels, W.De Graaf,J.M.H.Levelt & P.Louwerse Physica 25,123,(1959)

162. J.Buchmann Z.Physik.Chem.(Leipzig) A163,461,(1933)

163. J.H.Hildebrand & R.L.Scott "Regular Solutions" (Prentice Hall Inc. 1962)

164. J.H.Hildebrand & R.L.Scott "Solubility of Non Electrolytes" (Rienhold Co. 1950.)

165. J.H.Hildebrand Science 150,441,(1965)

166. J.H.Hildebrand & J.Walkley J.Phys.Chem.63,1174,(1959)

167. J.H.Hildebrand & E.B.Smith J.Chem.Phys.31,145,(1959)

168. " & H.Hiroaka J.Phys.Chem.67,1919,(1963)

169. " & J.Walkley J.Am.Chem.Soc.81,4439,(1959)

170. J.Horiuti "Sci. Papers Inst.Phys.Chem.Res.Tokyo 341,17,125,(1931)

171. H.Clever,J.H.Saylor,R.Batinno & P.M.Gross J.Phys.Chem 61,1078,(1957)

172. H.Clever,J.H.Saylor & P.M.Gross J.Phys.Chem.62,89,(1958)

173. " J.Phys.Chem.62,375,(1958)

174. Ref 164,p 152.

175. D.D.Eley Trans.Farad.Soc.35,1281,(1939)

176. " " " " 35,1421,(1939)

177. H.H.Uhlig J.Phys.Chem.41,1215(1937)

178. I.Kritchevsky & I.Iliinskya Act.Phys.Chem.URSS.20,327,(1945)

179. R.H.Schumm & O.Brown J.Am.Chem.Soc.75,2520,(1953)

180. R.Fujishiro,K.Shinoda & J.H.Hildebrand J.Phys.Chem. 65,2268,(1961)

181. Ref.163,p108.

182. L.W.Reeves & J.H.Hildebrand J.Phys.Chem.60,949,(1956)

183. J.C.Gjaldbaek Act.Chem.Scand.8,1398,(1952)

184. " & J.H.Hildebrand J.Am.Chem.Soc.71,3147,(1949)

185. G.Allen,G.Gee & G.J.Wilson J.Polymer.1,456,(1960)

186. K.E.MacCormack & W.G.Schneider J.Chem.Phys.19, ~~1269~~ 849, (1951)

187. J.C.McCoubrey & N.M.Singh Trans.Farad.Soc.55,1826,(1959)

188. I.H.Hillier & J.Walkley Nature,198,257,(1963)

189. Ref.35,Table 1A,pp 1110-1112.

190. R.L.Scott J.Chem.Phys.25,193,(1956)

191. R.A.Pierotti J.Phys.Chem.67,1841,(1963)

192. " " " " 69,281,(1965)

193. H.Reiss,H.L.Fersch & J.L.Lebowitz J.Chem.Phys.31,369,(1959)

194. " " " " & E.Helfland J.Chem.Phys 32,119,(1960)

195 H.Reiss,H.L.Fersch,J.L.Lebowitz & E.Helfland J.Chem.Phys 33,1379,(1960)

196. J.M.Prausnitz A.Inst.Chem.Eng.Jnl.4,269,(1958)

197. C.S.Barret &L.Mayer J.Chem.Phys.41,1078,(1964)

198. W.Kauzmann "Quantum Chemistry"(Achademic Press. 1957) p187.

199. J.Walkley - unpublished data.

200. Ref.16B,Table A5.1

201. Z.Salsberg & J.G.Kirkwood J.Chem.Phys.21,2169,(1953)

202. R.B.Bird,J.O.Hirschfelder & L.Spotz J.Chem.Phys. 18,1398,(1950)

203. H.G.David,S.D.Hamann & R.B.Thomas Aus.J.Chem.12,309,(1959)

204. G.H.Hudson & J.C.McCoubrey Trans.Farad.Soc. 56,761,(1960)

205. Ref.16B,p42.

206. D.N.Glew & J.H.Hildebrand J.Phys.Chem.60,618,(1956)

207. J.E.Lennard-Jones & A.E.Ingham Proc.Roy.Soc.A107,636,(1925)

208. J.A.Barker Disc.Farad.Soc.40,126,(1965)

APPENDICIES

Appendix 1. - Appendix 8.

(inclusive)

Appendix 1 (A.1). The Solution of the Schroedinger Equation Through the W.K.B. Approximation.

In this section we do not use flow diagrams to illustrate the computational process, but rather we briefly describe the problem and in a qualitative manner show how it was attacked in the program.

(i) Theory

The quantum partition function (4.2.5) involves energy levels that can only be obtained by solving the Schroedinger equation (4.2.6), which under suitable conditions & separation of variables reduces to:-

$$S''(R) + \left\{ \frac{8\pi^2}{\Lambda^{*2}} \lambda_{l,n} - \frac{l(l+1)}{R^2} - \frac{8\pi^2}{\Lambda^{*2}} W(R) \right\} S(R) = 0. \quad (A.1.1)$$

The W.K.B. approximation expands S(R) as a power series in in R, thus:-

$$S(R) = S_0(R) + \hbar S_1(R) + \frac{\hbar^2}{2} S_2(R) + \cdots \quad (A.1.2)$$

and retains only the first two terms in this series.

The energy levels come as the solutions of

$$\int_a^b \left[\frac{8\pi^2}{\Lambda^{*2}} \lambda_{l,n} - \frac{(l+\frac{1}{2})^2}{R^2} - \frac{8\pi^2}{\Lambda^{*2}} W(R) \right]^{\frac{1}{2}} dR = (n+\tfrac{1}{2})\pi$$

which may be written as:-

$$\int_a^b \varphi^{\frac{1}{2}} dR = (n+\tfrac{1}{2})\pi \quad (A.1.3)$$

(A.1.3) is solved by first defining a cell size, subdividing this interval and then moving across the cell, evaluating Q until Q changes sign. It does this at the classical turning points a and b which may therefore be found approximately and refined by a Newton iterative technique.

The integration in (A.1.3) is performed by a Gauss quadrature procedure over 20 Gauss points giving an accuracy of 10^{-3}. The solution, λ_0, of this same equation is obtained by iteration to a specified degree of accuracy using a Newton method.

We also need the volume derivative of the eigen-value (4.2.14) and this is found from:-

$$\int_a^b \frac{1}{2}\left[\frac{8\pi^2}{\Lambda^{*2}}\frac{d\lambda}{d\alpha} - \frac{8\pi^2}{\Lambda^{*2}}\frac{d\overline{W(R)}}{d\alpha}\right] Q^{-\frac{1}{2}} dR = 0 \qquad (A.1.4)$$

in a similar manner.

(ii) The Program

The program was written in CHLF Autocode and was run on the Atlas computer of the University of London Institute of Computing Science. For further information on the programming language the reader is referred to the publications of the Institute.

The program itself was subdivided into chapters and routines and rather than give these in their Autocode form we content ourselves with a general description of their function.

The basic requirement is to compute thermodynamic properties for a quantum particle of given Λ^*, obeying a specific "m:n" potential. This is done for a set V^*, over a range of T^*, using the W.K.B. approximation to derive the energy levels and obtaining preliminary values of λ_0 and $d\lambda_0/dV$ from a harmonic oscillator approximation.

(a) Chapter 0

This is chiefly the input chapter. It reads m and n, the potential coefficients, stores temperature range in T^*, reads

in number of neighbours in each shell, number of Gauss points, quantum parameter and evaluates further neighbour distances.

Reads initial guesses for λ_o and $d\lambda_o/dV$, sets up α, $Rc(0.5527\alpha)$ and prints cell radius.

Sums potential over required number of shells, stores λ, $d\lambda/dV$ from Chapter 1.

Increases quantum number, L, imposes connection formula.

(b) Chapter 1.

Uses Newton iterative method to refine turning points, then calculates λ, $d\lambda/dV$.

Sets up Gauss points, calculates Q(R) and dQ(R)/dR at turning points $\underline{a}$ and $\underline{b}$ (via Routine 1000).

Using Newton method refines $\underline{a}$ and $\underline{b}$ and then moves into Gauss integration (Routine 10).

Solves $Q(R)^{\frac{1}{2}} = (n+\frac{1}{2})\pi$, when this true λ value is obtained. Solution by Newton Raphson method. When λ is known to specified accuracy it is printed (via Anelex lay out Routine 1) and stored for calculation of thermodynamic properties. A similar procedure is adopted for $d\lambda/dV$.

Increases n, increases L. New turning points evaluated. Continues until the maximum level (set in input data) for λ values has been obtained.

(c) Chapter 2

Fault chapter; detects negative λ, or positive $d\lambda/dV$.

(d) Chapter 3

Output chapter. Sets up temperature count and count on energy levels. Brings eigen-values and their volume derivatives out of storage. Sums over all available L,n.

Determines accuracies of thermodynamic properties. Calculates and prints these for all set T*.

(e) Routine 1000

Most used part of program. Is entered with differnet calues of R to calculate $\overline{W(R)}$, $d\overline{W(R)}/dR$, Q(R) and dQ(R)/dR.

Further it gives $(Q(R))^{\frac{1}{2}}$ and $dW(R)/d\alpha$.

(f) Routine 9

Calculates all terms that depend solely on m and n i.e. the constant K, where:-

$$K = \left[(n/m)^{n/n-m} - (n/m)^{m/m-n} \right]^{-1}$$

It also evaluates the asymptotic correction term.

(g) Routine 11

Evaluates turning points by "chord method". Splits search area into units of $\alpha/50$ then increases R stepwise by $\alpha/50$. Calculates Q(R) and after finding where it changes sign applies the "chord method"

(h) Routine 10

Gauss integration. Integrates all functions over appropriate a and b interval. Continually moves control into Routing 1000 to evaluate Q(R) etc.

Appendix 2 (A.2). Evaluation of the Potential Parameters

(a) Graphical Method

This will be illustrated by a resume of its application to neon where:-

U_o=-448.0cal/mole(115)

V_o=13.39cc/mole (117)

and m=20.183/(6.02x10^{23}), where m is the mass of the molecule.

(i) Utilising the equations in (4.3) we find (for zero pressure:-

$$\mu_o^* = \mu_o/N = \lambda_o^* + \omega^*(0)/2 \qquad (A.2.1)$$

$$d\lambda_o^*/dV^* = -\tfrac{1}{2}\, d\omega^*(0)/dV^* \qquad (A.2.2)$$

λ_o^*; $(d\lambda_o^*/dV^*)$ are computed directly from the W.K.B. approximation and:-

$$\omega^*(0) = \frac{12}{T^*}\left[\frac{1.0109}{V^{*2}} - \frac{2.4090}{V^{*4}}\right] \qquad (A.2.3)$$

$dW^*(0)/dV^*$ comes from the derivative of (A.2.3) with respect to V^*.

(ii) Solutions of (A.2.2) are obtained from a graphical plot (see Fig.4.1). This gives unique sets of Λ^* and V^* values, and from a plot of Λ^* vs. λ_o^* corresponding unique values of λ_o^* are obtained

(iii) The molecular diameter σ is obtained from:-

$$V^* = V/N\sigma^3 = V_o/N\sigma^3 \text{ (at } 0^\circ K). \qquad (A.2.4)$$

For neon $$\sigma = (13.39/V^*N)^{1/3} \qquad (A.2.5)$$

(iv) To evaluate ϵ/k at varying Λ^*

$$\Lambda^* = h/(m\epsilon)^{\frac{1}{2}}\sigma \qquad (A.2.6)$$

hence $$\epsilon/k = \frac{h^2}{k}\left(\Lambda^{*2} m \sigma^2\right)^{-1} \qquad (A.2.7)$$

where h and k are the Planck and Boltzmann constants respectively. Hence from (ii),(iii) and (iv) we may compute or evaluate unique sets of $\Lambda^*, V^*, \sigma, \epsilon/k$ and λ_o^*.

(v) The solution of (A.2.1) requires that:-

$$U_o^* - \lambda_o^* = W^*(0)/2 \qquad (A.2.8)$$

which may be "normalised" to:-

$$\mu_o - \frac{R}{k}\lambda_o^* = \frac{R}{2}\frac{\epsilon}{k}\omega^*(o). \qquad (A.2.9)$$

where R=1.98 cal./mole deg.

Plots of $U_o - (R\epsilon/k)\lambda_o^*$ and $(R\epsilon/2k)W^*(0)$ against V^* intersected at a unique V^* for the system. Table (A2.1) gives abbreviated data for the neon investigation.

Table (A2.1)

V^*	Λ^*	$N\sigma^3$	$\sigma(\text{Å})$	$\epsilon/k(^\circ K)$	λ_o^*	$\mu_o - \frac{R}{k}\lambda_o^*$	$[\omega^*(o)\frac{R}{2}\frac{\epsilon}{k}]$
1.01	0.460	13.328	2.798	57.03	1.73	-643	941
1.02	0.500	13.108	2.792	48.48	1.84	-625	795
1.03	0.540	12.980	2.783	41.83	1.95	-610	682
1.04	0.580	12.856	2.774	36.50	2.04	-596	591

The intersection of the curves in Fig.(A2.1) is at $V^*=1.0395$. From data in Table (A2.1) and further data from higher V^*, Fig. (A2.2) is constructed with ϵ/k plotted against V^*. The intercept on this curve for $V^*=1.0395$ is at $\epsilon/k=36.6^\circ K$. which is the unique value for the energy parameter for the system.

Hence for neon:- $V^*=1.0395$

$$N\sigma^3 = 13.39/1.0395 \text{ cc/mole}$$

$$\sigma = 2.777\text{Å}$$

and the experimental and computed data give for the zero point

Fig A2.1 Determination of $N6^3$ (=V/V* at 0°K.) for Neon through the solution of (A.2.1)

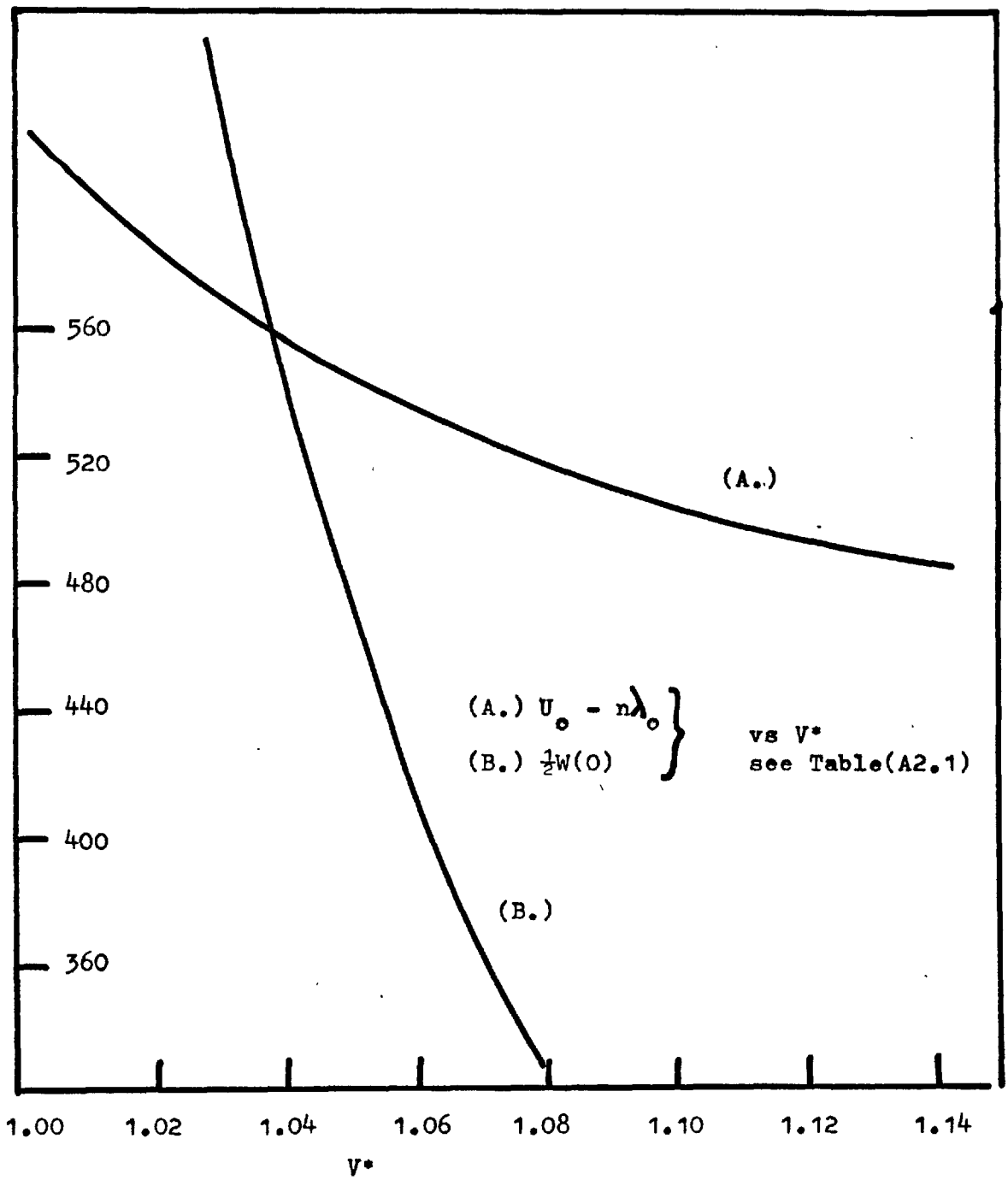

Fig A2.2 Neon 12-6 potential $\epsilon/k(^{\circ}K)$ vs V^{*}

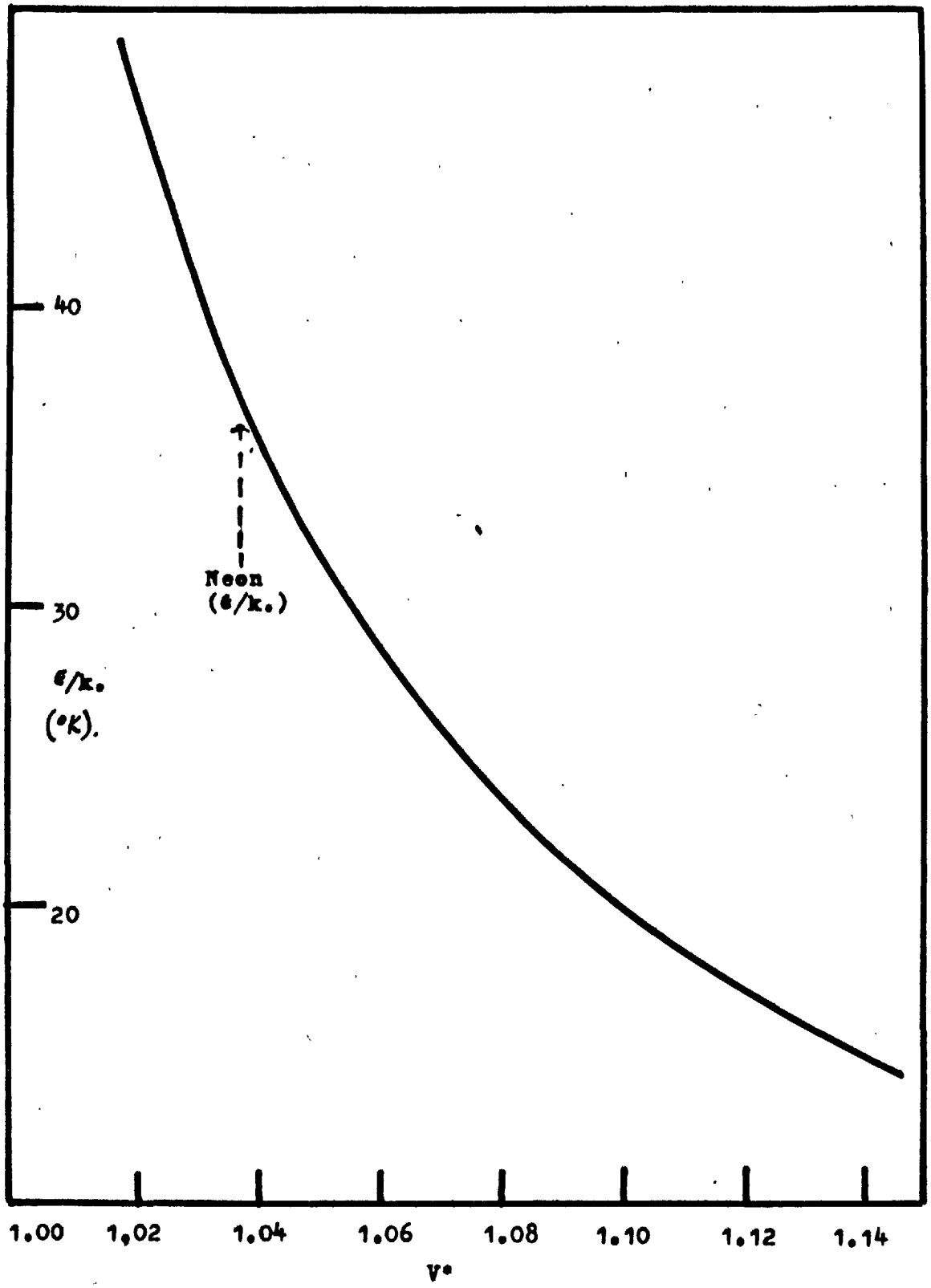

parameters of neon:-

σ =2.777Å; ϵ/k=36.6°K;

$N\sigma^3$=12.89 cc./mole; Λ^*=0.580.

(b) Iterative Method (as developed by B.D.Utting Ref.(71))

Consider (4.3.3) and (4.3.4) as:-

$$U_0/N\epsilon = \lambda_0^* + w^*(0)/2 \qquad (A.2.10)$$

$$-P_0\sigma^3/\epsilon = d\lambda_0^*/dv^* + \tfrac{1}{2}\, dw^*(0)/dv^* \qquad (A.2.11)$$

(NB. this treatment is general for any P_0)

(A.2.10) and (A.2.11) are both functions of ϵ and σ and may be written as:-

$$F_i(\sigma,\epsilon) = 0 \quad (i=1,2) \qquad (A.2.12)$$

If $(\sigma_{10}, \epsilon_{10})$ is the first approximation to ths solution and if $(\sigma_{10}+h_1, \epsilon_{10}+h_2)$ is a better approximation we may write:-

$$F_i(\sigma_{10}+h_1, \epsilon_{10}+h_2) = 0 \quad (i=1,2) \qquad (A.2.13)$$

Expanding (A.2.13) as Taylor series and truncating after temms linear in h_1, h_2 we obtain:-

$$F_i(\sigma_{10}, \epsilon_{10}) + h_1\left(\partial F_i/\partial\sigma\right)_{\sigma=\sigma_{10}} + h_2\left(\partial F_i/\partial\epsilon\right)_{\epsilon=\epsilon_{10}} = 0 \qquad (A.2.14)$$

(A.2.14) is two linear simultaneous equations in h_1, h_2 which may be solved for h_1, h_2 providing that $F_i(\sigma_{10}, \epsilon_{10})$ and the partial derivatives may be calculated. The partial derivatives may be replaced by the difference quotients so:-

$$F_i(\sigma_{10}, \epsilon_{10}) + h_1\left(\Delta F_i/\Delta\sigma\right)_{\sigma=\sigma_{10}} + h_2\left(\Delta F_i/\Delta\epsilon\right)_{\epsilon=\epsilon_{10}} = 0 \qquad (A.2.15)$$

where

$$\left(\frac{\Delta F_i}{\Delta\sigma}\right)_{\sigma=\sigma_{10}} = \frac{F_i(\sigma_{10},\epsilon_{10}) - F_i(\sigma_{10}-\delta\sigma_{10},\epsilon_{10})}{\delta\sigma_{10}} \quad (i=1,2) \qquad (A.2.16)$$

and $\delta\sigma_{10}$ is chosen as $0.01\sigma_{10}$ (arbitrary).

A similar expression to (A.2.16) gives $\left(\Delta F_i/\Delta\epsilon\right)_{\epsilon=\epsilon_{10}}$.

Equations (A.2.15) may be easily solved for h_1, h_2. The new solution is then iterated to a specified accuracy.

The process as described above can be integrated into the W.K.B. program.

Appendix 3 (A.3) Argon experimental & theoretical data.

(i) Experimental Molar volume vs Temperature data

T(°K)	V^a	T(°K)	V^a	T(°K)	V^a	T(°K)	V^b
4	22.55	30	22.80	60	23.61	15	22.55
8	22.65	35	22.91	65	23.79	25	22.69
10	22.56	40	23.02	70	23.98	35	22.88
15	22.59	45	23.15	75	24.20	50	23.31
20	22.64	50	23.29	80	24.43	61	23.64
25	22.71	55	23.45				

(all molar volumes expressed as cc/mole.)

a Calculated from X ray density ρ (gm/cc.) as given by Batchelder (117) : $V = M/\rho$ where M is 39.984 gms. and ρ is quoted to $\pm$ 0.0001 gm/cc.

b Data of Barrett & Mayer(197.)

(ii) Theoretical Molar volume vs Temperature data

T(°K)	V(cc/mole)[a]	T(°K)	V(cc/mole)[b]
9.78	22.54	25.88	22.54
15.34	22.57	32.59	22.68
19.82	22.63	41.33	22.89
26.09	22.71	51.12	23.19
32.86	22.85	61.10	23.52
41.68	23.06	69.96	23.87
52.20	23.37		
62.30	23.70		
70.55	24.06		

a Theoretical data for $\rho^* = 0.185$ normalised with zero point params. $\epsilon/k = 120.8^\circ K.$; $N\sigma^3 = 23.68$ cc/mole.

b Normalised with virial params. $\epsilon/k = 119.8^\circ K.$; $N\sigma^3 = 23.50$cc/mole

(iii) Experimental Heat Capacity Data.

T(°K)	C_p [a]	T(°K)	C_p [a]	T(°K)	C_v [b]	T(°K)	C_v [c]
5	0.088	40	5.387	10	0.787	60	5.118
10	0.790	50	6.006	15	1.910	70	5.453
15	1.940	60	6.528	20	2.894	75	5.740
20	2.990	70	7.100	25	3.632	80	5.788
25	3.828	75	7.488	30	4.145		
30	4.463	80	7.928	40	4.674		
				50	5.046		

(all heat capacaties in cals/deg.mole.)

a Data of Morrison et al (116)

b As a but obtained through (4.4.1)

c From work of Clusius et al (115).

(iv) Theoretical Heat Capacaties.

T(°K)	C_v	T(°K)	C_v	T(°K)	C_v
9.78	0.380	26.09	3.954	52.20	5.040
15.34	1.600	32.86	4.290	62.40	5.124
19.82	2.742	41.68	4.760	70.55	5.162

(smoothed plot of above gives C_v values below.)

T(°K)	C_v	$\alpha \times 10^4 (deg^{-1})$ [a]	$\beta \times 10^5 (atm^{-1})$ [a]	$\alpha^2 VT/\beta$	C_p
0	2.676	4.903	3.427	0.065	2.741
30	4.176	8.764	4.045	0.292	4.468
40	4.720	11.300	4.263	0.586	5.306
50	5.008	13.241	4.861	0.931	5.949
60	5.110	14.953	5.316	1.278	6.427
70	5.158	16.882	6.009	1.550	6.744
80	5.200	19.301	7.447	2.099	7.299

(for legends see overleaf.)

all specific heats are in cals/deg.mole.

a α , β calculated from fitting of polynomial to experimental data - Hillier & Walkley (106). Values of V from theoretical V vs T(^{o}K.) curve. C_p linked to C_v by (4.4.1)

(v) Theoretical & Experimental entropy.

T(^{o}K)	S_i^a(cals/deg.mole.)	T(^{o}K)	S_i^b(cals/deg.mole)
10	0.282	26.09	2.092
20	1.256	32.86	3.052
30	3.008	41.68	4.118
40	4.406	52.20	5.500
50	5.688	62.30	6.670
60	6.802	70.55	7.546
70	7.900		
80	8.547		

a Calculated from (4.4.2)

b Theoretical data from (115).

Appendix 4 (A.4) Neon Experimental & theoretical data.

(i) Experimental Molar volume vs Temperature data.

T(°K)	V(cc/mole)^A	a_o(A)^A	V(cc/mole)^B	a_o(A)^B
3.0	13.389	4.4617		
4.0	13.390	4.4619	13.393	4.4622
6.0	13.394	4.4622	13.400	4.4630
8.0	13.404	4.4634	13.408	4.4639
10.0	13.425	4.4658	13.435	4.4669
12.0	13.460	4.4696	13.471	4.4709
14.0	13.509	4.4750	13.526	4.4771
16.0	13.574	4.4822	13.570	4.4818
18.0	13.655	4.4912	13.672	4.4951
20.0	13.775	4.5043	13.753	4.5109
22.0	13.877	4.5154	13.864	4.5139
23.5	13.982	4.5269		

A Data of Batchelder (117)
B " " Bolz & Mauer (132)
} a_o and V connected via (4.6.3)

(ii) Theoretical Data Molar volume, lattice constant, heat capacity & entropy (normalising with zero pt. params.)

T(°K)	a_o(A)	V(cc/mole)	C_v	S_i
10.25	4.4637	13.407	0.970	0.140
15.52	4.4782	13.536	2.516	0.953
18.81	4.4923	13.665	3.244	1.582
21.23	4.5064	13.794	3.622	2.053
23.02	4.5203	13.992	3.876	2.492
24.60	(4.5340)	(14.051)	(3.972)	(2.813)

( ) values must be doubtful since temp. is above triple point.
C_v, S_i are in cals/deg.mole.
Z.pt. params. ϵ/k = 36.60°K, $N6^3$ = 12.89cc/mole, Λ^* = 0.580.

(iii) Theoretical data for Λ^*=0.590, normalised with params. of Brown (138)(ϵ/k=35.28°K., $N\delta^3$= 12.86 cc/mole.)

T(°K)	a_o(A)	V(cc/mole)	C_v(cal/mole.deg.)
8.6	4.4637	13.405	0.680
14.29	4.4748	13.507	2.280
17.46	4.4893	13.636	3.044
19.58	4.5030	13.764	3.462
21.70	4.5173	13.893	3.770
23.36	4.5308	14.022	3.940

(iv) Molar Volume vs Temperature data(theoretical values normalised by appropriate parameters.)

T(°K)[a]	V(cc/mole)[a]	T(°K)[b]	V(cc/mole)[b]	T(°K)[c]	V[c]
11.13	13.241	12.24	12.033	6.43	12.940
15.42	13.367	16.96	12.148	10.22	12.962
18.05	13.619	19.85	12.262	15.17	13.021
21.66	13.745	23.82	12.491	18.54	13.146
23.38	13.871			20.98	13.271
				23.04	13.396
				24.80	13.522

a Virial params of Nicholson & Schneider (119), ϵ/k=33.74°K $N\delta^3$ =12.61 cc/mole. Λ^*=0.608

b "Self-consistant" params. Boato & Casanova (136) ϵ/k=37.10°K. $N\delta^3$ =11.46 cc/mole, Λ^*=0.596.

c Solid state params. Mullin (135), ϵ/k=35.76°K, $N\delta^3$= 12.52 cc/mole Λ^*=0.593

(v) Experimental Heat Capacity Data.

T(°K)	C_p [a]	$\bar{C}_p$ [a]	$\bar{C}_v$ [b]
8	0.586	0.580	0.577
10	1.238	1.206	1.202
12	1.883	1.825	1.786
14	2.520	2.350	2.311
16	3.310	2.815	2.763
20	4.358	3.569	3.571
22	5.030	(3.898)	
24	5.755	(3.999)	

(all heat capacities expressed as cal/mol.deg.

a Data of Clusius et al (115) C_v obtained from C_p via (4.6.4

b Data of Batchelder (117) C_v obtained from Clusius C_p data via (4.4.1) using α and β from X ray measurements.

(vi) Theoretical values of C_p

T(°K)	C_v	$\alpha^2 VT/\beta$	C_p
14.29	2.280	0.174	2.454
17.46	3.044	0.545	3.589
19.58	3.462	0.620	4.082
21.70	3.770	1.222	4.992

a Obtained via (4.6.5)

(vii) Entropy

T(°K)	S_i [a]	S_i [b]	T(°K)	S_i [a]	S_i
5.0	0.069				
10.0	0.428	0.398	20.0	2.278	2.225
15.0	1.253	1.204	22.0	2.728	2.672
18.0	1.849	1.800	24.0	3.197	3.140

a From Clusius data (115) and (4.4.2)

b " Batchelder (117) calculated by machine integration.

Appendix 5 (A.5) Theoretical and Experimental data for Quantum corresponding states

(i) Hydrogen & Deuterium (64.5°K) experimental data of Hamann(102)

Hydrogen $\Lambda^*=1.729$		Deuterium $\Lambda^*=1.223$	
V*	C.	V*	C.
1.342	4.791	1.396	3.587
1.417	4.406	1.484	2.965
1.504	3.394	1.622	2.317
1.710	2.441	1.737	1.984
1.924	1.922	1.902	1.629
		2.235	1.277

Throughout A.5 C = PV/NkT

Experimental data reduced with $\epsilon/k=37.0°K, N\sigma^3=15.11$cc/mole.

(ii) Theoretical data for H_2, D_2 from U.P.Approximation

U.P.Data $\Lambda^*=1.729$				$\Lambda^*=1.223$		
V*	ΔC^a_{UP}	C^b	$\sum C^c$	ΔC^a_{UP}	C	$\sum C^c$
1.350	2.060	2.028*	4.089	1.390	2.028*	3.418
1.611	1.380	1.322	2.702	0.890	1.322	2.212
2.000	0.980	0.844	1.864	0.580	0.884	1.464
2.500				0.402	0.738	1.140

a From U.P. theoretical data, compressibility for various V* over a range of T* evaluated with $\Lambda^*=\Lambda^*_{H_2}$. At experimental T* unique set of C_{UP} for various V* evaluated then

$$\Delta C = (C_{UP} - C_{class})$$

where C_{class} is at same V*

b This is argon data of Levelt obtained from graphical plots of experimental data and interpolated under required conditions (i.e. V* and T*)

c $\sum C = \Delta C + C_{expt}$

* this value was obtained by extrapolation of expt. data.

(iii) Theoretical data from L.J. Model for H_2 & D_2 at T*=1.748

L.J.Data Λ^*=1.729				Λ^*=1.223		
V*	ΔC^a	C^b_{expt}	ΣC^c	ΔC^a	C^b_{expt}	ΣC^c
1.350	0.795	2.028*	2.823	0.345	2.028*	2.373
1.611	0.275	1.322	1.597	0.040	1.322	1.362
2.000	0.137	0.884	1.019	0.034	0.884	0.918
2.500	-0.077	0.738	0.731			

a, b and c obtained similarly to U.P.case but with $\Delta C=(C_{LJ}- C_{clas})$

(iv) Experimental H_2 & D_2 data at 123°K.(T*=3.32) from Michels et al (161).

Hydrogen*		Deuterium*	
V*	C	V*	C
1.48	3.428	1.48	3.102
1.64	2.793	1.64	2.578
1.85	2.296	1.85	2.128
2.11	1.912	2.11	1.799
2.64	1.623		

* Compressibility was expressed as a polynomial in powers of the density. This was evaluated using coefficients given for 123°K., resulting values were in amergats and were converted to normal compressibilities using the fact that A amergats of PV = 543.082 cals/mole x A.

(v) H_2 & D_2 U.P.Data T* = 3.32

U.P.Data Λ^*=1.729				Λ^*=1.223		
V*	ΔC	C^a_{expt}	ΣC	ΔC	C^a_{expt}	ΣC
1.350	1.390	2.885	4.275	0.840	2.885*	3.725
1.611	0.900	2.157	3.057	0.580	2.157	2.737
2.000	0.560	1.619	2.179	0.380	1.619	1.999
2.500				0.260	1.337	1.597

a Evaluated from argon data of Levelt (160) at approptiate T*,V*

(vi) Experimental Helium data of Buchmann (162) ($T^*=1.996(20.4^\circ K)$ $\epsilon/k = 10.22^\circ K, N\delta^3 = 10.06$ cc/mole)

V^*	C	V^*	C
1.242	12.67	1.488	8.16
1.284	11.57	1.613	6.93
1.335	10.47	1.806	5.64
1.401	9.33	2.167	4.21

(vii) Helium U.P. theoretical data $\Lambda^* = 2.674$

V^*	ΔC	C_{expt} [a]	ΣC
1.350	5.010	2.320*	7.330
1.611	2.758	1.604	4.462
2.000	1.599	1.093	2.693
2.500	1.026	0.905	1.931

a From argon data of Levelt $T^*=1.996$, V^* as appropriate.

(viii) Experimental data H_2 & D_2 when $T^*=8.74(323^\circ K)$

Michels et al (161)

Hydrogen		Deuterium	
V^*	C [a]	V^*	C [a]
1.48	2.897	1.48	2.798
1.64	2.535	1.64	2.465
1.85	2.226	1.85	2.174
2.11	1.966	2.11	1.927
2.47	1.745	2.47	1.538

a Calculated as in (iv) via a polynomial.

From above, three "theoretical" argon points may be obtained where $C_{Ar} = C_{expt} - \Delta C_{UP}$

V^*	ΔC	C_{expt}	C_{Ar}	
1.48	0.545	2.897	2.332	
1.64	0.460	2.535	2.075	for H_2 $\Lambda^*=1.729$
1.85	0.380	2.226	1.846	

(viii) -cont.

V^*	ΔC	C_{expt}	C_{Ar}	
1.48	0.405	2.798	2.393	
1.64	0.300	2.465	2.165	D_2 at Λ^*=1.2
1.85	2.174	2.174	1.924	

	Hydrogen			Deuterium		
V^*	ΔC	C_{exp}	C_{Ar}	ΔC	C_{exp}	C_{Ar}
1.350	0.710	3.250	2.540	0.550	3.130	2.580
1.611	0.480	2.590	2.110	0.320	3.520	2.200
2.000	0.320	2.075	1.755	0.220	2.030	1.810

The above were evaluated at V^* corresponding to those for the U.P.

From the six points for C_{Ar} (= $C_{exp} - \Delta C_{UP}$) the two "theoretical" curves for argon at T^*=8.74 were constructed.

Appendix 6 (A.6) The Uniform Potential approximation (after Hillier & Walkley (157))

The quantum partition function Z_{qu} may be written for a single particle theory as (4.2.5) and the resulting energy levels for the particle in the cell are found by a solution of the wave equation -

$$\left(-\hbar^2/2m\right)\nabla^2\psi + \left[W(r) - E\right]\psi = 0 \qquad (A.6.1)$$

Assuming a uniform potential

$$W(r) = W(0) \quad r < r_m \quad : \quad W(r) = \infty \quad r > r_m$$

the wave equation (A.6.1) may be transformed into the appropriate polar co-ordinates and the solution(198) given as -

$$\psi = Ap_l^{|m|}(\cos\theta)\exp(im\phi)(1/r).J_{(l+\frac{1}{2})}(Kr) \qquad (A.6.2)$$

where $K=(2mE)^{\frac{1}{2}}/\hbar$ is an associated Legendre function and $J_{(l+\frac{1}{2})}$ is a Bessel function. Applying the conditions that the wave equation falls to zero when $r = r_m$ it is found -

$$J_{(l+\frac{1}{2})}(Kr_m) = 0 \qquad (A.6.3)$$

As a direct result of (A.6.3) the energy levels are given as:-

$$E_l = \pi^2\hbar^2 C_l/2r_m^2 \qquad (A.6.4)$$

where C_l is obtained numerically from zeros of half integral Bessels using Newton's recurrance relationships.

This gives a partition function:-

$$Z_{qu} = \left\{ \sum_l (2l+1)\exp(-h^2 C_l/8mkTr_m^2) \right\}^N \times \exp(-NW(0)/2kT) \qquad (A.6.5)$$

The value of r_m is determined by adopting the assumption of Hamman (101,102) that r_m, on account of the strongly

repulsive potential in the cell, may be evaluated by equating W(r) to zero. Thus -

$$r_m^* = V^{*\frac{1}{3}} y_m^{*\frac{1}{2}} 2^{1/6} \qquad (A.6.6)$$

where $r_m^*=(r_m/\sigma)$ and $y_m^*=(r_m/a)^2$

and (A.6.5) becomes

$$Z_{qu} = \left\{ \sum_l (2l+1) \exp(-D^* C_1 / T^* V^{*\frac{2}{3}} y_m^*) \right\}^N \times \exp(-NW^*(0)/2T^*) \qquad (A.6.7)$$

where $D^* = h^2/8m\epsilon\sigma^2 2^{1/3}$, and from which the compressibility & other thermodynamic properties are readily derived.

Appendix 7 (A.7) Experimental data for the system Deuterium-Cyclohexane at 25°C.

(i) Pressure -Volume readings before DoseI (Atmos.Press. = 76.875 cms.Hg)

V [a]	m_1 [b]	m_2 [b]	Δm	P_T [c]	$1/P_T \times 10^2$
23.01	22.884	22.953	0.069	76.944	1.300
21.06	27.167	32.927	5.760	82.635	1.210
18.95	31.804	44.761	12.957	89.832	1.113
19.95	29.624	39.057	9.433	86.308	1.159

a Volume reading of gas burette in cc.

b m_1, m_2 are heights of mercury levels in left and right arms of burette; $\Delta m = m_2 - m_1$

c P_T = atmos. pressure + Δm

(ii) Pressure-Volume readings after Dose I(before Dose II)

V	m_1	m_2	Δm	P_T	$1/P_T \times 10^2$
20.51	28.313	28.459	0.146	76.891	1.299
18.60	32.546	38.865	6.319	83.154	1.203
16.50	37.181	51.561	14.380	91.225	
17.45	35.072	45.628	10.556	87.491	1.143
19.45	30.679	34.153	3.474	80.309	1.245

(iii) Pressure-Volume readings after Dose II(before Dose III)

V	m_1	m_2	Δm	P_T	$1/P_T \times 10^2$
17.55	34.864	34.958	0.094	76.914	1.300
15.55	39.272	46.770	7.498	84.318	1.186
13.35	43.685	60.055	16.370	93.190	1.073
14.47	41.648	53.706	12.058	88.788	1.125
16.55	37.089	40.664	3.575	80.395	1.244

(iv) Pressure-Volume readings after Dose III(before Dose IV)
(Atmos. pressure =76,775 cms.Hg.)

V	m_1	m_2	Δm	P_T	$1/P_T$ x 10^2
14.81	40.914	40.976	0.062	76.837	1.301
12.78	45.391	54.139	8.748	85.523	1.169
10.90	49.555	68.219	18.664	95.439	1.048
11.80	47.548	61.109	13.562	90.336	1.107
13.85	43.013	46.926	3.913	80.688	1.239

(v) Pressure-Volume readings after Dose IV(Atmos.Press. = 76.770 cms.Hg.)

V	m_1	m_2	Δm	P_T	$1/P_T$ x10^2
12.25	46.578	46.586	0.008	76.778	1.302
10.19	51.108	61.317	10.209	86.979	1.150
8.56	54.680	75.072	20.392	97.162	1.029
9.34	52.984	68.279	15.295	92.065	1.086
11.14	49.020	54.159	5.139	81.909	1.220

Results of (i) - (v) inclusive, are used to construct V vs $1/P_T$ plots in Fig (8.5)

(vi) Dose I, Dilatometer levels etc

Before Dose

Time	m_1	m_2	S(div)	Beck(^oC)	R.Temp
09.55	35.916	36.461	5.8-6.2	3.081	20.65
10.00	"	36.454	5.7-6.1	"	20.50
10.05	35.917	36.452	"	"	"
10.10	"	"	5.8-6.1	"	"

After Dose:-

10.49	36.692	36.974	5.7-6.2	3.081	21.60
10.54	36.690	36.971	5.6-5.9	"	21.70
10.59	36.692	36.974	5.7-6.1	"	"

(N.B. in all above and subsequent tables m_1 is capillary height in closed arm of dilatometer; m_2 height in open arm; S the galvanometer reading in scale divisions over time interval between measurements.)

(vi) -cont

After dose-partial pressure applied.

Time	m_1	m_2	S(div)	Beck(°C)	R.Temp
11.05	35.917	37.898	5.7-6.1	3.081	21.70
11.10	"	37.872	"	"	21.80
11.15	"	37.898	"	"	"
11.21	"	37.881	5.8-6.1	"	22.0
11.27	"	37.878	"	"	"

(vii) Dose II

Before dose:-

11.45	36.679	36.995	5.8-6.1	3.081	22.05
11.50	36.676	36.995	5.6-5.9	"	22.20
11.53	36.682	36.996	5.6-6.0	"	"

After dose:-

12.45	37.284	37.894	5.7-6.2	3.081	22.20
12.50	37.287	37.896	5.9-6.1	"	"
12.53	37.284	37.896	5.8-6.1	"	21.90

Pressure applied,L.H.limb at level as before Dose II

13.00	36.679	38.606	5.8-6.1	3.081	22.30
13.04	"	38.580	5.7-6.0	"	"
13.10	"	38.606	5.7-6.1	"	22.50
13.13	"	38.631	5.8-6.1	"	"
13.16	"	38.614	"	"	"
13.20	"	38.640	"	"	"

Pressure applied,L.H.limb at level as before DoseI

13.22	35.917	39.546	5.8-6.0	3.081	22.40
13.25	"	39.500	"	"	"
13.28	"	39.496	"	"	"
13.32	"	39.504	5.7-6.0	"	"
13.37	"	39.516	"	"	22.15

(viii) Dose III

Before dose

Time	m_1	m_2	S(div)	Beck(°C)	R.Temp
13.48	37.279	37.852	5.8-6.0	3.081	22.40
13.53	37.283	"	5.8-6.1	"	"
13.58	"	37.857	"	"	"

After dose:-

14.50	37.974	38.634	5.7-6.2	3.081	22.20
14.55	37.974	38.636	"	"	22.45
15.00	37.971	"	5.7-6.0	"	"

Pressure applied, L.H. limb at level as before Dose III

15.03	37.282	39.400	5.8-6.1	3.081	22.60
15.07	"	39.479	"	"	"
15.10	"	39.404	"	"	"
15.14	"	39.422	"	"	"
15.18	"	39.382	"	"	22.70

Pressure applied, L.H. limb at level as before Dose I

15.20	35.917	40.994	5.7-6.2	3.081	22.60
15.25	"	40.990	5.7-6.0	"	"
15.28	"	40.984	"	"	22.30
15.31	"	41.004	"	"	"
15.37	"	41.005	5.6-5.9	"	"

(ix) Dose IV

Before dose

15.48	37.978	38.566	5.8-6.1	3.081	22.70
15.53	"	38.569	"	"	"
15.57	"	"		"	"

After dose

16.45	38.651	39.239	5.8-6.1	3.081	22.80
16.49	38.650	39.234	5.7-6.1	"	"
16.53	38.649	39.236	"	"	"

(ix) Dose IV- cont:- Press. applied,L.H.limb at level as before Dose IV

Time	m_1	m_2	S(div)	Beck(^{o}C)	R.Temp
16.55	37.978	40.021	5.8-6.1	3.081	22.80
16.59	"	40.030	5.8-6.0	"	"
17.03	"	40.001	"	"	22.70
17.07	"	40.009	5.7-6.0	"	"
Pressure applied,L.H.limb at level as before Dose I					
17.11	35.917	42,469	5.7-6.0	3.081	22.80
17.15	"	42.452	"	"	"
17.20	"	42.454	"	"	"
17.31	"	42.442	"	"	"

From data given in (vi) - (ix) inclusive Table 8.2 is constructed.

Appendix 8 (A.8)

Experimental Partial Molar Volume data at 25°C.

Argon in Benzene at 25°C.

Table A8.1 Experimental Data

Dose	V. (cc.)	V(tot) (cc.)	N x10^4 (moles)	N x10^4	l^a (cms)	l^b (cms.)	V_2^a	V_2^b
I	2.37	(2.37)	0.968	(0.968)	1.480	(1.480)	44.32	(44.32)
II	2.89	5.26	1.180	2.148	1.800	3.312	44.22	44.70
III	2.78	8.04	1.135	3.283	1.736	5.047	44.34	44.57
IV	2.75	10.79	1.123	4.406	1.112	6.815	44.55	44.84

l^a - Extension from right hand arm alone.

l^b - " " " " " refered to it's position before dose I.

V_2^a, V_2^b -Respective partial molar volumes obtained from above, for individual doses.

V_2 calculated from plot of l^b(cms.) vs V(tot) in cc:-Fig A8.1

$$V_2 = (dl/dV)_{slope} \times 298.36 \times 82.07 \times 2.899 \times 10^{-3} (cc/mole)$$

$$= 6.28 \times 70.986 \ (cc/mole)$$

$$V_2 = 44.58 \ (cc/mole)$$

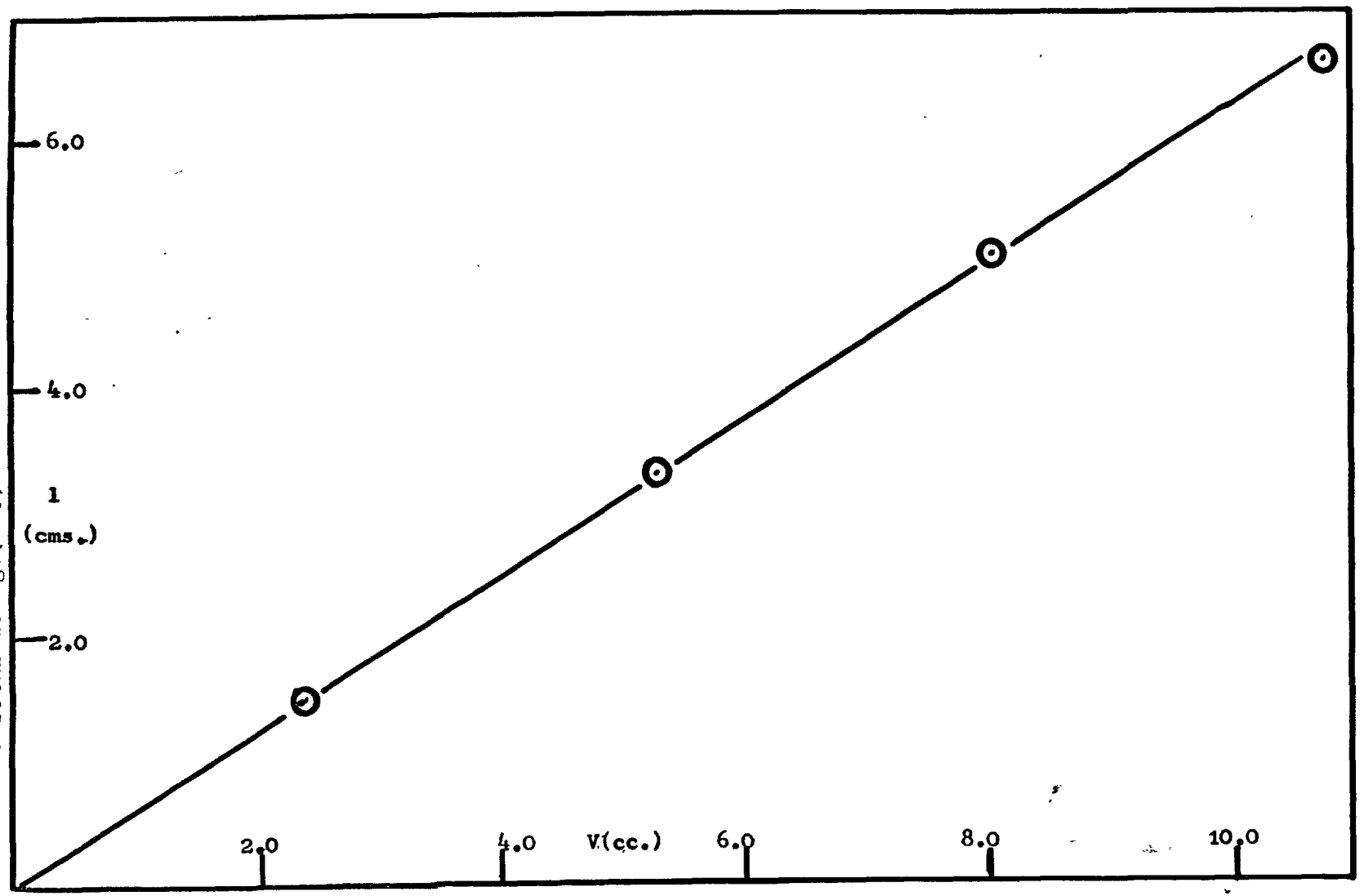

Fig A8.1 Argon in Benzene at 25°C. Total extension(cms.) vs Total dosage(cc.)

Argon in Cyclohexane at 25°C.

Table A8.2 Experimental data.

Dose	V. (cc.)	V(tot)	N x10^4 (moles)	N x10^4	l^a (cms)	l^b (cms)	V_2^a	V^b_2
I	2.70	(2.70)	1.103	(1.103)	1.837	(1.837)	48.30	(48.30)
II	2.63	5.33	1.074	2.177	1.783	3.574	47.60	47.12
III	2.49	7.82	1.017	3.194	1.666	5.190	46.19	46.74
IV	2.34	10.16	0.956	4.150	1.619	6.612	45.48	45.73

Columns superscripted as in previous tables.

V_2 calculated from slope of l^b(cms) vs V(tot)-total dosage in cc.Plot given as Fig A8.2

$V_2 = (dl/dv)_{slope} \times 70.986$ cc/mol

$= 5.00/7.45 \times$ " "

$V_2 = 46.85$ cc/mol

Fig A8.2 Argon in Cyclohexane at 25°C. Total extension(cms.) vs Total dosage(cc.)

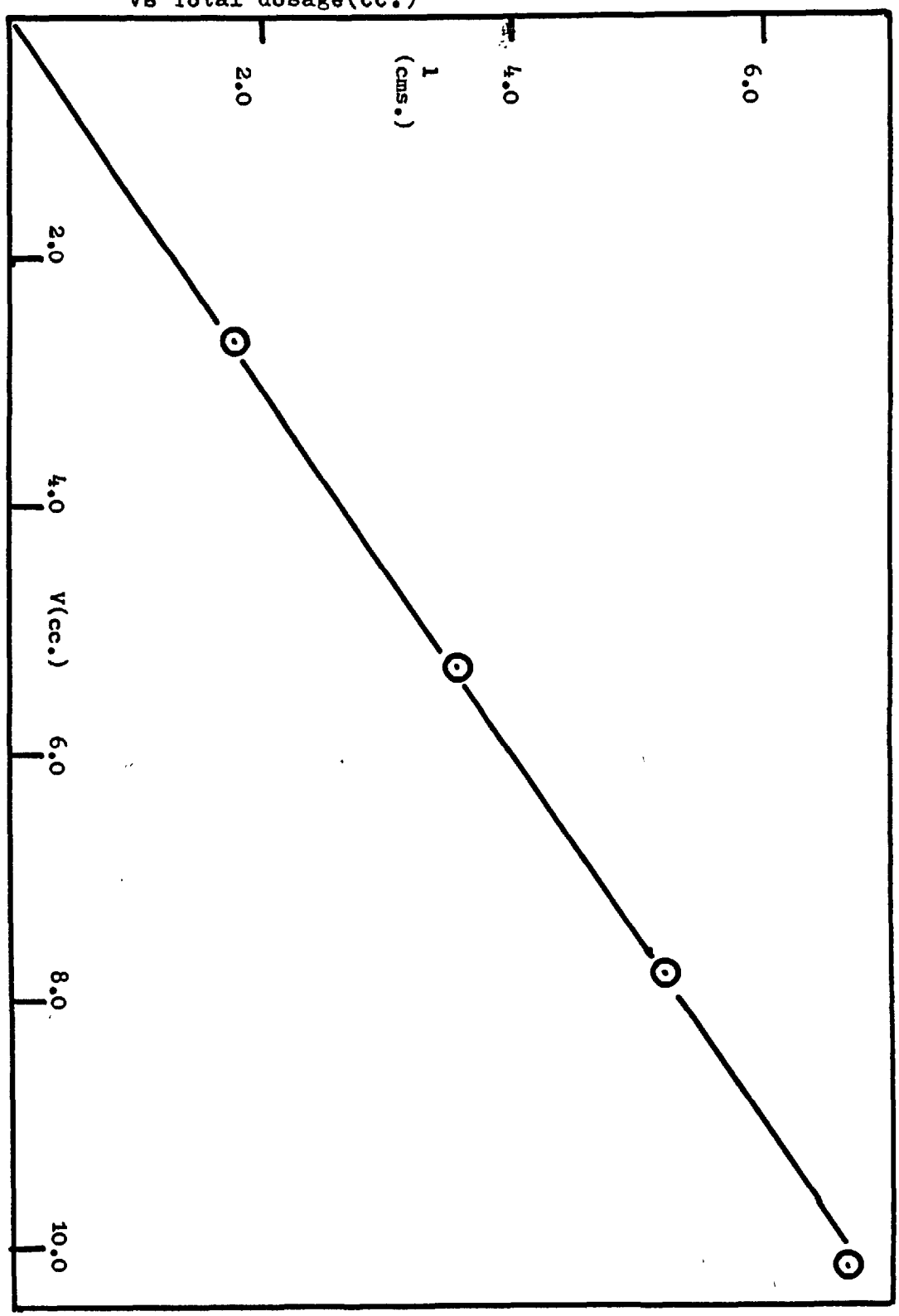

Argon in n-Heptane at 25°C.

Table A8.3 Experimental Data.

Dose	V. (cc.)	V(tot)	N x10^4 (moles)	N x10^4 (tot.)	l^a (cms.)	l^b (cms.)	V_2^a	V_2^b
I	2.27	(2.27)	0.927	(0.927)	1.550	(1.550)	48.47	(48.47)
II	1.90	4.17	0.776	1.703	1.307	2.831	48.82	48.19
III	2.11	6.28	0.862	2.565	1.466	4.331	49.31	48.95
IV	2.84	9.12	1.160	3.725	1.761	6.136	44.01	48.95
V	2.39	11.51	0.976	4.701	1.681	7.744	49.93	47.76

Columns superscripted as in previous tables

V_2 calculated from slope of l^b(cms) vs V(tot),in cc.Plot given as Fig A8.3

$$V_2 = (dl/dV)_{slope} \times 70.986 \text{ cc/mole}$$
$$= 6.80/10.00 \quad " \quad " \quad "$$

$$V_2 = 48.27 \text{ cc/mole}$$

Fig A8.3 Argon in n-Heptane at 25°C. Total extension(cms.) vs Total dosage(cc.)

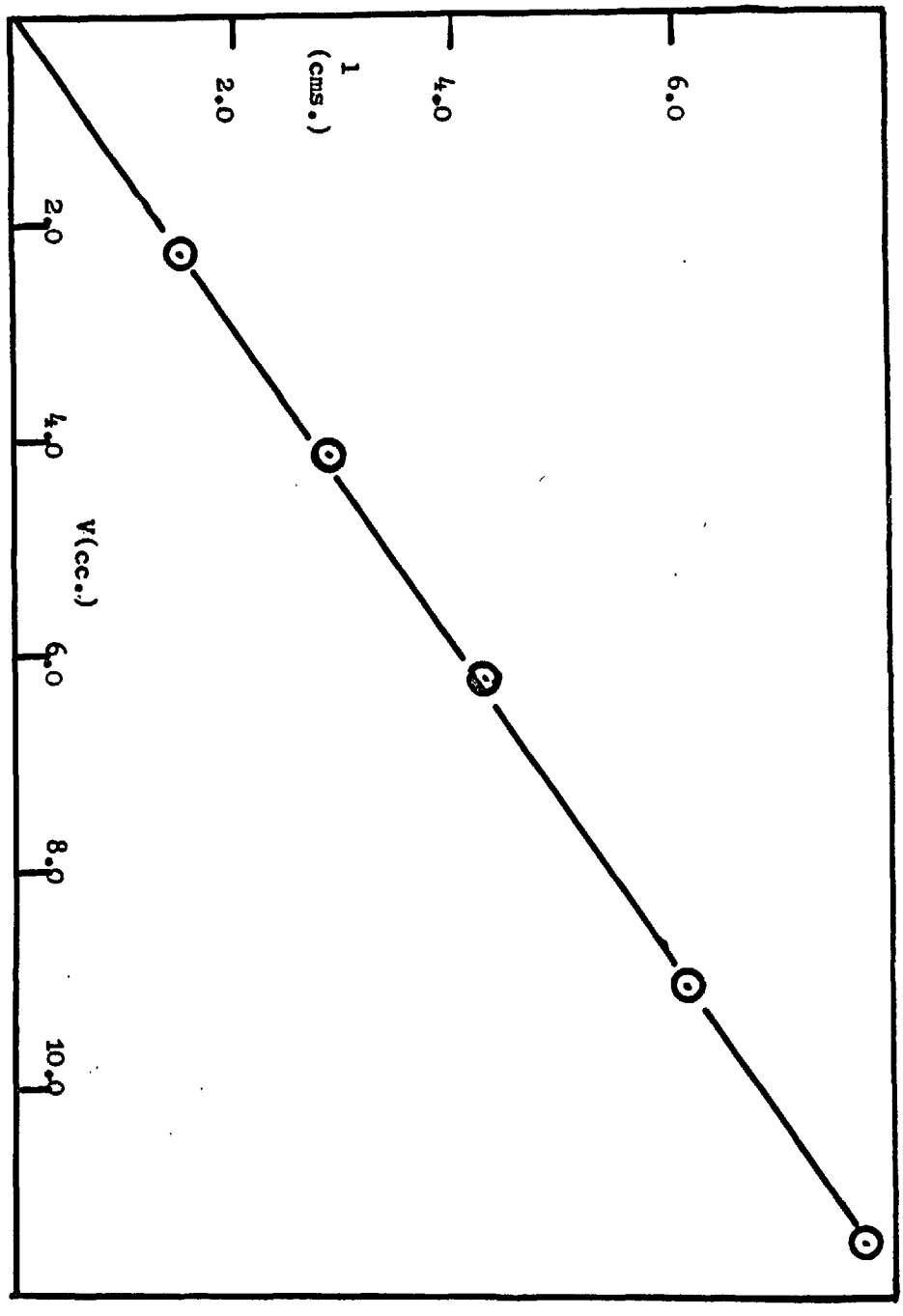

Argon in i-Octane at 25°C.

Table A8.4 Experimental Data

Dose	V. (cc.)	V(tot)	N x10^4 (moles)	N x10^4 (tot)	l^a (cms.)	l^b (cms.)	V_2^a	V_2^b
I	2.03	(2.03)	0.829	(0.829)	1.497	(1.497)	52.35	(52.35)
II	2.41	4.44	0.984	1.813	1.625	3.053	47.87	48.82
III	2.22	6.66	0.907	2.72.	1.593	4.675	50.23	49.83
IV	2.23	8.89	0.911	3.631	1.590	6.195	50.60	49.46
V	2.10	10.99	0.858	4.489	1.483	7.645	50.12	49.37

Columns superscripted as in previous tables

V_2 calculated from slope of l^b(cms) vs V(tot),in cc.Plot given as Fig A8.4

V_2 = (dl/dV) x 70.986 cc/mole

= 5.94/8.50 " "

V_2 = 49.61 cc/mole

Fig A8.4 Argon in i-Octane at 25°C. Total extension(cms.) vs Total dosage(cc.)

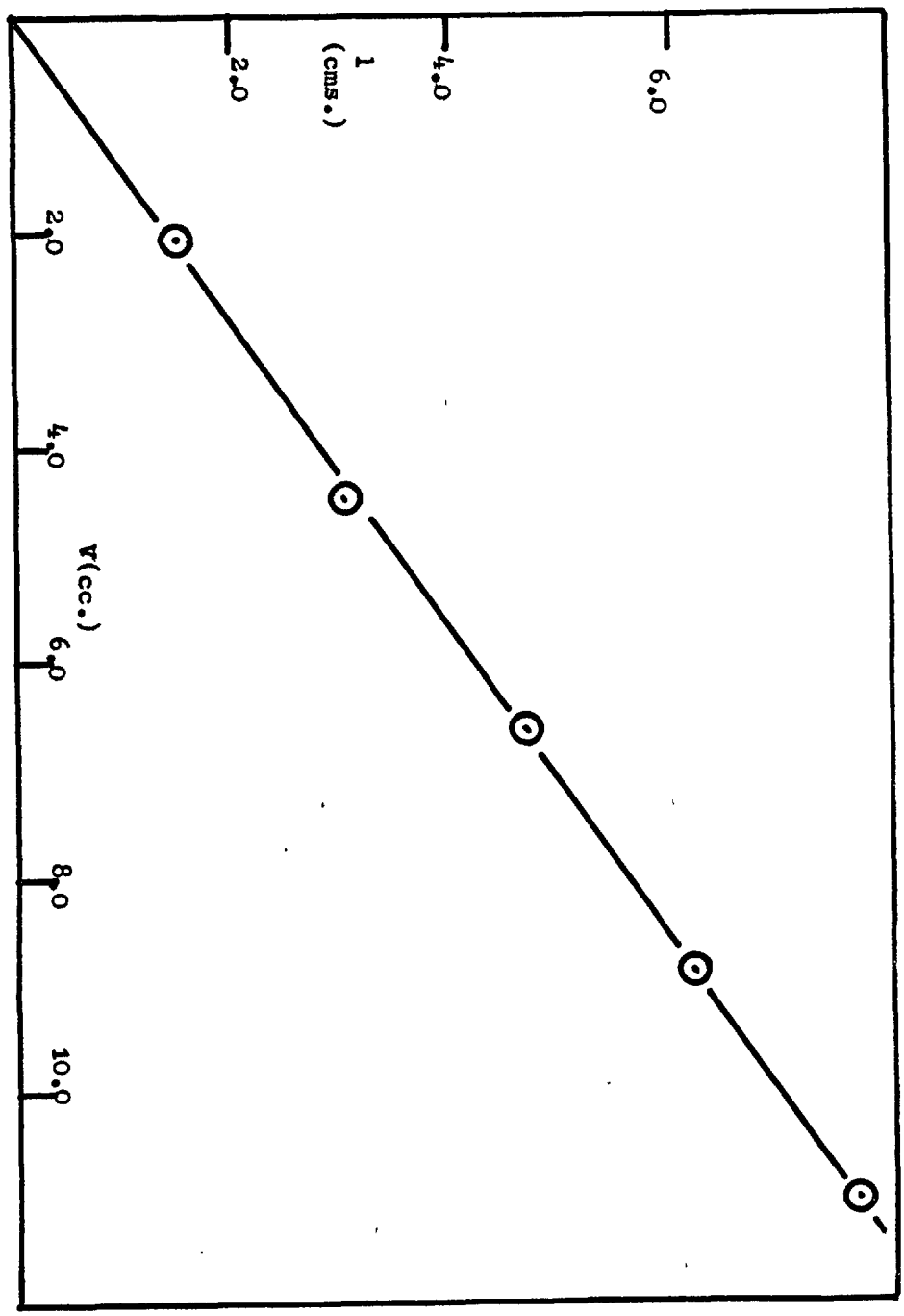

Methane in Benzene at 25°C.

Table A8.5 Experimental Data.

Dose	V. (cc.)	V(tot)	N x10^4 (mole)	N x10^4	l^a (cms.)	l^b (cms.)	V_2^a	V^a_2
I	1.55	(1.55)	0.633	(0.633)	1.183	(1.183)	54.18	(54.18)
II	2.07	3.62	0.895	1.478	1.586	2.800	53.80	54.92
III	1.93	5.55	0.788	2.666	1.367	4.180	50.29	53.46
IV	1.80	7.35	0.735	3.001	1.375	5.515	54.23	53.26

Columns superscripted as in previous tables.

V_2 calculated from the slope of l^b(cms) vs V(tot),in cc.Plot given as Fig A8.5.

$V_2 = (dl/dV)_{slope} \times 70.986$ cc/mole

$= 3.76/5.00$ " " "

$V_2 = 53.38$ cc/mole

Fig A8.5 Methane in Benzene at 25°C, Total extension(cms.) vs Total dosage(cc.)

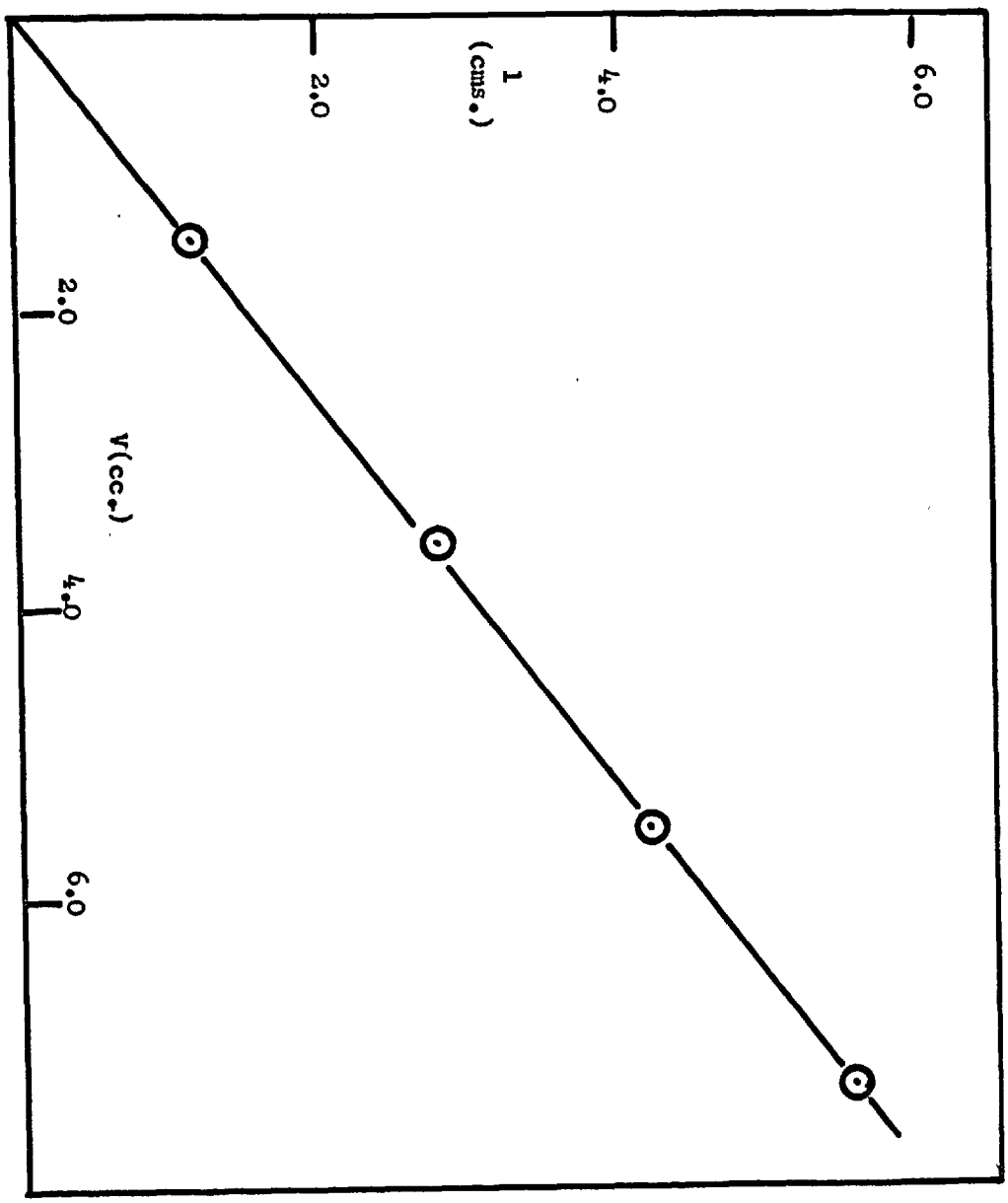

Methane in Cyclohexane at 25°C.

Table A8.6 Experimental Data.

Dose	V. (cc)	V(tot)	N x10^4 (moles)	N x10^4 (tot)	l^a (cms)	l^b (cms)	V_2^a	V_2^b
I	1.94	(1.94)	0.792	(0.792)	1.629	(1.629)	59.63	(59.63)
II	2.67	4.61	1.090	1.882	2.010	3.605	53.46	55.53
III	2.45	7.06	1.001	2.883	1.853	5.421	53.46	54.51
IV	2.50	9.56	1.021	3.904	1.945	7.460	59.22	54.40
V	2.52	12.08	1.032	4.936	1.786	9.260	50.17	54.39

Columns superscripted as in previous tables.

V_2 calculated from slope of l^b(cms) vs V(tot),in cc.Plot given as Fig A8.6

$V_2 = (dl/dV)_{slope} \times 70.986$ cc/mole

$= 7.75/10.00$ " " "

$V_2 = 55.01$ cc/mole

Fig A8.6 Methane in Cyclohexane at 25°C, Total extension(cms.) vs Total dosage(cc.)

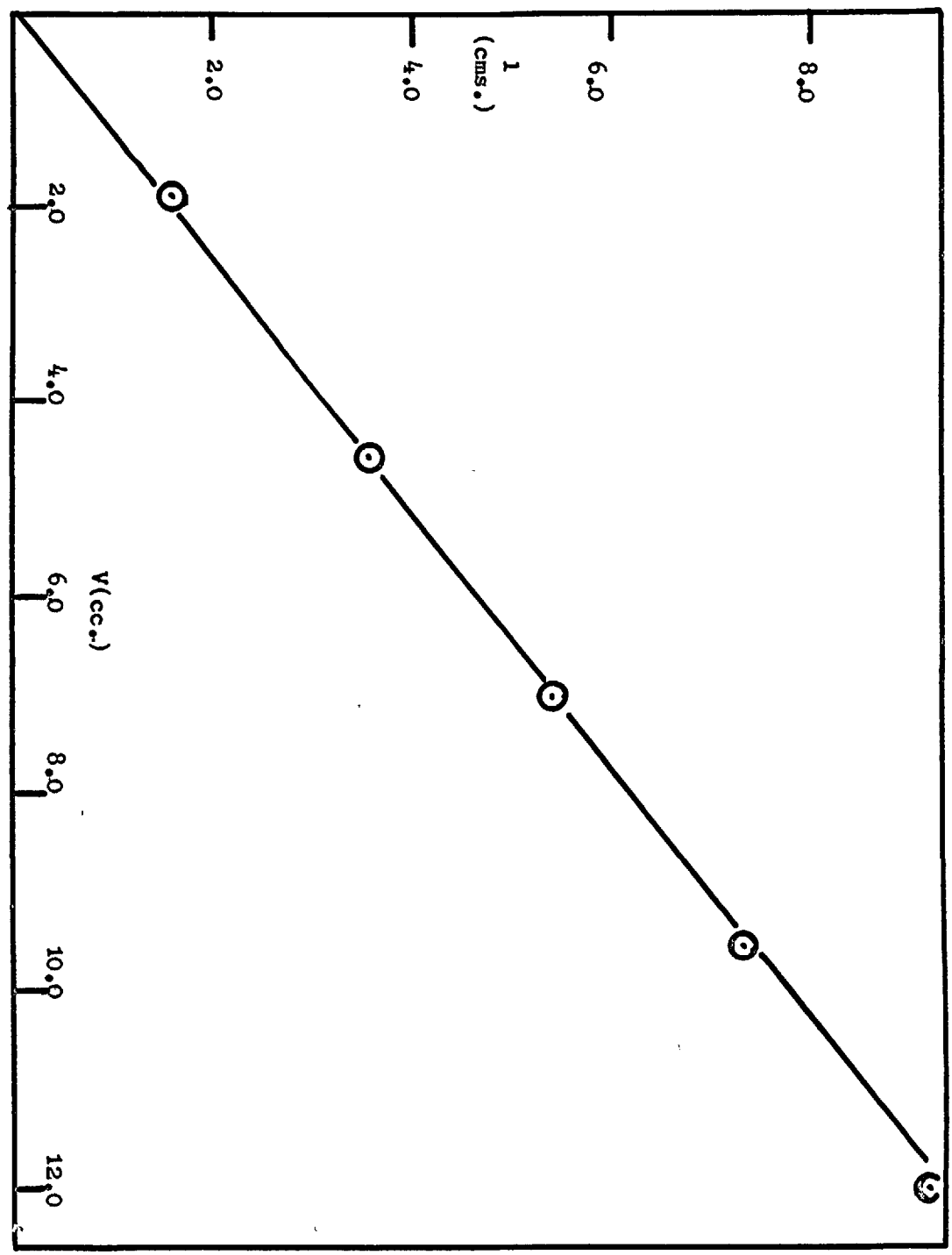

Methane in n-Heptane at 25°C.

Table A8.7 Experimental Data

Dose	V. (cc)	V(tot)	N x10^4 (mole)	N x10^4 (tot)	l^a (cms)	l^b (cms)	V_2^a	V_2^a
I	2.05	(2.05)	0.837	(0.837)	1.724	(1.724)	59.71	(59.71)
II	2.45	4.50	1.003	1.840	2.008	3.743	58.04	58.97
III	2.62	7.12	1.070	2.910	2.290	6.081	62.04	60.58
IV	2.43	9.55	0.992	3.902	1.887	8.021	55.15	59.59
V	2.53	12.08	1.033	4.935	2.023	10.039	56.77	58.97

Columns superscripted as in previous tables.

V_2 calculated from the slope of l^b(cms) vs V(tot), in cc. Plot is given as Fig A8.7

$V_2 = (dl/dV)_{slope} \times 70.986$ cc/mole

$= 8.39/10.0$ " " "

$V_2 = 59.56$ cc/mole

Fig A8.7 Methane in n-Heptane at 25°C, Total extension(cms.) vs Total dosage(cc.)

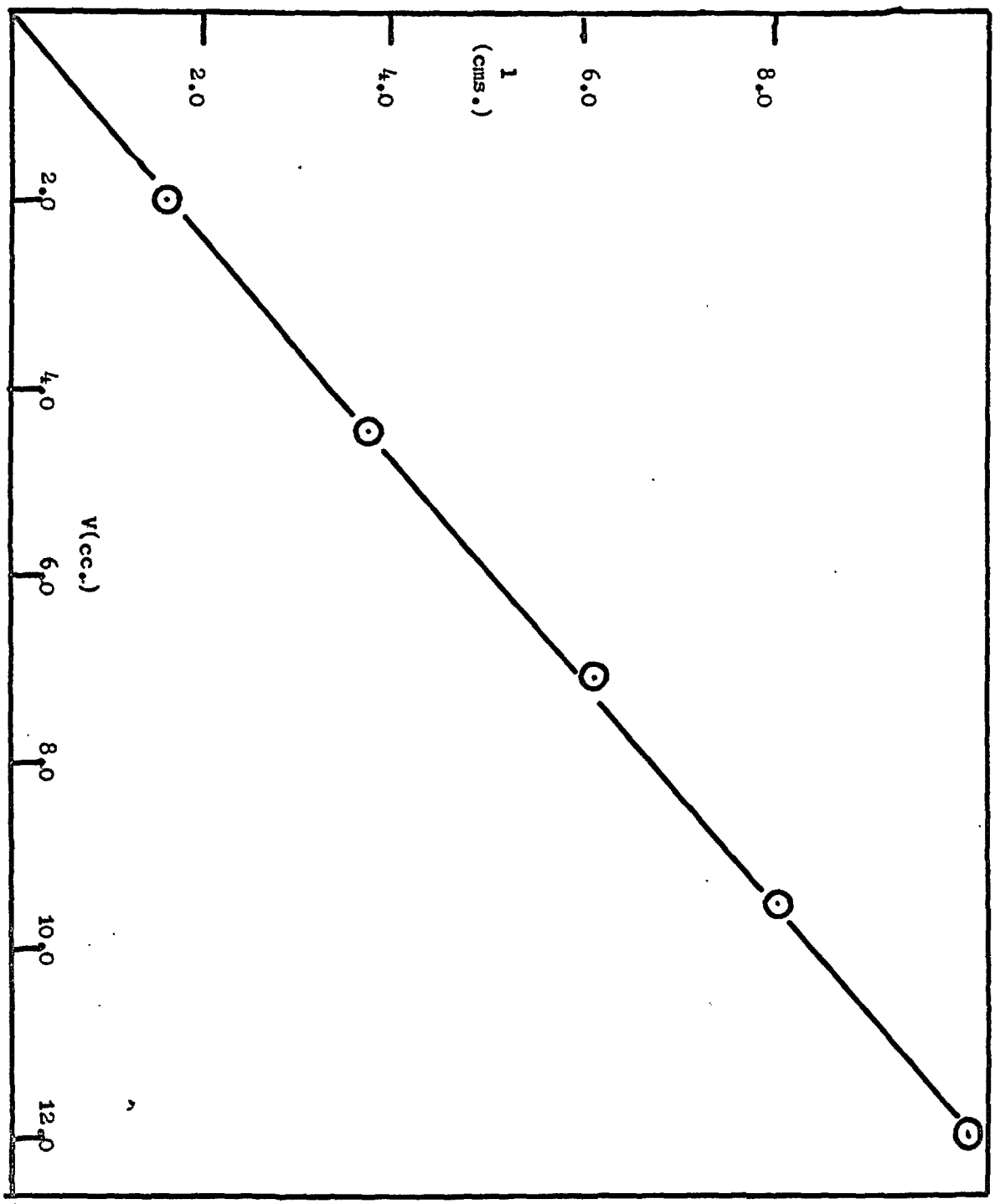

Methane in i-Octane at 25°C.

Table A8.8 Experimetal Data.

Dose	V. (cc)	V(tot)	N x10^4 (moles)	N x 10^4 (tot)	l^a (cms)	l^b (cms)	V_2^a	V_2^b
I	2.49	(2.49)	1.017	(1.017)	2.055	(2.055)	53.38	(53.38)
II	2.36	4.85	0.964	1.981	1.859	3.851	55.90	56.36
III	2.41	7.25	0.984	2.965	1.882	5.750	55.45	56.22
IV	2.49	9.74	1.017	3.982	1.910	7.618	54.45	55.56

Columns superscripted as in previous tables.

V_2 calculated from the slope of l^b(cms) vs V(tot),in cc.
Plot is given as Fig A8.8

$V_2 = (dl/dV)_{slope} \times 70.986$ cc/mole

$= 3.99/5.0$ " " "

$V_2 = 56.65$ cc/mole

Fig A8.8 Methane in i-Octane at 25°C, Total extension(cms.) vs Total dosage(cc.)

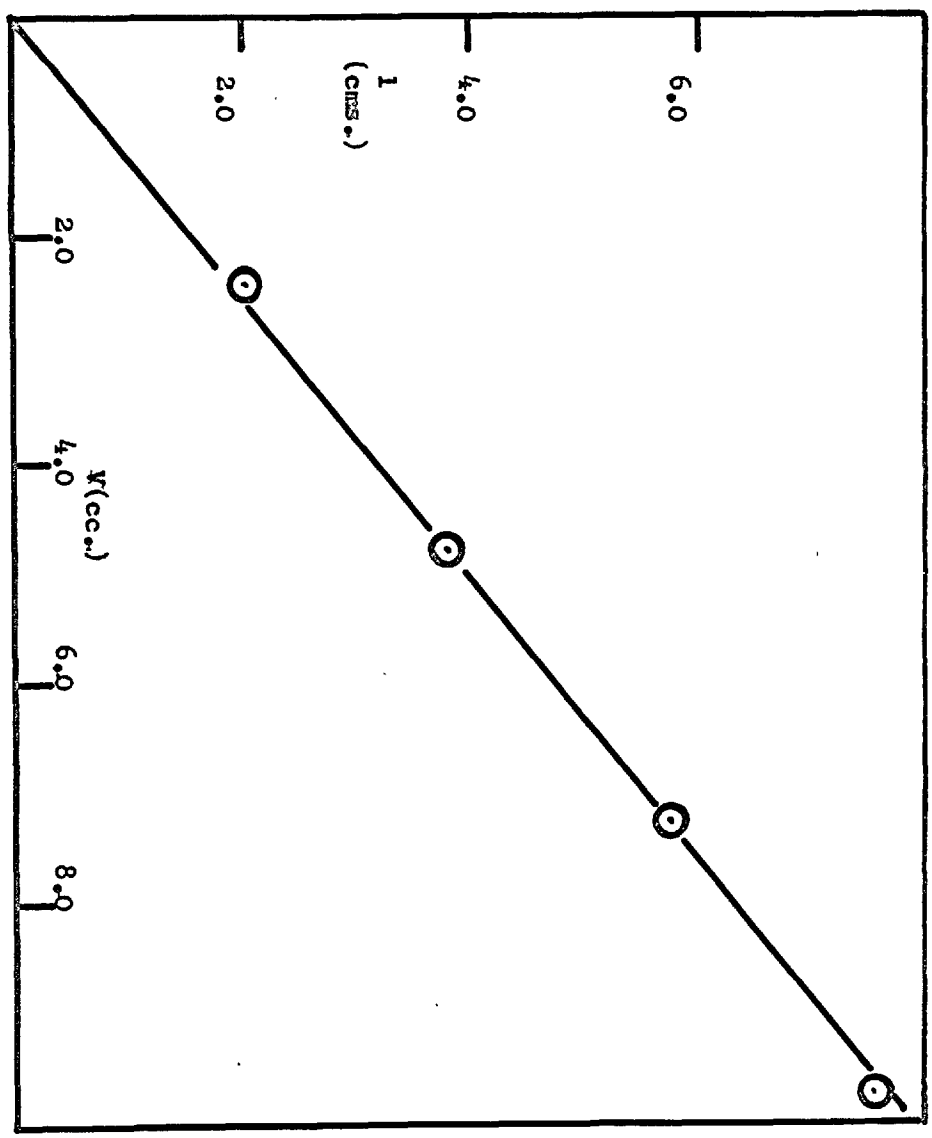

Freon in Benzene at 25°C.

Table A8.9 Experimental Data.

Dose	V. (cc)	V(tot)	N x10^4 (mol)	N x10^4 (tot)	l^a (cms)	l^b (cms)	V_2^a	V_2^b
** Ia	1.70	(1.70)	0.694	(0.694)	1.974	(1.974)	82.46	(82.46)
I	1.78	(1.78)	0.727	(0.727)	2.052	(2.052)	81.82	(81.82)
II	2.15	3.93	0.878	1.605	2.516	4.573	83.07	82.60
III	1.93	5.86	0.788	2.393	2.196	6.835	81.20	82.80

** Thermostating control lost after Ia, hence V_2 estimated from Doses I-III.

Columns superscripted as in previous tables

V_2 calculated from the slope of l^b(cms) vs V(tot), in cc. Plot is given as Fig A8.9.

$$V_2 = (dl/dV)_{slope} \times 70.986 \text{ cc/mole}$$

$$= 5.80/5.00 \quad " \quad " \quad "$$

$$V_2 = 82.34 \text{ cc/mole}$$

Fig A8.9 Freon in Benzene at 25°C, Total extension(cms.) vs Total dosage(cc.)

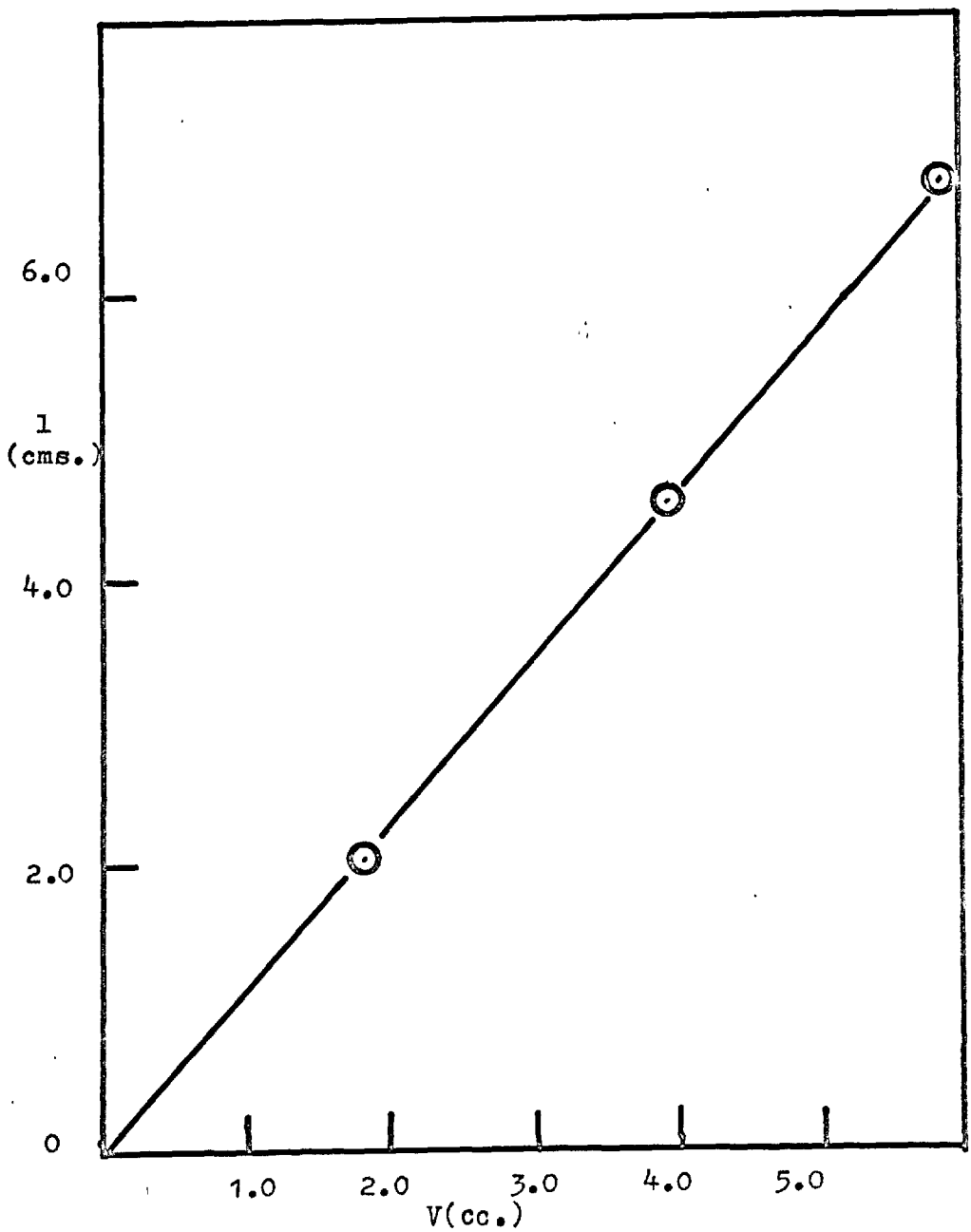

Freon in Cyclohexane at 25°C.

Table A8.10 Experimental Data

Dose	V. (cc)	V(tot)	N x10^4 (mole)	N x10^4 (tot)	l^a (cms)	l^b (cms)	V_2^a	V_2^b
I	1.68	(1.68)	0.686	(0.686)	2.198	(2.198)	92.88	(92.88)
II	1.72	3.40	0.702	1.338	2.101	4.298	86.76	89.76
III	1.78	5.18	0.727	2.115	2.165	6.379	86.33	87.44
IV	1.70	6.88	0.694	2.809	2.064	8.461	86.22	87.32
V	1.80	8.68	0.735	3.544	2.134	10.545	84.17	86.26

Columns superscripted as in previous tables

V_2 calculated from the slope of l^b (cms) vs V(tot), in cc. Plot is given as Fig A8.10

$V_2 = (dl/dV)_{slope} \times 70.986$ cc/mole

$= 9.23/7.50$ " " "

$V_2 = 87.36$ cc/mole

Fig A8.10 Freon in Cyclohexane at 25°C, Total extension(cms.) vs Total dosage(cc.)

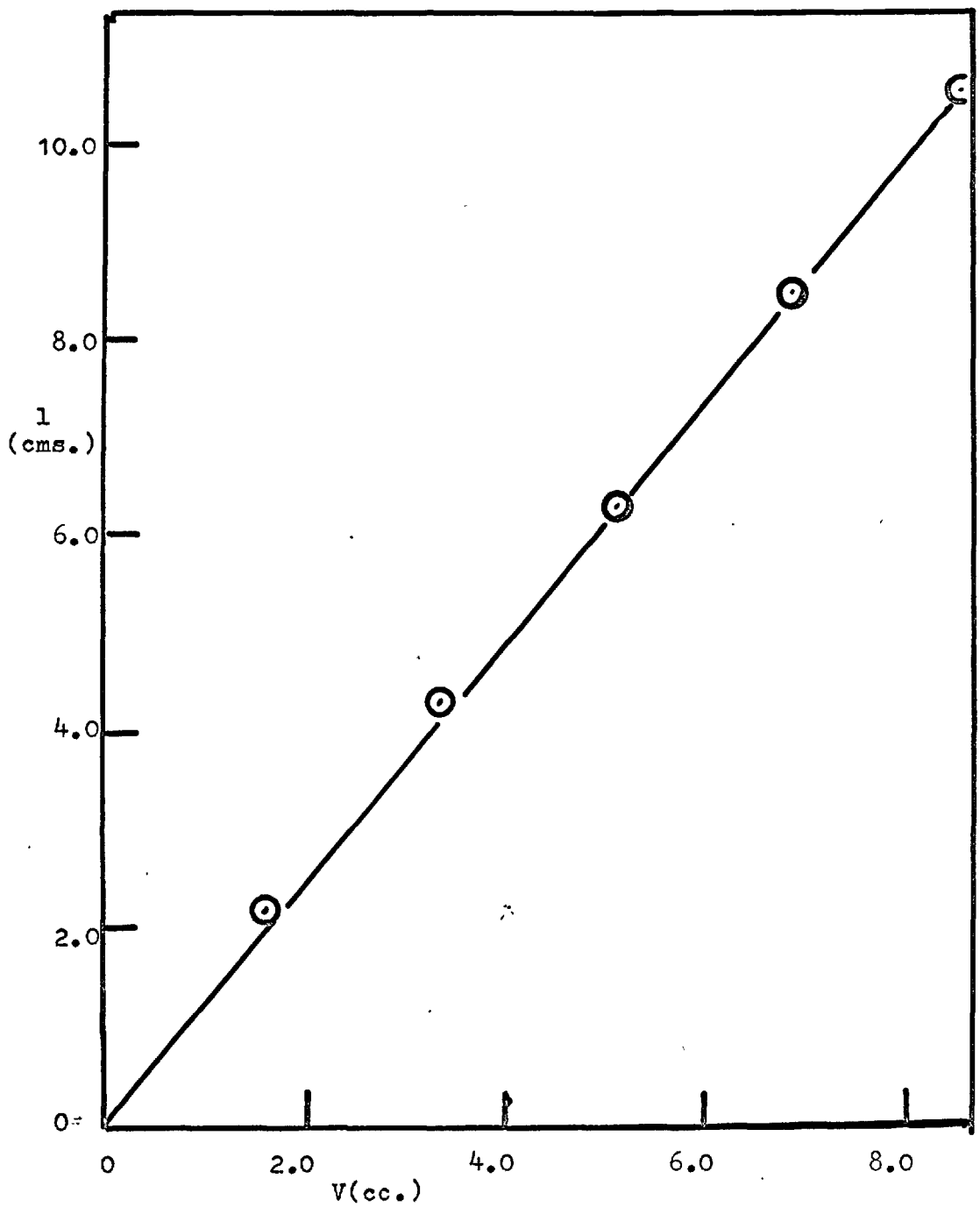

Freon in n-Heptane at 25°C.

Table A8.11 Experimental Data.

Dose	V. (cc)	V(tot)	N x10^4 (mol)	N x10^4 (tot)	l^a (cms)	l^b (cms)	V_2^a	V_2^b
I	1.96	(1.96)	0.800	(0.800)	2.453	(2.453)	88.89	(88.89)
II	1.55	3.51	0.633	1.433	2.090	4.397	95.72	88.93
III	1.38	4.89	0.564	1.997	1.612	6.175	82.92	89.64
IV	1.61	6.49	0.658	2.655	1.583	7.780	69.74	84.95
V	1.56	8.05	0.637	3.292	1.965	9.773	89.43	86.06

Columns superscripted as in previous tables

V_2 calculated from slope of l^b(cms) vs V(tot), in cc.
Plot is given as Fig A8.11

$V_2 = (dl/dV)_{slope} \times 70.986$ cc/mol

$= 6.24/5.00$ " " "

$V_2 = 88.59$ cc/mol

Fig A8.11 Freon in n-Heptane at 25°C, Total extension(cms.) vs Total dosage.(cc.)

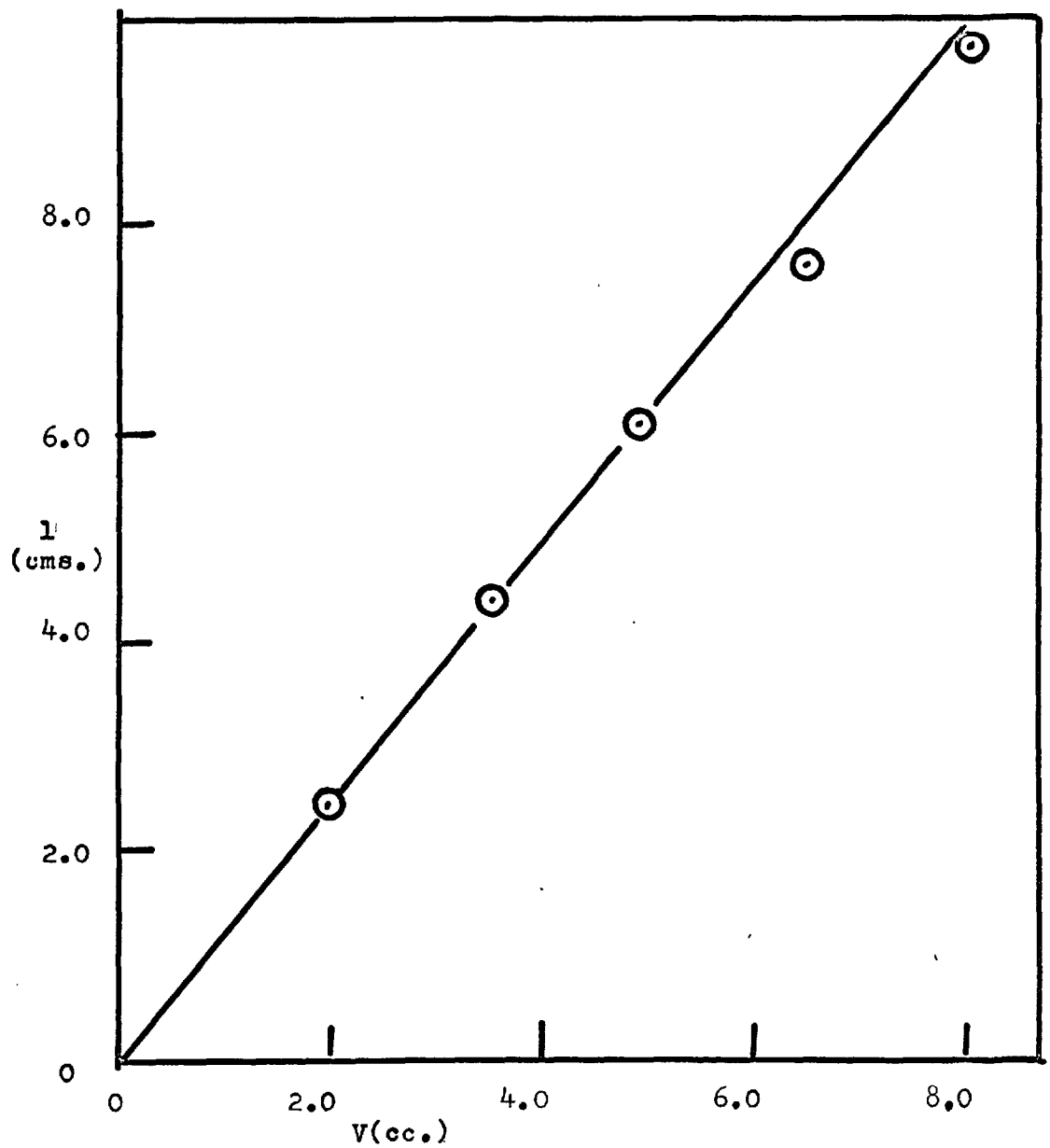

Freon in i-Octane at 25°C.

Table A8.12 Experimental data.

Dose	V. (cc)	V(tot)	N x10^4 (mole)	N x10^4 (tot)	l^a (cms)	l^b (cms)	V_2^a	V_2^a
I	1.27	(1.27)	0.519	(0.519)	1.516	(1.516)	85.57	(85.67)
II	1.77	3.04	0.723	1.242	2.236	3.728	89.66	87.02
III	1.54	4.58	0.629	1.871	1.865	5.585	85.96	86.54
IV	1.78	6.36	0.727	2.598	2.249	7.805	89.68	87.09
V	1.87	8.23	0.764	3.362	2.214	10.002	84.01	86.25

Columns superscripted as in previous tables

V_2 is calculated from the slope of l^b(cms) vs V(tot),in cc. Plot is given as Fig A8.12

$V_2 = (dl/dV)_{slope} \times 70.986$ cc/mole

$= 8.00/6.55$ " " "

$V_2 = 86.70$ cc/mole

Fig A8.12 Freon in i-Octane at 25°C, Total extension(cms.) vs Total dosage(cc.)

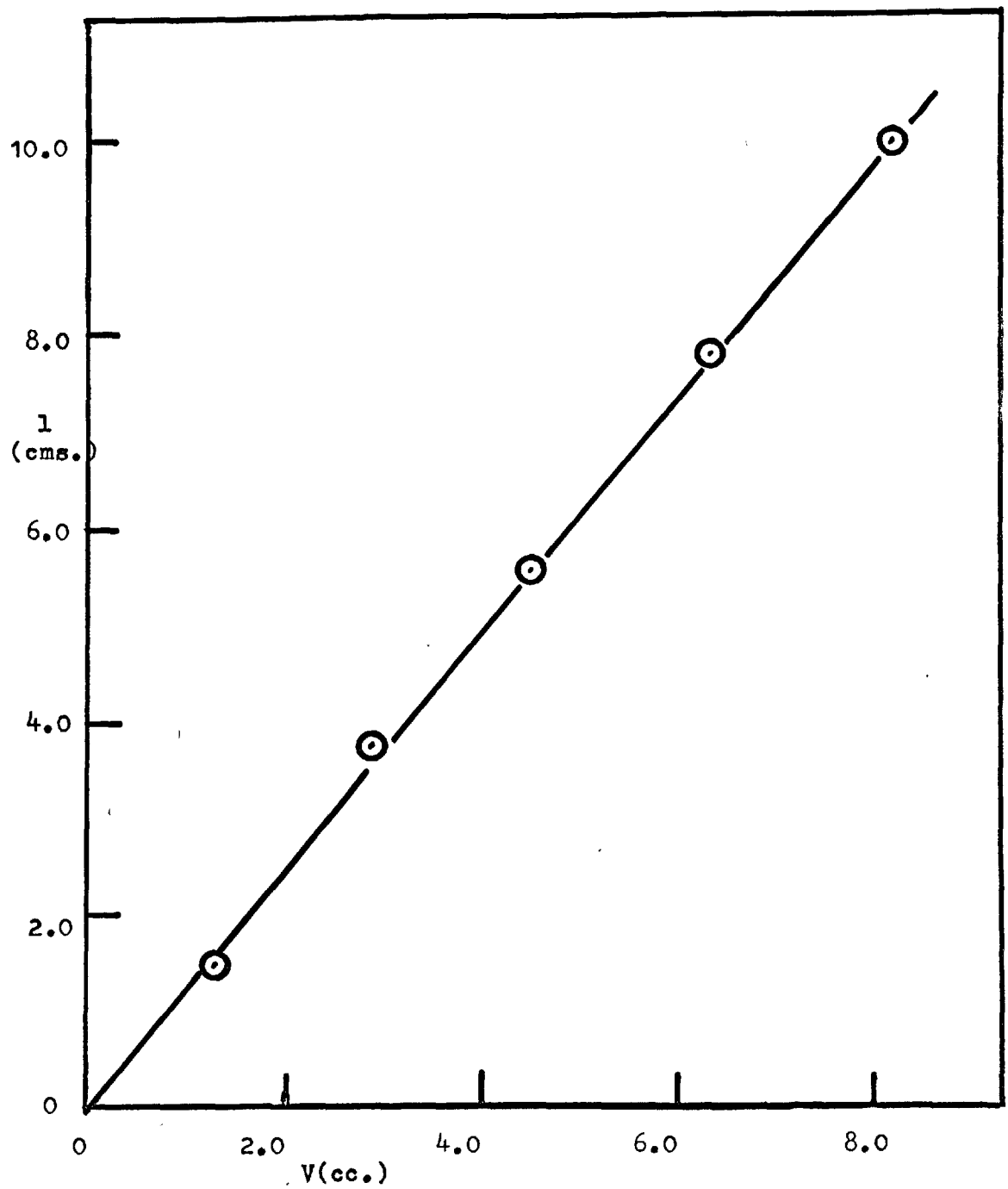

Sulphur Hexafluoride in Benzene at 25°C,(1st Series.)

Table A8.13 Experimental Data.

Dose	V. (cc.)	V(tot)	N x10^4 (mol)	N x10^4	l^a (cms)	l^b (cms)	V_2^a	V_2^b
I	1.30	(1.30)	0.532	(0.532)	1.789	(1.789)	97.49	97.49
II	2.19	3.49	0.895	1.427	3.026	4.804	98.05	97.71
III	2.06	5.55	0.842	2.269	2.528	7.670	98.00	98.00
IV	1.58	7.13	0.646	2.915	2.052	9.773	92.09	97.19
V	1.54	8.67	0.630	3.545	2.137	11.766	98.34	96.22

Columns superscripted as in previous tables

V_2 is calculated from the slope of l^b(cms) vs V(tot),in cc.The Plot is given as Fig A8.13

$V_2 = (dl/dV)_{slope} \times 70.986$ cc/mol

$= 11.5/8.4$ " " "

$V_2 = 97.07$ cc/mol

Fig A8.13 Sulphur Hexafluoride in Benzene at 25°C, Total extension(cms.) vs Total dosage(cc.)--Series 1.

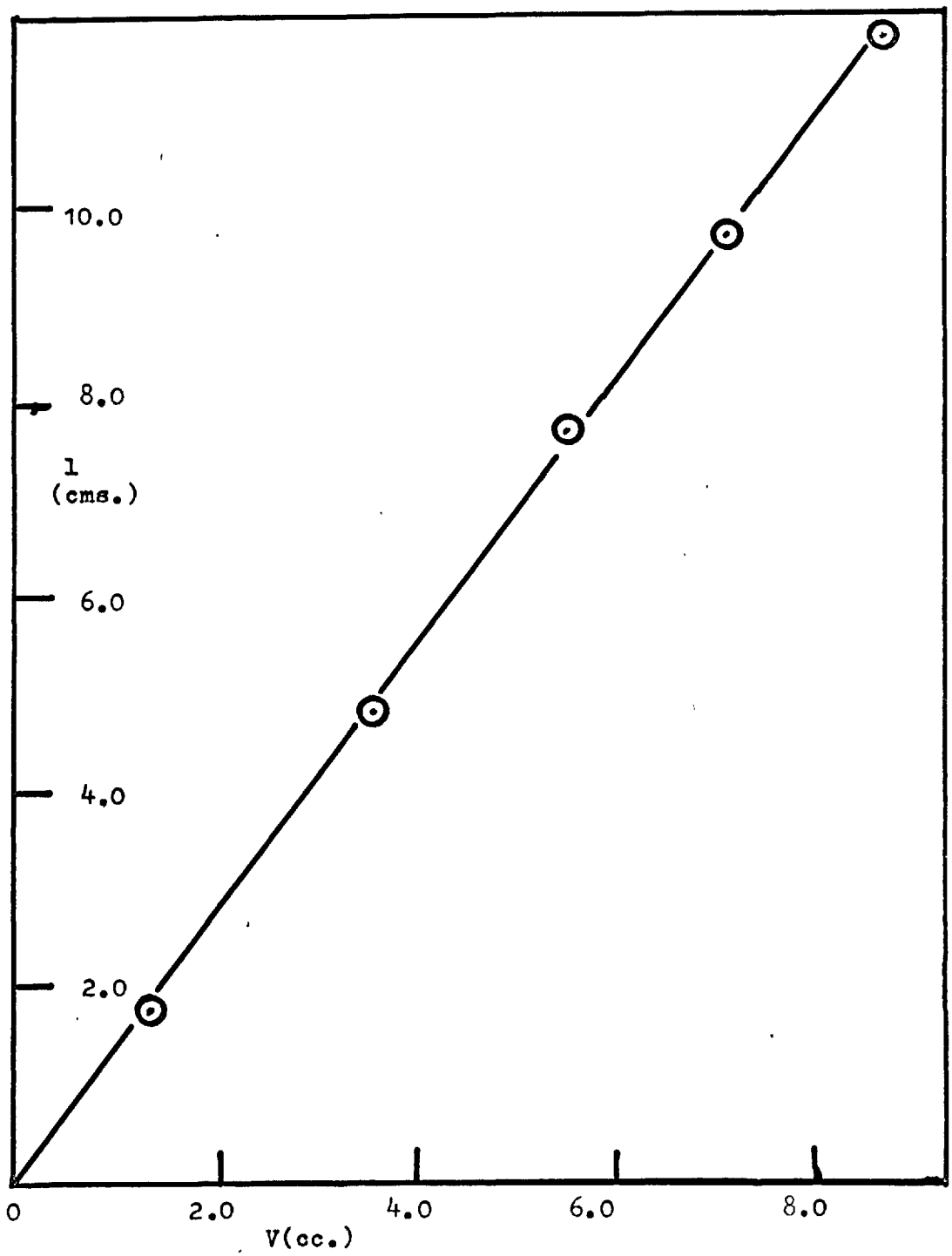

Sulphur Hexafluoride in Benzene at 25°C.(2nd Series)

Table A8.14 Experimental Data.

Dose	V. (cc.)	V(tot)	N x10^4 (moles)	N x10^4 (tot)	l^a (cms)	l^b (cms)	V_2^a	V_2^b
I	1.67	(1.67)	0.683	(0.683)	2.328	(2.328)	98.81	(98.81)
II	2.97	4.64	1.214	1.897	4.205	6.436	100.41	98.36
III	1.46	6.10	0.597	2.494	1.948	8.281	94.59	96.26
IV	2.11	8.21	0.863	3.357	2.967	11.073	99.67	95.62

Columns superscripted as in previous tables.

V_2 is calculated from the slope of l^b(cms) vs V(tot),in cc.The plot is given as Fig A8.14

$V_2 = (dl/dV)_{slope} \times 70.986$ cc/mole

$= 8.15/6.00$ " " "

$V_2 = 96.42$ cc/mole

Fig A8.14 Sulphur Hexafluoride in Benzene at 25°C, Total extension(cms.) vs Total dosage(cc.)--Series 2.

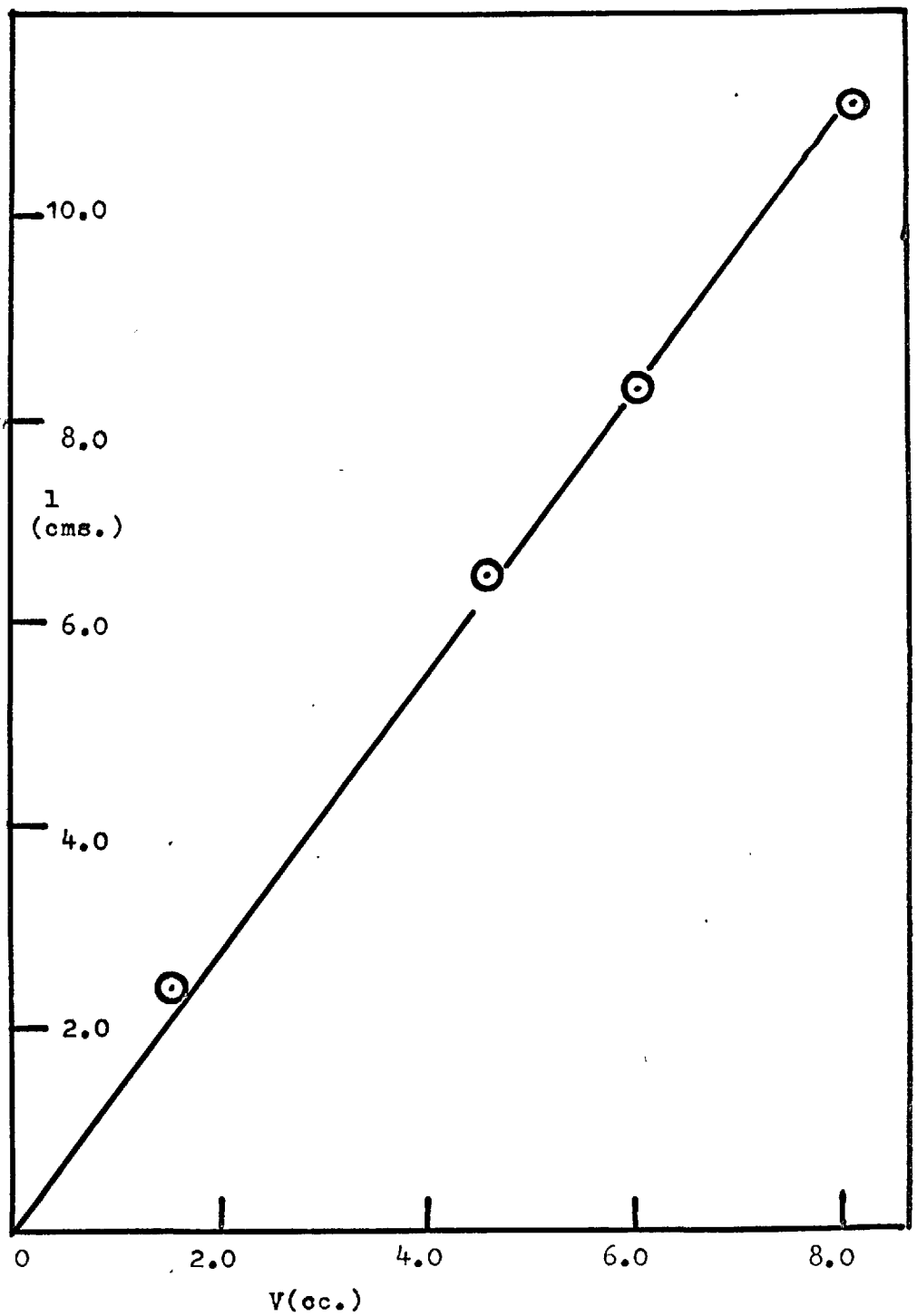

Sulphur Hexafluoride in Cyclohexane at 25°C.

Table A8.15 Experimental Data

Dose	V. (cc)	V(tot)	N x10^4 (mols)	N x10^4 (tot)	l^a (cms)	l^b (cms)	V_2^a	V_2^b
I	1.52	(1.52)	0.621	(0.621)	2.128	(2.128)	99.34	(99.34)
II	1.79	3.31	0.731	1.352	2.646	4.745	104.94	101.71
III	1.66	4.97	0.678	2.030	2.367	7.232	101.24	103.28
IV	1.58	6.55	0.645	2,675	2.028	9.286	91.15	100.64

Columns superscripted as in previous tables.

V_2 is calculated from the slope of l^b(cms) vs V(tot),in cc. The plot is given as Fig A8.15

V_2 = (dl/dV) x 70.986 cc/mole

= 9.0/6.3 " " "

V_2 = 101.41 cc/mole

Fig A8.15 Sulphur Hexafluoride in Cyclohexane at 25° C,
Total extension(cms.) vs Total dosage(cc.)

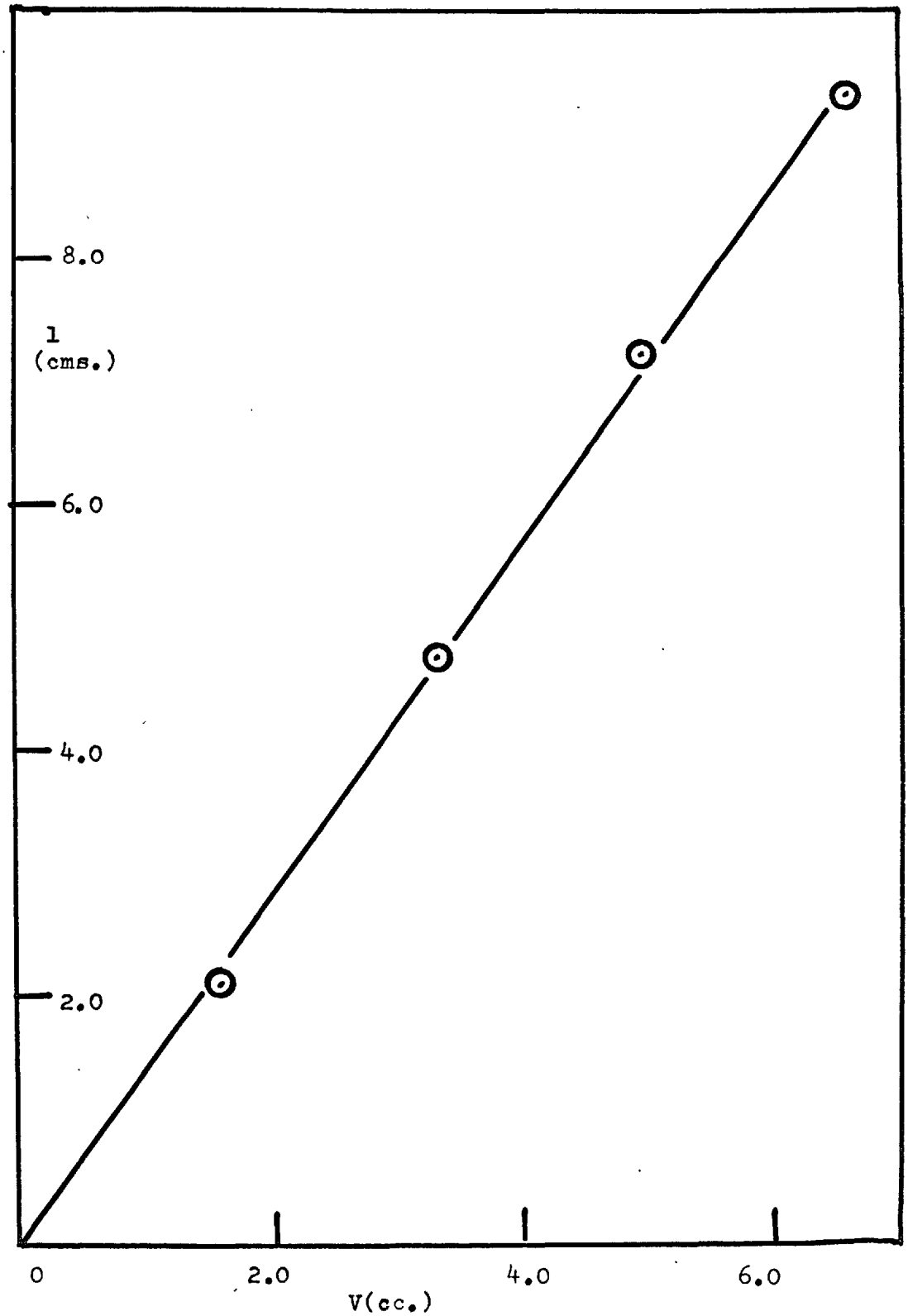

Sulphur Hexafluoride in n-Heptane at 25°C.
Table A8.16 Experimental Data

Dose	V. (cc.)	V(tot)	N x10^4 (mole)	N x10^4 (tot)	l^a (cms)	l^b (cms)	V_2^a	V_2^a
I	1.48	(1.48)	0.604	(0,604)	2.146	(2.146)	102.93	(102.93)
II	1.64	3.12	0.670	1.274	2.356	4.484	101.94	102.03
III	1.82	4.94	0.743	2.017	2.632	7.164	102.69	102.96
IV	1.62	6.56	0.662	2.679	2.315	9.482	101.37	102.61

Columns superscripted as in previous tables.

V_2 is calculated from the slope of l^b(cms) vs V(tot), in cc.
The plot is given as Fig A8.16

$V_2 = (dl/dV)_{slope} \times 70.986$ cc/mole

$= 7.95/5.50$ " " "

$V_2 = 102.61$ cc/mole

Fig A8.16 Sulphur Hexafluoride in n-Heptane at 25°C, Total extension(cms.) vs Total dosage(cc.)

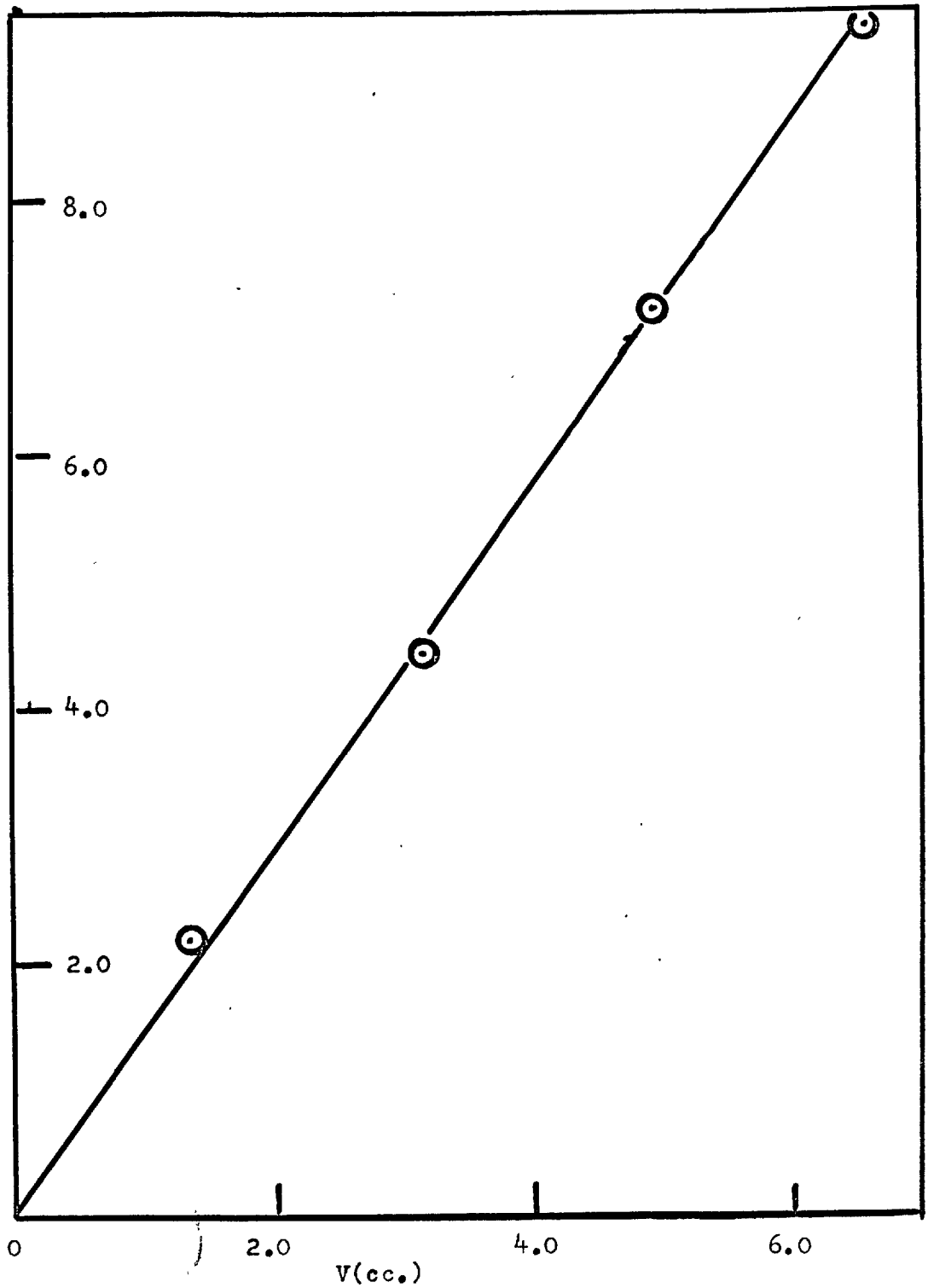

Sulphur Hexafluoride in i-Octane at 25°C.

Table A8.17 Experimental Data

Dose	V. (cc.)	V(tot)	N x10^4 (mole)	N x10^4 (tot)	l^a (cms)	l^b (cms)	V_2^a	V_2^b
I	1.65	(1.65)	0.674	(0.674)	2.431	(2.431)	104.58	(104.58)
II	2.38	4.03	0.972	1.646	3.354	5.993	100.0	104.49
III	1.61	5.64	0.657	2.303	2.468	8.346	108.9	105.06
IV	1.58	7.22	0.645	2.948	2.169	10.447	97.49	102.73
V	0.98	8.20	0.400	3.348	1.439	11.833	104.29	102.46

Columns superscripted as in previous tables

V_2 is calculated from the slope of l^b(cms) vs V(tot), in cc. The plot is given as Fig A8.17

V_2 = (dl/dV) x 70.986 cc/mole

= 11.65/8.00 " "

V_2 = 103.38 cc/mole

Fig A8.17 Sulphur Hexafluoride in i-Octane at 25°C, Total extension(cms.) vs Total dosage(cc.)

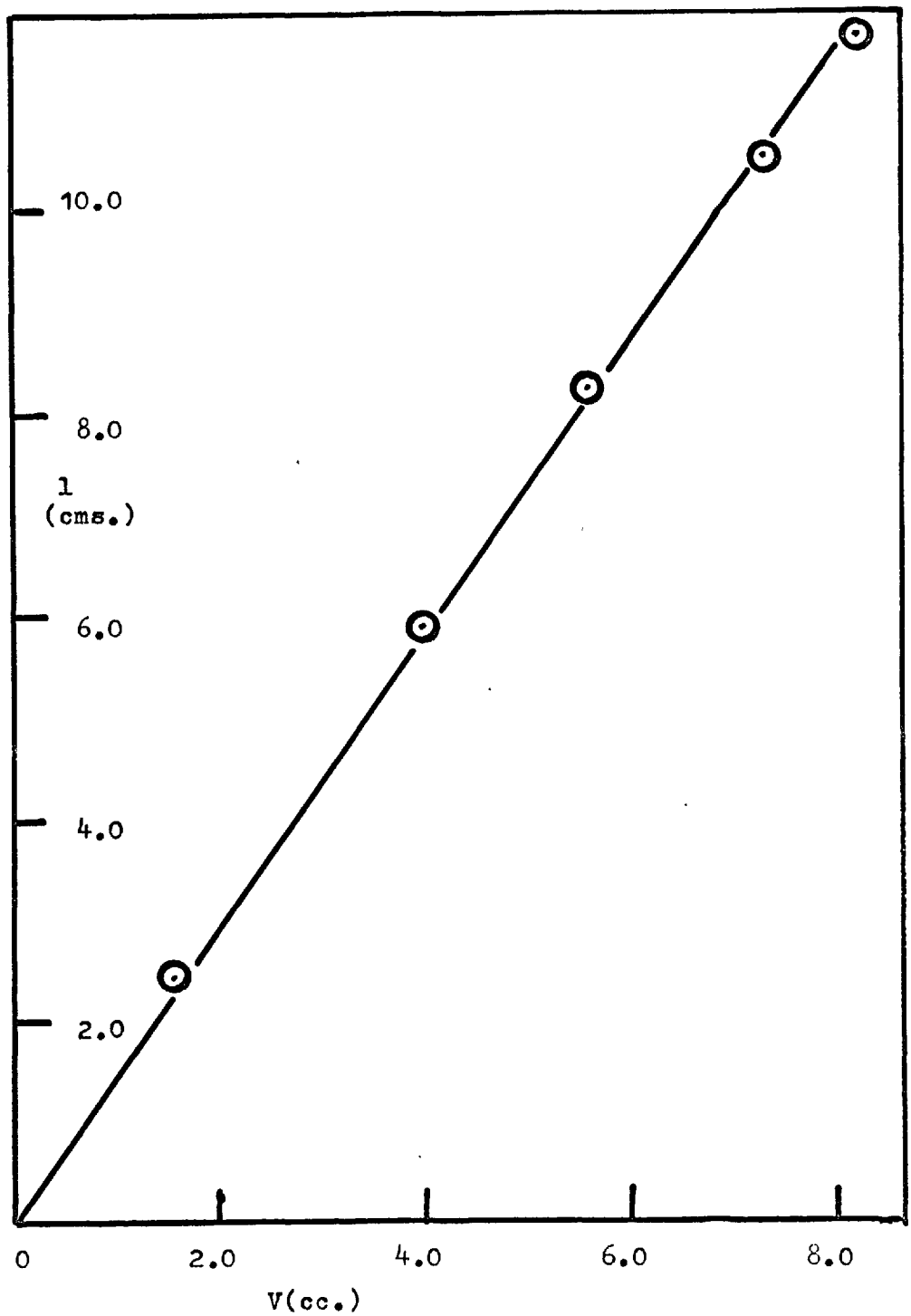

Hydrogen in Benzene at 25°C.

Table A8.18 Experimental Data

Dose	V. (cc.)	V(tot)	N x10^4 (moles)	N x 10^4 (tot)	l^a (cms)	l^b (cms)	V_2^a	V_2^b
I	2.79	(2.79)	1.139	(1.139)	1.388	(1.388)	35.33	(35.33)
II	2.97	5.76	1.213	2.352	1.518	2.863	37.27	35.29
III	2.72	8.48	1.111	3.463	1.470	4.303	38.35	36.02
IV	2.26	10.74	0.923	4.386	1.041	5.282	32.70	34.91

Columns superscripted as in previous tables

V_2 is calculated from the slope of l^b(cms) vs V(tot),in cc.

Plot is given as Fig A8.18

V_2 = (dl/dV) x 70.986 cc/mole

= 4.98/10.00 " "

V_2 = 35.35 cc/mole

Fig A8.18 Hydrogen in Benzene at 25°C, Total extension(cms.) vs Total dosage(cc.)

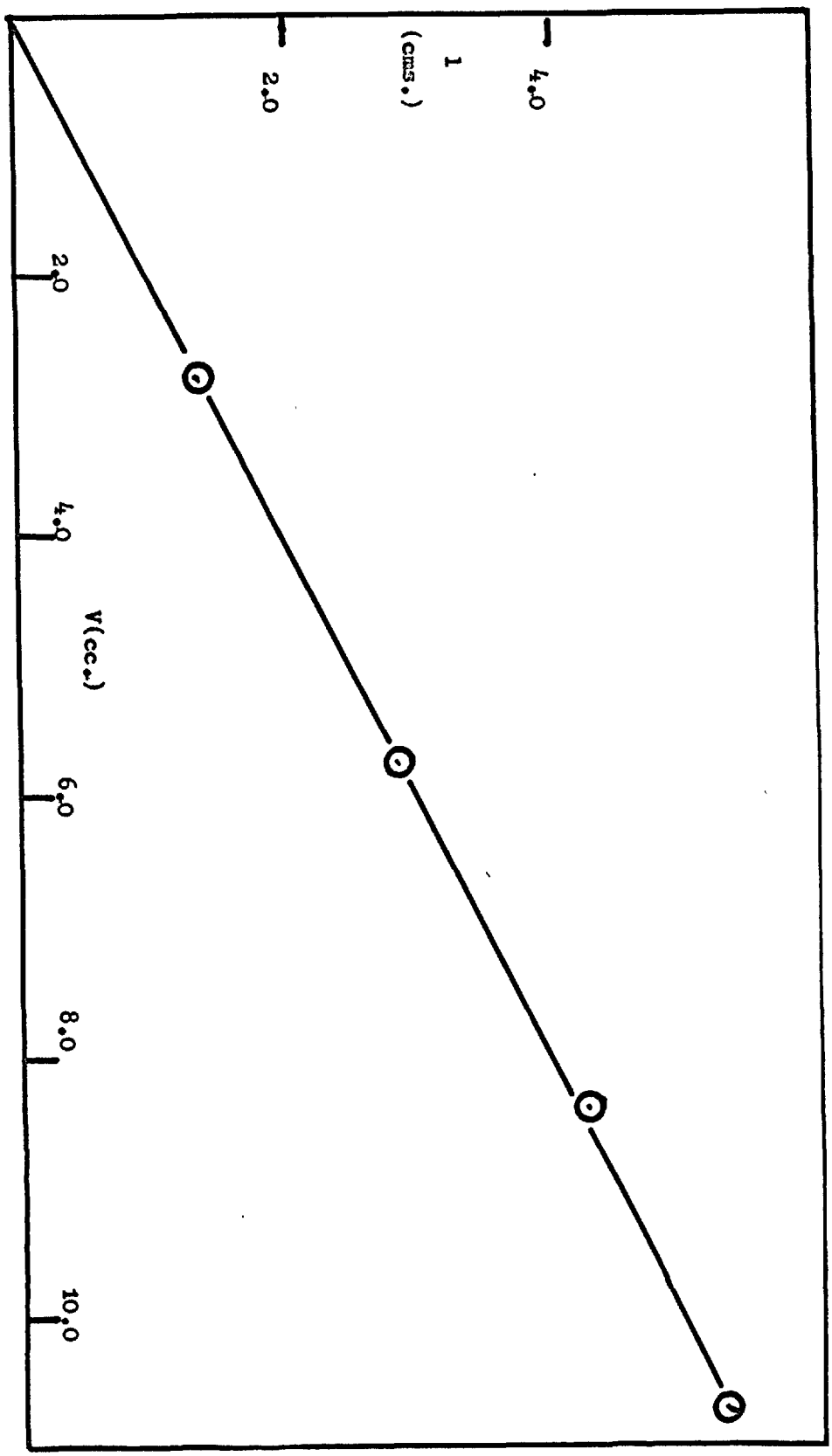

Hydrogen in Cyclohexane at 25°C.

Table A8.19 Experimental Data.

Dose	V. (cc)	V(tot)	N x 10^4 (moles)	N x10^4 (tot)	l^a (cms)	l^b (cms)	V_2^a	V_2^b
I	2.45	(2.45)	1.001	(1.001)	1.437	(1.437)	41.66	(41.66)
II	2.94	5.39	1.201	2.202	1.740	3.151	42.00	41.48
III	2.84	8.23	1.160	3.362	1.593	4.750	40.28	40.96
IV	2.65	10.88	1.082	4.444	1.416	6.116	37.94	39.90

Columns superscripted as in previous tables

V_2 is calculated from the slope of l^b(cms) vs V(tot),in cc.

Plot is given as Fig A8.19

V_2 = (dl/dV) x 70.986 cc/mole

= 5.79/10.00 " "

V_2 = 41.10 cc/mole

Fig A8.19 Hydrogen in Cyclohexane, Total extension(cms.) vs Total dosage(cc.)

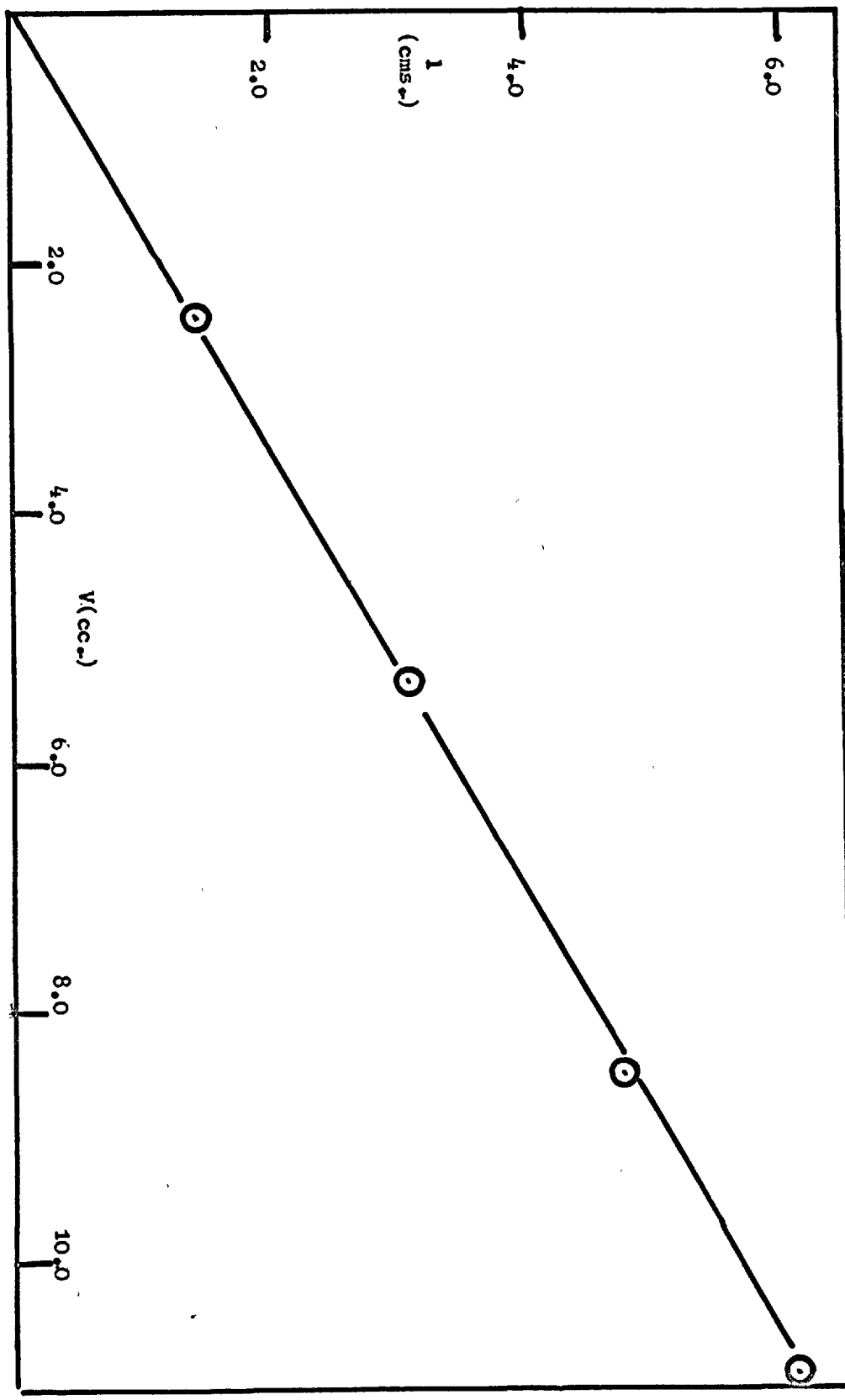

Hydrogen in n-Heptane at 25°C

Table A8.20 Experimental Data

Dose	V. (cc.)	V(tot)	N x10^4 (mol)	N x10^4 (tot)	l^a (cms)	l^b (cms)	V_2^a	V_2^b
I	2.84	(2.84)	1.160	(1.160)	1.969	(1.969)	49.21	(49.21
II	2.60	5.44	1.062	2.222	1.424	3.433	38.87	44.79
III	2.52	7.96	1.029	3,251	1.388	4.702	37.70	41.93
IV	2.90	10.86	1.184	4.435	1.894	6.552	46.37	42.82
V	2.78	13.64	1.135	5.570	1.739	8.201	44.42	42.68

Columns superscripted as in previous tables

V_2 is calculated from the slope of l^b(cms) vs V(tot),in cc. Plot is given as Fig A8.20

$V_2 = (dl/dV)_{slope} \times 70.986$ cc/mol.

$= 6.08/10.00$ " " "

$V_2 = 43.16$ cc/mol

Fig A8.20 Hydrogen in n-Heptane at 25°C, Total extension(cms.) vs Total dosage(cc.)

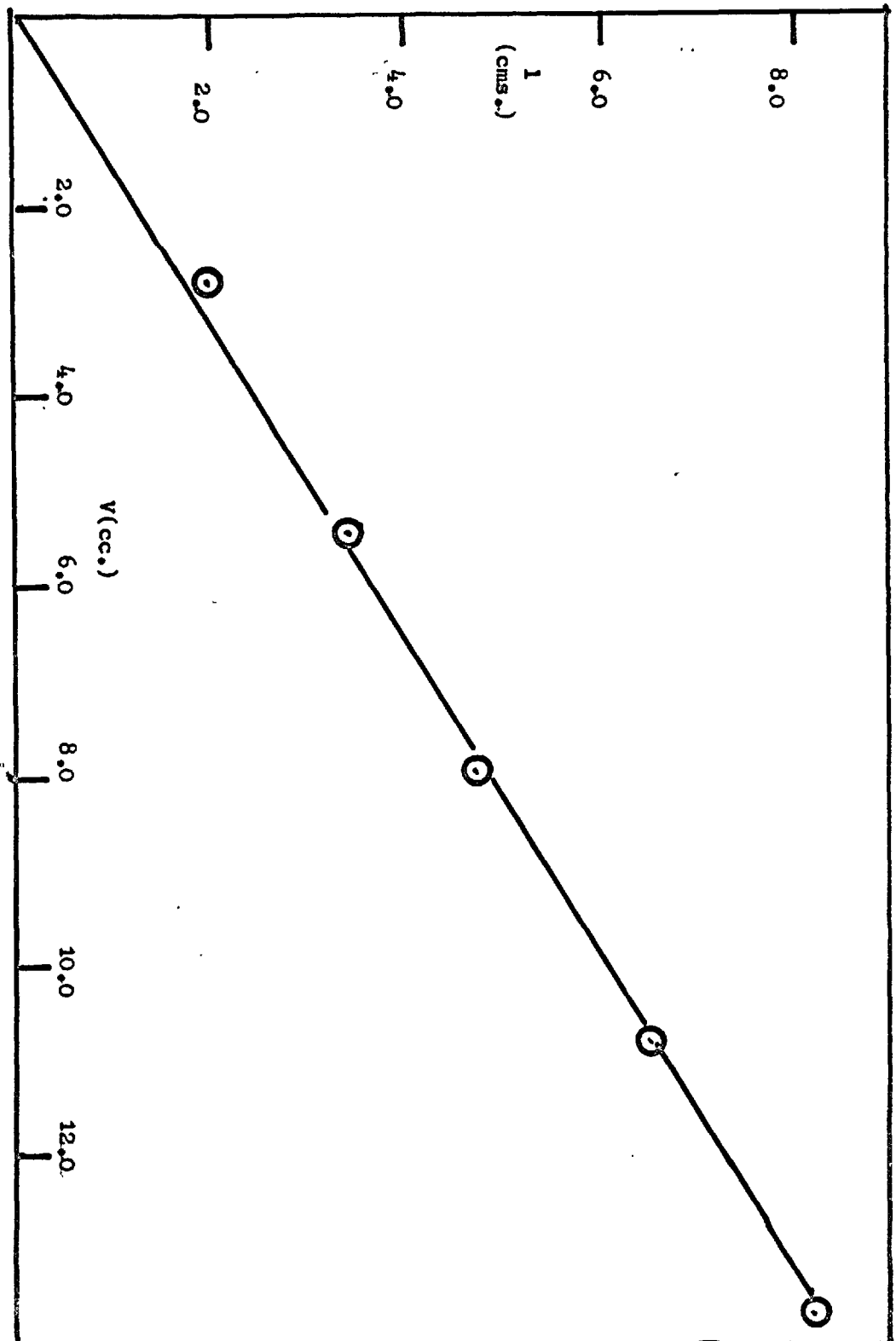

Hydrogen in i-Octane at 25°C.

Table A8.21 Experimental Data.

Dose	V_+ (cc.)	V(tot)	N x10^4 (moles)	N x10^4 (tot)	l^a (cms)	l^b (cms)	V_2^a	V_2^b
I	2.18	(2.18)	0 890	(0.890)	1.509	(1.509)	49.15	(49.15)
II	2.73	4.91	1.115	2.005	1.745	3.252	45.37	47.02
III	2.88	7.79	1.176	3.181	1.875	5.104	46.22	46.52
IV	2.74	10.53	1.119	4.300	1.719	6.845	44.53	46.15
V	2.65	13.18	1.082	5.382	1.551	8.348	41.56	44.97

Columns superscripted as in previous tables.

V_2 is calculated from the slope of l^b(cms) vs V(tot) in cc. The Plot is given as Fig A8.21

V_2 = (dl/dV) x 70.986 cc/mole

= 8.00/12.30 " "

V_2 = 46.17 cc/mole

Fig A8.21 Hydrogen in i-Octane at 25°C, Total extension(cms.) vs Total dosage(cc.)

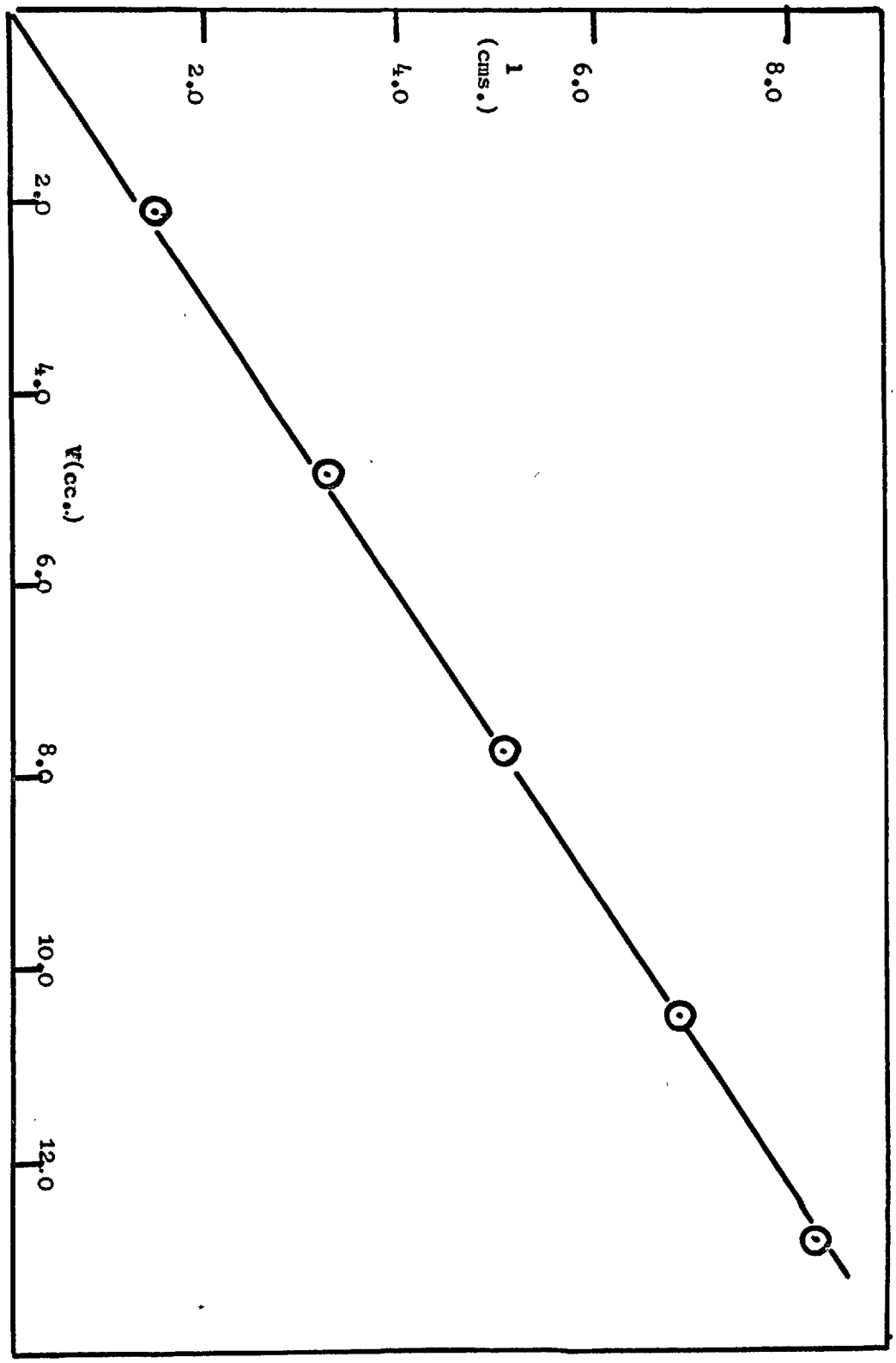

Deuterium in Benzene at 25°C.

Table A8.22 Experimental Data.

Dose	V. (cc.)	V(tot)	N x10^4 (mole)	N x10^4 (tot)	l^a (cms)	l^b (cms)	V_2^a	V_2^b
I	3.30	(3.30)	1.348	(1.348)	1.518	(1.518)	32.65	(32.65)
II	2.97	6.27	1.213	2.561	1.274	2.841	30.45	32.16
III	2.84	9.11	1.160.	3.721	1.356	4.212	33.89	32.82

Columns superscripted as in previous tables.

V_2 is calculated from the slope of l^b(cms) vs V(tot),in cc.

The plot is given as Fig A8.22

V_2 = (dl/dV) x 70.986 cc/mole

= 6.10/10.00 " "

V_2 = 32.72 cc/mole

Fig A8.22 Deuterium in Benzene at 25°C.Total extension(cms.) vs Total dosage(cc.)

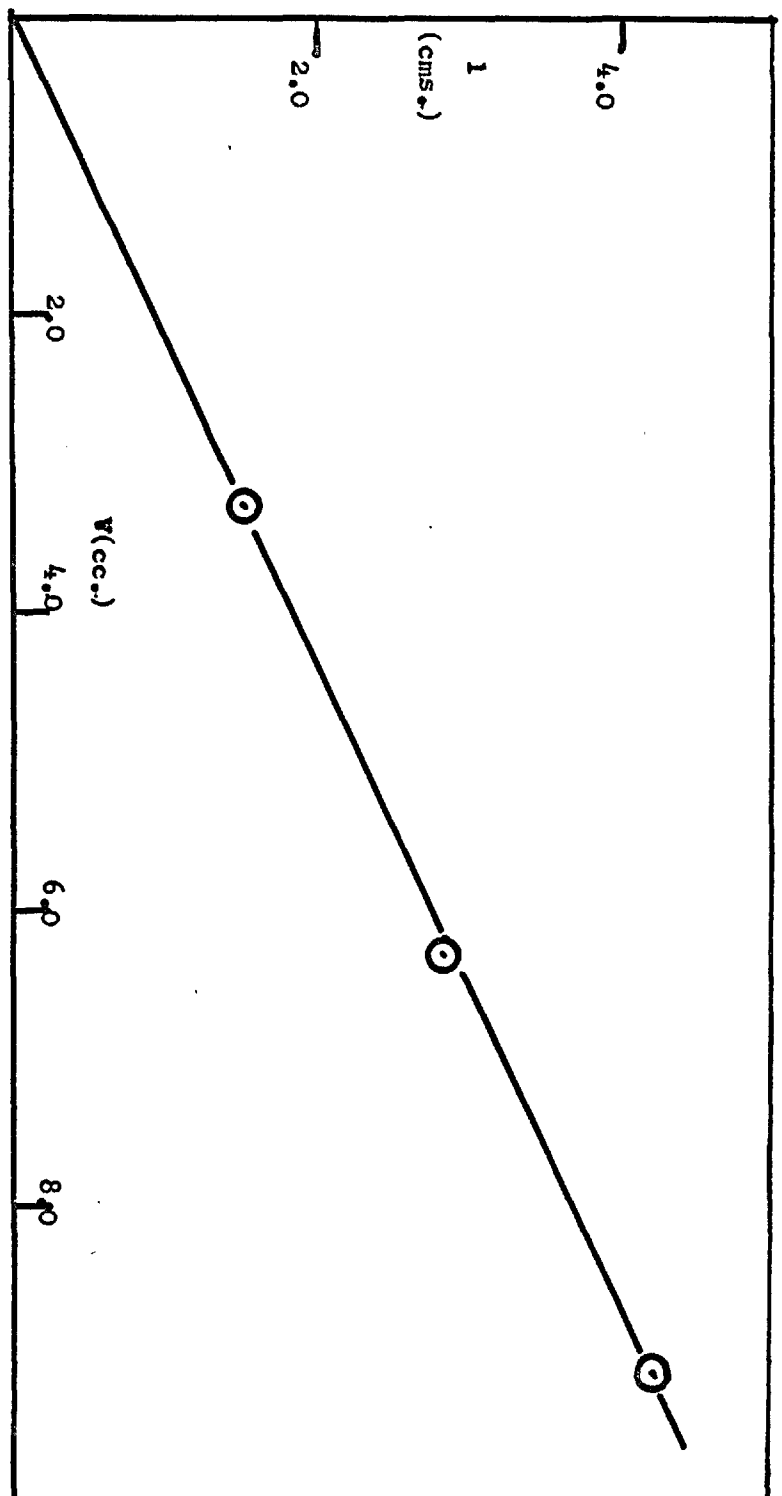

Deuterium in n-Heptane at 25°C.

Table A8.23 Experimental Data

Dose	V. (cc.)	V(tot)	N x10^4 (mole)	N x10^4 (tot)	l^a (cms)	l^b (cms)	V_2^a	V_2^b
I	3.18	(3.18)	1.299	(1.299)	1.819	(1.819)	40.59	(40.59)
II	3.25	6.43	1.327	2.626	1.847	3.698	40.35	40.82
III	3.09	9.52	1.262	3.888	1.789	5.542	41.10	41.32
IV	3.13	12.65	1.278	5.166	1.879	7.338	42.62	41.17

Columns superscripted as in previous tables.

V_2 is calculated from the slope of l^b(cms) vs V(tot), in cc.

The Plot is given as Fig A8.23

$$V_2 = (dl/dV)_{slope} \times 70.986 \text{ cc/mole}$$

$$= 5.80/10.00 \text{ " " "}$$

$$V_2 = 41.17 \text{ cc/mole}$$

Fig A8.23 Deuterium in n-Heptane at 25°C, Total extension(cms.) vs Total dosage(cc.)

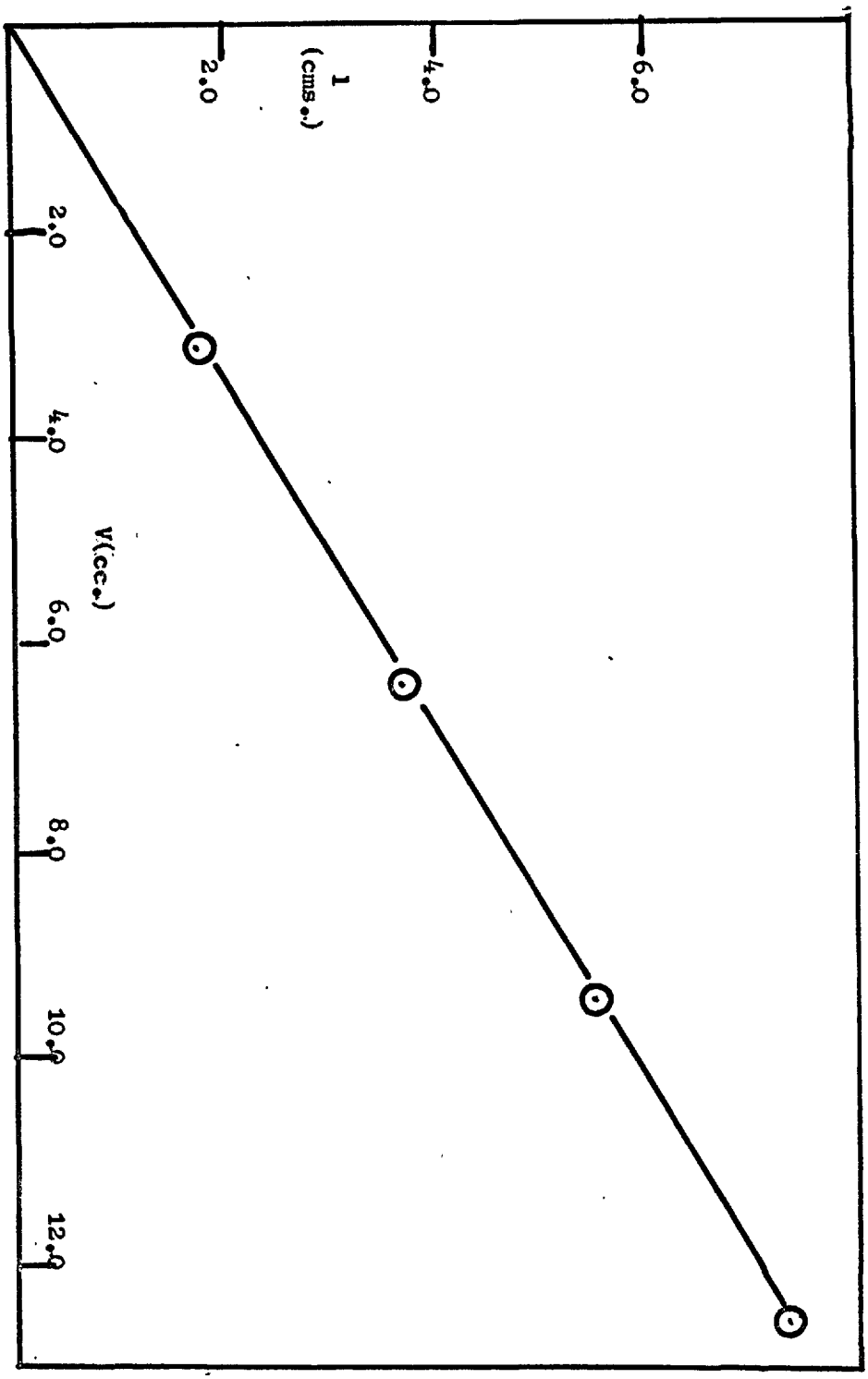

Deuterium in i-Octane at 25°C.

Table A8.24 Experimental Data.

Dose	V. (cc.)	V(tot)	N x10^4 (mole)	N x10^4 (tot)	l^a (cms)	l^b (cms)	V_2^a	V_2^b
I	2.81	(2.81)	1.148	(1.148)	1.703	(1.703)	43.01	(43.01)
II	2.95	5.76	1.205	2.353	1.732	3.461	41.67	42.64
III	2.86	8.62	1.168	3.251	1.725	5.250	42.81	43.23
IV	2.80	11.42	1.143	4.664	1.739	6.967	44.11	43.30
V	2.70	14.12	1.103	5.767	1.663	8.582	43.71	43.14

Columns superscripted as in previous tables.

V_2 is calculated from the slope of l^b(cms) vs V(tot) in cc. The Plot is given in Fig A8.24

$V_2 = (dl/dV)_{slope} \times 70.986$ cc/mole

$= 7.50/12.35$ " " "

$V_2 = 43.11$ cc/mole

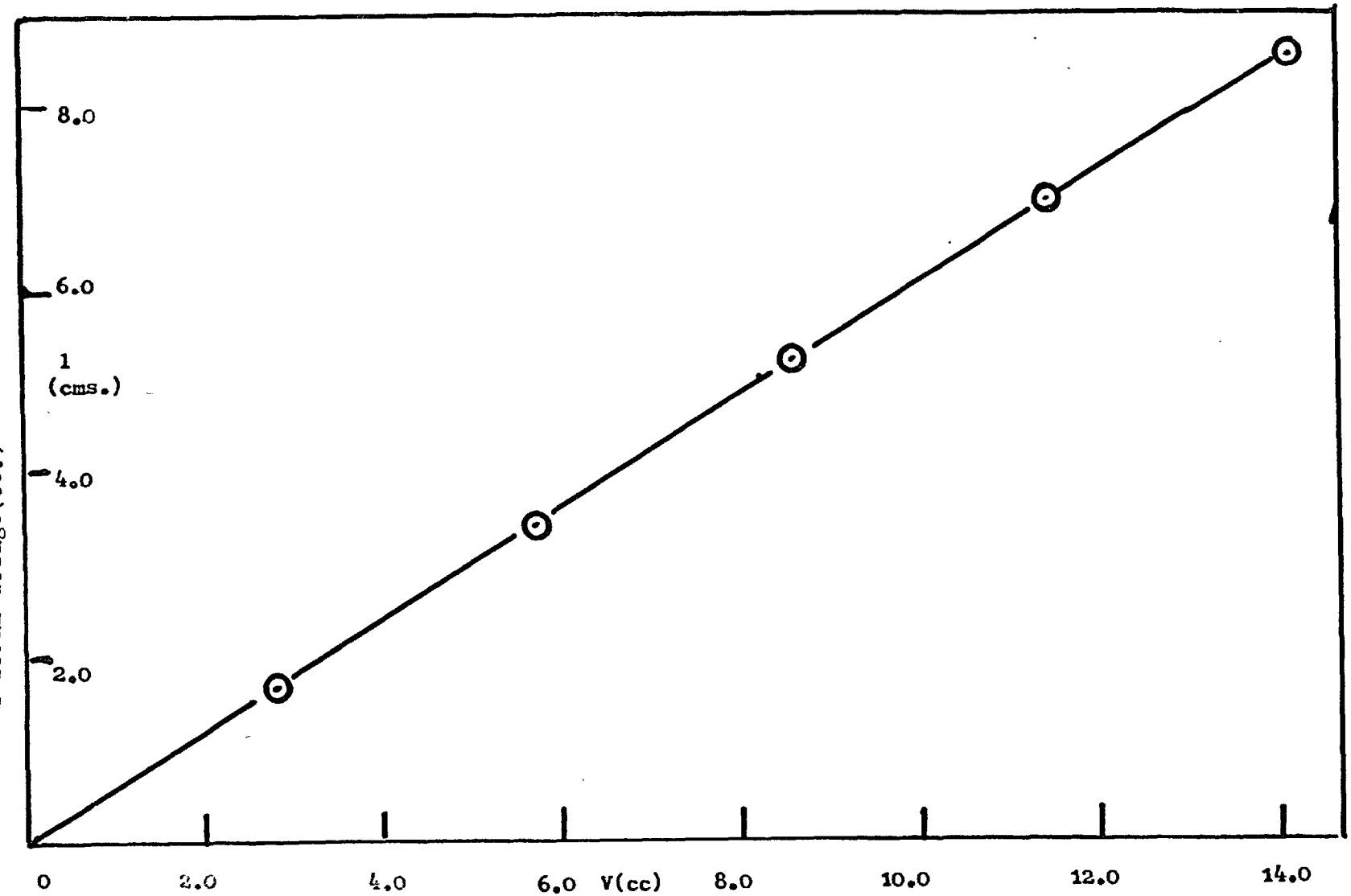

Fig A8.24 Deuterium in 1-Octane at 25°C. Total extension (cms.) vs Total dosage (cc.)